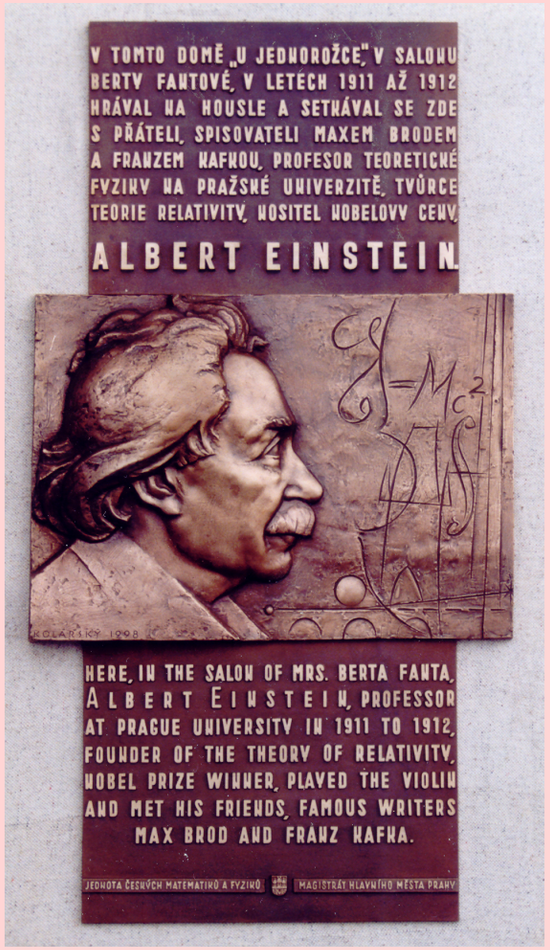

Memorial plaque of Albert Einstein in the Old Town Square No. 17.

ISBN 978-80-85823-70-7

COSMOLOGY ON SMALL SCALES 2020

Proceedings of the International Conference

Cosmology on Small Scales 2020

Exessive Extrapolations and Selected Controversies in Cosmology

Prague, September 23–26, 2020

Edited by
Michal Křížek and Yurii V. Dumin

Institute of Mathematics
Czech Academy of Sciences

Proceedings of the International Conference

COSMOLOGY ON SMALL SCALES 2020

Excessive Extrapolations and Selected Controversies in Cosmology

Prague, September 23–26, 2020

Edited by
Michal Křížek and Yurii V. Dumin

Institute of Mathematics
Czech Academy of Sciences
Prague 2020

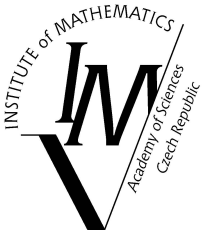

ISBN 978-80-85823-70-7
Institute of Mathematics
Czech Academy of Sciences
Prague 2020
LaTeX typesetting prepared by Hana Bílková

The important thing is not to stop questioning.
Albert Einstein

CONTENTS

Alternative cosmological theories

PREFACE

According to the modern cosmological paradigm, about 2/3 of the energy of the Universe is in dark form and about 5/6 of the matter is invisible. However, numerous recent independent attempts to detect dark-matter particles failed, and a number of other problems with the existence of dark energy and dark matter (such as the anomalous friction in the dark-matter halos of galaxies) become now more and more obvious. All these problems raise the question if the "dark" substance is merely a result of the use of erroneous assumptions or incorrect models based e.g. on excessive extrapolations. Consequently, it is timely to gather specialists from various branches of astronomy and astrophysics to discuss these questions.

Yet another subtle issue is that the Friedmann equation – the cornerstone of modern cosmology – was derived from the system of ten Einstein equations applied to a perfectly symmetric universe, which is homogeneous and isotropic for every fixed time instant. The question is whether this is justified and, in particular, at which scale the effect of Hubble expansion begins to be manifest.

For instance, recently it was found by the sky survey programs GALEX, SDSS and Spitzer S^4G imaging that the expansion speed of our Galaxy is about $0.6 - 1\,\mathrm{kpc/Gyr}$ (i.e. $600 - 1000$ m/s) even though the extragalactic gas and dust continuously fall on the galactic disk, see C. Martínez-Lombilla et al., MNRAS 483 (2019), 664–691. It is interesting that this number is of the same order as the Hubble constant $H_0 = 68\,\mathrm{km/(s\,Mpc)}$ recalculated to the Galactic radius $R = 16$ kpc, namely $H_0 \approx 1000\,\mathrm{m/(s\,}R)$. The expansion speed of the Solar system is of order H_0, too.

To shed more light onto these topics, we decided to organize the International Conference *Cosmology on Small Scales 2020: Excessive Extrapolations and Selected Controversies in Cosmology*. It was held at the Institute of Mathematics of the Czech Academy of Sciences at Žitná 25, Prague 1, from 23 to 26 September 2020 (see `css2020.math.cas.cz`). It was a continuation of our previous conferences *Cosmology on Small Scales 2016: Local Hubble Expansion and Selected Controversies in Cosmology*, and *Cosmology on Small Scales 2018: Dark Matter Problem and Selected Controversies in Cosmology* which took place four and two years ago (see `css2016.math.cas.cz, css2018.math.cas.cz`).

The main topics of the conference "Cosmology on Small Scales 2020" were:

- ▷ Mathematical aspects of the extrapolations used in cosmology
- ▷ Arguments for and against dark matter, and revisiting the foundations of physics
- ▷ Alternative models for dark matter and dark energy
- ▷ The systematic disagreement on the value of the Hubble constant computed by different methods
- ▷ Theoretical possibility and observational evidence for small-scale cosmological effects

- ▷ Complementary redshifts of non-cosmological nature
- ▷ Quantum effects on the early universe and their observational imprints at the present time

In these Proceedings we present several papers showing that the claimed amount of dark matter and dark energy can be a result of vast overestimation and may not conform with reality. At the end of the Proceedings, there are several papers on "history and philosophy of cosmology" and "alternative cosmological theories". Although they may be questionable and the Scientific Committee is not responsible for their content, we believe that it is reasonable to present them to the wide audience.

The Scientific Committee consisted of

Assoc. Prof. Yurii Dumin (Moscow State University & Space Research Institute of RAS, Russia)
Prof. Itzhak Goldman (Afeka College, Israel)
Prof. Igor Karachentsev (Special Astrophysical Observatory of RAS, Russia)
Prof. Sergei Kopeikin (University of Missouri, USA)
Prof. Pavel Kroupa (University of Bonn, Germany)
Prof. André Maeder (Geneva Observatory, Switzerland)
Assoc. Prof. Attila Mészáros (Charles University, Czech Republic)
Prof. Marek Nowakowski (Universidad de los Andes, Colombia)
Prof. Lawrence Somer (Catholic University of America, USA)
Prof. Alessandro Spallicci (University of Orleans, CNRS, France)
Prof. Alexei Starobinsky (Landau Institute of RAS, Russia)

Local Organizing Committee consisted of

Prof. Michal Křížek — Chair (Czech Academy of Sciences, Czech Republic)
Assoc. Prof. Yurii Dumin — Vice-Chair (Moscow State University & Space Research Institute of RAS, Russia)
Assoc. Prof. Tomáš Vejchodský (Czech Academy of Sciences, Czech Republic)
Hana Bílková (Czech Academy of Sciences, Czech Republic)

The Local Organizing Committee is deeply grateful to all authors for their contributions and the support of RVO 67985840 (Institute of Mathematics of the Czech Academy of Sciences). Out sincere thanks go also to all active members of the Cosmological Section of the Czech Astronomical Society for their continual help. Finally, we are indebted to Hana Bílková for technical assistance in the final typesetting and Tomáš Vejchodský for his helpful cooperation.

These Proceedings can be downloaded from the website:

`http://users.math.cas.cz/~krizek/list.html`

Michal Křížek and Yurii V. Dumin

Conference *Cosmology on Small Scales 2020*
Michal Křížek and Yurii Dumin (Eds.)
Institute of Mathematics CAS, Prague

EXCESSIVE EXTRAPOLATIONS OF EINSTEIN'S EQUATIONS

Michal Křížek[1], Lawrence Somer[2]

[1]Institute of Mathematics, Czech Academy of Sciences
Žitná 25, 115 67 Prague 1, Czech Republic
krizek@cesnet.cz
[2]Department of Mathematics, Catholic University of America
Washington, D.C. 20064, U.S.A.
somer@cua.edu

Cordially dedicated to Assoc. Prof. Jan Chleboun on his 60th birthday

Abstract: The standard cosmological model is surprisingly quite thoroughly investigated even though it possesses many paradoxes. We present several arguments indicating why excessive extrapolations of Einstein's equations to cosmological distances are questionable. First, we show how to express explicitly the first of Einstein's 10 partial differential equations to demonstrate their extremely large complexity. Therefore, it would be very difficult to find their solution for two or more bodies to model, e.g., the evolution of the Solar system. Further, we present some unexpected failures of the Schwarzschild and Friedmann solution of these equations. Then we explain why application of Einstein's equations to the whole universe represents incorrect extrapolations that lead to dark matter, dark energy, and several unrealistic situations. Finally, we give 10 further arguments showing why celebrated Einstein's equations do not describe reality well.

Keywords: Einstein's equations, Schwarzschild solution, Friedmann equation, modeling error, incorrect extrapolations, dark matter, dark energy

PACS: 4.20.-q, 95.35.+d, 98.80.-k

1. Introduction

Einstein's field equations of general relativity consist of 10 equations (cf. [13])

$$R_{\mu\nu} - \frac{1}{2}Rg_{\mu\nu} = \frac{8\pi G}{c^4}T_{\mu\nu}, \quad \mu,\nu = 0,1,2,3, \tag{1}$$

for 10 components of the unknown symmetric metric tensor $g_{\mu\nu}$ (sometimes called *gravitational potentials*) of one timelike coordinate $x^0 = ct$ and three Cartesian or curvilinear space coordinates x^1, x^2, x^3, i.e. $g_{\mu\nu} = g_{\mu\nu}(x^0, x^1, x^2, x^3)$ (for simplicity

the dependence of all functions from (1) on these coordinates will be nowhere indicated), where $c = 299\,792\,458$ m/s is the speed of light in vacuum, $G = 6.674 \cdot 10^{-11}$ $\mathrm{m^3 kg^{-1} s^{-2}}$ is the gravitational constant,

$$R_{\mu\nu} = \sum_{\varkappa=0}^{3} R^{\varkappa}{}_{\mu\varkappa\nu} \tag{2}$$

is the symmetric *Ricci tensor*,

$$R = \sum_{\mu,\nu=0}^{3} g^{\mu\nu} R_{\mu\nu} \tag{3}$$

is the *Ricci scalar* (i.e. the scalar curvature), $T_{\mu\nu}$ is the symmetric *tensor of density of energy and momentum*,

$$R^{\varkappa}{}_{\mu\sigma\nu} = \frac{\partial \Gamma^{\varkappa}{}_{\mu\nu}}{\partial x^{\sigma}} - \frac{\partial \Gamma^{\varkappa}{}_{\mu\sigma}}{\partial x^{\nu}} + \sum_{\lambda=0}^{3} \Gamma^{\lambda}{}_{\mu\nu}\Gamma^{\varkappa}{}_{\lambda\sigma} - \sum_{\lambda=0}^{3} \Gamma^{\lambda}{}_{\mu\sigma}\Gamma^{\varkappa}{}_{\lambda\nu}, \quad \varkappa,\, \mu,\, \sigma,\, \nu = 0,1,2,3, \tag{4}$$

is the *Riemann curvature tensor* that has 20 independent components from the total number of $4^4 = 256$ components due to several symmetries

$$R^{\varkappa}{}_{\mu\sigma\nu} + R^{\varkappa}{}_{\sigma\nu\mu} + R^{\varkappa}{}_{\nu\mu\sigma} = 0, \quad R_{\lambda\mu\sigma\nu} = -R_{\mu\lambda\sigma\nu} = -R_{\lambda\mu\nu\sigma}, \quad R_{\lambda\mu\sigma\nu} = \sum_{\varkappa} g_{\lambda\varkappa} R^{\varkappa}{}_{\mu\sigma\nu},$$

where the first equality is called the *first Bianchi identity* and

$$\Gamma^{\mu}{}_{\varkappa\sigma} = \frac{1}{2} \sum_{\nu=0}^{3} g^{\mu\nu} \Big(\frac{\partial g_{\varkappa\nu}}{\partial x^{\sigma}} + \frac{\partial g_{\sigma\nu}}{\partial x^{\varkappa}} - \frac{\partial g_{\varkappa\sigma}}{\partial x^{\nu}} \Big) = \frac{1}{2} \sum_{\nu=0}^{3} g^{\mu\nu} (g_{\varkappa\nu,\sigma} + g_{\sigma\nu,\varkappa} - g_{\varkappa\sigma,\nu}) \tag{5}$$

are the *Christoffel symbols of the second kind* (also called the *connection coefficients*). All derivatives are supposed to be classical (for simplicity we shall write $g_{\varkappa\nu,\sigma} := \partial g_{\varkappa\nu}/\partial x^{\sigma}$ to reduce notation). From this and the relation $g_{\varkappa\sigma} = g_{\sigma\varkappa}$ one can derive the symmetry

$$\Gamma^{\mu}{}_{\varkappa\sigma} = \Gamma^{\mu}{}_{\sigma\varkappa} \quad \text{for } \mu = 0,1,2,3.$$

Thus altogether we have $40 = 4 \times (1+2+3+4)$ independent components. Finally, the contravariant symmetric 4×4 metric tensor $g^{\mu\nu}$ is inverse to the covariant metric tensor $g_{\mu\nu}$, i.e.

$$g^{\mu\nu} = \frac{g^{*}_{\mu\nu}}{\det(g_{\mu\nu})}, \qquad \det(g_{\mu\nu}) := \sum_{\pi \in S_4} (-1)^{\operatorname{sgn}\pi} g_{0\nu_0} g_{1\nu_1} g_{2\nu_2} g_{3\nu_3}, \tag{6}$$

where the entries $g^{*}_{\mu\nu}$ form the 4×4 matrix of 3×3 algebraic adjoints of $g_{\mu\nu}$, S_4 is the symmetric group of 24 permutations π of indices $(\nu_0, \nu_1, \nu_2, \nu_3)$, $\operatorname{sgn}\pi = 0$ for an even permutation and $\operatorname{sgn}\pi = 1$ for an odd permutation.

Theorem 1. *If $g_{\mu\nu}$ is a solution of* (1)*, then* $(-g_{\mu\nu})$ *also solves* (1).

Proof. From (5), we find that the Christoffel symbols remain the same if we replace $g_{\mu\nu}$ by $(-g_{\mu\nu})$, namely,

$$\Gamma^{\mu}_{\varkappa\sigma} = \frac{1}{2}(-g^{\mu\nu})\Big(-\frac{\partial g_{\varkappa\nu}}{\partial x^{\sigma}} - \frac{\partial g_{\sigma\nu}}{\partial x^{\varkappa}} + \frac{\partial g_{\varkappa\sigma}}{\partial x^{\nu}}\Big).$$

Using (2) and (4), we find that the Ricci tensor $R_{\mu\nu}$ in (1) does not change as well. Concerning the second term on the left-hand side of (1), we observe from (3) that $\big(-\frac{1}{2}Rg_{\mu\nu}\big)$ also remains unchanged if we replace $g_{\mu\nu}$ by $(-g_{\mu\nu})$. □

2. On explicit form of the first Einstein equation

In this section we want to point out the extreme complexity of Einstein's equations. In (1), the dependence of the Ricci scalar R and the Ricci tensor $R_{\mu\nu}$ on the metric tensor $g_{\mu\nu}$ is not indicated. Therefore, Einstein's equations (1) seem to be quite simple. To avoid this deceptive opinion, we will now derive the explicit form of the first Einstein equation.

We will consider only the simplest case when $T_{\mu\nu} = 0$ (and without the cosmological constant, cf. (17)). Multiplying (1) by $g^{\mu\nu}$ and summing over all μ and ν, we obtain by (3) that

$$0 = \sum_{\mu,\nu=0}^{3} g^{\mu\nu}R_{\mu\nu} - \frac{1}{2}R\sum_{\mu,\nu=0}^{3} g^{\mu\nu}g_{\mu\nu} = R - \frac{1}{2}R\sum_{\mu=0}^{3}\delta^{\mu}_{\ \mu} = R - \frac{1}{2}4R,$$

where $\delta^{\mu}_{\ \nu}$ is the Kronecker delta. Thus, $R = 0$ and Einstein's vacuum equations can be rewritten as[1]

$$R_{\mu\nu} = 0.$$

Applying (2) and (4), we can express the first Einstein equation as follows

$$0 = R_{00} = \sum_{\varkappa=0}^{3} R^{\varkappa}_{\ 0\varkappa 0} = \sum_{\varkappa=0}^{3}\left(\Gamma^{\varkappa}_{\ 00,\varkappa} - \Gamma^{\varkappa}_{\ 0\varkappa,0} + \sum_{\lambda=0}^{3}(\Gamma^{\lambda}_{\ 00}\Gamma^{\varkappa}_{\ \lambda\varkappa} - \Gamma^{\lambda}_{\ 0\varkappa}\Gamma^{\varkappa}_{\ 0\lambda})\right)$$

$$\begin{aligned}
=&\underline{\Gamma^{0}_{\ 00,0}} + \Gamma^{1}_{\ 00,1} + \Gamma^{2}_{\ 00,2} + \Gamma^{3}_{\ 00,3} - \underline{\Gamma^{0}_{\ 00,0}} - \Gamma^{1}_{\ 01,0} - \Gamma^{2}_{\ 02,0} - \Gamma^{3}_{\ 03,0}\\
&+ \underline{\Gamma^{0}_{\ 00}}(\Gamma^{0}_{\ 00} + \Gamma^{1}_{\ 01} + \Gamma^{2}_{\ 02} + \Gamma^{3}_{\ 03}) + \underline{\underline{\Gamma^{1}_{\ 00}}}(\Gamma^{0}_{\ 10} + \Gamma^{1}_{\ 11} + \Gamma^{2}_{\ 12} + \Gamma^{3}_{\ 13})\\
&+ \underline{\underline{\Gamma^{2}_{\ 00}}}(\Gamma^{0}_{\ 20} + \Gamma^{1}_{\ 21} + \Gamma^{2}_{\ 22} + \Gamma^{3}_{\ 23}) + \underline{\Gamma^{3}_{\ 00}}(\Gamma^{0}_{\ 30} + \Gamma^{1}_{\ 31} + \Gamma^{2}_{\ 32} + \Gamma^{3}_{\ 33})\\
&- \underline{\Gamma^{0}_{\ 00}\Gamma^{0}_{\ 00}} - \Gamma^{0}_{\ 01}\Gamma^{1}_{\ 00} - \Gamma^{0}_{\ 02}\Gamma^{2}_{\ 00} - \Gamma^{0}_{\ 03}\Gamma^{3}_{\ 00} - \underline{\underline{\Gamma^{1}_{\ 00}\Gamma^{0}_{\ 01}}} - \Gamma^{1}_{\ 01}\Gamma^{1}_{\ 01}\\
&- \Gamma^{1}_{\ 02}\Gamma^{2}_{\ 01} - \Gamma^{1}_{\ 03}\Gamma^{3}_{\ 01}\\
&- \underline{\underline{\Gamma^{2}_{\ 00}\Gamma^{0}_{\ 02}}} - \Gamma^{2}_{\ 01}\Gamma^{1}_{\ 02} - \Gamma^{2}_{\ 02}\Gamma^{2}_{\ 02} - \Gamma^{2}_{\ 03}\Gamma^{3}_{\ 02} - \underline{\Gamma^{3}_{\ 00}\Gamma^{0}_{\ 03}} - \Gamma^{3}_{\ 01}\Gamma^{1}_{\ 03}\\
&- \Gamma^{3}_{\ 02}\Gamma^{2}_{\ 03} - \Gamma^{3}_{\ 03}\Gamma^{3}_{\ 03},
\end{aligned}$$

[1]Concerning nonuniqueness expressed by Theorem 1, we observe from (5) that we can add any constant to any component of $g_{\mu\nu}$ and Einstein's equations $R_{\mu\nu} = 0$ will still be valid.

where the underlined terms cancel. Hence, the first Einstein equation can be rewritten by means of the Christoffel symbols in the following way:

$$\begin{aligned}
0 =&\Gamma^1{}_{00,1} + \Gamma^2{}_{00,2} + \Gamma^3{}_{00,3} - \Gamma^1{}_{01,0} - \Gamma^2{}_{02,0} - \Gamma^3{}_{03,0} \\
&+ \Gamma^0{}_{00}(\Gamma^1{}_{01} + \Gamma^2{}_{02} + \Gamma^3{}_{03}) + \Gamma^1{}_{00}(-\Gamma^0{}_{10} + \Gamma^1{}_{11} + \Gamma^2{}_{12} + \Gamma^3{}_{13}) \\
&+ \Gamma^2{}_{00}(-\Gamma^0{}_{20} + \Gamma^1{}_{21} + \Gamma^2{}_{22} + \Gamma^3{}_{23}) + \Gamma^3{}_{00}(-\Gamma^0{}_{30} + \Gamma^1{}_{31} + \Gamma^2{}_{32} + \Gamma^3{}_{33}) \\
&- 2\Gamma^1{}_{02}\Gamma^2{}_{01} - 2\Gamma^1{}_{03}\Gamma^3{}_{01} - 2\Gamma^2{}_{03}\Gamma^3{}_{02} - (\Gamma^1{}_{01})^2 - (\Gamma^2{}_{02})^2 - (\Gamma^3{}_{03})^2. \qquad (7)
\end{aligned}$$

Using (5), we obtain

$$\begin{aligned}
2\Gamma^\mu{}_{\varkappa\sigma} =&g^{\mu 0}(g_{\varkappa 0,\sigma} + g_{\sigma 0,\varkappa} - g_{\varkappa\sigma,0}) + g^{\mu 1}(g_{\varkappa 1,\sigma} + g_{\sigma 1,\varkappa} - g_{\varkappa\sigma,1}) \\
&+ g^{\mu 2}(g_{\varkappa 2,\sigma} + g_{\sigma 2,\varkappa} - g_{\varkappa\sigma,2}) + g^{\mu 3}(g_{\varkappa 3,\sigma} + g_{\sigma 3,\varkappa} - g_{\varkappa\sigma,3})
\end{aligned}$$

and thus by (7) we can express the first Einstein equation $R_{00} = 0$ by means of the metric coefficients and their first and second order derivatives as follows:

$$\begin{aligned}
0 =&4R_{00} = 2[g^{10}_{,1} g_{00,0} + g^{11}_{,1}(2g_{01,0} - g_{00,1}) + g^{12}_{,1}(2g_{02,0} - g_{00,2}) + g^{13}_{,1}(2g_{03,0} - g_{00,3}) \qquad (8) \\
&+ g^{10} g_{00,01} + g^{11}(2g_{01,01} - g_{00,11}) + g^{12}(2g_{02,01} - g_{00,21}) + g^{13}(2g_{03,01} - g_{00,31}) \qquad (9) \\
&+ g^{20}_{,2} g_{00,0} + g^{21}_{,2}(2g_{01,0} - g_{00,1}) + g^{22}_{,2}(2g_{02,0} - g_{00,2}) + g^{23}_{,2}(2g_{03,0} - g_{00,3}) \\
&+ g^{20} g_{00,02} + g^{21}(2g_{01,02} - g_{00,12}) + g^{22}(2g_{02,02} - g_{00,22}) + g^{23}(2g_{03,02} - g_{00,32}) \\
&+ g^{30}_{,3} g_{00,0} + g^{31}_{,3}(2g_{01,0} - g_{00,1}) + g^{32}_{,3}(2g_{02,0} - g_{00,2}) + g^{33}_{,3}(2g_{03,0} - g_{00,3}) \\
&+ g^{30} g_{00,03} + g^{31}(2g_{01,03} - g_{00,13}) + g^{32}(2g_{02,03} - g_{00,23}) + g^{33}(2g_{03,03} - g_{00,33}) \\
&- g^{10}_{,0} g_{00,1} - g^{11}_{,0} g_{11,0} - g^{12}_{,0}(g_{02,1} + g_{12,0} - g_{01,2}) - g^{13}_{,0}(g_{03,1} + g_{13,0} - g_{01,3}) \\
&- g^{10} g_{00,10} - g^{11} g_{11,00} - g^{12}(g_{02,10} + g_{12,00} - g_{01,20}) - g^{13}(g_{03,10} + g_{13,00} - g_{01,30}) \\
&- g^{20}_{,0} g_{00,2} - g^{21}_{,0}(g_{01,2} + g_{21,0} - g_{02,1}) - g^{22}_{,0} g_{22,0} - g^{23}_{,0}(g_{03,2} + g_{23,0} - g_{02,3}) \\
&- g^{20} g_{00,20} - g^{21}(g_{01,20} + g_{21,00} - g_{02,10}) - g^{22} g_{22,00} - g^{23}(g_{03,20} + g_{23,00} - g_{02,30}) \\
&- g^{30}_{,0} g_{00,3} - g^{31}_{,0}(g_{01,3} + g_{31,0} - g_{03,1}) - g^{32}_{,0}(g_{02,3} + g_{32,0} - g_{03,2}) - g^{33}_{,0} g_{33,0} \\
&- g^{30} g_{00,30} - g^{31}(g_{01,30} + g_{31,00} - g_{03,10}) - g^{32}(g_{02,30} + g_{32,00} - g_{03,20}) - g^{33} g_{33,00}]
\end{aligned}$$

$$
\begin{aligned}
&+ (g^{00}g_{00,0} - g^{01}g_{00,1} - g^{02}g_{00,2} - g^{03}g_{00,3}) \\
&\times [g^{10}(2g_{10,1} - g_{11,0}) + g^{11}g_{11,1} + g^{12}(2g_{12,1} - g_{11,2}) + g^{13}(2g_{13,1} - g_{11,3}) \\
&+ g^{20}(g_{10,2} + g_{20,1} - g_{12,0}) + g^{21}g_{11,2} + g^{22}g_{22,1} + g^{23}(g_{13,2} + g_{23,1} - g_{12,3}) \\
&+ g^{30}(g_{10,3} + g_{30,1} - g_{13,0}) + g^{31}g_{11,3} + g^{32}(g_{12,3} + g_{32,1} - g_{13,2}) + g^{33}g_{33,1}]
\end{aligned}
$$

$$
\begin{aligned}
&+ (g^{10}g_{00,0} + g^{11}g_{11,1} - g^{12}g_{11,2} - g^{13}g_{11,3}) \\
&\times [-g^{00}g_{00,1} - g^{01}g_{11,0} - g^{02}(g_{12,0} + g_{02,1} - g_{10,2}) - g^{03}(g_{13,0} + g_{03,1} - g_{10,3}) \\
&+ g^{10}(2g_{10,1} - g_{11,0}) + g^{11}g_{11,1} + g^{12}(2g_{12,1} - g_{11,2}) + g^{13}(2g_{13,1} - g_{11,3}) \\
&+ g^{20}(g_{10,2} + g_{20,1} - g_{12,0}) + g^{21}g_{11,2} + g^{22}g_{22,1} + g^{23}(g_{13,2} + g_{23,1} - g_{12,3}) \\
&+ g^{30}(g_{10,3} + g_{30,1} - g_{13,0}) + g^{31}g_{11,3} + g^{32}(g_{12,3} + g_{32,1} - g_{13,2}) + g^{33}g_{33,1}]
\end{aligned}
$$

$$
\begin{aligned}
&+ [g^{20}g_{00,0} + g^{21}(2g_{01,0} - g_{00,1}) + g^{22}(2g_{02,0} - g_{00,2}) + g^{23}(2g_{03,0} - g_{00,3})] \\
&\times [-g^{00}g_{00,2} - g^{01}(g_{21,0} + g_{01,2} - g_{20,1}) - g^{02}g_{22,0} - g^{03}(g_{23,0} + g_{03,2} - g_{20,3}) \\
&+ g^{10}(g_{20,1} + g_{10,2} - g_{21,0}) + g^{11}g_{11,2} + g^{12}g_{22,1} + g^{13}(g_{23,1} + g_{13,2} - g_{21,3}) \\
&+ g^{20}(2g_{20,2} - g_{22,0}) + g^{21}(2g_{21,2} - g_{22,1}) + g^{22}g_{22,2} + g^{23}(2g_{23,2} - g_{22,3}) \\
&+ g^{30}(g_{20,3} + g_{30,2} - g_{23,0}) + g^{31}(g_{21,3} + g_{31,2} - g_{23,1}) + g^{32}g_{22,3} + g^{33}g_{33,2}]
\end{aligned}
$$

$$
\begin{aligned}
&+ [g^{30}g_{00,0} + g^{31}(2g_{01,0} - g_{00,1}) + g^{32}(2g_{02,0} - g_{00,2}) + g^{33}(2g_{03,0} - g_{00,3})] \\
&\times [-g^{00}g_{00,3} - g^{01}g_{01,3} - g^{02}(g_{32,0} + g_{02,3} - g_{30,2}) - g^{03}g_{33,0} \\
&+ g^{10}(g_{30,1} + g_{10,3} - g_{31,0}) + g^{11}g_{11,3} + g^{12}(g_{32,1} + g_{12,3} - g_{31,2}) + g^{13}g_{33,1} \\
&+ g^{20}(g_{30,2} + g_{20,3} - g_{32,0}) + g^{21}(g_{31,2} + g_{21,3} - g_{32,1}) + g^{22}g_{22,3} + g^{23}g_{33,2} \\
&+ g^{30}(2g_{30,3} - g_{33,0}) + g^{31}(2g_{31,3} - g_{33,1}) + g^{32}(2g_{32,3} - g_{33,2}) + g^{33}g_{33,3}]
\end{aligned}
$$

$$
\begin{aligned}
&- 2[g^{10}g_{00,2} + g^{11}(g_{01,2} + g_{21,0} - g_{02,1}) + g^{12}g_{22,0} + g^{13}(g_{03,2} + g_{23,0} - g_{02,3})] \\
&\times [g^{20}g_{00,1} + g^{21}g_{11,0} + g^{22}(g_{02,1} + g_{12,0} - g_{01,2}) + g^{23}(g_{03,1} + g_{13,0} - g_{01,3})]
\end{aligned}
$$

$$
\begin{aligned}
&- 2[g^{10}g_{00,3} + g^{11}(g_{01,3} + g_{31,0} - g_{03,1}) + g^{12}(g_{02,3} + g_{32,0} - g_{03,2}) + g^{13}g_{33,0}] \\
&\times [g^{30}g_{00,1} + g^{31}g_{11,0} + g^{32}(g_{02,1} + g_{12,0} - g_{01,2}) + g^{33}(g_{03,1} + g_{13,0} - g_{01,3})]
\end{aligned}
$$

$$
\begin{aligned}
&- 2[g^{20}g_{00,3} + g^{21}(g_{01,3} + g_{31,0} - g_{03,1}) + g^{22}(g_{02,3} + g_{32,0} - g_{03,2}) + g^{23}g_{33,0}] \\
&\times [g^{30}g_{00,2} + g^{31}(g_{01,2} + g_{21,0} - g_{02,1}) + g^{32}g_{22,0} + g^{33}(g_{03,2} + g_{23,0} - g_{02,3})]
\end{aligned}
$$

$$
\begin{aligned}
&- [g^{10}g_{00,1} + g^{11}g_{11,0} + g^{12}(g_{02,1} + g_{12,0} - g_{01,2}) + g^{13}(g_{03,1} + g_{13,0} - g_{01,3})]^2 \\
&- [g^{20}g_{00,2} + g^{21}(g_{01,2} + g_{21,0} - g_{02,1}) + g^{22}g_{22,0} + g^{23}(g_{03,2} + g_{23,0} - g_{02,3})]^2
\end{aligned}
$$

$$- [g^{30}g_{00,3} + g^{31}(g_{01,3} + g_{31,0} - g_{03,1}) + g^{32}(g_{02,3} + g_{32,0} - g_{03,2}) + g^{33}g_{33,0}]^2. \quad (10)$$

Now we should substitute (6) to all entries with double upper indices to (10). For instance, the entry g^{11} in line (9) could be rewritten by means of the Sarrus rule for 3×3 symmetric matrices g^*_{11} by

$$\begin{aligned} g^{11} =& \frac{g^*_{11}}{\det(g_{\mu\nu})} \\ =& \frac{g_{00}g_{22}g_{33} + 2g_{02}g_{03}g_{23} - g_{00}(g_{23})^2 - g_{22}(g_{03})^2 - g_{33}(g_{02})^2}{\sum_{\pi\in S_4}(-1)^{\operatorname{sgn}\pi} g_{0\nu_0}g_{1\nu_1}g_{2\nu_2}g_{3\nu_3}}, \end{aligned} \quad (11)$$

where the sum in the denominator contains $4! = 24$ terms. Note that the optimal expression for the minimum number of arithmetic operations to calculate the inverse of a 4×4 matrix is not known, yet. The other nine entries g^{00}, g^{01}, g^{02}, g^{03}, g^{12}, g^{13}, g^{22}, g^{23}, and g^{33} can be expressed similarly.

However, we have to evaluate also the first derivatives of $g^{\mu\nu}$. Consider for instance the entry $g^{11}_{,1}$ in line (8). Then by (11) we get

$$\begin{aligned} g^{11}_{,1} =& \frac{\partial}{\partial x_1}\Big(\frac{g^*_{11}}{\det(g_{\mu\nu})}\Big) \\ =& \Big(\frac{1}{\sum_{\pi\in S_4}(-1)^{\operatorname{sgn}\pi} g_{0\nu_0}g_{1\nu_1}g_{2\nu_2}g_{3\nu_3}} \\ & \qquad \times (g_{00}g_{22}g_{33} + 2g_{02}g_{03}g_{23} - g_{00}(g_{23})^2 - g_{22}(g_{03})^2 - g_{33}(g_{02})^2)\Big)_{,1} \\ =& \Big[\big(g_{00,1}g_{22}g_{33} + 2g_{02,1}g_{03}g_{23} - g_{00,1}(g_{23})^2 - g_{22,1}(g_{03})^2 - g_{33,1}(g_{02})^2 + g_{00}g_{22,1}g_{33} \\ & + 2g_{02}g_{03,1}g_{23} + g_{00}g_{22}g_{33,1} + 2g_{02}g_{03}g_{23,1} - 2g_{00}g_{23,1} - 2g_{22}g_{03,1} - 2g_{33}g_{02,1}\big) \\ & \times \Big(\sum_{\pi\in S_4}(-1)^{\operatorname{sgn}\pi} g_{0\nu_0}g_{1\nu_1}g_{2\nu_2}g_{3\nu_3}\Big) \\ & - \big(g_{00}g_{22}g_{33} + 2g_{02}g_{03}g_{23} - g_{00}(g_{23})^2 - g_{22}(g_{03})^2 - g_{33}(g_{02})^2\big) \\ & \times \sum_{\pi\in S_4}(-1)^{\operatorname{sgn}\pi}(g_{0\nu_0,1}g_{1\nu_1}g_{2\nu_2}g_{3\nu_3} + g_{0\nu_0}g_{1\nu_1,1}g_{2\nu_2}g_{3\nu_3} + g_{0\nu_0}g_{1\nu_1}g_{2\nu_2,1}g_{3\nu_3} \\ & + g_{0\nu_0}g_{1\nu_1}g_{2\nu_2}g_{3\nu_3,1})\Big]\Big(\sum_{\pi\in S_4}(-1)^{\operatorname{sgn}\pi} g_{0\nu_0}g_{1\nu_1}g_{2\nu_2}g_{3\nu_3}\Big)^{-2}. \end{aligned} \quad (12)$$

Substituting all $g^{\mu\nu}$ and also its first derivatives into (10), we get the explicit form of the first Einstein equation $R_{00} = 0$ of the second order for 10 unknowns g_{00}, g_{01}, $g_{02}, \ldots, g_{33}$. It is evident that such an equation is extremely complicated. Relation (8) takes only 4 lines, relation (10) takes 40 lines and after substitution of determinants into (10) the equation $R_{00} = 0$ takes several pages. The other nine equations $R_{\mu\nu} = 0$ can be expressed similarly. Therefore, the explicit form of all 10 Einstein equations will occupy a huge amount of pages. **This fact prevents**

us to verify whether Einstein's equations describe, for instance, the Solar system better than Newtonian mechanics by N-body simulations.

For comparison note that the Laplace equation $\Delta u = 0$ has only three terms $\partial^2 u/\partial x_i^2$ on its left-hand side, $i = 1, 2, 3$, and the famous Navier-Stokes equations 24 terms.

3. Non-differentiability of the Schwarzschild composite solution

In 1915, Karl Schwarzschild wrote to Albert Einstein that he has found a solution [47] for the case $T_{\mu\nu} = 0$ (for the English translation of Schwarzschild's original letter by R. A. Rydin see [12]). It can be written as the following diagonal tensor

$$g_{\mu\mu} = \operatorname{diag}\Big(-\frac{r-S}{r}, \frac{r}{r-S}, r^2\sin^2\theta, r^2\Big), \tag{13}$$

$g_{\mu\nu} = 0$ for $\mu \neq \nu$, where $r > S$, the constant S is given by (14) below, (r, φ, θ) are the standard spherical coordinates, $\varphi \in [0, 2\pi)$, $\theta \in [0, \pi]$, i.e.,

$$\begin{aligned} x^1 &= r\sin\theta\cos\varphi, \\ x^2 &= r\sin\theta\sin\varphi, \\ x^3 &= r\cos\theta. \end{aligned}$$

Schwarzschild assumed that the gravitational field has the following properties: it is static (meaning that it does not change over time), it is spherically symmetric, the spacetime is empty, and the spacetime is asymptotically flat. For a fixed nonrotating ball in vacuum with mass $M > 0$ and with a spherically symmetric mass distribution we set

$$S = \frac{2MG}{c^2} \tag{14}$$

which is called the *Schwarzschild gravitational radius* and (13) is called the *exterior Schwarzschild metric*.

In 1916 Karl Schwarzschild (see [48]) found the first nonvacuum solution[2] of Einstein's equations (1). He assumed that the ball with coordinate radius $r_0 > 0$ is formed by an ideal incompressible non-rotating fluid with constant density to avoid a possible internal mechanical stress that may have a non-negligible influence on the resulting gravitational field. He also assumed zero pressure at the surface. Then the corresponding metric is (see e.g. [15], [16, p. 529], [49, p. 213], [53])

$$g_{\mu\mu} = \operatorname{diag}\bigg(-\frac{1}{4}\bigg(3\sqrt{1-\frac{S}{r_0}} - \sqrt{1-\frac{Sr^2}{r_0^3}}\bigg)^2, \frac{r_0^3}{r_0^3 - Sr^2}, r^2\sin^2\theta, r^2\bigg), \tag{15}$$

[2]The Schwarzschild solution is static. On the other hand, the well-known Kerr metric [39, p. 878] is stationary, which means that there exists a coordinate system where we can express the metric tensor independent of the time coordinate. Every static solution is stationary, but not vice versa.

where $r \in [0, r_0]$, S is given by (14), and we assume that $r_0 > S$. The corresponding metric tensor is called the *interior Schwarzschild solution*. It is again a static solution and the corresponding right-hand side $T_{\mu\nu}$ is also a diagonal tensor for which $T_{00} = 0$, since it does not change over time.

Using (13) and (15), we can easily verify that the exterior and interior metric have the same values for $r = r_0$, i.e., each component $g_{\mu\mu} = g_{\mu\mu}(r)$ is a continuous function on $[0, \infty)$ for $\mu = 0, 1, 2, 3$. However, the first derivatives of g_{11} of the exterior and interior Schwarzschild solution do not match (see Figure 1), since they have a jump on the common boundary $r = r_0$. Note that the 2nd order Einstein equations contain classical derivatives of $g_{\mu\nu}$ which are supposed to be continuous in definition (5). Therefore, the corresponding space manifold described by the Riemann curvature tensor is not differentiable, since the tangent hyperplane for $r = r_0$ cannot be uniquely defined. All Riemannian manifolds must be locally flat which is not true in this particular case (see also [26]).

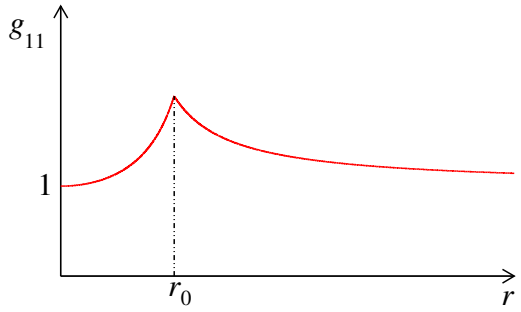

Figure 1: The behavior of the non-differentiable component $g_{11} = g_{11}(r)$ of the metric tensor from (13) and (15). The first derivative $(\partial g_{11}/\partial r)(r_0)$ is not defined. The piecewise rational function g_{11} cannot be smoothed near r_0, since then Einstein's equations (1) would not be valid in a close neighborhood of r_0.

From (13) we observe that the one-sided limit of the derivative of the component $g_{11}(r) = r/(r - S)$ of the exterior solution is negative

$$\lim_{r \to r_0^+} \frac{\partial g_{11}}{\partial r}(r) < 0,$$

whereas the component $g_{11}(r)$ of the interior solution (15) is an increasing function on $[0, r_0]$ (cf. Figure 1). It is increasing even for a variable spherically symmetric density $\rho = \rho(r)$, see [8, 39]. Consequently, the Schwarzschild solution cannot be used inside the ball with radius $r_1 > r_0$ to model our Sun or any other star with radius r_0 together with its spherically symmetric vacuum neighborhood (see Figure 2 and (5)). This is a serious drawback, since the composite metric tensor (13)+(15) is not differentiable for $r = r_0$. Consequently, (13) and (15) are only local solutions and together they do not form a global solution in the ball with radius r_1.

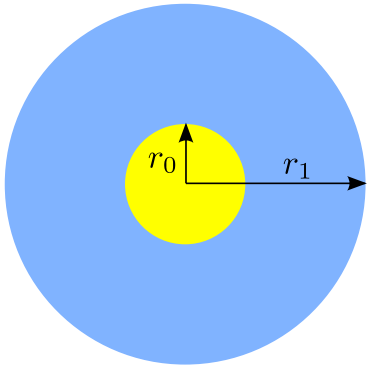

Figure 2: Spherical shell $\{(x,y,z) \in \mathbb{E}^3 \,|\, r_0^2 \le x^2+y^2+z^2 \le r_1^2\}$ is the region between two concentric spheres.

Similarly, the function $u(x) = |x|$ is a local classical solution of the second order ordinary differential equation $u'' = 0$ on the intervals $[-1,0]$ and $[0,1]$, but it is not a global solution over the interval $[-1,1]$. It is not even a weak solution there.

Example 1. For comparison, we also note that the first order classical derivatives of the Newton potential u for the situation sketched in Figure 2 are continuous. It is described by the Poisson equation

$$\Delta u = 4\pi G\rho,$$

where ρ is the mass density. Let the right-hand $f = 4\pi G\rho$ side be spherically symmetric and such that $f(r) = 1$ for $r \in [0,1]$ and $f(r) = 0$ otherwise. The Laplace operator in spherical coordinates reads (see [44, Sect. 7.2])

$$\Delta u = \frac{\partial^2 u}{\partial r^2} + \frac{2}{r}\frac{\partial u}{\partial r} + \frac{1}{r^2}\Big(\frac{\partial^2 u}{\partial \theta^2} + \operatorname{cotan}\theta \frac{\partial u}{\partial \theta} + \frac{1}{\sin^2\theta}\frac{\partial^2 u}{\partial \varphi^2}\Big).$$

The sum in parenthesis on the right-hand side is zero for the spherically symmetric case. By the well-known method of variations of constants, we find the following solution of the above Poisson equation

$$u(r,\varphi,\theta) = \frac{1}{6}r^2 - \frac{1}{2} \quad \text{for } r \in [0,1],$$

$$u(r,\varphi,\theta) = -\frac{1}{3r} \quad \text{otherwise.}$$

Hence, both u and $\partial u/\partial r$ are continuous at $r_0 = 1$. □

Finally, let us emphasize that the covariant divergence of the right-hand side of (1) has to be zero, see (30) and [39, p. 146]. Therefore, the covariant divergence of the left-hand side of (1) is zero, too. However, this requires the existence of the third order derivatives of the metric tensor $g_{\mu\nu}$ at r_0.

4. Another unexpected property of the Schwarzschild solution

For positive numbers $r_0 < r_1$ consider a spherical shell with interior radius r_0 and exterior radius r_1 (see Figure 2). Its volume in the Euclidean space $\mathbb{E}^3$ is clearly given by

$$V = \frac{4}{3}\pi(r_1^3 - r_0^3). \tag{16}$$

Now we will derive a formula for the proper volume $\tilde{V}$ of the spherical shell with coordinate radii $r_0 < r_1$ in a curved space around the mass ball with coordinate radius r_0. Here the tilde indicates a curved space. By (13) we find that the exterior spatial volume element is equal to

$$\mathrm{d}\widetilde{V} = \sqrt{\frac{r}{r-S}}\,\mathrm{d}r \cdot (r\sin\theta\,\mathrm{d}\varphi) \cdot (r\,\mathrm{d}\theta).$$

Therefore, the *proper (relativistic) volume* is defined as

$$\widetilde{V} = \int_{r_0}^{r_1} r^2\sqrt{\frac{r}{r-S}}\,\mathrm{d}r \cdot \int_0^{\pi}\Big(\int_0^{2\pi}\sin\theta\,\mathrm{d}\varphi\Big)\mathrm{d}\theta = 4\pi\int_{r_0}^{r_1} r^2\sqrt{\frac{r}{r-S}}\,\mathrm{d}r. \tag{17}$$

Theorem 2. *If $M > 0$ and $r_0 > S$ are any fixed numbers satisfying* (14)*, then*

$$\widetilde{V} - V \to \infty \quad \text{as } r_1 \to \infty.$$

Proof. By differentiation, we can easily check that

$$\int r^2\sqrt{\frac{r}{r-S}}\,\mathrm{d}r = \Big(\frac{r^2}{3} + \frac{5Sr}{12} + \frac{5S^2}{8}\Big)\sqrt{r(r-S)} + \frac{5S^3}{16}\ln(2\sqrt{r(r-S)} + 2r - S).$$

From this, (17), and (16) we get

$$\begin{aligned}
\widetilde{V} - V =& 4\pi\int_{r_0}^{r_1} r^2\sqrt{\frac{r}{r-S}}\,\mathrm{d}r - \frac{4}{3}\pi(r_1^3 - r_0^3)\\
=& \frac{4\pi}{3}\Big[\Big(r_1^2 + \frac{5Sr_1}{4} + \frac{15S^2}{8}\Big)\sqrt{r_1(r_1-S)} + \frac{15S^3}{16}\ln(2\sqrt{r_1(r_1-S)} + 2r_1 - S)\\
&- \Big(r_0^2 + \frac{5Sr_0}{4} + \frac{15S^2}{8}\Big)\sqrt{r_0(r_0-S)} - \frac{15S^3}{16}\ln(2\sqrt{r_0(r_0-S)} + 2r_0 - S)\\
&- r_1^3 + r_0^3\Big].
\end{aligned} \tag{18}$$

Since

$$r_1 > r_0 > S$$

and since the logarithmic function is increasing, the difference of the two terms containing ln in (18) is positive.[3] Thus from the inequality

$$\sqrt{r_1(r_1 - S)} > r_1 - S$$

we obtain the following lower bound

$$\widetilde{V} - V > \Big(r_1^2 + \frac{5Sr_1}{4} + \frac{15S^2}{8}\Big)(r_1 - S) - r_1^3 + C = \frac{Sr_1^2}{4} + \frac{5S^2r_1}{8} + \overline{C},$$

where C contains all remaining terms not depending on r_1 and where $\overline{C} = C - 15S^3/8$. Letting $r_1 \to \infty$, we obtain the statement of the theorem. □

We observe that the difference of volumes $\tilde{V} - V$ increases over all limits for $r_1 \to \infty$, which is a quite surprising property. Namely, Theorem 2 can be applied for instance to a billiard ball or a small steel ball bearing (see Example 2 below) or an imperceptible pinhead, since the mass $M > 0$ can be arbitrarily small. Consequently, a natural question arises: How large can r_1 be so that the relativistic relation (17) approximates reality well.

Example 2. Setting $M = 0.033$ kg, $r_0 = 0.01$ m, and $r_1 = 5 \cdot 10^{20}$ m, which is the radius of our Galaxy, we find that $S = 5 \cdot 10^{-29}$ m and by (18) the difference

$$\widetilde{V} - V \approx 10\,000 \text{ km}^3.$$

This is about 10^{19} times more than the volume of the ball itself. From this we see that the use of Einstein's equations to galactic distances is questionable. Further drawbacks of the Schwarzschild metric are surveyed in [20]. □

5. Division by zero in the Friedmann normalized equation

Einstein's equations (1) were derived for a local description of the universe. They were "tested" in a neighborhood of the Sun [12, 24, 39]. However, in 1917 Einstein applied his equations to the whole universe [14]. At that time he did not know what is its real size. Now we know that the size of the observable universe is at least 10^{15} astronomical units.

We will show that these excessive extrapolations by many orders of magnitude may lead to a division by zero in Einstein's equations. To avoid a gravitational collapse of the whole universe Einstein introduced a new form of his equations (see [14])

$$R_{\mu\nu} - \frac{1}{2}Rg_{\mu\nu} + \Lambda g_{\mu\nu} = \frac{8\pi G}{c^4}T_{\mu\nu} \tag{19}$$

with non-zero cosmological constant Λ.

[3] The argument in parenthesis after ln is dimensionless, because $\ln a - \ln b = \ln(a/b)$.

At present there are thousands of papers on the cosmological constant Λ. However, for the time being, we do not know any of its significant digit (nor even its sign). The standard cosmological model (see [42]) assumes that

$$\Lambda \approx 10^{-52}\ \mathrm{m}^{-2}. \tag{20}$$

Einstein's equations were not developed for a dynamical evolution of the universe. This was done later in 1922 by Alexander Friedmann [18, 19] who derived from the first Einstein equation the following ordinary differential equation for the *expansion function* $a = a(t)$

$$\dot{a}^2 = \frac{8\pi G\rho a^2}{3} + \frac{\Lambda c^2 a^2}{3} - kc^2, \tag{21}$$

where the dot denotes the time derivative, $k \in \{-1, 0, 1\}$ is the curvature index, and $\rho = \rho(t) > 0$ is the mean mass density. At present it is assumed that (21) should be considered only for $t > \tau$, where

$$\tau \approx 380\,000\ \mathrm{yr}$$

is the time of decoupling of the cosmic microwave background radiation (CMB). Note that Friedmann derived (21) exactly from (19) without any approximations, i.e., (21) is a direct mathematical consequence of Einstein's equations for a homogeneous and isotropic universe which is described by a maximally symmetric manifold for $k \in \{-1, 0, 1\}$. In particular, it is a consequence only of the first Einstein equation (8)–(12) enriched by the cosmological constant (see [30] for a detailed proof),

$$\boxed{\text{Einstein's equations } + \text{ maximum symmetry } \Longrightarrow \text{ Friedmann equation.}} \tag{22}$$

We shall suppose that

$$\dot{a}(\tau) > 0, \tag{23}$$

since the universe was expanding at time τ. Furthermore, assume that $\dot{a}(t) \neq 0$ for all $t > \tau$ and divide equation (21) by $\dot{a}^2$. Then the Friedmann equation reads

$$\Omega_{\mathrm{M}}(t) + \Omega_{\Lambda}(t) + \Omega_k(t) = 1 \quad \text{for all } t > \tau, \tag{24}$$

where

$$\Omega_{\mathrm{M}}(t) = \frac{8\pi G\rho(t)}{3H^2(t)} > 0, \quad \Omega_{\Lambda}(t) = \frac{\Lambda c^2}{3H^2(t)}, \quad \text{and} \quad \Omega_k(t) = -\frac{kc^2}{a^2(t)H^2(t)}, \tag{25}$$

are normalized cosmological parameters called (see [41, p. 58], [43, p. 37]) the *density of dark and baryonic matter, density of dark (or vaccum) energy,* and the *curvature parameter*, respectively, and

$$H(t) = \frac{\dot{a}(t)}{a(t)} \tag{26}$$

is the *Hubble-Lemaître parameter*. Note that (24) is really a differential equation, since the derivative $\dot{a}$ is hidden in the Hubble-Lemaître parameter.

In the literature on cosmology, the division of (21) by the square $\dot{a}^2 \geq 0$ is usually done without any preliminary warning that we may possibly divide by zero which may lead to various paradoxes. For instance, we see by (25) and (26) that

$$\dot{a}(t) \to 0 \quad \Longrightarrow \quad \Omega_{\mathrm{M}}(t) \to \infty \quad \text{and} \quad \Omega_{\Lambda}(t) \to \pm\infty \quad \text{for} \quad \Lambda \neq 0, \tag{27}$$

corresponding e.g. to an oscillating (cyclic) universe, or a loitering universe or a bouncing universe by de Sitter with $\rho \equiv 0$ and $\Lambda > 0$, see Figure 3,

$$a(t) = \frac{1}{\alpha}\cosh(\alpha c t) \quad \text{for } \alpha = \sqrt{\frac{\Lambda}{3}}.$$

In the last case the Friedmann equation (21) is satisfied for $k = 1$, namely,

$$(\dot{a}(t))^2 = c^2\sinh^2(\alpha c t) = c^2\cosh^2(\alpha c t) - c^2 = c^2\alpha^2 a^2(t) - c^2 = \frac{\Lambda c^2}{3}a^2(t) - kc^2$$

and we have $\dot{a}(0) = 0$. Note that de Sitter solution does not describe reality well due to the unrealistic assumption $\rho \equiv 0$.

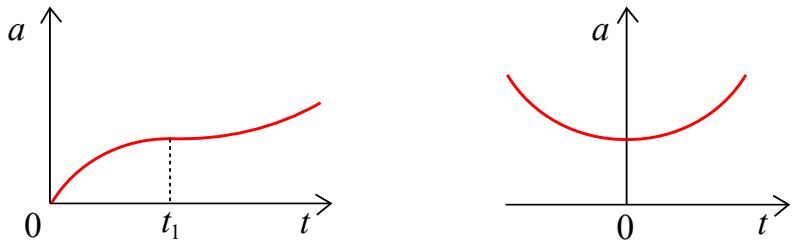

Figure 3: Graph of the expansion function $a = a(t)$ for 1) a loitering universe for which there exists $t_1 > 0$ such that $\dot{a}(t_1) = 0$, amd for 2) a bouncing universe.

The Einstein static solution (see Figure 4)

$$a(t) \equiv \Lambda^{-1/2}$$

with $\Lambda > 0$ satisfies $\dot{a} \equiv 0$ which leads to division by zero in (25), too. The Friedmann equation (21) is satisfied again for $k = 1$ and $\rho = \Lambda c^2/(4\pi G)$, namely,

$$0 \equiv \dot{a}^2 = \frac{8\pi G}{3}\rho a^2 + \frac{\Lambda c^2}{3}a^2 - c^2 = \frac{8\pi G}{3}\frac{\Lambda c^2}{4\pi G}\frac{1}{\Lambda} + \frac{\Lambda c^2}{3}\frac{1}{\Lambda} - c^2 = 0.$$

However, the Einstein static solution also does not describe reality well, since the universe is expanding and the condition (23) does not hold. Moreover, this solution is unstable [6, 9, 14, 35], i.e., small fluctuations can make it either expand or contract (cf. Figure 3 for $a(t_1) = \Lambda^{-1/2}$).

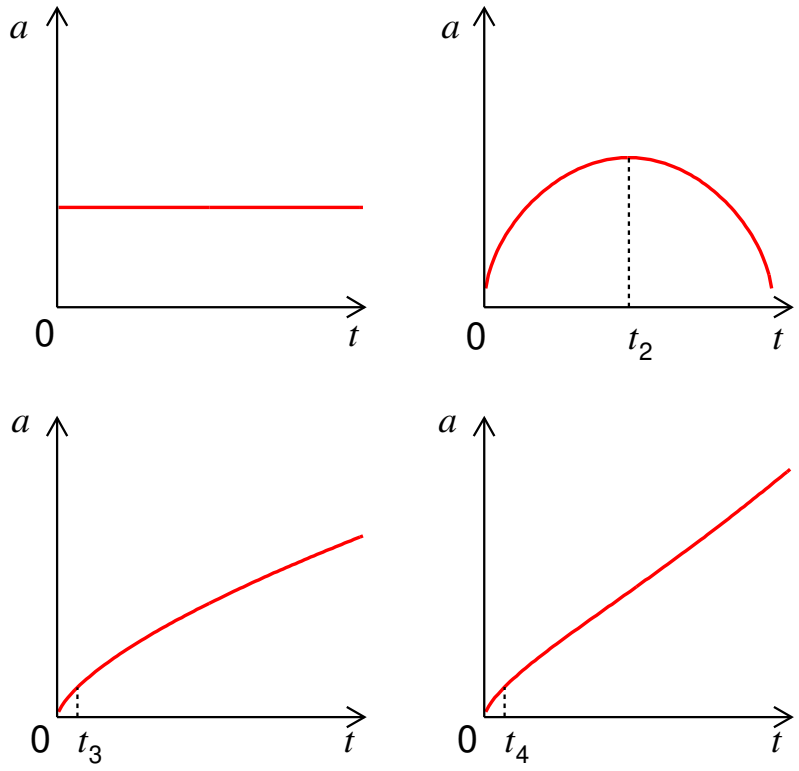

Figure 4: The expansion function for 1) the Einstein static universe, 2) the cyclic universe (the expansion stops at some time $t_2 > 0$ and then starts to shrink), 3) the universe with zero cosmological constant, and for 4) the currently proposed expansion of the universe with a positive cosmological constant. Here $t_4 = \tau$ denotes the time instant of the origin of the cosmic microwave background radiation.

Is there really an infinite density of dark matter and dark energy, when $a = a(t)$ reaches its extremal values? The true density of baryonic matter is surely finite. For an oscillating universe (see the upper right of Figure 4), when the density of dark energy reaches an infinite value (27), the universe starts to shrink. This is a quite paradoxical result, see [30, p. 169].

The behavior of the curvature parameter is also strange. Applying (26), we see that $\Omega_k(t) = -kc^2/\dot{a}^2(t)$, i.e., $\Omega_k(t) \approx 0$ when the universe has originated (cf. Figure 4).

In [26] we show that division by zero in (25) may appear for Λ negative, vanishing, and also positive. If $\Lambda < 0$, we always divide by zero in (25).

In the model with $\Lambda = 0$ we again divide by zero in (25) if $k = 1$ and $\rho = \rho(t)$ is larger than the so-called critical density $\rho_{\text{crit}}(t) = 3H^2(t)/(8\pi G)$. For $k = -1$ the expansion function is strictly convex and increasing for $t > t_3 > 0$ (see the bottom left part of Figure 4).

If $\Lambda > 0$ then the division by zero in (25) may appear for $k = 1$. Otherwise the expansion function satisfying (23) changes from strictly concave to strictly convex on the interval (9,14) Gyr (see the bottom right part of Figure 4).

6. Incorrect extrapolations lead to dark matter and dark energy

By the scientific results of the Planck satellite [43], our universe is composed of about 68 % of some mysterious dark energy (i.e., the present value $\Omega_\Lambda = 0.68$ in (25)), 27 % of some exotic dark matter, and less than 5 % of ordinary baryonic matter. In truth, it is more likely that the measured data just indicate that the extrapolation is wrong, since it requires one to introduce some hypothetical dark matter and dark energy.[4]

The above cosmological parameters were obtained by the three seemingly independent methods of Baryonic Acoustic Oscillations (BAO), Cosmic Microwave Background Radiation[5] (CMB), and Supernovae type Ia explosions (SNe). However, these methods are not independent, since they are all based on the same normalized Friedmann equation (24).

According to the standard cosmological model [43], our universe contains more dark matter than ordinary baryonic matter and

$$\text{the ratio of masses of dark matter to baryonic matter} \approx \mathbf{6} : \mathbf{1}. \tag{28}$$

In [25] we present ten arguments showing that this proclaimed amount of dark matter is highly overestimated. The ratio (28) was again obtained from the standard ΛCDM cosmological model which is based on excessive extrapolations [32]. For instance, most of the observed galaxies have spiral structure. If these galaxies would contain six times more uniformly distributed nonbaryonic matter than baryonic matter, then they could not exhibit such a high symmetry of structured baryonic matter. Moreover, their disks would be more thicker due to dark matter halos.

In [28] we suggest that nonbaryonic dark matter need not be taken into account to explain the observed rapid rotation of spiral galaxies. The main reason is a special form of the gravitational potential of a flat disk which guarantees large orbital velocities of stars at the galaxy edge. In particular, we proved that a star orbiting a central mass point along a circular trajectory of radius R has a smaller speed than if it were to orbit a flat disk of radius R and the same mass with an arbitrary rotationally symmetric density distribution, see also [25, 33, 52].

At the end of the 20th century (when Perlmutter et al. published their famous paper [42]) it was thought that red dwarfs of the spectral class M form only 3 % of the total number of stars, see [5, p. 93]. Nevertheless, the Gaia satellite estimated that

[4] There are hundreds of popularization books on dark matter and dark energy, since people like mysteries. This trend is difficult to stop, since almost nobody would buy a book stating that there is no dark matter and dark energy.

[5] For a trustworthy criticism of this method we refer to [50].

red dwarfs are in the vast majority — about 75 %. This large proportion essentially contributes to invisible baryonic matter.

The density of dark and baryonic matter is defined by means of the Friedmann equation by (25), i.e. via Einstein's equation, cf. (22). However, sometimes Newton laws are used to describe dynamic manifestations of galaxy clusters. Einstein's equations should thus not be substituted by Newtonian mechanics to "prove" the existence of dark matter.

For the luminosity distance of supernovae type Ia explosions, Perlmutter et al. [42, p. 566] used a formula which was derived from the Friedmann equation. This distance thus essentially depends on the fact whether Einstein's equations on cosmological distances sufficiently well approximate reality, since the Friedmann equation (21) is a mathematical consequence of (19) for a homogeneous and isotropic universe, see (22).

If this approximation is poor, the luminosity distances are not correct. Moreover, the method SNe treats type Ia supernovae as standard candles. However, they cannot be considered in this way due to a possible large extinction of light from the supernova [51]. This essentially depends on its location in the host galaxy, if it is at its edge or in the middle completely surrounded by galactic gas and dust. It also depends on the direction of the supernova rotational axis. In this way we may receive several orders of magnitude weaker light.

Further, let us introduce the dimensionless *deceleration parameter*

$$q := -\frac{\ddot{a}a}{\dot{a}^2} = -\frac{\ddot{a}}{a}H^{-2} = -\dot{H}H^{-2} - 1,$$

where the second equality follows directly from (26). From this we see that the deceleration parameter $q_0 = q(t_0)$ at the present time t_0 appears at the quadratic term in the Taylor expansion (see e.g. [39, p. 781], [44, p. 652])

$$\begin{aligned} a(t) &= a(t_0) + \dot{a}(t_0)(t-t_0) + \frac{1}{2}\ddot{a}(t_0)(t-t_0)^2 + \dots \\ &= a(t_0)\Big(1 + H_0(t-t_0) - \frac{1}{2}q_0H_0^2(t-t_0)^2 + \dots\Big), \end{aligned} \tag{29}$$

where $H_0 = H(t_0)$ is the present value of $H(t)$ called the *Hubble constant*. In the paper [45, p. 110], a negative value of the parameter

$$q_0 \approx -0.6$$

was found, i.e., a is strictly convex in a neighborhood of t_0 and the expansion of the universe accelerates (see the last graph in Figure 4). Using (29), we observe that the linear term is much larger than the quadratic term for t close to t_0, namely,

$$|H_0(t-t_0)| \gg \frac{1}{2}|q_0|H_0^2(t-t_0)^2 = \frac{1}{2}|q_0|\frac{\Lambda c^2}{3\Omega_\Lambda(t_0)}(t-t_0)^2,$$

where the last equality is due to (25). The single quadratic term is so small that the linear term in (29) essentially dominates not only in a close neighborhood of t_0, but also for the other $t < t_0$,

$$0.3|H_0(t-t_0)| > \frac{1}{2}|q_0|H_0^2(t-t_0)^2,$$

where $\frac{1}{2}|q_0| = 0.3$.

7. Further counter-arguments

We shall present 10 further counter-arguments showing that Einstein's equations do not describe reality well, especially on cosmological distances.

7.1. Problems with initial and boundary conditions

It is generally impossible to prescribe explicitly any appropriate initial and boundary conditions for non-spherically symmetric regions (e.g. on a cube) for $g_{\mu\nu}$ which satisfies (1) or (19). The reason is that spacetime tells matter how to move and matter tells spacetime how to curve [39]. So the initial space manifold is a priori not known for nontrivial cases. Thus we have serious problems to prove the uniqueness and also the existence of the solution of Einstein's equations and compare it with reality. Furthermore, suitable function spaces, where we look for the true solution, are usually not specified in the literature.

Let us also point out that Einstein's equations are fully deterministic whereas the universe (with its biological systems) does not operate solely gravitationally due to quantum phenomena. Their effects can be observed not only on microscopic scales. For instance, in our brain we can decide to change the trajectory of an asteroid in arbitrary direction by the famous kinetic impactor method. Hence, the evolution of the real world is very unstable with respect to initial conditions including our decision. Imperceptible quantum fluctuations may thus cause large changes of trajectories of celestial bodies and this process is definitely not described by Einstein's equations.

7.2. Nonuniqueness of the topology

The knowledge of the metric tensor $g_{\mu\nu}$ does not determine uniquely the topology of the corresponding space-time manifold. For instance, the Euclidean space $\mathbb{E}^3$ has obviously the same metric $g_{\mu\nu} = \delta_{\mu\nu}$, $\mu, \nu = 1, 2, 3$, as $\mathbb{S}^1 \times \mathbb{E}^2$, but different topology for a time-independent case with $T_{\mu\nu} = 0$ in (1). Here $\mathbb{S}^1$ stands for the unit circle. Hence, solving Einstein's equations does not mean that we obtain the shape of the associated manifold. Other examples can be found in [39, p. 725].

7.3. Law of conservation of energy

In general relativity the energy-momentum conservation is true only locally, which is expressed in the covariant divergence form as

$$T^{\mu\nu}{}_{;\nu} := \frac{\partial T^{\mu\nu}}{\partial x^\nu} + \Gamma^\mu{}_{\lambda\nu}T^{\lambda\nu} + \Gamma^\nu{}_{\lambda\nu}T^{\mu\lambda} = 0, \tag{30}$$

see e.g. [39, p. 146]. So the law of conservation of energy holds for Einstein's equations (19). However, in [29] we presented 10 independent observational arguments showing that the Solar system slowly expands and the expansion rate is comparable to H_0, cf. (29). For instance, the measured mean speed of the Moon from the Earth is 3.84 cm/yr while tidal forces can explain only one half of this value. The corresponding remainder is approximately equal to $0.67H_0$, see [10], [11], [29, p. 187].

Slight violation of the laws of conservation of energy and of momentum in static spacetime can easily explain a wide range of puzzles such as the faint young Sun paradox, the formation of Neptune and Uranus closer to the Sun, the existence of rivers on Mars, the paradox of tidal forces of the Moon, the paradox of the large orbital momentum of the Moon, Triton and Charon, migration of planets, the slow rotation of Mercury, the absence of its moons, rapid orbital expansion of Titan [34], etc.

In [29, Chapt. 16] we also show that galaxies themselves slightly expand at rate comparable with H_0. For instance, by [37, Sect. 8] the observed conservative expansion rate of the Milky Way is $0.6 - 1$ kpc/Gyr, which is approximately 600–1000 m/s and the Hubble constant recalculated on the diameter D of our Galaxy is $H_0 = 2\,\mathrm{km}/(\mathrm{s}D)$, see [29, p. 241].

The angular momentum of spiral galaxies is also not conserved, cf. [36, 40]. This is naturally expressed by the galactic angular momentum paradox: *How is it possible that spiral galaxies (originating from small random fluctuations in a hot homogeneous and isotropic universe) rotate so fast?*

7.4. Modeling error

The difference between physical reality and the solution of Einstein's equations is called the modeling error. In Figure 5 there is a general computational scheme of numerical solutions of problems of mathematical physics on a computer [29], where we always commit three basic errors: modeling error $e_0 = e_0(t)$, discretization error $e_1 = e_1(t)$, and rounding errors $e_2 = e_2(t)$. The size of e_0 is often not taken into account in the theory of general relativity even though it can be much larger than $e_1 + e_2$.

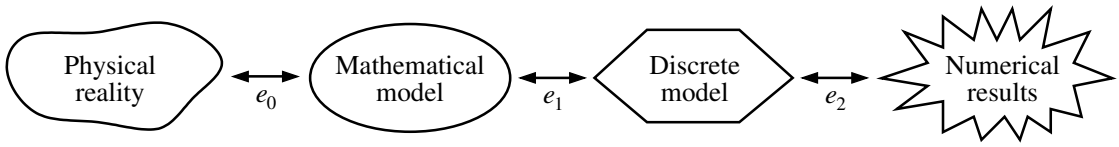

Figure 5: Modeling error $e_0(t)$ is the difference between physical reality and the solution of its mathematical model (mathematical-physical description). The discretization error $e_1(t)$ is the difference between solutions of the mathematical model and the discrete computer model. Finally, in $e_2(t)$ rounding errors (or iteration errors) are included.

Setting $A = \frac{1}{3}\Lambda c^2$ and $B = -kc^2$, the Friedmann equation (21) can be rewritten as the following simple autonomous ordinary differential equation with constant coefficients

$$\dot{a}^2 = Aa^2 + B + \frac{C}{a}, \tag{31}$$

where $C = \frac{8}{3}\pi G\rho a^3 > 0$ is constant by the law of conservation of mass for zero pressure, i.e. $\rho(t)a^3(t) = \rho(t_0)a^3(t_0)$ for all $t > \tau$, where t_0 is the present time (see [31, p. 100]). E.g. $C = \frac{2}{3}c^2\sqrt{\Lambda}$ for the Einstein universe and $C = 0$ for the de Sitter universe, where $k = 1$ and $\Lambda > 0$. However, the analytical solution of (31) is not known when $ABC \neq 0$, in general. Therefore, we cannot separate particular terms of the sum e_0+e_1 to establish the modeling error e_0. Hence, from equation (31) we should not make any categorical conclusions about the deep past and the future of the universe, about its age, origin, size, curvature, composition, expansion speed, etc., as is often done.

Moreover, we should not perform the backward integration of the Friedmann equation close to the Big Bang (cf. Figure 4), when quantum phenomena played an essential role, since they are not described by Einstein's equations.

7.5. Scale non-invariance

No equation of mathematical physics describes reality absolutely exactly on any scale. The reason is that the laws of physics are not unchanged under a change of scale, in general. For instance, Einstein's equations (19) are not scale-invariant, since they are highly nonlinear and contain fixed physical constants Λ, c, and G. They do not describe phenomena at an atomic level in a trustworthy manner. In this case, the modeling is very large (see Figure 6). If the curvature index $k = 1$, then the corresponding space manifold (hypersphere) is bounded, i.e., the scale invariance again cannot hold.

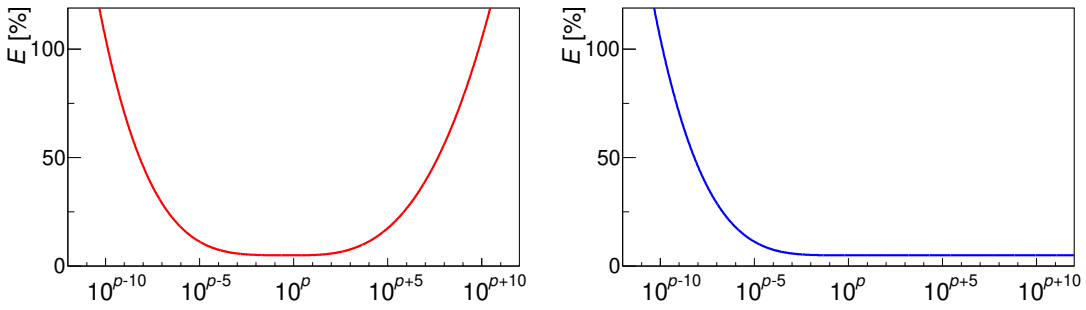

Figure 6: Left: A schematic illustration of a general behavior of the relative modeling error E for equations of mathematical physics. The horizontal axis has a logarithmic scale and p is the exponent for which the modeling error is the smallest. Right: Behavior of the modeling error for Einstein's equations promoted by the standard cosmological model.

The standard cosmological model is based on the unrealistic assumption that Einstein's equations are scale invariant, i.e., one can apply them to arbitrarily large objects — like the whole universe. This is, of course, an unjustified extrapolation, see Section 5.

7.6. Unconvincing general relativity tests

Classical tests of the theory of general relativity [38, 39], such as bending of light, Mercury's perihelion shift, gravitational redshift, and also Shapiro's fourth test of general relativity, are usually being verified by very simple algebraic formulae derived by various simplifications and approximations from the exterior Schwarzschild solution (13) without any guaranteed estimates of the modeling error. However, we cannot verify the validity of Einstein's equations (1) by means of the Schwarzschild solution.[6] This could be used only to disprove their validity (more precisely, to disprove their good approximation properties of reality).

For instance, Mercury's perihelion shift is thought to be one of the fundamental tests of the validity of the general theory of relativity. Recall Einstein's formula for this shift [12] during one period $T = 7.6005 \cdot 10^6$ s,

$$\varepsilon = 24\pi^3 \frac{a^2}{T^2 c^2 (1 - e^2)} = 5.012 \cdot 10^{-7} \text{ rad}, \tag{32}$$

where $e = 0.2056$ is the eccentricity of its elliptic orbit and $a = 57.909 \cdot 10^9$ m the length of its semimajor axis. From this we find an incredibly small perihelion advance

$$\mathcal{E} = 43'' \text{ per century}.$$

Let us point out that formula (32) was published already in 1898 by Paul Gerber [21]. In [12], the planet Mercury is replaced by a massless point (which is again called Mercury) that does not curve the surrounding spacetime[7] and the influence of the other planets is not taken into account. According to [17, p. 147], the relativistic perihelion shift $43''$ is in excellent agreement with observed values. However, the observed perihelion shift is $\mathcal{O} \approx 575''$ per century due to the gravitational tug of other planets. From this value general relativists subtract the value $\mathcal{C} \approx 532''$ calculated by Newtonian mechanics with infinite speed of gravity. This has to be done numerically, since the analytical solution of the n-body problem corresponding to the Solar system is not known. Hence, we necessarily meet all kinds of errors marked in Figure 4. In spite of that general relativists claim that

$$\mathcal{E} = \mathcal{O} - \mathcal{C}.$$

[6] Similarly, good approximation properties of reality modeled by the Laplace equation $\Delta u = 0$ cannot be verified by testing its linear solution $u(x_1, x_2, x_3) = x_1 + x_2 + x_3$, since there exist infinitely many other equations having the same solution.

[7] For comparison note that the Earth ($18\times$ heavier than Mercury) curves the surrounding spacetime by maintaining the Moon's motion at a speed of 1 km/s at a very large distance of 384 400 km. The generalized 3rd law of Kepler yields the difference 13 000 km in positions after one century if Mercury is replaced by a massless point.

However, the quantities $\mathcal{O}$ and $\mathcal{C}$ are not uniquely defined. Thus, the proposed relativistic shift $43''$ per century comes from the subtraction of two quite inexact numbers of almost equal magnitude (Observed minus Calculated). As such, this shift is highly uncertain and may not correspond to reality. We present a thorough numerical analysis of this ill-conditioned problem in [24].

The observed twist of line of apsides of binary pulsars does not imply that Einstein's equations describe reality well. The reason is that we do not know any of their solutions for two massive bodies, since they are extremely complicated, cf. (8)–(12). Nevertheless, we can apply formula (32) to the star S2 orbiting the super-massive black hole Sgr A*. For the corresponding values $a \approx 970$ au $\approx 145 \cdot 10^{12}$ m, $e \approx 0.885$, and the period $T \approx 16.052$ yr $\approx 507 \cdot 10^6$ s (see [1]) formula (32) yields a relatively large value $\varepsilon = 10.74$ arc minutes. However, we see that formula (32) contains squares of a, e, and T, so it is very sensitive to their precise determination. Moreover, the trajectory of S2 is seen only in the projection on the celestial sphere, so it is difficult to get precise values[8] of a and e, see [27]. Hence, we have to wait for several periods to verify, whether the proposed value $\varepsilon = 10.74'$ corresponds to reality.

7.7. Hubble-Lemaître constant

In 2016, the Planck Collaboration stated that

$$H_0 = 66.93 \pm 0.62 \text{ km s}^{-1}\text{Mpc}^{-1}. \tag{33}$$

This value is based on the standard cosmological model (i.e. Einstein's equations), while the Gaia and Hubble Space Telescope measurements of Cepheids and RR Lyrae yield the 10 % larger value $H_0 = 73.52 \pm 1.62$ km s^{-1}Mpc^{-1}, see [46]. We again get a disagreement between theory and observations. For a substantial discordance in estimating another cosmological parameter σ_8, see [22].

7.8. The age of the universe

The age of the universe was derived from the ΛCDM model up to four significant digits

$$t_0 = 13.79 \text{ Gyr} \tag{34}$$

using the backward integration of the Friedmann equation (21) and the present value of the Hubble-Lemaître constant (33). Nevertheless, from such a simple equation we should not make any categorical conclusions about the real age of the universe, since it was derived from Einstein's equations by excessive extrapolations to cosmological scales. For instance, by [7] the star HD 140283 is 14.46 ± 0.8 Gyr old, which contradicts (34). Moreover, this star is quite close to our Sun, so it is very probable that there are older stars in the whole universe.

[8] The angular size of the (projected) semimajor axis a was measured quite precisely, but the Earth-Sgr A* distance is known only approximately, i.e., the presented value of a in meters is very rough.

The existence of super-massive black holes $\approx 10^{10}\ M_\odot$ at distances $z \approx 7$, when the universe was only 700 000 yr old, also indicates that its real age is probably higher than (34).

7.9. Time delay variables

Einstein's equations do not contain delays (in time variables) corresponding to the finite speed of gravity. This does not allow us to properly treat aberration effects. The actual angle of gravitational aberration has to be necessarily positive, since the zero aberration angle would contradict causality [29]. In fact, the causality principle should be prior to the law of conservation of energy.

7.10. Measurements of vacuum energy

The main argument against the proposed amount of vacuum (dark) energy is the 120-order-of-magnitude discrepancy between the measured and theoretically derived density of vacuum energy (see [2]). From this it is evident that the standard cosmological model, which is a direct mathematical consequence of Einstein's equations (22), does not approximate reality well.

For further cosmological paradoxes we refer e.g. to [3, 4].

8. Concluding remarks

The main problem of the standard cosmological model lies in the hidden assumption that Einstein's equations describe the evolution of the whole universe very well. Unfortunately, this unjustified assumption sits at the origin of all paradoxes of the current cosmology. It resembles the situation of the PhD thesis of J. N. He defined the so-called canal surfaces and proved many surprising lemmas and theorems about them. Later it was found that his set of canal surfaces is empty.

In 1922 astronomers had no idea about the real size of the universe, because galaxies (other than the Milky Way) were discovered by Edwin Hubble in 1925, see [23]. Their typical size is about 10^{10} astronomical units, and the size of the observable universe is at least five orders of magnitude larger. In spite of that, Alexander Friedmann [18] (and before him also Albert Einstein [14]) applied Einstein's equations to the whole universe, even though they are being tested on much smaller scales.

This excessive extrapolation has caused the current crisis of the standard cosmological model.

The standard cosmological model assumes that time flows completely uniformly from the Big Bang on (cf. Subsection 7.8). However, it is important to realize that in the observable universe we actually look in any direction into the vast spacetime singularity. The more distant the objects that are observed, the more it seems to us that time passes more slowly due to the cosmological redshift. For instance, if there were a huge clock placed at $z = 1$ from the Earth, then we would see that it runs twice as slow. For the largest currently observed distance corresponding to the CMB with redshift $z = 1089$, a similar clock would seem to tick $1090\times$ slower than

on the Earth. Moreover, time flows more slowly close to dense massive objects which applies to the early universe when also quantum phenomena were present.

Acknowledgement. The authors are indebted to J. Brandts, A. Mészáros, and A. Ženíšek for inspiration and valuable suggestions, and F. Křížek for drawing some figures. Supported by RVO 67985840 of the Czech Republic.

References

[1] Abuter, R. et al.: Detection of the gravitational redshift in the orbit of the star S2 near the Galactic centre massive black hole. Astron. Astrophys. **615** (2018), L15.

[2] Adler, J. R., Casey, B., Jacob, O. C.: Vacuum catastrophe: An elementary exposition of the cosmological constant problem. Amer. J. Phys. **63** (1995), 620–626.

[3] Baryshev, Y.: Paradoxes of cosmological physics in the beginning of the 21-st century, arXiv: 1501.01919v1, 2015, 1–11.

[4] Baryshev, Y., Teerikorpi, P.: Fundamental questions of practical cosmology. Springer, Dordrecht, Heidelberg, London, New York, 2012.

[5] Binney, J., Merrifield, M.: Galactic astronomy. Princeton, 1998.

[6] Carroll, S. M., Press, H. W., Turner, E. L.: The cosmological constant. Annu. Rev. Astron. Astrophys. **30** (1992), 499–542.

[7] Cowen, R.: Nearby star is almost as old as the Universe. Nature 2013, January 10, doi: 10.1038/nature.2013.12196.

[8] Delgaty, M. S. R., Lake, K.: Physical acceptability of isolated, static, spherically symmetric, perfect fluid solutions of Einstein's equations. Comput. Phys. Commun. **115** (1998), 395–415.

[9] de Sitter, W.: On the relativity of inertia. Remarks concerning Einstein latest hypothesis. Proc. Kon. Ned. Acad. Wet. **19** (1917), 1217–1225.

[10] Dumin, Y. V.: A new application of the Lunar laser retroreflectors: Searching for the "local" Hubble expansion. Adv. Space Res. **31** (2003), 2461–2466.

[11] Dumin, Y. V.: Testing the dark-energy-dominated cosmology by the Solar-System experiments. Proc. of the 11th Marcel Grossmann Meeting on General Relativity (eds. H. Kleinert, R. T. Jantzen, R. Ruffini), World Sci., Singapore, 2008, 1752–1754, arXiv: 0808.1302.

[12] Einstein, A.: Erklärung der Perihelbewegung des Merkur aus der allgemeinen Relativitätstheorie. Königlich-Preußische Akad. Wiss. Berlin, (1915), 831–839. Eng. trans. Explanation of the perihelion motion of Mercury from general relativity theory, by R. A. Rydin with comments by A. A. Vankov, pp. 1–34.

[13] Einstein, A.: The foundation of the general theory of relativity. Ann. Phys. **49** (1916), 769–822.

[14] Einstein, A.: Kosmologische Betrachtungen zur allgemeinen Relativitätstheorie. Königlich-Preuss. Akad. Wiss., Berlin, 1917, 142–152. Eng. trans. in The principle of relativity. New York, Dover, 1952.

[15] Ellis, H. G.: Gravity inside a nonrotating, homogeneous, spherical body. ArXiv: 1203.4750v2, 2012, pp. 1–6.

[16] Florides, P. S.: A new interior Schwarzschild solution. Proc. Roy. Soc. London A **337** (1974), 529–535.

[17] Foster, J., Nightingale, J. D.: A short course in general relativity. Springer, New York, 1995.

[18] Friedman, A.: Über die Krümmung des Raumes. Z. Phys. **10** (1922), 377–386. Eng. trans. On the curvature of space. General Relativity and Gravitation **31** (1999), 1991–2000.

[19] Friedmann, A.: Über die Möglichkeit einer Welt mit konstanter negativer Krümmung des Raumes. Z. Phys. **21** (1924), 326–332. Eng. trans. On the possibility of a world with constant negative curvature of space. General Relativity and Gravitation **31** (1999), 2001–2008.

[20] Fromholz, P., Poisson, E., Will, C. M.: The Schwarzschild metric: It's the coordinates, stupid! Amer. J. Phys. **82** (2014), 295–300.

[21] Gerber, P.: Die räumliche und zeitliche Ausbreitung der Gravitation. Zeitschrift Math. Phys. **43** (1898), 93–104.

[22] Hildebrandt, H. et al.: KiDS-450: Cosmological parameter constraints from tomographic weak gravitational lensing. Mon. Not. R. Astron. Soc. **465** (2017), 1454–1498.

[23] Hubble, E.: Cepheids in spiral nebulae. The Observatory **48** (1925), 139–142.

[24] Křížek, M.: Influence of celestial parameters on Mercury's perihelion shift. Bulg. Astron. J. **27** (2017), 41–56.

[25] Křížek, M.: Ten arguments against the proclaimed amount of dark matter. Gravit. Cosmol. **24** (2018), 350–359.

[26] Křížek, M.: Do Einstein's equations describe reality well? Neural Netw. World **29** (2019), 255–283.

[27] Křížek, M.: Possible distribution of mass inside a black hole. It there any upper limit on mass density? Astrophys. Space Sci. **364** (2019), Article 188, 1–5.

[28] Křížek, M., Křížek, F., Somer, L.: Dark matter and rotation curves of spiral galaxies. Bulg. Astron. J. **25** (2016), 64–77.

[29] Křížek, M., Křížek, F., Somer, L.: Antigravity — its origin and manifestations Lambert Acad. Publ., Saarbrücken, 2015, xiv + 348 pp.

[30] Křížek, M., Mészáros, A.: On the Friedmann equation for the three-dimensional hypersphere. Proc. Conf. Cosmology on Small Scales 2016, Local Hubble Expansion and Selected Controversies in Cosmology (eds. M. Křížek, Y. V. Dumin), Inst. of Math., Prague, 2016, 159–178.

[31] Křížek, M., Mészáros, A.: Classification of distances in cosmology. Proc. Conf. Cosmology on Small Scales 2018, Dark Matter Problem and Selected Controversies in Cosmology (eds. M. Křížek, Y. V. Dumin), Inst. of Math., Prague, 2018, pp. 92–118.

[32] Křížek, M., Somer, L.: Excessive extrapolations in cosmology. Gravit. Cosmol. **22** (2016), 270–280.

[33] Kroupa, P.: The dark matter crisis: Falsification of the current standard model of cosmology. Publ. Astron. Soc. Australia **29** (2012), 395–433.

[34] Lainey, V. et al.: Resonance locking in giant planets indicated by the rapid orbital expansion of Titan. Nat. Astron., June 2020, 1–16.

[35] Lanczos, C.: Über eine stationäre kosmologie im sinne der Einsteinischen Gravitationstheories. Zeitschr. f. Phys. **21** (1924), 73–110.

[36] Lelli, F., McGaugh, S. S., Schombert, J. M., Pawlowski, M. S.: One law to rule them all: The radial acceleration relation of galaxies. Astrophys. J. **836** (2017), arcicle id. 152, 23 pp.

[37] Martínez-Lombilla, C., Trujillo, I., Knapen, J. H.: Discovery of disc truncations above the galaxies' mid-plane in Milky Way-like galaxies. Mon. Not. R. Astron. Soc. **483** (2019), 664–691.

[38] McCausland, I.: Anomalies in the history of relativity. J. Sci. Exploration **13** (1999), 271–290.

[39] Misner, C. W., Thorne, K. S., Wheller, J. A.: Gravitation, 20th edition. New York, W. H. Freeman, 1997.

[40] Obreschkow, D. et al. (eds.): Galactic angular momentum. Proc. XXXth IAU General Assembly, Focus Meeting 6, Vienna, August, 2018.

[41] Perlmutter, S.: Supernovae, dark energy, and the accelerating universe. Physics Today **56** (2003), April, 53–60.

[42] Perlmutter, S. et al.: Measurements of the cosmological parameters Ω and Λ from the first seven supernovae at $z \geq 0.35$. Astrophys. J. **483** (1997), 565–581.

[43] Planck Collaboration: Planck 2013 results, I. Overview of products and scientific results. Astron. Astrophys. **571** (2014), A1, 1–48.

[44] Rektorys, K. et al.: Survey of applicable mathematics I. Kluwer Acad. Publ., Dordrecht, 1994.

[45] Riess, A. G. et al.: New Hubble space telescope discoveries of type Ia supernovae at $z >= 1$: Narrowing constraints on the early behavior of dark energy. Astrophys. J. **659** (2007), 98–121.

[46] Riess, A. G. et al.: Milky Way Cepheid standards for measuring cosmic distances and application to GAIA DR2: Implications for the Hubble constant. Astrophys. J. **861** (2018), Article ID 126.

[47] Schwarzschild, K.: Über das Gravitationsfeld eines Massenpunktes nach der Einsteinschen Theorie. Sitzungsber. Preuss. Akad. Wiss. (1916), 189–196. Eng. trans. On the gravitational field of a point-mass, according to Einstein's theory. The Abraham Zelmanov Journal **1** (2008), 10–19.

[48] Schwarzschild, K.: Über das Gravitationsfeld einer Kugel aus incompressiebler Flüssigkeit nach der Einsteinschen Theorie. Sitzungsber. Preuss. Akad. Wiss. (1916), 424–435. Eng. trans. On the gravitational field of a sphere of incompressible liquid, according to Einstein's theory. The Abraham Zelmanov Journal **1** (2008), 20–32.

[49] Stephani, H.: Relativity: An introduction to special and general relativity, 3rd edition. Cambridge Univ. Press, Cambridge, 2004.

[50] Vavryčuk, V.: Universe opacity and CMB. Mon. Not. R. Astron. Soc. **478** (2018), 283–301.

[51] Vavryčuk, V.: Universe opacity and Type Ia supernova dimming. Mon. Not. R. Astron. Soc. **489** (2019), L63–L68.

[52] Yahalom, A.: The effect of retardation on galactic rotation curves. J. Phys.: Conf. Ser. **1239** (2019), 012006.

[53] https://en.wikipedia.org/wiki/Interior_Schwarzschild_metric

Conference *Cosmology on Small Scales 2020*
Michal Křížek and Yurii Dumin (Eds.)
Institute of Mathematics CAS, Prague

A POSSIBLE CONSTRAINT ON THE VALIDITY OF GENERAL RELATIVITY FOR STRONG GRAVITATIONAL FIELDS?

W. Oehm

Bonn, Germany
physik@wolfgang-oehm.com

Abstract: The axiomatic foundation of Einstein's theory of General Relativity is discussed based on an epistemological point of view, yielding a possible restriction on the range of validity regarding the strength of gravitational fields.

Keywords: General theory of relativity, Einstein's elevator, Lorentz frame, Minkowski metric

PACS: 4.20.-q

1. Introduction

As there are various forms of the equivalence principle circulating, this is the form suggested by [2, p. 22]:

> Weak Equivalence Principle (WEP): *"If an uncharged test body is placed at an initial event in spacetime and given an initial velocity there, then its subsequent trajectory will be independent of its mass,*[1] *internal structure and composition."*

> Einstein Equivalence Principle (EEP): *(i) WEP is valid, (ii) the outcome of any local non-gravitational test experiment is independent of the velocity of the (freely falling) apparatus, and (iii) the outcome of any local non-gravitational test experiment is independent of where and when in the universe it is performed.*

Here the local non-gravitational test experiment is represented by the local Lorentz frame which is the freely falling reference frame in which the laws of Special Relativity are valid, and the term *local* indicates arbitrarily small spatial extensions.

[1] Here the term "*mass*" was added by the author for the sake of clarity. In [2] it is clear from the context upon discussing the equivalence of inertial and passive gravitational mass.

The world-line of a force-free test particle in a Lorentz frame with coordinates $\tilde{x}$ and proper time τ is given by

$$\frac{\mathrm{d}^2\widetilde{x}^a}{\mathrm{d}\tau^2} = 0. \tag{1}$$

The transformation to the reference frame of an observer with coordinates x

$$\frac{\mathrm{d}\widetilde{x}^a}{\mathrm{d}\tau} = \frac{\partial\widetilde{x}^a}{\partial x^b}\frac{\mathrm{d}x^b}{\mathrm{d}\tau} \tag{2}$$

yields

$$\ddot{x}^a + \Gamma^a{}_{bc}\,\dot{x}^b\dot{x}^c = 0, \tag{3}$$

where the derivative to the proper time τ is denoted by the dot, and $\Gamma^a{}_{bc}$ is the affine (metric) connection. The metric g_{ab} of the observer's reference frame relates to the Minkowski metric η_{bc} via

$$g_{ab} = \frac{\partial\widetilde{x}^c}{\partial x^a}\frac{\partial\widetilde{x}^d}{\partial x^b}\,\eta_{cd}\ . \tag{4}$$

Regarding experimental and observational tests, General Relativity is *quantitatively* confirmed for *weak* gravitational fields within the Solar system only. Observations of black holes and gravitational waves are essentially of phenomenological character without thorough quantitative examination so far. Actually, this also is a matter of fact for the recently published observation of the pericentral drift of the star S2 orbiting the compact radio source Sgr A* (see [1]), which is assumed to represent the massive black hole in the Galactic centre. In this case obviously only vague estimates for the essential physical entities like the mass of the black hole are at our disposal.

2. Einstein's elevator

The assumption of a local Lorentz frame is based on Einstein's thought experiment where an observer situated in an closed elevator is not able to distinguish between gravitational forces, and inertial forces due to acceleration. Since gravitational fields are inhomogeneous, it is clear that the observer would be able to distinguish a gravitational field from an homogeneous acceleration field *if he was able to measure with sufficient accuracy*, depending on the size of the elevator and the inhomogeneity of the gravitational field. Commonly accepted is the way out to reduce the size of the elevator to infinitesimal small values, resulting in the local Lorentz frame with an approximate metric

$$\eta_{ab} + o(\widetilde{x}^2)\ . \tag{5}$$

3. *A priori* vs. *a posteriori* relation between theory and accuracy of measurements

Thus the axiomatic mathematical formulation of General Relativity apparently is directly related to the issue of the measurement capabilities of observers. If the observers where able to measure with sufficient accuracy then they would not consider their elevator as inertial (Lorentz) frame, and in principal this stays true down to infinitesimal extensions.

This suggests that the variety of axiomatic formulations in physics be distinguished between those with an *a posteriori* only relation to measurement capabilities and those with an additional *a priori* relation to measurement capabilities in the following sense:

- For an *a posteriori* formulation, only the predictions derived from a mathematical axiom are compared to observations and experimental results. Clearly have the capabilities of measurement an impact on this comparison but the formulation of the mathematical axiom itself is independent of the question of measurement accuracy.

- As already explained, General Relativity represents an *a priori* formulation, because this formulation "stands and falls" with measurement capabilities. This is an additional feature to the *a posteriori* comparison of mathematical predictions with measurement results, which of course also applies here.

4. Locality, a different view

As mentioned in Chapter 1, there are no *quantitative* experiments for strong gravitational fields available. Furthermore, referring to Chapter 3, the essential issue is the fact that the *a priori* relation to the measurement capabilities of an real existing *observer on Earth* is completely separated from the objects under investigation (black holes, Big Bang). With pithy words: What is the concern of cosmological objects regarding the measurement capabilities of an *observer on Earth*? Apparently (iii) of EEP manifests a vague extrapolation to situations which are incompatible to our local situation (Solar system). In that regard the *a priori* aspect of EEP establishes a fundamental distinction from *a posteriori* axiomatic formulations of basic physical concepts applied to cosmology[2].

5. Conclusion

Based on a given size of the "elevator" and a certain measurement accuracy, it is clear that there is a limiting ceiling value for the strength of the gravitational field in that sense that beyond this ceiling value the observer would be able to distinguish between acceleration and gravitation. As a possible logical consequence, this implies

[2]Inventions like *dark matter* or *dark energy* are here not considered as basic physical concepts like the foundations of Mechanics, Electrodynamics, Quantum Mechanics etc.

an *intrinsic* restriction on the validity range of General Relativity regarding the strength of gravitational forces. However, due to the locality aspect of Chapter 4 and the *a priori* feature of EEP in combination with the arbitrariness of a given measurement accuracy, an explicit quantification appears to be hardly possible.

6. Outlook

The author perceives this document as basis for a discussion forum at the conference.

Acknowledgements

The author would like to thank P. Kroupa, M. Olschowy, and M. Křížek for encouraging discussions and communications.

References

[1] GRAVITY Collaboration et al.: Detection of the Schwarzschild precession in the orbit of the star S2 near the Galactic centre massive black hole, arXiv:2004.07187 (2020).

[2] Will, C. M.: *Theory and experiment in gravitational physics*. Cambridge University Press, Cambridge, 1993.

Conference *Cosmology on Small Scales 2020*
Michal Křížek and Yurii Dumin (Eds.)
Institute of Mathematics CAS, Prague

THE PROBLEM OF CAUSALITY IN THE UNCERTAINTY-MEDIATED INFLATIONARY MODEL*

Yurii V. Dumin

Sternberg Astronomical Institute (GAISh) of Lomonosov Moscow State University,
Universitetskii prosp. 13, Moscow, 119234 Russia

Space Research Institute (IKI) of Russian Academy of Sciences,
Profsoyuznaya str. 84/32, Moscow, 117997 Russia

dumin@yahoo.com, dumin@sai.msu.ru

Abstract: It was suggested in our previous works [Y.V. Dumin. In: *Cosmology on Small Scales 2018*, p. 136; Grav. Cosmol., **25** (2019), 169] that the Dark Energy (effective Λ-term) can be mediated by the time–energy uncertainty relation in the Mandelstam–Tamm form, which is applicable to the long-term evolution of quantum systems. Then, the amount of Dark Energy gradually decays with time, and the corresponding scale factor of the Universe increases by a "quasi-exponential" law (namely, proportional to the exponent of the square root of time) throughout the entire history of the Universe. While this universal behavior looks quite appealing, an important question arises: Does the quasi-exponential expansion resolve the major problems of the early Universe in the same way as the standard inflationary scenario? Here, we try to elucidate this issue by analyzing a causal structure of the respective space–time. It is found that the observed region of the Universe (the past light cone) covers a single causally-connected domain developing from the Planckian time (the future light cone). Consequently, there should be no appreciable inhomogeneity and anisotropy in the early Universe, creation of the topological defects will be suppressed, etc. From this point of view, the uncertainty-mediated Dark Energy can serve as a viable alternative to the standard (exponential) inflationary scenario.

Keywords: Dark Energy, uncertainty relation, inflationary model, causal structure

PACS: 98.80.Bp, 98.80.Cq, 98.80.Es, 95.36.+x

*A short version of this article is published in Grav. Cosmol. **26** (3) (2020), 259.

1. Introduction

The Dark Energy (or the effective Λ-term) is one of cornerstones of the modern cosmology, however little is known about its nature and origin till now. In particular, it is unclear if it is a new fundamental physical constant or just an effective contribution from the underlying field theory. Yet another interpretation of this entity was proposed in our recent works [4, 5], where we assumed that the amount of Dark Energy could be derived from the quantum uncertainty relation between the time and energy in the Mandelstam–Tamm form [11]. As distinct from the well-known Heisenberg relation, which is used mostly in the context of measurements, the Mandelstam–Tamm relation is applicable to the long-term evolution of quantum systems and widely employed now in such branches of physics as quantum optics, quantum information processing, etc. [3]. So, its application to the quantum cosmology is well in the mainstream of the modern physics. (It should be mentioned that some qualitative conjectures about a possible role of the uncertainty relation in explanation of the Dark Energy were put forward even earlier by A. Coe in preprint [2], but the quantitative analysis undertaken there looked absolutely unreasonable.)

Briefly speaking, the main points of our treatment [4, 5] were as follows. We begin with the standard Robertson–Walker metric,

$$\mathrm{d}s^2 = c^2\mathrm{d}t^2 - R^2(t)\biggl[\frac{\mathrm{d}r^2}{1-kr^2} + r^2(\mathrm{d}\theta^2 + \sin^2\theta\,\mathrm{d}\varphi^2)\biggr]\,, \tag{1}$$

whose temporal evolution is described by the Friedmann equation, e.g., [15]:

$$H^2 \equiv \left(\frac{\dot{R}}{R}\right)^2 = \frac{8\pi G}{3c^2}\,\rho \,-\, kc^2\frac{1}{R^2} \,+\, \frac{c^2}{3}\,\Lambda\,. \tag{2}$$

Here, r, θ, and φ are the dimensionless spherical coordinates, the coefficient k equals 1, 0, and -1 for the closed, flat, and open 3D space, respectively; R is the scale factor (called sometimes also the expansion function) of the Universe, H is the Hubble parameter, ρ is the energy density of matter in the Universe, G is the gravitational constant, and c is the speed of light in vacuum. (Since the resulting formulas for the uncertainty-mediated Dark Energy will look a bit unusual, we prefer to keep here all the dimensional constants.)

The Λ-term appearing in (2) can be formally associated with the vacuum energy density ρ_{v}:

$$\Lambda = \frac{8\pi G\rho_{\mathrm{v}}}{c^4}\,. \tag{3}$$

So, our main conjecture is to express ρ_{v} through the vacuum energy in the Planck volume,

$$\Delta E = \rho_{\mathrm{v}} l_{\mathrm{P}}^3 \tag{4}$$

(where $l_{\mathrm{P}}{=}\sqrt{G\hbar/c^3}$ is the Planck length, $\hbar = h/2\pi$), and then to estimate this energy through the uncertainty relation with the equality sign:

$$\Delta E\,\Delta t \approx \frac{C_{\mathrm{UR}}}{2}\,\hbar\,, \tag{5}$$

where $\Delta t \equiv t$ is the total time of cosmological evolution (i.e., the age of the Universe). The numerical coefficient $C_{\rm UR}$ equals 1 in the well-known Heisenberg's case (related mostly to the measurement problems) and π in the Mandelstam–Tamm's situation (referring to the long-term evolution) [3]. Anyway, this coefficient gives only the lower bound on the product of the corresponding uncertainties. So, all subsequent formulas will be valid, strictly speaking, only up to this numerical coefficient.

As a result, we get the effective time-dependent Λ-term,

$$\Lambda(t) = \frac{4\pi C_{\rm UR}}{c\, l_{\rm P}}\,\frac{1}{t}\,, \tag{6}$$

and its substitution into (2) leads to the master equation of our cosmological model:

$$H^2 \equiv \left(\frac{\dot R}{R}\right)^2 = \frac{8\pi G}{3c^2}\,\rho \,-\, kc^2\frac{1}{R^2} \,+\, \frac{4\pi C_{\rm UR}}{3\tau}\,\frac{1}{t}\,, \tag{7}$$

where $\tau = l_{\rm P}/c = \sqrt{G\hbar/c^5}$ is the Planck time. From the mathematical point of view, this differential equation is non-autonomous, i.e., it involves the explicit dependence on time, which is a quite unusual situation in cosmology. However, as follows from the detailed analysis, this fact does not result in any substantial peculiarities of the solution: it turns out to be well between the solutions of usual cosmological equations obtained under the various assumptions.

The simplest case, already considered in our previous works [4, 5], corresponds to the spatially-flat Universe ($k = 0$) and the ignorable energy density of matter ($\rho \approx 0$). Then, formula (7) is reduced to

$$H^2 \equiv \left(\frac{\dot R}{R}\right)^2 = \frac{4\pi C_{\rm UR}}{3\tau}\,\frac{1}{t}\,, \tag{8}$$

which can be trivially integrated:

$$R(t) = R^*\exp\!\left(\sqrt{\frac{16\pi C_{\rm UR}}{3}}\,\sqrt{\frac{t}{\tau}}\,\right), \tag{9}$$

where $R^* = R(0)$ is the integration constant; and we consider only the solution increasing with time, i.e., the expanding Universe.

Therefore, the entire cosmological evolution is described by the universal "quasi-exponential" function (9) instead of being composed of a few absolutely different stages (dominated by the Dark Energy, radiation, dust-like matter, and again the Dark Energy) in the standard cosmological scenario, as illustrated in Figure 1 from the paper [4]. So, the puzzle of two absolutely different Λ-terms in the very early Universe and nowadays [14] becomes naturally resolved.

Yet another important feature of the new model is a considerably increased age of the Universe T as compared to its value T^* in the standard cosmology. Really, as follows from (8),

$$T \approx (T^*/\tau)\,T^*, \tag{10}$$

where $(T^*/\tau) \approx 10^{61}$ is a huge numerical factor; for more details, see Eq. (10) in [5]. In other words, although the Universe is expanding, it becomes in some sense "quasi-perpetual". This is not surprising, because function (9) grows much slower than the pure exponent.

In principle, employing the perturbation theory, it is not difficult to get a refined solution of the equation (7), when a small contribution from the ordinary matter is taken into account; for more details, see Eqs. (10)–(14) in [4]. Unfortunately, the corresponding solution is not so interesting, because the first-order correction becomes noticeable only at the Planckian scale.

2. Application to the early Universe

As is known, the dominant modern paradigm for the description of the early Universe is the inflationary scenario; e.g., reviews [6, 12]. Its emergence in the early 1980's was caused by the fact that, in the framework of the hot Big-Bang model with a power-law expansion, the observed region of the Universe (i.e., the past light cone) contains a large number of the subregions developing independently from the Big Bang (the future light cones). Therefore, one should expect a considerable variation between the properties of such subregions, resulting in a huge inhomogeneity of the fundamental characteristics of the observed Universe, e.g., temperature of the cosmic microwave background radiation (CMB), etc. Besides, if the Universe contains the fields experiencing the symmetry-breaking phase transformations (e.g., Higgs fields, responsible for a generation of mass of the elementary particles), then various kinds of the topological defects should be formed at the boundaries between the subregions, while we do not detect them in observations.

The best remedy for this situation is to modify the expansion law of the Universe, e.g., from the power to exponential one [7]. Then, the observed region of the Universe will cover only one causally-connected subregion developing from the initial instant of time. So, its physical characteristics will be sufficiently homogenized in the course of its evolution, and all the above-mentioned problems should disappear. The stage of the exponential expansion can be naturally produced by the Λ-term in Friedmann equation (2); but it remains unclear how such Λ-term emerges in the early Universe?

The most popular idea in the early 1980's was that the effective Λ-term is associated with the potential energy of the non-linear scalar field in the overcooled state formed after the strongly non-equilibrium symmetry-breaking phase transformation; for a review of this approach, see [10]. Unfortunately, the attempts to find a suitable candidate for such scalar field in the theory of elementary particles (e.g., Higgs field in the electroweak theory) failed. So, a common tendency in the inflationary cosmology became to introduce the inflaton potentials quite arbitrarily (irrelevant to any particular model of elementary particles) and just to check the corresponding cosmological predictions.

Yet another approach to derive the approximately exponential expansion is to

consider the gravitational Lagrangians with the high-order (e.g., quadratic) terms of curvature [17]. From the physical point of view, such terms could be attributed to the expectation values of the matter fields distorted by the curved space–time [16]. Unfortunately, since we still do not have a comprehensive theory of elementary particles, the exact functional form and numerical coefficients of the high-order terms remain unknown and are postulated a priori.

In view of the above-mentioned drawbacks, it would be desirable to find a more solid physical basis for the inflationary cosmology; and the effective Λ-term mediated by the quantum uncertainty relation could be one of the promising options. However, it should be kept in mind that it predicts the quasi-exponential expansion (9) rather than a pure exponent. So, it is unclear in advance if this mechanism can resolve the standard problems of the early Universe as efficiently as the exponential scenario? To answer this question, we need to analyse a causal structure of the respective space–time; and a convenient way to do so is to use the conformal diagrams.

First of all, it will be convenient to measure the time t from the instant of observation (so that the preceding cosmological evolution occurs at the negative times). Then, formula (9) should be rewritten as

$$R(t) = R_0 \exp\left(\sqrt{\frac{16\pi C_{\rm UR}}{3}}\ \frac{\sqrt{t+T}-\sqrt{T}}{\sqrt{\tau}}\right), \tag{11}$$

where R_0 is the present-day value of the scale factor, and $t = -T$ is the beginning of the Universe. (We prefer to not call it the Big Bang, because in the modern literature this term often refers to the onset of the "hot" stage, when the ordinary matter becomes dominant.

The conformal time, as usual, is defined as

$$\eta = \int \frac{{\rm d}t}{R(t)}\,. \tag{12}$$

Then, the domains of causality (i.e., the light cones) will be shaped just by the straight lines [13].

A crucial problem of the old, "pre-inflationary" cosmology was that the observable region of space (e.g., by the instant of symmetry-breaking phase transition, when the ordinary matter was formed, or by the instant of recombination, when the Universe became transparent), $\eta = -\eta^*$, contains a large number of the subregions developing independently from the initial instant of time, $\eta = -\eta_0$ (which is assumed to be at the Planckian scale), as illustrated in the top panel of Figure 1. Really, as follows from the evident geometrical consideration, the number of causally-disconnected domains (represented by the lower triangles) inside the observed region of space (the upper triangle) is given by

$$N_{\rm CD} \approx \left(\frac{\eta_0}{\eta^*} - 1\right)^{-3}. \tag{13}$$

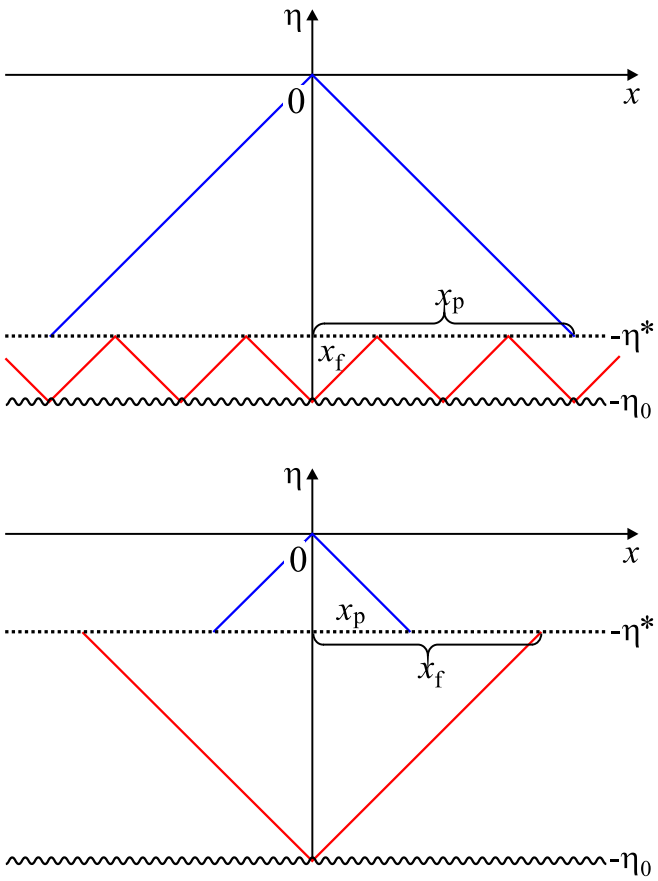

Figure 1: Conformal diagrams of the space–time corresponding to the "pre-inflationary" models, governed by the ordinary matter (top panel), and the inflationary models, governed by the Λ-term (bottom panel). Here, $x_{\rm p}$ is the size (radius) of the past light cone observable at the present time, and $x_{\rm f}$ is the size of the future light cone originating at the beginning of the Universe.

So, for the law of expansion of the ordinary matter,

$$R(t) = R_0 \left(\frac{t+T}{T} \right)^{\frac{2}{3(1+w)}} \tag{14}$$

(where $t = -T$ is the instant of the "classical" Big Bang, and w is the parameter appearing in the equation of state, $p = w\rho$), the conformal time depends on the physical time as

$$\eta(t) = \frac{cT}{R_0} \, \frac{3(1+w)}{1+3w} \left[\left(\frac{t+T}{T} \right)^{\frac{1+3w}{3(1+w)}} - 1 \right]. \tag{15}$$

Substituting this formula to (13), we get:

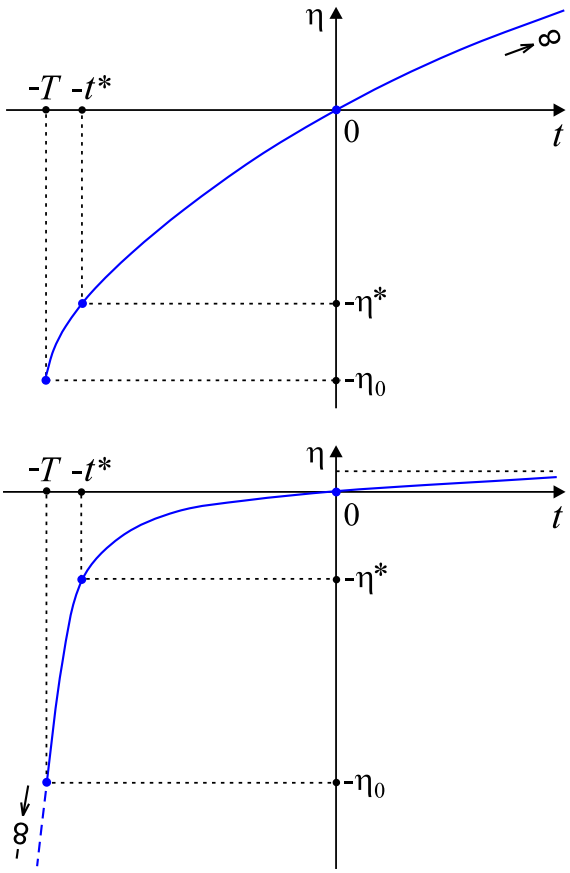

Figure 2: Characteristic behavior of the conformal time η as function of the physical time t in the "pre-inflationary" models, governed by the ordinary matter, (top panel) vs. the inflationary models (bottom panel). The dashed part of the curve, tending to $-\infty$, refers only to the standard (exponential) inflation.

$$N_{\rm CD} \approx \left\{ \left[1 - \left(\frac{T - t^*}{T} \right)^{\frac{1+3w}{3(1+w)}} \right]^{-1} - 1 \right\}^{-3} \gg 1. \tag{16}$$

Consequently, as was already mentioned before, there should be a considerable inhomogeneity of physical characteristics within the observed region of the Universe. Moreover, if the Universe is filled with a Higgs field, giving the masses to the elementary particles, then its non-zero values will be established independently in the causally-disconnected domains [1, 18]. As a result, various kinds of the topological defects (such as monopoles, strings/vortexes, and domain walls/kinks, depending on the symmetry group involved) should be formed at the boundaries between the subregions [8, 19], while we actually do not see them in astronomical observations [9].

From the mathematical point of view, all these drawbacks stem from the fact that the conformal time η increases immediately after the Big Bang not so quickly and,

as a result, the difference $\eta_0 - \eta^*$ remains quite small (top panel in Figure 2). This problem is naturally resolved in the standard (exponential) inflationary scenario, where the scale factor changes as

$$R(t) = R_0 \exp\Bigl(\sqrt{\Lambda/3}\, c\, t\Bigr) \tag{17}$$

and, consequently, the conformal time depends on the physical time as

$$\eta(t) = \frac{1 - \exp\Bigl(-\sqrt{\Lambda/3}\, c\, t\Bigr)}{R_0 \sqrt{\Lambda/3}}\,. \tag{18}$$

As a result, the interval of the conformal time before the instant at which we observe the Universe, $\eta_0 - \eta^*$, becomes much greater (bottom panel in Figure 2); it formally tends to infinity for the purely exponential inflation without singularity. Then, substituting (18) into (13), we find:

$$N_{\rm CD} \approx \exp\Bigl[-\sqrt{3\Lambda}\, c\,(T - t^*)\Bigr] \ll 1\,. \tag{19}$$

So, the entire observable region of the Universe turns out to be within the same causally-connected light cone originating in the past.

Will the same behavior take place in the quasi-exponential model, following from the principle of quantum uncertainty? In this case, relation between the physical and conformal time corresponding to the expansion law (9) will be

$$\begin{aligned} \eta(t) \;\; = \;\; & \sqrt{\frac{3}{4\pi C_{\rm UR}}}\, \frac{c\tau}{R_0} \biggl[\biggl(\sqrt{\frac{T}{\tau}} + \sqrt{\frac{3}{16\pi C_{\rm UR}}} \biggr) \\ & - \biggl(\sqrt{\frac{t+T}{\tau}} + \sqrt{\frac{3}{16\pi C_{\rm UR}}} \biggr) \exp\left(\sqrt{\frac{16\pi C_{\rm UR}}{3}}\, \frac{\sqrt{T} - \sqrt{t+T}}{\sqrt{\tau}} \right) \biggr]. \end{aligned} \tag{20}$$

Apart from the Planckian region, $t + T \sim \tau$, behavior of this function is qualitatively similar to the case of classical (exponential) inflation, except that it terminates at $t = -T$; see bottom panel in Figure 2. (In principle, our equations might be favourable for constructing the bounce-type model of the Universe, but we prefer to not speculate here about the processes at Planckian times.) In other words, the difference of the conformal times when the causally-connected subregion if formed, $\eta_0 - \eta^*$, turns out to be sufficiently large.

Next, substituting (20) to (13), we get:

$$N_{\rm CD} \approx \left(\frac{16\pi C_{\rm UR}}{3}\right)^{3/2} \left(\frac{T - t^*}{\tau}\right)^{3/2} \exp\left[-4\sqrt{3\pi C_{\rm UR}} \left(\frac{T - t^*}{\tau}\right)^{1/2} \right] \ll 1\,, \tag{21}$$

i.e., the same inequality as in the standard inflationary scenario.

3. Conclusions

1. Since the Universe expanding by law (9) possesses qualitatively the same causal structure as in the classical inflationary scenario, the problems of homogeneity and isotropy of the space–time, the absence of topological defects, etc. should be naturally resolved. Therefore, our model can serve as a viable alternative to other inflationary models. Its main advantage is a more solid physical basis, because it does not require any artificial assumptions about the form of the inflaton potential or the higher-order curvature terms in the Lagrangian.

2. Yet another advantage of the proposed model is that inflation is not anymore a separate, very specific stage in the history of the Universe; instead, all physical parameters change smoothly throughout the entire cosmological evolution. In particular, the puzzle of two very different Λ-terms in the early Universe and nowadays becomes naturally resolved.

3. A few other well-known problems of the early Universe, e.g., formation of the approximately flat three-dimensional space and the spectrum of the primordial perturbations, still need to be studied in more detail. They will be discussed in the separate papers.

Acknowledgements

I am grateful to A. Starobinsky, J.-P. Uzan, C. Wetterich, C. Kiefer and members of his group for valuable discussions and critical comments. I am also grateful to the Max Planck Institute for the Physics of Complex Systems (Dresden, Germany) and Institute of Mathematics of Czech Academy of Sciences (Prague, Czech Republic) for fruitful working environment during my visits there.

References

[1] Bogoliubov, N.N.: Field-theoretical methods in physics. Suppl. Nuovo Cimento (Ser. prima) **4** (1966), 346.

[2] Coe, A.: *Observable Universe topology and Heisenberg uncertainty principle.* Preprint viXra:1710.0143, 2017.

[3] Deffner, S., Campbell, S.: Quantum speed limits: from Heisenberg's uncertainty principle to optimal quantum control. J. Phys. A: Math. Theor. **50** (2017), 453001.

[4] Dumin, Y. V.: Cosmological inflation from the quantum-mechanical uncertainty relation. In: M. Křížek, Y. Dumin (Eds.), *Cosmology on Small Scales 2018*, *Dark matter problem and selected controversies in cosmology.* Inst. of Math., Prague, 2018, p. 136.

[5] Dumin, Y. V.: A unified model of Dark Energy based on the Mandelstam–Tamm uncertainty relation. Grav. Cosmol. **25** (2019), 169.

[6] Ellis J., Wands, D.: Inflation. In: Patrignani, C., et al. (Particle Data Group), *Review of Particle Physics*. Chin. Phys. C **40** (2016), 100001, p. 367.

[7] Guth, A. H.: The inflationary Universe: A possible solution to the horizon and flatness problems. Phys. Rev. D **23** (1981), 347.

[8] Kibble, T. W. B.: Topology of cosmic domains and strings. J. Phys. A: Math. Gen. **9** (1976), 1387.

[9] Klapdor-Kleingrothaus, H. V., Zuber, K.: *Particle Astrophysics*. Inst. Phys. Publ., Bristol, 1997.

[10] Linde, A. D.: The inflationary Universe. Rep. Prog. Phys. **47** (1984), 925.

[11] Mandelstam, L. I., Tamm, I. E.: The energy-time uncertainty relation in non-relativistic quantum mechanics. Izv. Akad. Nauk SSSR (Ser. Fiz.) **9** (1945), 122, in Russian.

[12] Martin, J., Ringeval, C., Vennin, V.: Encyclopædia inflationaris. Phys. Dark Universe **5-6** (2014), 75.

[13] Misner, C. W.: Mixmaster Universe. Phys. Rev. Lett. **22** (1969), 1071.

[14] Mortonson, M. J., Weinberg, D. H., White, M.: Dark Energy. In: Patrignani, C., et al. (Particle Data Group), *Review of Particle Physics*. Chin. Phys. C **40** (2016), 100001, p. 402.

[15] Olive K. A., Peacock, J. A.: Big-Bang cosmology. In: Patrignani, C., et al. (Particle Data Group), *Review of Particle Physics*. Chin. Phys. C **40** (2016), 100001, p. 355.

[16] Sakharov, A. D.: Vacuum quantum fluctuations in curved space and the theory of gravitation. Dokl. Akad. Nauk SSSR **177** (1967), 70, in Russian.

[17] Starobinsky, A. A.: A new type of isotropic cosmological models without singularity. Phys. Lett. B **91** (1980), 99.

[18] Zeldovich, Ia. B., Kobzarev, I. Yu., Okun, L. B.: Cosmological consequences of a spontaneous breakdown of a discrete symmetry. Sov. Phys.—JETP **40** (1975), 1.

[19] Zurek, W. H.: Cosmological experiments in superfluid helium? Nature **317** (1985), 505.

Conference *Cosmology on Small Scales 2020*
Michal Křížek and Yurii Dumin (Eds.)
Institute of Mathematics CAS, Prague

COSMIC MICROWAVE BACKGROUND AS THERMAL RADIATION OF INTERGALACTIC DUST?

Václav Vavryčuk[1], Jana Žďárská[2]

[1]Institute of Geophysics, Czech Academy of Sciences
Boční 2, CZ-141 00 Prague 4, Czech Republic
vv@ig.cas.cz
[2]Institute of Physics, Czech Academy of Sciences
Na Slovance 2, CZ-182 21 Prague 8, Czech Republic
zdarskaj@fzu.cz

Abstract: This paper is an interview about an alternative theory of evolution of the Universe with dr. Václav Vavryčuk from the Institute of Geophysics of the Czech Academy of Sciences.

Keywords: Olbers' paradox, adiabatic expansion, Big Bang nucleosynthesis, thermal radiation

PACS: 98.80.-k

Cosmic microwave background (CMB) is a strong and uniform radiation coming from the Universe from all directions and is assumed to be relic radiation arising shortly after the Big Bang. It is the most important source of knowledge about the early Universe and is intensively studied by astrophysicists. Arno Penzias and Robert Wilson (see Figure 1) received the Nobel Prize in 1978 for the CMB discovery and George Smoot and John Mather received the Nobel Prize in 2006 for a discovery of the CMB anisotropy. In this interview, we talk with dr. Václav Vavryčuk from the Institute of Geophysics of the Czech Academy of Sciences about another possible origin of the CMB, and we debate how this alternative theory could affect the currently accepted cosmological model.

Jana Žďárská: Most astrophysicists and cosmologists consider the cosmic microwave background (CMB) as relic radiation originating in the epoch shortly after the Big Bang. However, you propose to explain the CMB as thermal radiation of intergalactic dust. Why?

Václav Vavryčuk: This alternative explanation of the CMB is closely related to the so-called Olbers' paradox, which addresses an apparent discrepancy between observed amount of light coming from the universe and predictions for a model of

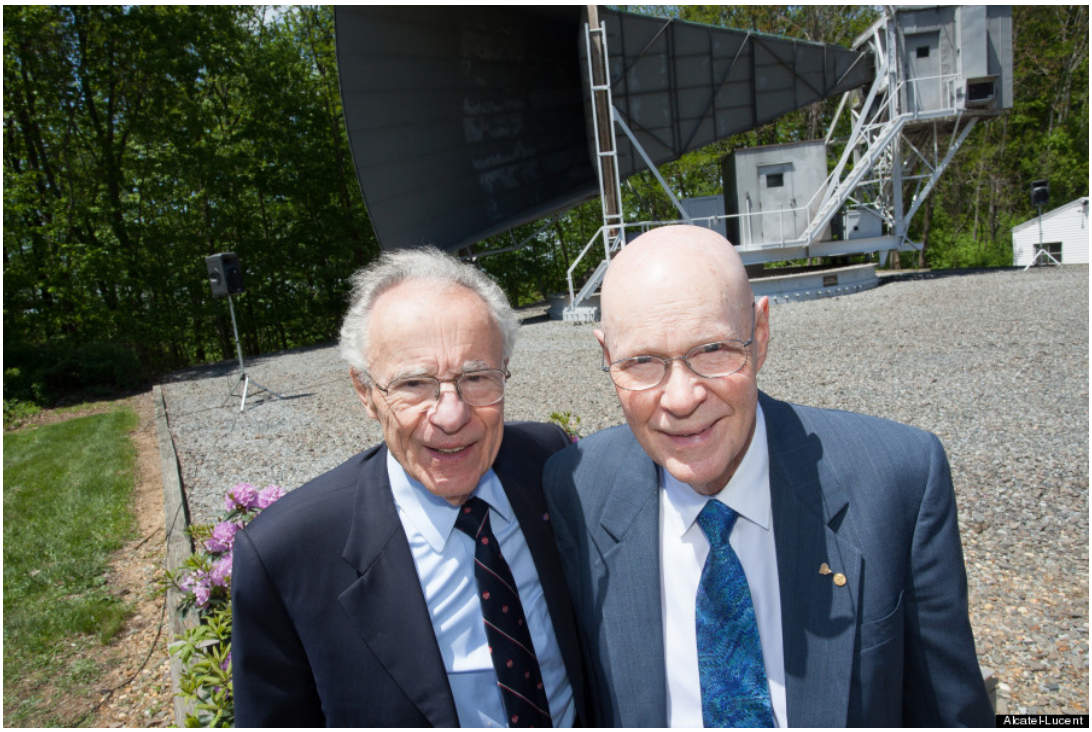

Figure 1: The Nobel Prize laureates Arno Penzias (left) and Robert Wilson (right) for the discovery of the Cosmic Microwave Background.

stationary infinite universe. The model predicts the intensity of light in the night almost 13 orders higher than that actually observed. In 1823, Olbers explained this paradox by light attenuation when photons travel through the universe. However, the Olbers' solution was rejected and the paradox is now explained by an idea of the universe with a finite age, where the finite age prevents accumulating too many photons in the universe. In my theory, I adopt the idea of Olbers and explain the low intensity of light in cosmic space by attenuation of photons by intergalactic dust. Dust grains are present in interstellar and intergalactic matter, they are rich in carbon and they have a complex fluffy shape with size of μm. The dust grains well absorb light in a broad range of wavelengths.

J.Ž.: You mean that the energy of photons absorbed by dust causes that dust is heated up and emits thermal radiation into the cosmic space?

V.V.: Exactly. Dust is present in galaxies but also in intergalactic space. Galaxies produce light and electromagnetic waves at other wavelengths, and dust is warmed up due light absorption. Subsequently, dust emits thermal radiation according to the Planck's law. Light of stars in galaxies can heat up galactic dust grains up to 10–40 K, and in the galaxy centres even to 80 K. However, light intensity in intergalactic space is much lower and the temperature of intergalactic dust is below 5 K.

J.Ž.: Is it possible to calculate the temperature of intergalactic dust more accurately?

V.V.: Yes, we can do that. If we take into account the amount of galactic and intergalactic dust and the amount of light in intergalactic space, it is possible to show that intergalactic dust should have temperature of 2.7 K that is the observed temperature of the CMB (see Figure 2). Hence, my theory suggests that the CMB is not relic radiation originating in the Big Bang but thermal radiation of intergalactic dust.

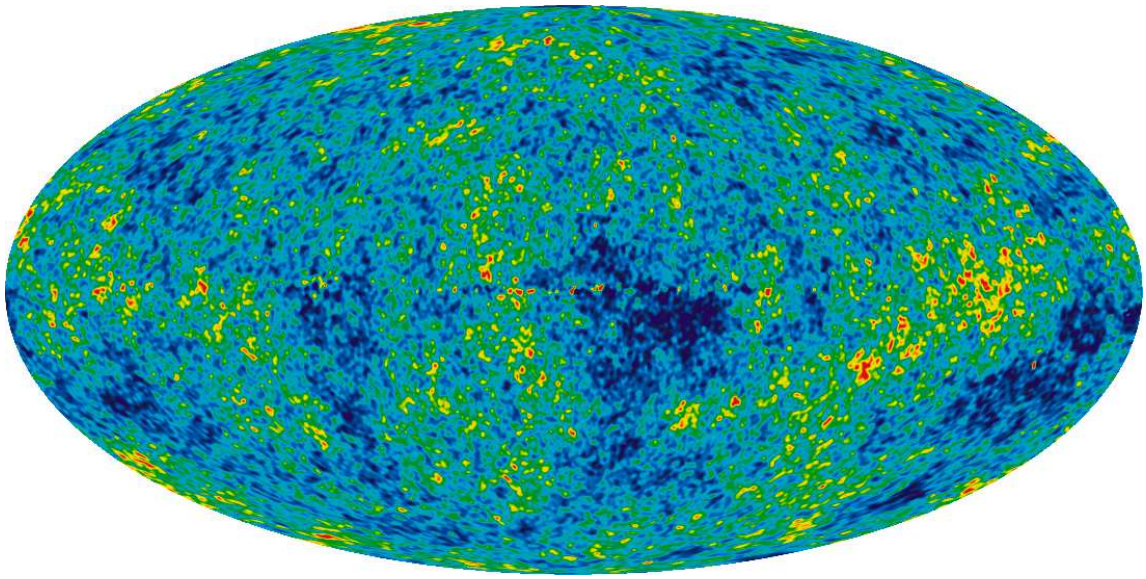

Figure 2: Map of temperature anisotropies of the Cosmic Microwave Background with temperature 2.725 K obtained by the WMAP spacecraft. The colour scale has a range $\pm 70 \mu$K. Source: `http://wmap.gsfc.nasa.gov/media/101080`

J.Ž.: But why the temperature is not continuously increasing by persistent absorption of star light?

V.V.: This is an important question. Intergalactic dust absorbs light from galaxies and is heated up. However, it also emits thermal radiation. Hence, it loses energy and this energy is absorbed back by galaxies. Both energies – absorbed by dust and emitted by dust — are equal and dust is in energy balance. Nevertheless, it does not mean that the temperature of dust was 2.7 K also in the past epochs of the universe. When the universe occupied a smaller volume, galaxies were closer each to the other and the intensity of light was higher in intergalactic space. Consequently, also the dust temperature was higher.

J.Ž.: Does it mean that intergalactic dust is cooling due to the expansion of the universe?

V.V.: Yes, you are right. The process of dust cooling is caused by an adiabatic expansion of the universe. The same property is attributed also to relic radiation of the Big Bang. Light with the temperature of $\sim 3000\,\mathrm{K}$ decoupled from the matter in the early universe with the redshift of ~ 1100, and then it was cooling due to the universe expansion down to the temperature of 2.7 K. However, this theory is not capable to explain, why light was not dimmed and why its spectrum was not disturbed by absorption by galactic and intergalactic dust over the whole history of the universe.

J.Ž.: Your theory provokes many questions and has many important consequences. Can you mention some of them?

V.V.: There are many open questions, which must be explained consistently, the proposed theory to be accepted. For example, why do we observe small temperature fluctuations in the CMB called the CMB anisotropies, and why are they associated with polarization anomalies? In recent years, these anomalies are mapped very accurately by the Planck spacecraft (see Figure 3) and their properties are intensively studied. Interestingly, the origin of the CMB anisotropies is very easy to understand. The thermal radiation of dust depends on the density of galaxies in the universe; hence, it is warmed up to a higher or lower temperature according to the local density of galaxies. Inside galaxy clusters and superclusters, the dust temperature is high, near voids and supervoids with the absence of galaxies, the dust temperature is low. Consequently, we observe a slightly different CMB properties from different directions of the universe. The polarization anomalies can also be explained easily. They just map magnetic fields around galaxy clusters in the universe. The carbon present in dust grains is in the form of graphite and it is conductive. Hence, the dust grains are aligned according to the magnetic field of galaxy clusters and emit polarized light.

J.Ž.: Have you already published your theory?

V.V.: Yes, the theory has been published in several papers [1]–[4]. However, it was not easy, because the idea of the CMB as thermal radiation of intergalactic dust is not new, and it was rejected by the astronomical community many years ago. I had to persuade the editor and reviewers that rejecting this idea was unjustified.

J.Ž.: Your theory can cause a revolution in the modern cosmology. Are there any reactions to your papers?

V.V.: So far, I have noticed just a few reactions to my results. Indeed, my theory is in an essential contradiction with the currently accepted universe model. It refutes fundamentals of the modern cosmology. Obviously, it invokes doubts and suspicions.

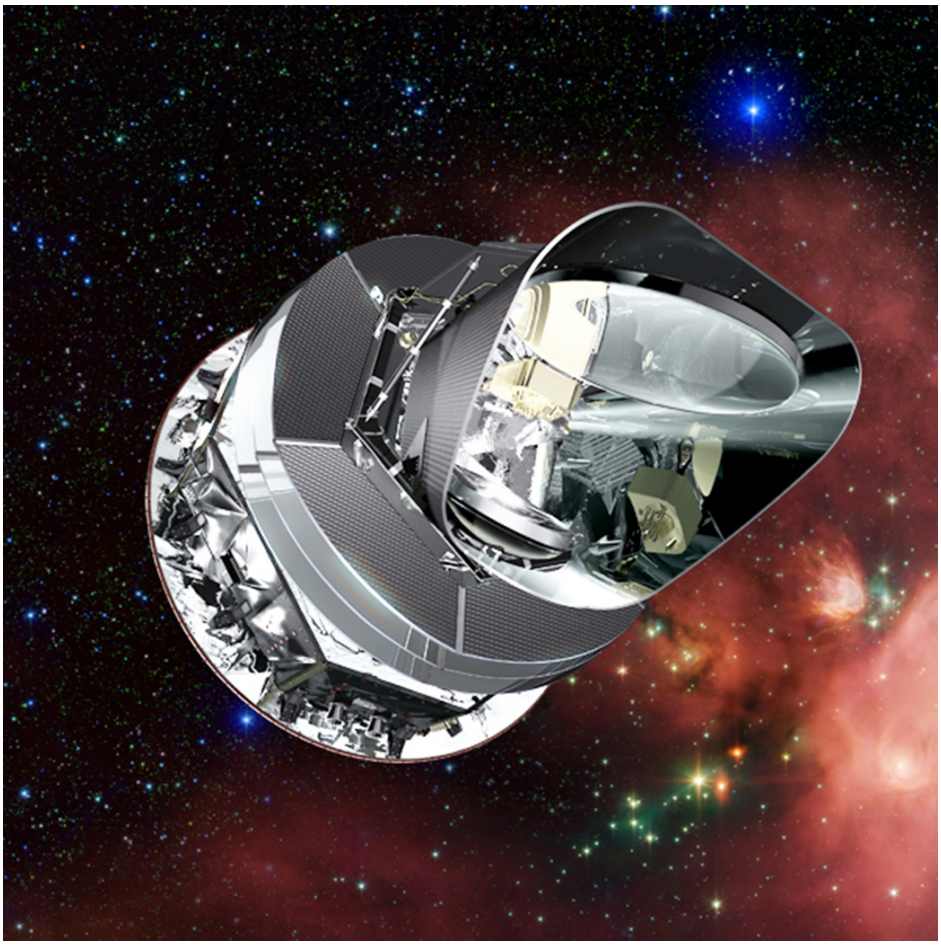

Figure 3: Planck is a space laboratory of the European Space Agency that maps the early universe on wavelengths 0.3–11.1 mm, which corresponds to the Cosmic Microwave Background. Source: `https://www.nasa.gov/mission_pages/planck`

The review process was difficult and reviewers pointed to a negligible chance that my theory could be correct and disprove the accepted cosmological model. They asked for clear and persuasive arguments and calculations supporting my theory and urged me to find weak points of the Big Bang theory and discuss the impact of my results to it.

J.Ž.: You believe that there was no Big Bang. What are your arguments against the Big Bang theory?

V.V.: The main pillar supported the Big Bang theory is the existence of relic radiation. If we question the idea of the CMB as relic radiation of the Big Bang, only few arguments for the Big Bang remain. Moreover, they are rather indirect and not very persuasive.

J.Ž.: One of these arguments is the so-called Big Bang nucleosynthesis. Can you clarify it a little bit and discuss its validity?

V.V.: The Big Bang nucleosynthesis (BBN) predicts a composition of the universe just after the Big Bang. It is believed that the universe was formed by 75% of hydrogen (H) and almost of 25% of helium (^{4}He). Other elements in the early universe were present by less than 1%. For example, the BBN predicts very accurately relative abundances of helium (^{4}He) and lithium (^{7}Li) with respect to the hydrogen. As regards the helium, the first observations did not confirm the prediction, and a satisfactory fit with observations was achieved after two decades of efforts when a large number of random and systematic corrections had to be applied to observations. As regards the lithium, the prediction and observations are completely different with no possibility to remove this discrepancy.

J.Ž.: Is it possible to calculate a ratio between matter and light in the universe?

V.V.: Yes, based on the abundance of deuterium, the nucleosynthesis predicts a ratio between amounts of matter and light in the universe, specifically, the ratio between photons and other particles, such as protons and neutrons. We know well, how many photons are in the cosmic space, and thus we can calculate, how much matter should be there. However, the BBN predicts ten times less number of particles than expected from other observations (e.g., the observed curvature of the universe). Therefore, a new and exotic physical substance called 'dark matter' was introduced to remove this evident discrepancy. It is assumed that the dark matter is formed by unknown particles, which do not interact electromagnetically with the standard matter. Obviously, introducing such an unphysical quantity undermines the credibility of the Big Bang theory.

J.Ž.: You propose a cyclic model of the universe, which periodically expands and contracts with time. How did you come to this idea?

V.V.: A cyclic expansion-contraction of the universe is one of possible alternatives. In contrast to the standard model, I assume that the universe does not contract to a singularity, but just to a volume, which is about 5×10^3 times smaller than at present. Large-scale structures in the universe as galaxies would exist irrespective of the universe expansion history. The cyclic variation of the universe volume could be an analogy to Earth's tides. Of course, there must be forces controlling this cosmic dynamics.

J.Ž.: According to your theory, the universe exists infinitely long time. Do you think that stars could continually arise during such a long period?

V.V.: In my model, the global stellar mass density and the overall dust masses within galaxies and in intergalactic space are essentially constant with cosmic time. Consequently, the cosmic star formation rate should be balanced by the stellar mass-loss rate due to, for example, core-collapse supernova explosions (see Figure 4) and

Figure 4: Image of the remnant of the Type Ia supernova N103B located in the Large Magellanic Cloud taken by the Hubble Space Telescope.
Source: `http://www.sci-news.com/astronomy/type-ia-supernova-remnant-large-magellanic-cloud-04746.html`

stellar winds or superwinds. Hence, formations/destructions of stars and galaxies and complex recycling processes in galaxies and in the intergalactic medium play a central role in this model. Note that the production of heavy elements in stars due to the nuclear fusion can possibly be balanced by their destruction back to hydrogen by a strong radiation of quasars.

J.Ž.: Which highest redshift do we observe and why the current models of the universe are based on the idea of the universe expansion from a singularity?

V.V.: The universe expansion is documented on observations of redshifts measured for nearby and distant galaxies. The most distant known galaxies have redshift of about 11–12. We have no observational evidence about the expansion for earlier cosmic epochs. Hypothetical behaviour of the universe at redshifts higher than 12 is highly speculative and based on very simplistic Friedmann equations, which might be wrong. This includes a hypothesis of the initial singularity as the origin of the universe.

J.Ž.: How about concepts of dark matter and dark energy? Do you consider them in your theory?

V.V.: Dark matter and dark energy are notions contradicting physics and they are missing in my theory. At the present epoch, almost 95% of energy in the universe is attributed to dark matter and dark energy, which violate all known physical laws. In my opinion, these 95% of 'darkness' evidences our substantial ignorance of the universe evolution, and it rather measures how tiny fraction of processes in the universe can be rationally explained by the standard cosmological model.

J.Ž.: As far as I know, the dark energy was introduced in order to explain an unexpected dimming of the luminosity of supernovae, and Saul Perlmutter, Adam Riess and Brian Schmidt received the Nobel Prize in 2011 for this discovery. Can you explain details about this interesting phenomenon?

V.V.: You are right, the supernovae are a hot topic in the current astronomy. Namely, the so-called Type Ia supernovae (SNe Ia) are very useful for cosmology, because they explode with a roughly constant luminosity. Hence, the observed luminosity of these supernovae depends just on their distance. Based on measurements of their luminosity and redshift, we can trace the current velocity expansion and the expansion history of the universe. Surprisingly, the measurements revealed that the luminosity of the supernovae is dimming with distance faster than that predicted by the universe with decelerating expansion. In order to comply the model with the observed dimming, the idea of the expansion decelerating due to the gravity forces acting against the expansion was abandon and substituted by an idea of the accelerating expansion due to the outward repulsive forces associated with dark energy. However, the unexpected luminosity dimming of supernovae with distance is also possible to explain by absorption of light by intergalactic dust without any necessity to introduce dark energy as shown in my recent paper [5].

J.Ž.: Let's go back to your cyclic model of the universe with the absence of the Big Bang. How do you explain the dynamic contraction and expansion of the universe?

V.V.: The dynamic contraction is caused by gravity. The primary question is, however, which forces balance the gravity and give rise to the universe expansion. In my

concept, I assume that the universe works similarly as stars. Also stars are objects with gravity, but still they do not collapse. This is caused by their radiation of light and other electromagnetic waves. The repulsive radiation pressure in stars is so strong that it maintains stars in a balance with gravity and avoids their collapse. The stars collapse only when they are run out of fuel and are not able to radiate photons anymore.

J.Ž.: OK, but how this concept works for the universe with galaxies?

V.V.: In fact, the mechanism is simple. Galaxies are formed by stars, gas and galactic dust, and they emit light into the intergalactic space. This light produces pressure on galaxies and repels the galaxies each from the other similarly as wind acting on sail moves a sailing boat. The process is described by the standard physics and the radiation pressure acting on galaxies can easily be calculated. At present, the radiation pressure is negligible compared to gravity forces and the universe expansion must decelerate. After some time, the expansion will cease due to its deceleration and the universe contraction will begin. With decreasing the volume of the universe, the galaxies will be closer each to the other, and the intensity of light in the intergalactic space will rapidly increase and the contraction will be decelerating. I calculated that the contraction will stop for the universe volume corresponding to redshifts of about 15–20. At such redshifts, the radiation pressure will be so high that the universe will again start to expand. In this concept, the universe has no origin and is infinite in time. The number of galaxies would be roughly the same: the dying galaxies would be substituted by new born galaxies.

J.Ž.: Is there any experiment, which could confirm your theory?

V.V.: The progress in astronomy is based on gradually improving observations. A big step forward was the installation of the Hubble Space Telescope launched into low Earth orbit in 1990, which is capable to detect galaxies with redshifts up to 11–12. Surprisingly, we observe mature galaxies even at such very early universe. This observation belongs to many other puzzles in the Big Bang theory.

J.Ž.: Nevertheless, we need observations even from earlier epochs of the universe using a telescope of higher resolution ...

V.V.: With some delay, a new telescope called the James Webb Telescope (see Figure 5) will be launched in 2021. This telescope should be of about 100 times more sensitive than the Hubble Telescope and should be able to explore very early universe epochs. I expect that it brings many surprising discoveries and it will confirm that the number of galaxies in the universe is roughly constant with time. Now, we observe only the biggest and most luminous galaxies in the early universe, because the luminosity rapidly decreases with distance. With a more sensitive telescope we could observe galaxies in epochs, when no galaxies should exist according to the Big Bang theory. If such galaxies are detected, my cosmological model will be strongly supported.

Figure 5: James Webb Telescope prepared by the cosmic space agency NASA should be launched in 2021. Its sensitivity will be 100× higher than for the Hubble Telescope. Source: `https://bigthink.com/jazzy-quick/the-james-webb-space-telescope-will-bring-us-closer-to-a-galaxy-far-far-away`

J.Ž.: How about the discovery of gravitational waves in the universe, for which Rainer Weiss, Barry Barish and Kip Thorn received the Nobel Prize in 2017*? Can observations of gravitational waves contribute to verification of your theory?*

V.V.: Partially yes. Gravitational waves excited by mergers of neutron star-neutron star or of the black hole-neutron star can serve for measuring the speed of the universe expansion similarly as the luminosity measurements of supernovae. Observations of gravitational waves would be better than those of supernovae, because they are not affected by the presence of intergalactic dust. Hence, they can uniquely confirm or disprove, whether the universe expansion is accelerating according to the Big Bang theory or decelerating according to my cosmological model. However, we need a very sensitive detector of gravity waves, as the planned Einstein Telescope, a third generation detector proposed by a consortium of European institutions, the installation of which is scheduled to 2025.

J.Ž.: Recently, you presented your theory at an international astronomical workshop in Bonn, Germany. How were your ideas received?

V.V.: It was a workshop organized by prof. Pavel Kroupa and his collaborators from the University of Bonn, and devoted to gravity, specifically to difficulties and

controversies in the galaxy dynamics produced by the presence of hypothetical dark matter. My talk was received with interest and invoked a long and eager discussion. However, persuading a broad astronomical community that my cosmological model is correct or at least a reasonable alternative to the Big Bang theory will not be easy and will take time.

J.Ž.: In your opinion, how long time does it take the current cosmological model to be abandon?

V.V.: It is difficult to estimate when the Big Bang idea will definitely be rejected. The most of astronomers and cosmologists accepted this theory, even though it is full of many discrepancies, contradictions and puzzles. Instead of developing new alternative theories, they used to live with these puzzles and became resistant to a critique of the Big Bang. For example, a very old star (denoted as HD 140283) with age of 14.5 billion years was discovered at distance of 60 pc from the Sun. Paradoxically, the age of the universe predicted by the Big Bang theory is estimated to be 13.8 billion years only. Even after this revolutionary discovery, the mainstream opinion on the Big Bang did not change.

J.Ž.: Does it mean that even such evident discrepancy between theory and observations did not wake up astronomers from their lethargy?

V.V.: Yes. This is partly caused by firmly rooted preconceived opinions of astronomers, and by reluctance of scientists, who developed the Big Bang theory, to admit their mistakes. However, the critique of and the unsatisfaction with the current cosmological model are continuously increasing, and a deep crisis in cosmology is coming near. I expect that enough evidence against the Big Bang will be accumulated in the horizon of 5–10 years. It will very much depend on observations of the future James Web Space Telescope, and possibly on the Einstein Telescope for detection of gravitational waves.

J.Ž.: What do you find most fascinating in the universe?

V.V.: I guess, the universe fascinates everybody. As a student of the grammar school, I often visited observatory and admired a variety of stars and galaxies and the immense space among them. In particular, I was excited by the fact that the universe is a subject to simple physical laws. Understanding the universe evolution is a big challenge for us, and I recommend to all scientists, who like solving demanding and ambitious problems, to work in astrophysics and cosmology.

J.Ž.: Thank you very much for the interesting interview and I wish you success with your novel cosmological ideas.

Acknowledgements

We thank Michal Křížek for interesting discussions and fruitful comments.

References

[1] Vavryčuk V.: Impact of galactic and intergalactic dust on the stellar EBL. Astrophys. Space Sci. **361** (6) (2016), art. no. 198.

[2] Vavryčuk V.: Universe opacity and EBL. Mon. Not. R. Astron. Soc. **465** (2) (2016) 1532–1542.

[3] Vavryčuk V.: Missing dust signature in the cosmic microwave background. Mon. Not. R. Astron. Soc. **470** (1), (2017) L44–L48.

[4] Vavryčuk V.: Universe opacity and CMB. Mon. Not. R. Astron. Soc. **478** (1), (2018) 283–301.

[5] Vavryčuk V.: Universe opacity and Type Ia supernova dimming. Mon. Not. R. Astron. Soc. **489** (1) (2019), L63–L68.

Conference *Cosmology on Small Scales 2020*
Michal Křížek and Yurii Dumin (Eds.)
Institute of Mathematics CAS, Prague

A CRITICAL REVIEW OF PARADOXES IN THE SPECIAL THEORY OF RELATIVITY

Michal Křížek

Institute of Mathematics, Czech Academy of Sciences
Žitná 25, CZ-115 67 Prague 1, Czech Republic
krizek@math.cas.cz

Abstract: We show that the Doppler effect and aberration of light can produce more dominant and entirely opposite effects for relativistic speeds than those predicted by the Special Theory of Relativity, in particular, the clock paradox, time dilatation, and length contraction. For instance, an observer will measure a higher frequency of an approaching clock than the same clock has at rest. We also prove that under certain conditions an approaching bar on a photo may seem to have a larger length for a relativistic speed than at rest.*

Keywords: Lorentz transformation, theory of groups, inertial systems, time dilatation, length contraction, twin paradox

PACS: 03.30.+p

1. Introduction

According to Newton's first law of inertia, a body will remain at rest or in uniform motion in a straight line unless acted upon by an external force. This fundamental physical principle serves to introduce the so-called inertial systems in the Special Theory of Relativity (STR), see [7, p. 211]. Consider a fixed coordinate system S with orthogonal axes x, y, z containing a fixed system of hypothetical synchronized clocks[1] that define the time coordinate $t \in (-\infty, \infty)$ of a uniformly flowing time. The coordinate system S is called *inertial* if it obeys Newton's first law of motion.

Let S' be another coordinate system with orthogonal axes x', y', z' which are for simplicity parallel with x, y, z and have the same scale at rest, see [25]. The time $t' \in (-\infty, \infty)$ in S' is introduced similarly using a fixed system of synchronized clocks in S' having also the same time scale at rest. Let the origin of S' move along

*Adapted and extended from the Czech version [12].

[1]This can be, in fact, interpreted so that all clocks are synchronized by an infinite speed of signal.

the x axis at a constant speed $v \in (-c, c)$, where c is the speed of light in vacuum[2], see Figure 1.

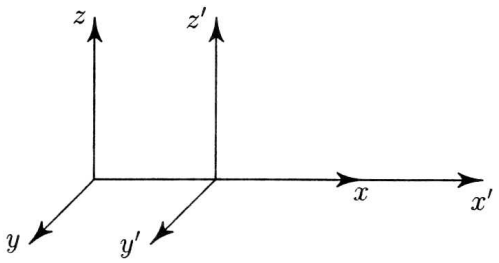

Figure 1: The inertial system S' is moving by speed $v \in (-c, c)$ with respect to the system S.

The Lorentz transformation (see [13]) is a fundamental tool of the STR. The parameter defined by

$$\gamma_v = \frac{1}{\sqrt{1 - \dfrac{v^2}{c^2}}} \geq 1 \tag{1}$$

is called the *Lorentz factor*. Points of the spacetime $\mathbb{R}^4$ are called *events*. Unless otherwise stated, we will restrict ourselves to one pair of the above described inertial systems, where the event is determined by the encounter of the origins of S and S' determines the beginning of time counting in the first and in the second inertial system, respectively, i.e., $t = 0$ in S and $t' = 0$ in S'. In this special case the *Lorentz transformation*[3] has the form $\mathcal{L}_v \colon \mathbb{R}^4 \to \mathbb{R}^4$,

$$x' = \gamma_v(x - vt), \tag{2}$$
$$y' = y,$$
$$z' = z,$$
$$t' = \gamma_v \left(t - \frac{v}{c^2} x \right), \tag{3}$$

where $x, y, z, t \in (-\infty, \infty)$ and the last equality expresses how to transform a uniformly flowing proper time during transition from S to S'. Events which are simultaneous[4] in S are given by the identity $t \equiv t_0$, where t_0 is a fixed constant. By (3)

[2]The basic postulate of the STR that the speed of light c has the same size in all inertial systems was verified experimentally on the Earth by the well-known Michelson's experiments, see [14].

[3]Albert Einstein uses the transformation (2)–(3) in his pioneering paper [5, p. 902] from 1905, but does not use the term intertial. He also does not cite Lorentz's paper [13, p. 185] from 1892 nor does he mention Hendrik Lorentz himself. Einstein probably knew Lorentz's work [13], since the titles of their two papers are very similar. Moreover, Lorentz was very famous after receiving the Nobel Prize in 1902.

[4]Let us emphasize that any two different events which are simultaneous in S are not causally connected. Thus, one can verify that they were really simultaneous only when their future light cones intersect (cf. Figure 5).

we see that the time t' depends not only on t but also on the position x, i.e., t' is not constant and thus the corresponding events do not have to be simultaneous in S' for $v \neq 0$.

Notice that the right-hand sides of relations (2) and (3) are linear functions in variables x and t for any fixed v. Thus, for $\boldsymbol{x} = (ct, x, y, z)$ and $\boldsymbol{x'} = (ct', x', y', z')$ the Lorentz transformation can be rewritten into the matrix form

$$\boldsymbol{x'} = \boldsymbol{L}_v \boldsymbol{x},$$

where

$$\boldsymbol{L}_v = \begin{pmatrix} \gamma_v & -\frac{v}{c}\gamma_v & 0 & 0 \\ -\frac{v}{c}\gamma_v & \gamma_v & 0 & 0 \\ 0 & 0 & 1 & 0 \\ 0 & 0 & 0 & 1 \end{pmatrix} \tag{4}$$

is a block diagonal symmetric and positive definite matrix. Note that the physical dimension of all entries of the vectors $\boldsymbol{x}$ and $\boldsymbol{x'}$ is one meter.

The inverse matrix $\boldsymbol{L}_v^{-1}$ has a similar form as $\boldsymbol{L}_v$, only the two minus signs in (4) have to be replaced by plus. Therefore, the Lorentz transformation $\mathcal{L}_v$ is a one-to-one mapping from $\mathbb{R}^4$ onto $\mathbb{R}^4$ for $v \in (-c, c)$.

Let us point out that in the limit case $|v| = c$, the matrix (4) becomes singular, since its two first rows are linearly dependent. Consequently, the Lorentz transformation should not be applied to the surface of the light cone. Its inverse does not exist.

2. Time dilatation

The relation (3) is to be understood only as the time which we would record at the moment when the two clocks in S and S' are closely passing each other at one single x-coordinate (e.g. at the origin). So we can compare only time data t and t' of local clocks, because the concept of the present is relative. By definition, all clocks in each inertial system at rest show the same time in the whole infinite three-dimensional space (e.g. at the beginning and at the end of a motionless bar). So when we are exactly in the middle between any two fixed clocks, they will show us the same time.

Consider a fixed time interval

$$\Delta t' = t'_2 - t'_1,$$

where t'_i are space independent coordinates in S'. For an arbitrary fixed point x in S we determine the corresponding t_2 and t_1 from formulae (cf. (3))

$$t'_2 = \gamma_v \left(t_2 - \frac{v}{c^2} x \right), \quad t'_1 = \gamma_v \left(t_1 - \frac{v}{c^2} x \right),$$

and we set $\Delta t = t_2 - t_1$. From this we get the so-called *time dilatation* (see e.g. [10, p. 430])

$$\Delta t' = \gamma_v \left(t_2 - \frac{v}{c^2} x - t_1 + \frac{v}{c^2} x \right) = \gamma_v \Delta t. \tag{5}$$

By (1) we see that $\Delta t' > \Delta t$ for any $v \neq 0$ independently of the sign of v. The relation (5) actually expresses that the time, measured by a clock in a moving system S', runs slower than the time measured by a clock that is at rest with respect to S.

The clock at rest is fastest.

The time dilation is usually theoretically justified as follows: A photon launched from the origin of the system S in the z direction flies obliquely at S' with speed c. Therefore, in terms of an observer in S' this photon needs longer time to reach the plane $z' = z = 1$ than in terms of an observer in the system S.

Remark 1. The experimental verification of time dilation can be demonstrated by means of particles called muons whose mean half-life time at rest is $\tau = 2.2 \cdot 10^{-6}$ s. From observations of cosmic rays we know that if muons move linearly at almost the speed of light, they will travel on average much longer distance than $c\tau = 660$ m. However, it should be emphasized that in the inertial system associated with muons their decay will not slow down. In another experiment [3], the time dilatation is verified by means of the transverse Doppler effect.[5] Lithium ions accelerated to the speed $v = 0.338c$ are used as clocks. Note that the Hafele-Keating experiment [9] with two atomic clocks in airplanes and one on the Earth is not too credible, since none of the corresponding three systems was inertial. □

The non-relativistic longitudinal Doppler effect[6] (see [4]) is described by the relation

$$f_v = \frac{c}{c - v} f, \tag{6}$$

where f is the source frequency at rest, v is the speed of the source approaching an observer along the axis x, f_v is the frequency measured by the observer, and c is the speed of signal. For relativistic speeds this relationship needs to be corrected by time dilation, see [7]. All physical processes including clock speed in S' will run by (3) slower when observed from S. Thus by (6), the new relation will be of the form

$$f_v = \frac{c}{c - v} f', \tag{7}$$

[5]The transverse relativistic Doppler effect was first measured by Ives in [11] already in 1938. In classical mechanics, this transverse effect does not occur, because it is given by time dilation (5) only.

[6]Olaf Rømer (in Journal des Sçavans, 1676) suggested an elegant method to measure the speed of light. When the Earth moved toward Jupiter, the time interval between successive eclipses of Jupiter's moon Io became steadily shorter with respect to the terrestrial time. When the Earth moved away from Jupiter these eclipses became steadily longer, i.e., they were behind the expected values. Rømer thus actually found a phenomenon, which was later named after Christian Doppler.

where c is the speed of light and

$$f' = \gamma_v^{-1} f \tag{8}$$

corresponds to the lower frequency calculated from (5). By (7), (8), and (1) we obtain a relativistic Doppler relation for the frequency detected in S (see [5]),

$$f_v = \frac{1}{1-\frac{v}{c}} f' = \frac{\gamma_v^{-1}}{1-\frac{v}{c}} f = \frac{\sqrt{1-\left(\frac{v}{c}\right)^2}}{1-\frac{v}{c}} f = \sqrt{\frac{c+v}{c-v}} f. \tag{9}$$

From this we immediately get the following theorem.

Theorem 1. *For any $v \in (0, c)$ we have that $f_v/f' > f_v/f > 1$. Moreover, $f_v/f \to \infty$ as $v \to c$.*

Consequently, the Doppler effect manifests more than the time dilation itself, whenever the clock approaches the observer. Hence, the higher the speed v, the greater the Doppler effect. Special relativity effects for large v are of higher order than those arising from the Doppler effect.

It is therefore very important to distinguish consistently between reconstructions (calculations by means of the Lorentz transformation) and observations (measurements, photographs, videos). The notion "observer" in the STR is somewhat confusing. It should not be a person who only applies relations (2)–(3). The observer performs real observations and measurements including all effects together as it is usually understood, i.e., the observer measures incoming frequencies.

Example 1. Suppose that a clock will be approaching the origin of S at relativistic speed $v = 0.8c$. Its proper time will pass slower than on clocks fixed in the system S, since by (1) and (5) we have

$$\gamma_v = \frac{1}{\sqrt{1-0.64}} = \frac{5}{3}$$

and

$$\Delta t' = \frac{5}{3}\Delta t.$$

However, substituting $v = 0.8c$ into (9), we find that

$$f_v = 3f \quad \text{and} \quad f_v = 5f', \tag{10}$$

i.e., the observer at the origin of S will detect a $3\times$ higher (blue-shifted) frequency than the same clock has at rest in the system S and even a $5\times$ higher frequency than the time dilatation predicts (see (8)). This may seem to be paradoxical. For a clock receding the origin by the speed $(-v)$, the observer will detect by (9) a $3\times$ lower (red-shifted) frequency than f. So there is a jump in these constant frequencies

at the origin and only in this single point the observer can theoretically detect the proper frequency f'. So the Doppler effect plays an essential role. □

Remark 2. The observer usually does not have a possibility to measure directly the speed v of some distant object so that he could immediately use the Lorentz transformation. However, he can measure the frequency f_v (blue-shifted or red-shifted) of some characteristic spectral line of a certain chemical compound and establish the corresponding quiescent frequency f. From this and (9) he can establish the speed v (or its radial component in general case). Then he can determine the factor γ_v^{-1} and find how significant are the corresponding relativistic effects (2)–(3). □

3. The Lorentz transformation does not allow superluminal velocities

First we recall Einstein's formula [5] for a relativistic addition of velocities, see also [17, Chapt. I.6].

Theorem 2 (Einstein). *Let $u \in (-c, c)$ and $w \in (-c, c)$ be constant velocities of a point-like object in the system S and S', respectively, in the direction of the horizontal axis. Then*

$$u = \frac{v + w}{1 + \dfrac{vw}{c^2}}, \tag{11}$$

where $v \in (-c, c)$ is a constant speed of S' with respect to S.

P r o o f: Velocities u and w are constant in S and S', respectively. Therefore,

$$u = \frac{\mathrm{d}x}{\mathrm{d}t} \quad \text{and} \quad w = \frac{\mathrm{d}x'}{\mathrm{d}t'}. \tag{12}$$

By (3) we get

$$\frac{\mathrm{d}t'}{\mathrm{d}t} = \gamma_v \left(1 - \frac{v}{c^2}\frac{\mathrm{d}x}{\mathrm{d}t}\right) = \gamma_v \left(1 - \frac{uv}{c^2}\right),$$

where the difference in parenthesis is obviously positive. Using this equality, (12), and (2) we find that

$$w = \frac{\mathrm{d}x'}{\mathrm{d}t'} = \frac{\mathrm{d}x'}{\mathrm{d}t}\frac{\mathrm{d}t}{\mathrm{d}t'} = \gamma_v \left(\frac{\mathrm{d}x}{\mathrm{d}t} - v\right) \gamma_v^{-1} \left(1 - \frac{uv}{c^2}\right)^{-1} = \frac{u - v}{1 - \dfrac{uv}{c^2}}.$$

From this it follows that

$$u - v = w - \frac{uvw}{c^2}.$$

Now it is enough to evaluate u and we obtain (11). □

For example, by Theorem 2 we see that for $v = w = \frac{2}{3}c$ the speed $u = \frac{12}{13}c$ is less than c. In the next theorem we prove that from (11) we can never get the speed of light or faster-than-light speed u, even if $|v|$ and $|w|$ are arbitrarily close to c.

First, let us recall that a *group* G is a set equipped with an associative binary operation $\circ\colon G \times G \to G$ and with the neutral element e such that for any $g \in G$ there exists exactly one inverse element $g^{-1} \in G$ for which

$$g \circ g^{-1} = e = g^{-1} \circ g.$$

The composition $\circ$ of two Lorentz transformations $\mathcal{L}_v$ and $\mathcal{L}_w$ given by relations (2)–(3) for $v, w \in (-c, c)$ is defined as follows

$$\mathcal{L}_u = \mathcal{L}_v \circ \mathcal{L}_w, \tag{13}$$

where u satisfies Einstein's formula (11).

Theorem 3. *Lorentz transformations $\mathcal{L}_v$ for all $v \in (-c, c)$ defined by* (2)–(3) *form an Abelian group.*

P r o o f: If $v, w \in (-c, c)$ then obviously

$$\left(1 + \frac{v}{c}\right)\left(1 + \frac{w}{c}\right) > 0 \quad \text{and} \quad \left(1 - \frac{v}{c}\right)\left(1 - \frac{w}{c}\right) > 0.$$

From this we find that

$$-\left(1 + \frac{vw}{c^2}\right) < \frac{v + w}{c} < 1 + \frac{vw}{c^2},$$

and thus

$$-c < \frac{v + w}{1 + \dfrac{vw}{c^2}} < c.$$

Comparing with Einstein's formula (11), we see that $u \in (-c, c)$, i.e., $|u|$ is always less than c.

Using (1) for $v = 0$, we find that $\gamma_0 = 1$ and the corresponding transformation $\mathcal{L}_0$ is the identity, i.e. the neutral element.

From (11) and (13) we immediately get that

$$\mathcal{L}_v \circ \mathcal{L}_{-v} = \mathcal{L}_0 = \mathcal{L}_{-v} \circ \mathcal{L}_v,$$

where $\mathcal{L}_{-v}$ is the inverse transformation, i.e., $x = \gamma_v(x' + vt')$, $t = \gamma_v(t' + vx'/c^2)$.

The composition $\circ$ is commutative, since the special block diagonal matrices $\boldsymbol{L}_v$ and $\boldsymbol{L}_w$ defined by (4) are commutative, i.e.

$$\begin{aligned}
\boldsymbol{L}_v\boldsymbol{L}_w &= \begin{pmatrix} \gamma_v & -\dfrac{v}{c}\gamma_v & 0 & 0 \\ -\dfrac{v}{c}\gamma_v & \gamma_v & 0 & 0 \\ 0 & 0 & 1 & 0 \\ 0 & 0 & 0 & 1 \end{pmatrix} \begin{pmatrix} \gamma_w & -\dfrac{w}{c}\gamma_w & 0 & 0 \\ -\dfrac{w}{c}\gamma_w & \gamma_w & 0 & 0 \\ 0 & 0 & 1 & 0 \\ 0 & 0 & 0 & 1 \end{pmatrix} \\
&= \begin{pmatrix} \gamma_v\gamma_w + \dfrac{vw}{c^2}\gamma_v\gamma_w & -\dfrac{v + w}{c}\gamma_v\gamma_w & 0 & 0 \\ -\dfrac{v + w}{c}\gamma_v\gamma_w & \gamma_v\gamma_w + \dfrac{vw}{c^2}\gamma_v\gamma_w & 0 & 0 \\ 0 & 0 & 1 & 0 \\ 0 & 0 & 0 & 1 \end{pmatrix} = \boldsymbol{L}_w\boldsymbol{L}_v
\end{aligned}$$

for all $v, w \in (-c, c)$. The associativity of the operation $\circ$ is due to the fact that matrix multiplication is associative. □

4. Length contraction

Lorentz's length contraction is an immediate consequence of the Lorentz transformation. On the horizontal axis x' consider a fixed bar which is at rest in the system S'. Denote its length by

$$\Delta x' = x'_2 - x'_1, \tag{14}$$

where x'_i are fixed time independent coordinates of its ends in S'. For an arbitrary fixed time instant t in S we determine the corresponding x_2 and x_1 from formulae (cf. (2))

$$x'_2 = \gamma_v(x_2 - vt), \quad x'_1 = \gamma_v(x_1 - vt),$$

and we set $\Delta x = x_2 - x_1$. Substituting this into (14), we get (cf. (5))

$$\Delta x' = \gamma_v(x_2 - vt - x_1 + vt) = \gamma_v \Delta x. \tag{15}$$

Denoting $\ell_0 = \Delta x'$ and $\ell = \Delta x$, we get by (1) the well-known *length contraction*

$$\ell = \ell_0 \sqrt{1 - \frac{v^2}{c^2}}. \tag{16}$$

The bar at rest has the greatest length.

Remark 3. For the time being there is no direct experimental evidence of length contraction (16). Anyway, we can verify it indirectly by means of muons mentioned in Remark 1. In the system S associated with these muons at rest we will observe their usual mean half-life time $\tau = 2.2 \cdot 10^{-6}$ s. However, in S' connected with Earth's atmosphere they will travel longer distance than $c\tau = 660$ m. This demonstrates the length contraction is S'. □

In 1959, Roger Penrose published a paper [18] (see also [19, p. 431], [20]) describing why we should see a quickly flying non-rotating ball in a photo again like a ball. In the same year, his thoughts were elaborated in more detail by James Terrell [21] using light aberration. Here is a specific example showing the substantial effect of light aberration for relativistic speeds.

Example 2. Consider a bar with length $\ell_0 = 1$ m. Assume that it moves from the left to the right along the axis x by the constant speed $v = 0.8c$ and that its front end just reached the origin of the coordinate system S. By (16) the bar is shortened to

$$\ell = \ell_0 \sqrt{1 - 0.64} = 0.6 \text{ m},$$

and thus the length of the straight line segment AC in Figure 2 is $|AC| = 0.4$ m. We will photograph this bar from the axis z by a fixed nonrotating camera which is placed at the distance

$$d = 0.75 \text{ m} \tag{17}$$

from the origin. Using the similarity of right triangles from Figure 2, we find that $|BC| = |AC|d/\ell_0 = 0.3$ m. From this we have $|AB| = \sqrt{0.4^2 + 0.3^2} = 0.5$ m. The segment on the hypotenuse from B to the camera has the same length in meters as d in (17),

$$\sqrt{1^2 + 0.75^2} - |AB| = 1.25 - 0.5 = d. \tag{18}$$

To avoid blurred photos, we assume that our idealized camera can take pictures within 1 picosecond. During this time period, the light will fly 0.3 mm only and a possible blurring will not play a significant role. For simplicity, we shall analyze only that photo, in which the front end of the bar just reached the coordinate origin of S. However, the rear end of the bar will be on the photo farther than ℓ, since the light from the front end flies along a shorter distance d than the light from the rear end (see Figure 2). That is why there will be recorded photons on the photo from the

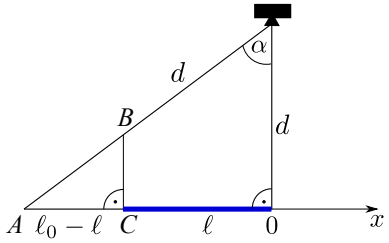

Figure 2: The length of the legs of the larger (or smaller) right triangle is 1 and 0.75 (or 0.4 and 0.3) meters. The ratio between the lengths of sides of the both triangles is 5 : 4 : 3. Due to light aberration the flying bar from the left to the right at the speed $0.8c$ has the same length in the photo as the same bar at rest. A photon emitted to the camera from the rear end of the moving bar will always have the same x coordinate as this rear end in this special case.

rear end of the bar that were emitted earlier than those from the front end. During the time period, when the rear end of the bar moves from A to C, a photon pointing from A to the camera will travel the distance $|AB|$, since $v/c = |AC|/|AB| = 0.8$. Hence, thanks to light aberration and (18) the moving bar will have on the photo the same length as the fixed one meter long bar. □

Let us point out that a photon will travel the distance d from the origin to the camera during the time period $\Delta t = d/c$. During this period, the bar will shift about $v\Delta t = 0.8d = 0.6$ m, i.e., it will be placed entirely to the right of point 0.

Example 3. Let again $\ell_0 = 1$ m and $v = 0.8c$. Hence, $\ell = 0.6$ m. This time, however, we place the camera closer to the axis x, i.e. $d < 0.75$ m. We shall again analyze the image, where the right end of the bar is at the origin. The left end of the

bar will shift from the point $A = (-a, 0)$ to the point $(-\ell, 0)$ during the time period $\Delta t = (a - \ell)/v$. During this period, a photon will travel the distance $c\Delta t$ from the point A to the camera. From the relation $a^2 + d^2 = ((a - \ell)c/v + d)^2$ we can derive the following inverse formula

$$d = \frac{a^2\left(\frac{v}{c} - \frac{c}{v}\right) + 2a\ell\frac{c}{v} - \ell^2\frac{c}{v}}{2(a - \ell)}.$$

For instance, when $a = 2$ m we obtain $d = \frac{15}{56} = 0.26\ldots$ m. So if we place the camera on the axis z at a distance of 26 cm from the origin, the one meter flying bar will appear extended in the photo as two meters long. Similarly for $v = 0.9$ and $d = 4$ cm we even get $a = 4$ m. The main reason for these surprising phenomena is that photons, which simultaneously passed through the lens, were not emitted simultaneously in S.

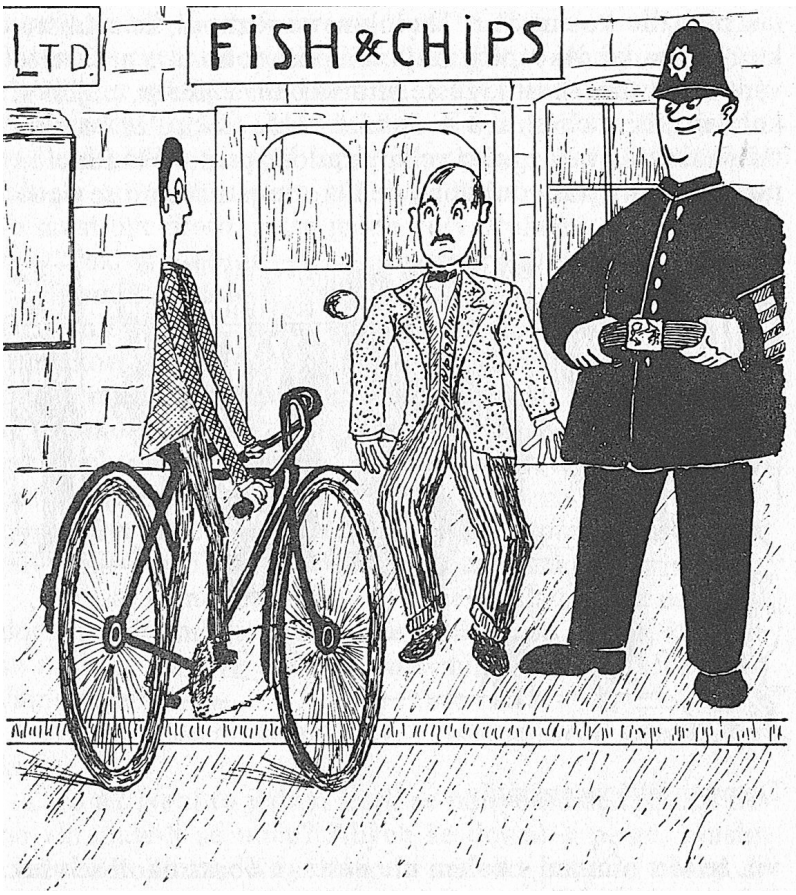

Figure 3: (see [8]). The man in the middle should observe much longer bicycle in the x-direction due to light aberration (compare with the observed bar from Example 3). Moreover, the wheels should not look like ellipses and its wires should be bent.

For $d = 0$ no aberration effect appears. The photon from the end of the bar will travel a distance of 3 m in the x-direction within 1 μs. During this time period, the end of the bar will move $3 \cdot 0.8 = 2.4$ m. Thus the photon just gets to the beginning of the bar, since $2.4 + 0.6 = 3$ m. □

Approaching objects are manifested by blue shift (i.e. shortening the wave length). However, due to aberration they may seem to be prolonged, which is paradoxical. On the other hand, receding objects that are manifested by red shift may seem to be shortened.

For $d > 0.75$ m we shall see the bar in the photo shorter than 1 meter. The same bar will also be shorter than ℓ, if we photograph it so that its left end is at the origin. If it is placed exactly symmetrically with respect to the origin, its length on the photo will be just ℓ, but nonlinearly deformed. In the article [23], Weisskopf describes an apparent deformation of a quickly flying cube on a photo.

Example 4. Due to Example 3, Figures 3 and 4 taken from the popularization book [8, Chapt. 1] are confusing. □

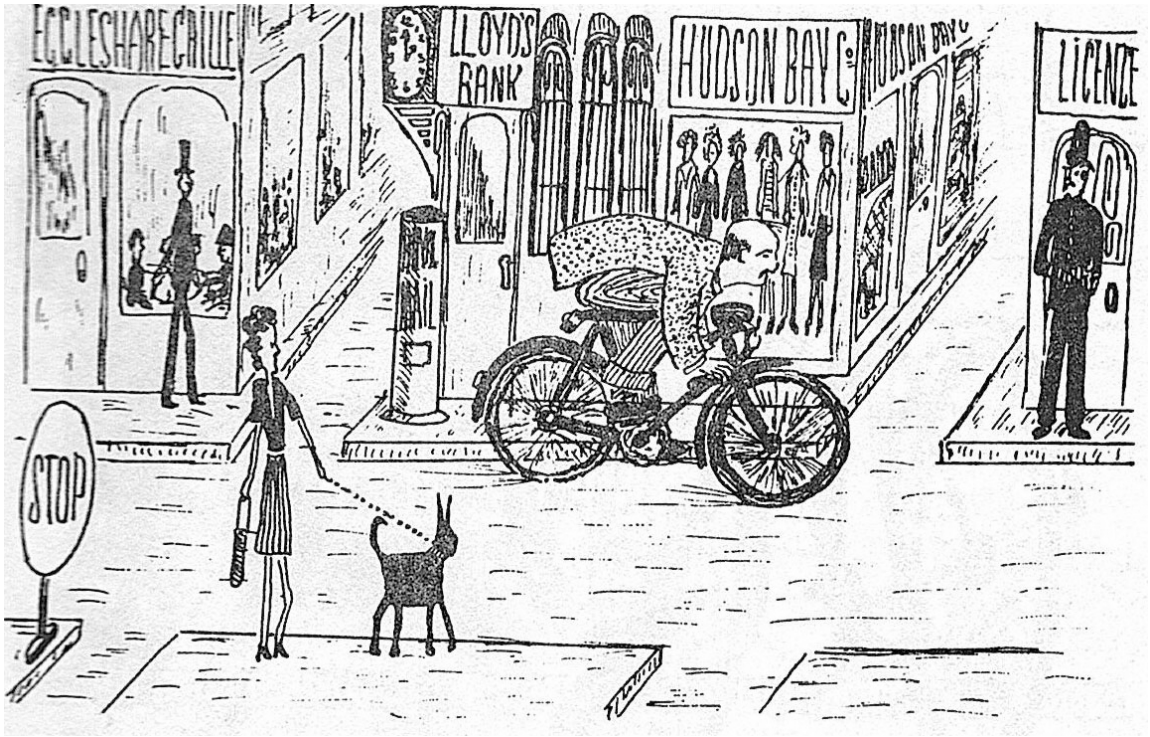

Figure 4: (see [8]). The man on the bicycle should see the policemen on the right thicker due to light aberration.

5. The twin paradox

In a series of publications [6], [8], [15, p. 167], [16], ... the twin paradox (called also the clock paradox) is described by means of time dilation as follows:

One of the twins Adam stays on Earth while the other twin Bob flies in a rocket e.g. to the star Sirius about 8 light years away with constant relativistic speed v. Bob's time runs slower due to time dilatation and his distance to Sirius is less than 8 light years due to length contraction. When Bob returns with velocity $(-v)$ back on Earth, he finds out that his brother Adam is much older than him.

Now let us look at the twin paradox in more detail. First we present a wrong argumentation which is sometimes proposed in the literature (and on internet).

Example 5 (Wrong argumentation). Let again $v = 0.8c$. For simplicity, the speed of light $c = 1$ ly/yr will be not explicitly marked in this example. According to Adam's time, Bob will reach Sirius within 10 years and the same amount of time he will fly back, i.e. 20 years altogether. The first half of Bob's trajectory is defined by the equation $x' = 0$ in the system S' implying by (2) that Bob will follow the line $t = \frac{5}{4}x$ in S (see the lower thick line in Figure 5). Its second half in the inertial system S'' associated with speed $(-v)$ is given by the equation $x'' = 0$ yielding $t = 20 - \frac{5}{4}x$.

Bob's proper time in the first half of his trip is $t' = \gamma_v(t - 0.8x)$ due to (3). From this for a constant time t' we obtain the equation $t = \frac{4}{5}x + \text{const}$ which determines in S the space of simultaneous events in S'. Its graph has to pass through the event given by $x = 8$ ly and $t = 10$ yr when Bob reaches Sirius. Hence, the corresponding space of simultaneity is given by the equation $t = \frac{4}{5}x + 3.6$, since $10 = \frac{4}{5} \times 8 + 3.6$ (see the dashed line passing through $t = 3.6$ on vertical axis in Figure 5). Similarly we find that the second space of simultaneous events in S'' is given by $t = -\frac{4}{5}x + 16.4$. During Bob's turn at Sirius, the time on Earth will jump about $20 - 2 \times 3.6 = 12.8$ yr. This time interval is not accounted by Bob and thus he will return 12.8 years younger than his twin Adam (see the left vertical axis t in Figure 5). □

Why is the above argumentation wrong? There are several reasons. Bob's proper time t' (and also t'') was not taken into account correctly as we shall see in Example 6. We saw in Theorem 1 and Example 1 that the Doppler effect plays an important role in the STR. However, it was also not taken into account in Example 5. Bob feels an infinite deceleration[7] during his turnover at Sirius. The reader is juggled that this is the main reason for the twin paradox, since Bob changes its inertial system. However, this is not true, since when Bob reaches Sirius, he can just transmit information about his real age in the system S' to another traveler who is fixed in the system S'' associated with speed $(-v)$. The same applies for Bob's departure and arrival back to the Earth.

Moreover, it is said that Bob will observe a large jump in time on Earth, since no event from the red interval (3.6, 16.4) on the vertical axis in Figure 5 is simultaneous

[7] Roger Penrose [19, p. 421] rounds the corresponding world lines on a small neighborhood around the three critical points to avoid an infinite acceleration or deceleration.

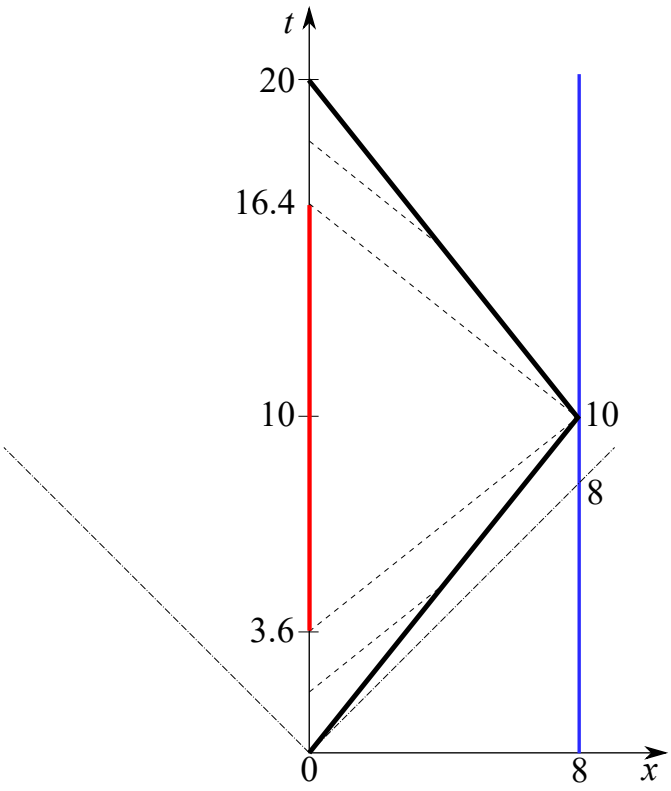

Figure 5: The vertical axis t shows the time in years and the horizontal axis x shows the distance in light years. The left vertical line is the world line of Adam who stays on Earth. The right vertical line corresponds to the world line of Sirius. The world line of flying Bob is marked with a thick piecewise linear line given by equations $t = \frac{5}{4}x$ and $t = 20 - \frac{5}{4}x$. The future light cone $t = |x|$ is marked by the dot-and-dash line and the dashed lines stand for events with simultaneous times in S' and S'' such that t' and t'' are constant.

with Bob. In Example 6, we will show that Bob will see only a jump in frequencies and no jump in time in S during his turnover (see Figure 6).

So further, we shall investigate the twin paradox from another point of view. We will get different values than in Example 5.

Theorem 4. *The difference $(ct)^2 - x^2$ is invariant with respect to the Lorentz transformation.*

P r o o f: From (2)–(3) we see that

$$\begin{aligned}(ct')^2 - x'^2 &= (ct' - x')(ct' + x') \\ &= \gamma_v \left(ct - \frac{vx}{c} - x + vt\right) \gamma_v \left(ct - \frac{vx}{c} + x - vt\right) \\ &= \gamma_v^2 \left(1 + \frac{v}{c}\right)(ct - x)\left(1 - \frac{v}{c}\right)(ct + x) = (ct)^2 - x^2. \end{aligned} \tag{19}$$

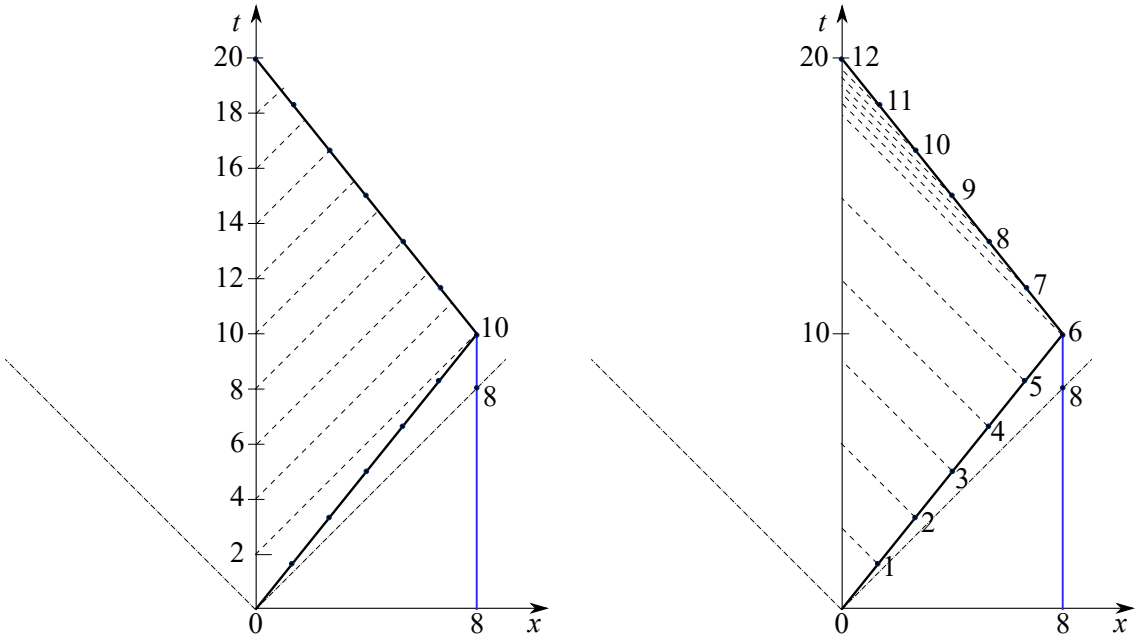

Figure 6: The notation is the same as in Figure 5 except for dashed lines. Here dashed lines indicate trajectories of photons launched every year by Adam and Bob. Left: Adam sends a periodic signal to Bob. Right: Bob sends a period signal to Adam. There is not jump in time — only a jump in received frequencies.

Hence, this difference of squares is invariant with respect to the Lorentz transformation. □

Example 6 (Right argumentation). Let again $v = 0.8c$. Since Bob is at rest in the system S', we have that $x' = 0$. Thus from (19) we get for $\Delta t = 10$ yr and $\Delta x = 8$ ly

$$c\Delta t' = \sqrt{(c\Delta t)^2 - (\Delta x)^2} = \sqrt{100 - 64} = 6 \text{ ly}. \tag{20}$$

Consequently, Bob will fly 6 years to Sirius according to his proper time (see bullets in Figure 6). Thus his clock at Sirius will show 6 years. On the other hand, the corresponding time interval on Earth is only 3.6 years (see Figure 5), since $\Delta t = \gamma_v^{-1}\Delta t' = \frac{3}{5} \cdot 6 = 3.6$ years by (5).

Let f be the same frequency of Adam's and Bob's clock at rest. Due to the relativistic Doppler relation (9), Adam will observe $3\times$ lower frequency from Bob's clock, since

$$f_{-v} = f\sqrt{\frac{c-v}{c+v}} = \frac{1}{3},$$

and after the turnover of Bob, Adam will observe the frequency $f_v = 3f$, see (10) and Figure 6. Adam will receive the same frequencies from Bob due to the relativity principle.

Obviously, Bob will fly after the turnover the same distance back to Earth with velocity $(-v)$ again 6 years according to his proper time. So he will be $20-2\times 6=8$ years younger than his twin Adam. This is a different result than in Example 5. Bob will see all instants on Earth, i.e., no time interval will be skipped. □

Example 7. How younger was Niel Armstrong when he returned from the Moon? For simplicity, assume that he was flying there and back by the constant speed $v = 10$ km/s and that $\Delta x = 384\,000$ km is the Earth-Moon distance. Hence, the one-way flight lasted

$$\Delta t = \frac{\Delta x}{v} = 38\,400 \text{ s} \tag{21}$$

with respect to Earth's clock. Then like in (20) we get

$$\Delta t' = \sqrt{(\Delta t)^2 - \frac{(\Delta x)^2}{c^2}} = \sqrt{38\,400^2 - 1.28^2} = \sqrt{1\,474\,559\,998.3616}$$
$$= 38\,399.999\,978\,\overline{666} \text{ s}$$

From this and (21) we find that

$$\Delta t - \Delta t' = 0.000\,021\,344\,\text{s}.$$

Thus, when Niel Armstrong returned, he was approximately 43 μs younger than if he stayed on Earth. □

6. Conclusions

The Special Theory of Relativity has a number of unexpected claims that contradict our intuition. According to the STR, no experiment can be made to decide whether the body is at rest or moving. All inertial systems for describing physical phenomena are equivalent and there is no preferred inertial system. However, at present we know that the cosmic microwave background radiation (CMB) actually determines a certain kind of a fixed reference system in our neighborhood. Thus there arise speculations whether the principle of relativity in the real universe holds.

In the limiting case $w = \pm c$, Einstein's formula (11) for $v \in (-c, c)$ gives $u = c$. Hence, every photon always has the speed of light in any inertial system.

It is often said that the Lorentz transformation for low speeds $|v| \ll c$ changes into the Galileo transformation

$$\begin{aligned} x' &= x - vt, \\ y' &= y, \\ z' &= z, \\ t' &= t. \end{aligned}$$

This is not true (see [2], [22]), since for an arbitrarily small fixed $v > 0$ we can always find x such that the term vx/c^2 in (3) will dominate significantly over t. However, from (2)–(3) it follows that the Lorentz transformation changes into the Galileo transformation for a fixed v, if we treat c as a parameter and assume that $c \to \infty$. However, for an infinite speed of light there would be no Doppler effect nor aberration of light.

Remark 4. For $\vec{x} = (x, y, z)$ and a constant velocity vector $\vec{v} \in \mathbb{R}^3$ with length $|\vec{v}| \in (0, c)$ the *general Lorentz transformation* is of the form (see e.g. [10, p. 434])

$$\vec{x}\,' = \vec{x} + \left(\frac{\gamma - 1}{|\vec{v}|^2} \vec{v} \cdot \vec{x} - \gamma t \right) \vec{v}, \tag{22}$$

$$t' = \gamma \left(t - \frac{\vec{v} \cdot \vec{x}}{c^2} \right). \tag{23}$$

Here the Lorentz factor γ is defined similarly as in (1), only v^2 needs to be rewritten as $|\vec{v}|^2$. It is easy to find that for nonzero $\vec{v} = (v, 0, 0)$, where $v \in (-c, c)$, relations (22)–(23) change to (2)–(3). By Wikipedia [24] (see also [1]), the Einstein addition of velocities is neither commutative nor associative, in general. □

We conclude by stating that the longitudinal Doppler effect and aberration of light may cause that we observe completely opposite phenomena than those predicted by the Special Theory of Relativity by meas of (2)–(3). Note that relations (2)–(3) represent only a transformation of spacetime coordinates of points from one inertial systems into spacetime coordinates of the second inertial system. We saw that some other effect than time dilatation and length contraction can manifest stronger and they cannot be shielded in any way. For a visualization of several further accompanying effects (like nonlinear distortion) we refer to `www.spacetimetravel.org`.

Acknowledgements

The author is indebted to J. Brandts, F. Křížek, M. Prunescu, and A. Ženíšek for inspiration and valuable suggestions, and H. Bílková for drawing some figures. Supported by RVO 67985840 of the Czech Republic.

References

[1] Ahmad, M., Alam, M. S.: Non-associativity of Lorentz transformation and associative reciprocal symmetric transformation. Iternat. J. Rec. Sym. Theor. Phys. **1** (2014), 9–19.

[2] Baierlein, R.: Two myths about special relativity. Amer. J. Phys. **74** (2006), 193–195.

[3] Botermann, B., et al.: Test of time dilatation using stored Li+ ions as clocks at relativistic speed. Phys. Rev. Lett. **113** (2014), 120405; errata **114** (2015), 239902.

[4] Doppler, Ch.: Ueber das farbige Licht der Doppelsterne und einiger anderer Gestirne des Himmels. Abh. böhm. Ges. Wiss. **2** (1842), 466–482.

[5] Einstein, A.: Zur Elektrodynamik bewegter Körper. Ann. der Phys. **322** (10) (1905), 891–921.

[6] Feynman, R. P., Leighton, R. B., Sand, M.: *The Feynman lectures of physics I.* Addison-Wesley Publ. Company, 1966.

[7] Foster, J., Nightingale, J. D.: *A short course in general relativity* (3rd edition). Springer, New York, 2006.

[8] Gamow, G.: *Mr. Tompkins in paperback*. Cambridge Univ. Press, London, 1965.

[9] Hafele, J. C., Keating, R. E.: Around-the-world atomic clocks: predicted relativistic time gains. Science **177** (1972), 166–168.

[10] Horák, Z., Krupka, F.: *Fyzika*, sv. 2 (in Czech). SNTL, Praha, 1976.

[11] Ives, H. E., Stilwell, G. R.: An experimental study of the rate of a moving atomic clock. J. Optic. Soc. Amer. **28** (1938), 215–226.

[12] Křížek, M.: O paradoxech ve speciální teorii relativity (in Czech). Obzory Mat. Fyz. Inf. **49**(1) (2020), 31–40.

[13] Lorentz, H. A.: La théorie électromagnetique de Maxwell et son application aux corps mouvants. Arch. Néerl. **25** (1892), 1–190.

[14] Michelson, A. A., Morley, E. W.: On the relative motion of the Earth and the luminiferous ether. Amer. J. Sci. **34** (1887), 333–345.

[15] Misner, C. W., Thorne, K. S., Wheeler, J. A.: *Gravitation*, 20th edition. W. H. Freeman, New York, 1997.

[16] Mixson, J. S.: *The twin paradox of special relativity is solved*. Infinity Publishing, 2014.

[17] Pauli, W.: *Theory of relativity*. Dover Publ., Inc., New York, 1981.

[18] Penrose, R.: The apparent shape of a relativistically moving sphere. Proc. Cambridge Phil. Soc. **55** (1959), 137–139.

[19] Penrose, R.: *The road to reality*. Vintage Books, London, 2005.

[20] Synge, J. L.: *Relativity: the special theory*. North-Holland Publ. Co., Amsterdam, 1956.

[21] Terrell, T.: Invisibility of Lorentz contraction. Phys. Rev. **116** (1959), 1041–1045.

[22] Vankov, A.: On controversies in special relativity. ArXiv: physics/0606130v1, 2006, 1–23.

[23] Weisskopf, V. F.: The visual appearance of rapidly moving objects. Physics Today **13**(9) (1960), 24–27.

[24] `https://en.wikipedia.org/wiki/Velocity-addition_formula`

[25] Ženíšek, A.: *Relativita do kapsy* (in Czech). Masaryk Univ., Brno, 2015.

Conference *Cosmology on Small Scales 2020*
Michal Křížek and Yurii Dumin (Eds.)
Institute of Mathematics CAS, Prague

MATHEMATICS OF THE HUBBLE LAW

Pavel N. Antonyuk

Faculty of Mechanics and Mathematics, Lomonosov Moscow State University, Moscow, Russia

Department of Philosophy, Moscow Institute of Physics and Technology, Dolgoprudny, Russia

pavera@bk.ru

Abstract: A generalization of the Hubble law in the framework of the special theory of relativity is obtained. The relativistic Doppler effect allows us to find a nonlinear relationship between the redshift and distance. It is concluded that the Universe is expanding with an acceleration.

Keywords: Hubble law, deceleration parameter, redshift, Galilean transformation, Lorentz transformation, Doppler effect

PACS: 03.30.+p, 98.80.-k, 98.80.Es

1. About Hubble's law

We consider the law of Edwin Hubble (1929), independently discovered also by Georges Lemaître (1927), see [1, 2]. In standard terms, the law has the form:

$$v = H \cdot R, \quad 0 \le R \le R_* = \frac{c}{H},$$

where c is the speed of light in vacuum and H is the Hubble constant.

It is known that the Hubble law (or the Hubble–Lemaître law) is invariant under the Galilean transformations. Let us prove the opposite: the velocity distribution of galaxies, which is invariant with respect to the Galilean transformations or the Lorentz transformations, leads only to the Hubble law or to its generalization.

2. The Hubble law as a consequence of the invariance of the velocity distribution law with respect to the Galilean transformations

According to the cosmological principle, we choose a homogeneous and isotropic model of the Universe, and write the dependence of speed on distance by the formula $v = f(R)$. Let us consider three galaxies I, J, and K moving along one straight line. The distance between I and J is equal to x, the distance between J and K is equal

to y, and the distance between I and K is equal to z. The galaxy J moves away from the galaxy I with speed U, the galaxy K moves away from the galaxy J with speed V, and the galaxy K moves away from the galaxy I with speed W. The following equalities hold:

$$U = f(x), \quad V = f(y), \quad W = f(z), \quad x + y = z, \quad U + V = W. \tag{1}$$

The last velocities-addition formula, given by Newton, is a consequence of the Galilean transformations. This formula is logically connected with the Corollary I from the Newton's laws of motion [3]. The five equalities (1) yield the functional equation:

$$f(x) + f(y) = f(x + y).$$

Augustin-Louis Cauchy found a solution to this equation in the class of continuous functions [4]:

$$f(x) = a \cdot x, \quad \text{where } a = \text{const}.$$

Equating this constant to the Hubble constant, we get the Hubble law, $v = H \cdot R$.

3. Relativistic generalization of the Hubble law as a consequence of the invariance of the velocity distribution law with respect to Lorentz transformations

We take the same three galaxies that move at high speeds and write five equalities for them:

$$U = f(x), \quad V = f(y), \quad W = f(z), \quad x + y = z, \quad \frac{U + V}{1 + \dfrac{U \cdot V}{c^2}} = W. \tag{2}$$

The last velocities-addition formula, given by Einstein in [5], is a consequence of the Lorentz transformations. The equalities (2) give a functional equation:

$$\frac{f(x) + f(y)}{1 + \dfrac{f(x) \cdot f(y)}{c^2}} = f(x + y).$$

The hyperbolic tangent gives the solution to this equation in the class of continuously differentiable functions:

$$f(x) = c \tanh \frac{a \cdot x}{c}, \quad \text{where } a = \text{const}.$$

Therefore, we get a generalization of the Hubble law:

$$v = c \tanh \frac{H \cdot R}{c}, \quad 0 \le R < \infty.$$

According to the correspondence principle, the generalization of the law goes over into the linear law for small values of R. Therefore, $a = H$. For large values of R, we obtain the asymptotic law $v = c$.

If $R = R_* = \dfrac{c}{H}$, then

$$v = \tanh(1) \cdot c \approx 0.76 \cdot c.$$

4. Redshift and distance to galaxies: Relativistic theory

In this section, z is the redshift, the remaining notation is standard. Einstein found the following formula for the relativistic Doppler effect, see [5]:

$$1+z=1+\frac{\Delta\lambda}{\lambda}=\sqrt{\frac{1+\dfrac{v}{c}}{1-\dfrac{v}{c}}}.$$

The new formula for the Hubble law gives the equality:

$$1+z=\sqrt{\frac{1+\tanh\dfrac{H\cdot R}{c}}{1-\tanh\dfrac{H\cdot R}{c}}}.$$

Taking into account the identity

$$\exp x=\sqrt{\frac{1+\tanh x}{1-\tanh x}},$$

we get a functional relationship between redshift and distance:

$$1+z=\exp\frac{H\cdot R}{c}\quad\text{or}\quad R=\frac{c}{H}\ln(1+z).$$

Therefore, we obtain the following correspondence of the quantities:

$$\begin{aligned}
&z=\mathrm{e}-1\approx 1.71828 \quad\Rightarrow\quad R=R_*,\\
&z=100 \quad\Rightarrow\quad R\approx 4.615\cdot R_*,\\
&z=1\,000\,000 \quad\Rightarrow\quad R\approx 13.8\cdot R_*.
\end{aligned}$$

For small values of R, we arrive at the well-known relation:

$$z=\frac{H\cdot R}{c}=\frac{v}{c},\qquad 0\le v\ll c.$$

Expanding the exponent in a power series, we obtain:

$$z=\frac{H\cdot R}{c}+\frac{1}{2}\left(\frac{H\cdot R}{c}\right)^2+O\left(\left(\frac{R}{R_*}\right)\right)^3.$$

The last formula is close to the empirical formulas for the redshift.

5. Hubble's law and rapidity

Rapidity is determined by the formula:

$$\theta = c \cdot \operatorname{arctanh}\frac{v}{c}.$$

The Croatian physicist Varićak and the English mathematician and astronomer Whittaker proposed the variable θ, see [6, 7].

A generalization of the Hubble law for rapidity gives the formula:

$$\theta = H \cdot R.$$

In other words, the transition from the Hubble linear law to its generalization is associated with the replacement of speed by rapidity.

6. The universe expanding with acceleration

For the scale factor R, we consider the equation:

$$\dot{R} = c \cdot \tanh \frac{H \cdot R}{c}, \quad 0 \le R < \infty.$$

This allows us to find the deceleration parameter:

$$q = -\frac{\ddot{R}\,R}{(\dot{R})^2} = -\frac{\dfrac{2\,HR}{c}}{\sinh \dfrac{2\,HR}{c}}\,.$$

Therefore, we get the double inequality:

$$-1 < q < 0 \quad (0 < R < \infty),$$

which allows us to draw a conclusion about the accelerated expansion of the Universe. If $R = R_* = \dfrac{c}{H}$, then

$$q = -\frac{2}{\sinh(2)} \approx -0.55.$$

Next, we consider the function:

$$q = -\frac{2X}{\sinh(2X)}, \quad \text{where } X = \frac{R}{R_*}.$$

The inflection point of the function graph gives the following values:

$$X \approx 0.803, \quad q \approx -0.67.$$

Expanding the function in a power series, we obtain:

$$q = -1 + \frac{2}{3}\left(\frac{R}{R_*}\right)^2 + O\left(\left(\frac{R}{R_*}\right)^4\right).$$

References

[1] Lemaître, G.: Un Univers homogène de masse constante et de rayon croissant rendant compte de la vitesse radiale des nébuleuses extragalactiques. Annales de la Société Scientifique de Bruxelles **A47** (1927), 49–59.

[2] Hubble, E.: A relation between distance and radial velocity among extra-galactic nebulae. Proceedings of the National Academy of Sciences of the United States of America **15** (1929), 168–173.

[3] Newton, I.: *Philosophiae naturalis principia mathematica*. Londini, 1687.

[4] Cauchy, A.-L.: *Analyse algébrique*. Paris, 1821.

[5] Einstein, A.: Zur Elektrodynamik bewekter Körper. Annalen der Physik **17** (1905), 891–921.

[6] Varićak, V.: Anwendung der Lobatschefskijschen Geometrie in der Relativtheorie. Physicalische Zeitschrift **11** (1910), 93–96.

[7] Whittaker, E. T.: *A History of the Theories of Aether and Electricity*. Dublin, 1910.

Conference *Cosmology on Small Scales 2020*
Michal Křížek and Yurii Dumin (Eds.)
Institute of Mathematics CAS, Prague

THE BARYONIC TULLY-FISHER LAW AND THE GAUGE THEORY OF CPT TRANSFORMATIONS

Kurt Koltko

P.O. Box 100595
Denver, CO 80250, U.S.A
localcpt@yahoo.com

Abstract: The gauge theory of CPT transformations is summarized. Properties of the Lagrangian and field equations are used to produce heuristic arguments explaining the Baryonic Tully-Fisher Law without need for dark matter or MOND.

Keywords: gauge theory, CPT symmetry, Tully-Fisher law, dark matter, Lagrangian

PACS: 4.20.-q, 95.35.+d, 98.80.-k

1. Introduction

General relativity (GR) is viewed as an incomplete theory because of its nonrenormalizability and, to a lesser extent, because of observable and experimental astrophysical issues difficult to explain with the Λ Cold Dark Matter (ΛCDM) paradigm such as the H_0 tension and nondetection of Dark Matter (DM). Additionally, there are the core-cusp, satellite galaxy distribution and abundance, and "too big to fail" problems when trying to model galaxies within the ΛCDM framework. Such shortcomings have led to various modified gravity theories.

The spin connection ($\omega_{\mu ab}$) formulation of GR used to handle fermions in curved spacetime allows an additional aspect on the incompleteness of GR – failure to include the entire group of proper Lorentz transformations. The spin connection formulation is derived from local Lorentz transformations acting on physical fields and the vierbein ($e_a{}^{\mu}$) used to describe spacetime. These Lorentz transformations (Lorentz rotations, λ) are the familiar spatial rotations and boosts from special relativity which form a group of proper, continuous transformations. However, the discrete transformation consisting of parity and time reversal together, PT, is also a proper transformation. Therefore, it would seem interesting to include local PT transformations as a natural physical extension of GR. The use of vierbein in the spin connection formalism accommodates a local PT transformation [1–4], whereas it is unclear how

to do so in the more well-known formulation of GR based on the metric tensor, $g_{\mu\nu}$, and Levi-Civita connection, $\Gamma^{\rho}_{\mu\nu}$.

Further motivation to extend GR along these lines is that PT is part of the discrete Charge Conjugation-Parity-Time Reversal (CPT) symmetry. The CPT symmetry is interesting for several reasons:

1) PT is not a universal symmetry whereas CPT is a universal symmetry.
2) The CPT symmetry has been verified experimentally and requires no extra dimensions.
3) CPT is born from the successful (i.e., renormalizable) union of special relativity with quantum theory.

The last point suggests that the CPT symmetry is a "bridge" between quantum theory and relativity and should be made a local symmetry included with local Lorentz rotations in order to construct an extension of GR which would be necessary in any approach to quantum gravity.

2. The transformations

At first glance it may not appear possible to gauge CPT, because there are no important continuously varying parameters involved with the CPT transformation. Also, locality would seem to be a problem. Except for an infinitesimal neighborhood around the origin of a Minkowski manifold, PT is not a local transformation.[1]

We examine the CPT transformation at the origin of an inertial reference frame in order to overcome the above obstacles. The effect of the global CPT transformation *at the origin* of a Minkowski spacetime coordinate system is to flip the coordinate axes and transform a Dirac wavefunction[2], ψ: $\psi \rightarrow \mathrm{i}\gamma^5\psi$. If a nontrivial *spacetime* analog of the charge conjugation operation exists, then we would have to include its effect. We assume no such operation exists, in other words, we assume there is no such thing as an "antispacetime" distinct from spacetime. An attempt to find a nontrivial "antispacetime" operation can be found in [1].

In order to extend this concept to a pseudo-Riemannian spacetime manifold, we introduce a vierbein field e^{μ}_{a}, where μ represents the manifold coordinates and a represents the local inertial frame coordinates. By viewing a vierbein at a given point x_μ as tiny coordinate axes with its origin centered at x_μ, we define a local CPT transformation at that point by $e^{\mu}_{a} \rightarrow -e^{\mu}_{a}$ (the coordinate axes flip), and $\psi(x_\mu) \rightarrow \mathrm{i}\gamma^5\psi(x_\mu)$. In the spirit of gauge theories, we define local CPT transformations as applying these "origin transformations" to the vierbein and wavefunctions at arbitrarily chosen points on the manifold.

The choice of *where* we want to perform a local CPT transformation will play the role of the continuous, arbitrary parameters appearing in gauge theories. In order to

[1] This section is revised from the version found in [3] in order to improve clarity, hopefully.

[2] We use the Bjorken-Drell conventions except for σ^{ab}, $\sigma^{ab} = \frac{1}{4}[\gamma^a, \gamma^b]$.

make this concept precise, we introduce a real differentiable function f, defined over the entire manifold to be used as the argument of step functions Θ. In the arbitrary regions where we choose to perform the local CPT transformations, we set $f > 0$ so that $\Theta[f] = 1$. In the arbitrary regions where we choose not to perform local CPT transformations, we set $f < 0$ so that $\Theta[-f] = 1$. The boundaries between regions where local CPT is carried out and where it is not are given by $f = 0$ with the convention that $\Theta[f] = 0$ if $f \leq 0$. By setting $f < 0$ everywhere, we retrieve the original action. By setting $f > 0$ everywhere in flat spacetime, one obtains the globally CPT transformed action.

We emphasize that f is not a physical field. The Θ are parameters which define when the local CPT transformations are carried out (or not). The Θ are just like the phases, ϕ, used in the gauging of $U(1)$ except that there are only two choices regarding the CPT symmetry instead of the continuum of choices for ϕ to be used in the $U(1)$ symmetry operation $\mathrm{e}^{\mathrm{i}\phi}$. To make the $U(1)$ operation local, one makes ϕ an *arbitrary* function of spacetime subject only to the condition that ϕ is differentiable. Similarly, the function f is introduced in order to make the arbitrary choice of carrying out local CPT ($f > 0$) or not ($f < 0$) at the points of interest. The function f plays the same role as replacing a constant ϕ by $\phi(x)$ in gauging $U(1)$. The only restriction placed on f is that it be differentiable so that $\partial_\mu \Theta[\pm f] = \pm\delta[f]\partial_\mu f$ makes sense (δ being the Dirac delta functional). *The function f must disappear in the field equations and any physical predictions.*

Because we are utilizing the proper spacetime transformation PT, it would be prudent to see if the metric spin connection, $\omega_{\mu ab}$, alone could accommodate local CPT transformations. So, we also include local, proper Lorentz rotations wherever $f > 0$. The local Lorentz rotations, $\lambda(x_\mu)$, are denoted by Λ_a^b and Λ_ψ for the vierbein and Dirac wavefunction respectively. In effect, we are gauging the CPTλ transformation[3] of the Dirac field to induce the gauging of the full group of proper spacetime Lorentz transformations.

Putting all of the above together, we have the following local CPTλ transformations:

$$\begin{aligned}
e_a^{\ \mu} &\rightarrow \Theta[-f]\, e_a^{\ \mu} - \Theta[f]\, e_b^{\ \mu} \Lambda_a^{\ b}, \\
\psi &\rightarrow \Theta[-f]\, \psi + \Theta[f]\, \mathrm{i}\gamma^5 \Lambda_\psi \psi, \\
\overline{\psi} &\rightarrow \Theta[-f]\, \overline{\psi} + \Theta[f]\, \mathrm{i}\overline{\psi}\gamma^5 \Lambda_{\overline{\psi}}, \\
\omega_{\mu ab} &\rightarrow \Theta[-f]\, \omega_{\mu ab} + \Theta[f]\, \widetilde{\omega}_{\mu ab} + \delta[f]\, \Theta[-f]\, \varsigma_{\mu ab} + \delta[f]\, \Theta[f]\, \widetilde{\varsigma}_{\mu ab},
\end{aligned}$$

where the metric spin connection is

$$\omega_{\mu ab} = \frac{1}{2} e_a^\nu \left(\partial_\mu e_{b\nu} - \partial_\nu e_{b\mu}\right) - \frac{1}{2} e_b^\nu \left(\partial_\mu e_{a\nu} - \partial_\nu e_{a\mu}\right) - \frac{1}{2} e_a^\rho e_b^\sigma \left(\partial_\rho e_{r\sigma} - \partial_\sigma e_{r\rho}\right) e_\mu^r$$

[3]In the author's previous work this has been called $CPT\Lambda$, where Λ denotes proper Lorentz rotations and has nothing to do with a cosmological constant.

and $\widetilde{\omega}_{\mu ab}$ is the transformation of $\omega_{\mu ab}$ under CPTλ which satisfies

$$\widetilde{\omega}_{\mu ab}\sigma^{ab} = \Lambda_{\psi}\omega_{\mu ab}\Lambda_{\overline{\psi}} - 2\left(\partial_{\mu}\Lambda_{\psi}\right)\Lambda_{\overline{\psi}}.$$

The $\varsigma_{\mu ab}$, $\widetilde{\varsigma}_{\mu ab}$ are boundary terms arising from the differentiation of the vierbein transformations in the metric spin connection. Explicit expressions for $\widetilde{\omega}_{\mu ab}$, $\varsigma_{\mu ab}$, $\widetilde{\varsigma}_{\mu ab}$ are found in [3]. The volume element, $|e|\,d^4x$, transforms as

$$|e|\,d^4x \rightarrow \left(\Theta\left[-f\right] + \Theta\left[f\right]\right)|e|\,d^4x.$$

Clearly, these transformations are well defined in curved spacetime.

3. Introduction of the gauge field X_{μ}

We take the action integral as the fundamental starting point, because delta functionals need to be in a definite integral in order to have meaning. Also, the action allows us to use variational principles from which we can deduce [3]:

1) The rules on how to handle the various products containing $\Theta\left[\pm f\right]$, $\delta\left[f\right]\partial_{\mu}f$.
2) The nontrivial, nonvanishing variation of the curved spacetime Dirac action under local CPTλ and the inability of the metric spin connection to compensate for this. Hence, the requirement of introducing the new minimally coupled gauge field, X_{μ}.
3) The structure of and transformation of X_{μ}. By using the above transformations in the Dirac action in curved spacetime, one obtains the gauge covariant derivative $D_{\mu}\psi = \partial_{\mu}\psi + \frac{1}{2}\omega_{\mu ab}\sigma^{ab}\psi + \beta X_{\mu}\psi$, where β is the coupling constant associated with X_{μ}. The structure of X_{μ} is determined to be $X_{\mu} = x_{\mu \mathrm{I}}\mathrm{I} + x_{\mu 5}\gamma^5 + x_{\mu ab}\sigma^{ab}$, where the $x_{\mu(\cdots)}$ are the dynamical field components. The transformation of X_{μ} is determined to be:

$$X_{\mu} \rightarrow \Theta\left[-f\right]X_{\mu} + \Theta\left[f\right]\Lambda_{\psi}X_{\mu}\Lambda_{\overline{\psi}} + \Theta\left[-f\right]\delta\left[f\right]Y_{\mu} + \Theta\left[f\right]\delta\left[f\right]\widetilde{Y}_{\mu},$$

where

$$\begin{aligned} Y_{\mu} =& \beta^{-1}\left[\partial_{\mu}f\left(\mathrm{I} - \mathrm{i}\gamma^5\Lambda_{\psi}\right) - \frac{1}{2}\varsigma_{\mu ab}\sigma^{ab}\right], \\ \widetilde{Y}_{\mu} =& \beta^{-1}\left[\partial_{\mu}f\left(-\mathrm{I} - \mathrm{i}\gamma^5\Lambda_{\overline{\psi}}\right) - \frac{1}{2}\widetilde{\varsigma}_{\mu ab}\sigma^{ab}\right]. \end{aligned}$$

Subsequent calculations using variational principles become complicated and difficult, for example, the proof that X_{μ} is massless [3]. So, the easier and more familiar "operator" approach found in [4] makes calculations easier and avoids some subtle issues regarding the variational approach. The usual machinery of gauge theories can be used. As examples, the proof that X_{μ} is massless becomes trivial, and

$D_\mu \to U D_\mu U^{-1}$. This approach begins with rewriting the transformation of ψ as $\psi \to U\psi$, where $U = \Theta[-f]\,\mathrm{I} + \Theta[f]\,\mathrm{i}\gamma^5\Lambda_\psi$. From this, one immediately obtains:

$$\begin{aligned} U^{-1} =& \Theta[-f]\,\mathrm{I} - \Theta[f]\,\mathrm{i}\gamma^5\Lambda_{\overline{\psi}}, \\ \partial_\mu U =& \Theta[f]\,\mathrm{i}\gamma^5\partial_\mu\Lambda_\psi + \delta[f]\,\partial_\mu f\left(\mathrm{i}\gamma^5\Lambda_\psi - \mathrm{I}\right), \end{aligned}$$

and

$$\begin{aligned} (\partial_\mu U)\,U^{-1} =& \Theta[f]\,(\partial_\mu\Lambda_\psi)\,\Lambda_{\overline{\psi}} + \Theta[-f]\,\delta[f]\,\partial_\mu f\left(\mathrm{i}\gamma^5\Lambda_\psi - \mathrm{I}\right) \\ &+ \Theta[f]\,\delta[f]\,\partial_\mu f\left(\mathrm{I} + \mathrm{i}\gamma^5\Lambda_{\overline{\psi}}\right). \end{aligned}$$

We denote the local CPTλ transformation by the customary U even though the transformation is not unitary. Unitarity is not necessary in making gauge theories. For example, λ is not unitary and is used to derive the metric spin connection formulation of GR as a gauge theory. For future reference, we also note that the presence or absence of a conservation law associated with a global symmetry transformation has no relevance to constructing the ensuing gauge theory. Again, returning to λ, we note that there are no conservation laws associated with global boosts.

We emphasize that X_μ *is required* in order to construct an expanded action which is well-behaved under local CPTλ. It is important to note that X_μ, its structure, and its transformation properties are *not* introduced ad-hoc. Rather, X_μ and its transformation properties are *derived* [1–4] from the requirement of constructing a Dirac action in curved spacetime which is well-behaved under local CPTλ transformations.

4. The Lagrangian

Once the transformation of X_μ is determined, then we can construct a Lagrangian density comprised of the expanded Dirac Lagrangian, free-field Lagrangian for X_μ, and a density containing the Einstein-Hilbert term of GR, κR, where $\kappa = (-16\pi G_N)^{-1}$. The total Lagrangian must satisfy the following requirements [1–4]:

1) gauge covariance under local CPTλ transformations,
2) absence of any Dirac delta functionals, $\delta[\dots]$, in the Lagrangian under local CPTλ transformations,
3) terms containing $x_{\mu ab}$ which are not solely constrained to appear within the combination $\left(\frac{1}{2}\omega_{\mu ab} + \beta x_{\mu ab}\right)\sigma^{ab}$, and
4) some components of X_μ appearing in both types of free-field Lagrangians used in GR and the standard model (SM).

The first requirement is obvious. The second prevents pathological variations of the expanded action under local CPTλ transformations. The third ensures that $x_{\mu ab}$ has physical significance and is not just a fancy way to ignore the delta functionals appearing in the transformation of $\omega_{\mu ab}$. The fourth reflects that CPT arises from both GR and SM. We also note that the minimal coupling term acting on matter,

$\left(\frac{1}{2}\omega_{\mu ab}+\beta x_{\mu ab}\right)\sigma^{ab}\psi$, implies replacing κR by $\kappa R_{X\omega}$, where $\kappa R_{X\omega}$ is the modified Einstein-Hilbert curvature term formed by replacing the metric spin connection $\omega_{\mu ab}$ in R by $\omega_{\mu ab}+2\beta x_{\mu ab}$. We obtain [4] for the Hermitian action S:

$$\begin{aligned}S=&\int\left\{\frac{\mathrm{i}}{2}e_a^{\mu}\overline{\psi}\gamma^a\left(\partial_\mu\psi+\frac{1}{2}\omega_{\mu bc}\sigma^{bc}\psi+\beta X_\mu\psi\right)-m\overline{\psi}\psi\right\}|e|\,\mathrm{d}^4x\\&-\int\left\{\frac{\mathrm{i}}{2}e_a{}^{\mu}\left(\partial_\mu\overline{\psi}-\frac{1}{2}\omega_{\mu bc}\overline{\psi}\sigma^{bc}+\beta\overline{\psi}\gamma^0X_\mu^\dagger\gamma^0\right)\gamma^a\psi\right\}|e|\,\mathrm{d}^4x\\&+\int\left\{\frac{1}{4}Tr\left(H_{\mu\nu}H^{\mu\nu\dagger}\right)+\frac{\kappa}{2}\left(R_{X\omega}+R_{X\omega}^\dagger\right)\right\}|e|\,\mathrm{d}^4x,\end{aligned}$$

where the term

$$H_{\mu\nu}=\frac{\beta}{2}\left(\omega_{\mu ab}\left[\sigma^{ab},X_\nu\right]-\omega_{\nu ab}\left[\sigma^{ab},X_\mu\right]\right)+\beta^2\left[X_\mu,X_\nu\right]+\beta\left(\partial_\mu X_\nu-\partial_\nu X_\mu\right)$$

reflects the quantum (SM) contribution to the origin of the CPT symmetry. The other symbols are the familiar Dirac terms. We note that a mass term for X_μ, $m\mathrm{Tr}\left(X_\mu X^{\mu\dagger}\right)$, is not gauge covariant and not allowed [1–4].

The Euler-Lagrange variation of S with respect to $x_{\mu ab}$ and $e_a{}^{\mu}$, respectively, gives the following two important equations: the $x_{\mu ab}$ field equation,

$$\begin{aligned}&4\beta D_\nu\left(\partial^\nu x_{cd}^\mu-\partial^\mu x_{cd}^\nu\right)\mathrm{Tr}\left[\left(\sigma^{ab}\right)^\dagger\sigma^{cd}\right]\\&\quad+2\beta\left\{\left(\omega_{\nu rs}+2\beta x_{\nu rs}^*\right)\left(\partial^\nu x_{cd}^\mu-\partial^\mu x_{cd}^\nu\right)Tr\left[\left[\sigma^{ab},\sigma^{rs}\right]^\dagger\sigma^{cd}\right]\right\}\\&\quad+2\beta D_\nu\left(2\beta x_{cd}^\nu x_{rs}^\mu+\omega_{cd}^\nu x_{rs}^\mu+\omega_{rs}^\mu x_{cd}^\nu\right)Tr\left[\left(\sigma^{ab}\right)^\dagger\left[\sigma^{cd},\sigma^{rs}\right]\right]\\&\quad-\left\{\beta\left(\omega_{\nu cd}+2\beta x_{\nu cd}^*\right)\left(2\beta x_{mk}^\mu x_{rs}^\nu+\omega_{mk}^\mu x_{rs}^\nu+\omega_{rs}^\nu x_{mk}^\mu\right)\mathrm{Tr}\left[\left[\sigma^{ab},\sigma^{cd}\right]^\dagger\left[\sigma^{mk},\sigma^{rs}\right]\right]\right\}\\&\quad+8\kappa\eta^{bc}\left(e^{a\mu}e^{n\rho}-e^{n\mu}e^{a\rho}\right)\left(\omega_{\rho cn}+2\beta x_{\rho cn}^*\right)\\&\quad+8\kappa\eta^{ac}\left(e^{b\mu}e^{n\rho}-e^{n\mu}e^{b\rho}\right)\left(\omega_{\rho nc}+2\beta x_{\rho nc}^*\right)\\=&4\mathrm{i}\overline{\psi}\sigma^{ab}\gamma^\mu\psi+8\kappa D_\nu\left(e^{a\nu}e^{b\mu}-e^{a\mu}e^{b\nu}\right),\end{aligned}$$

and the modified GR equation,

$$\frac{1}{2}\left\{\left(R_{X\omega}^{\mu\nu}+R_{X\omega}^{\mu\nu\dagger}\right)-\frac{1}{2}g^{\mu\nu}\left(R_{X\omega}+R_{X\omega}^\dagger\right)\right\}=\frac{1}{2\kappa}T^{\mu\nu},$$

where

$$\begin{aligned}T^{\mu\nu}=&\frac{g^{\mu\nu}}{4}Tr\left(H_{\rho\sigma}H^{\rho\sigma\dagger}\right)+\frac{\mathrm{i}}{2}\left[\left(D^\mu\overline{\psi}\right)\gamma^\nu\psi-\overline{\psi}\gamma^\nu D^\mu\psi\right]\\&+g^{\mu\nu}\left[\frac{\mathrm{i}}{2}\left(\overline{\psi}\gamma^\rho D_\rho\psi-\left(D_\rho\overline{\psi}\right)\gamma^\rho\psi\right)-m\overline{\psi}\psi\right].\end{aligned}$$

5. The Baryonic Tully-Fisher Law

We argue that the force arising from the $x_{\mu ab}$ components[4] follows an inverse square law for the following three reasons:

(1) $x_{\mu ab}$ affects matter (i.e., the Dirac spinor, ψ) in the exact same manner as $\omega_{\mu ab}$, since their only interaction with matter in S appears as the $\left(\frac{1}{2}\omega_{\mu ab} + \beta x_{\mu ab}\right)\sigma^{ab}\psi$ term.

(2) $x_{\mu ab}$ is massless.

(3) The free-field term for $x_{\mu ab}$ is contained in $R_{X\omega} + R^{\dagger}_{X\omega}$ and $\mathrm{Tr}\left(H_{\mu\nu}H^{\mu\nu\dagger}\right)$ both of which produce inverse square fields in GR and SM. An inverse square law allows us to use Gauss's law in the derivation of the Baryonic Tully-Fisher law (BTFL) [5].

We now argue that neutrinos are the source for the galactic scale force arising from $x_{\mu ab}$. First, by comparison with the second-order formalism definition of the metric spin connection, we notice that the terms in the $x_{\mu ab}$ field equations with coefficient κ create a new metric spin connection when replacing $\omega_{\mu ab}$ with $\omega_{\mu ab} + 2\beta x_{\mu ab}$. This interpretation is reinforced when taking the Palatini variation of the Lagrangian with respect to $\omega_{\mu ab}$ and seeing the same terms (with $2\beta x_{\mu ab}$ replaced by $\beta\left(x_{\mu ab} + x^{*}_{\mu ab}\right)$) appearing with coefficient κ. From the second-order formalism definition of the metric spin connection, these terms will cancel out. This allows us to linearize (i.e., weak field approximation) the $x_{\mu ab}$ field equations with respect to $\omega_{\mu ab}$, $x_{\mu ab}$ and focus on the remaining source term, $4\mathrm{i}\overline{\psi}\sigma^{ab}\gamma^{\mu}\psi$. Usually, this term will vanish [3], because of the random spin and momentum orientations of fermions in bulk matter. However, because of the fixed neutrino chirality, this term will not vanish for the neutrinos seen by an observer looking at a point neutrino source such as a star. So, we treat stars as point sources of this $4\mathrm{i}\overline{\psi}\sigma^{ab}\gamma^{\mu}\psi$ term which is proportional to the neutrino luminosity, I_{ν}. For a spiral galaxy the total neutrino flux will vanish at the center, so we expect no net force from the $x_{\mu ab}$ potential there. As we move towards the edge of the galaxy, the net neutrino flux starts to point outwards and increases as we move away from the center. Hence the force due to $x_{\mu ab}$ will increase along the way, and we avoid the core-cusp problem associated with the dark matter interpretation.

Because of the resemblance of the linearized $x_{\mu ab}$ field equation to electrodynamics and the expected inverse square behavior of the new force, we expect a weak field limit of the $x_{\mu ab}$ force to be of the Newtonian form $-kQ_{\nu}/r^2$, where k is the effective coupling constant, Q_{ν} is the source ("charge") term expected to be proportional to I_{ν}, and we have assumed an attractive force. So, the total field, $F(r)$ for a point source (or leading order term of an extended object such as a spiral galaxy) of mass M and I_{ν} would be [3]

$$F(r) = -\frac{G_N M}{r^2} - \frac{kQ_{\nu}}{r^2}.$$

[4] the physical implications of the $x_{\mu \mathrm{I}}$ and $x_{\mu 5}$ components are not considered in this paper

Because the neutrinos are ultrarelativistic, we would expect that the total Q_ν contained within r is given by $Q_\nu = I_\nu r/c$. So, using Gauss's law, we have

$$F(r) = -\frac{G_N M}{r^2} - \frac{kI_\nu}{cr}.$$

As $r \to \infty$, we see that

$$F(r) \to -\frac{kI_\nu}{cr}.$$

Therefore, the rotation curve, $v(r)$, flattens out at large r when

$$\frac{kI_\nu}{cr} = \frac{v^2}{r}, \quad \text{or} \quad v = \left(\frac{kI_\nu}{c}\right)^{\frac{1}{2}}.$$

Presumably, the MOND regime (a_M) is reached where the gravitational force is equal to the gauge CPT force instead of a modification to Newton's second law:

$$\frac{G_N M}{r^2} = \frac{kI_\nu}{cr} = a_M.$$

To obtain the slope of the BTFL, we have to be careful. First, we assume that the mass, M, of the galaxy is dominated by hydrogen and ignore the small amount of other elements. Then, we realize that because a small fraction of the H nuclei in the galaxy are undergoing fusion and emitting neutrinos, we have $I_\nu \propto M$. Unfortunately, this gives the asymptotic rotational speed to be $v \propto M^{\frac{1}{2}}$ from above and the wrong slope of the BTFL. To obtain the $(I_\nu)^{\frac{1}{2}}$ source dependence (instead of I_ν) required for the correct slope, we examine the behavior of the modified GR equation at the edge of a spiral galaxy. We use the weak field (linearized) version of modified GR because of the dearth of matter and the small acceleration (the deep MOND regime if one prefers) implying weak $\omega_{\mu ab}$ and $x_{\mu ab}$. Therefore, we neglect the term $(2\kappa)^{-1} T^{\mu\nu}$, because it is quadratic in the fields and because of the small value of $(2\kappa)^{-1}$. Next, we split the terms $R^{\mu\nu}_{X\omega} + R^{\mu\nu\dagger}_{X\omega}$ and $R_{X\omega} + R^{\dagger}_{X\omega}$ into $2R^{\mu\nu} + R^{\mu\nu}_X + R^{\mu\nu\dagger}_X$ and $2R + R_X + R^{\dagger}_X$, where $R^{\mu\nu}$, R are the usual curvature terms formed from the metric spin connection of the Einstein-Hilbert GR ("standard metric spin connection"), and $R^{\mu\nu}_X$, R_X are comprised of identical curvature terms with $\omega_{\mu ab}$ replaced by $2\beta x_{\mu ab}$ and additional terms containing products of $x_{\mu ab}\omega_{\nu cd}$ which are quadratic and therefore dropped. We use the standard metric spin connection as the basis for physical interpretation for a couple of reasons. First, the proof of covariance under local CPTλ [3, 4] used the standard metric spin connection of GR. Second, this allows for the standard GR interpretation of the linearized modified GR equation by moving everything containing $R^{\mu\nu}_X$, R_X, and their complex conjugates to the RHS thereby enabling us to interpret the RHS as an *effective* energy-momentum tensor source term, $\Upsilon_{\mu\nu}$: $R_{\mu\nu} - \frac{1}{2} g_{\mu\nu} R = \Upsilon_{\mu\nu}$. The *direct* (i.e., enhanced without the "middleman" of $T_{\mu\nu}$) effect of $x_{\mu ab}$ acting on spacetime by replacing $\omega_{\mu ab}$ with $\omega_{\mu ab} + 2\beta x_{\mu ab}$ is reflected by the absence of a κ^{-1} factor multiplying $\Upsilon_{\mu\nu}$. Importantly,

the linearized $\Upsilon_{\mu\nu} \sim (T_{X\mu\nu})^{\frac{1}{2}}$, where $T_{X\mu\nu}$ are the $x_{\mu ab}$ containing terms of $T_{\mu\nu}$. So, we take this as a cue to replace the source term I_ν of the Newtonian form of the weak field gauge CPT force by $(I_\nu)^{\frac{1}{2}}$ in order to reflect the behavior of $\Upsilon_{\mu\nu}$. This accounts for the origin of the $(I_\nu)^{\frac{1}{2}}$ dependence, hence the correct slope of the BTFL. We could also speculate that because everything is being interpreted in the standard GR framework, the new force is indeed attractive (instead of assuming it) and that light is also bent by the new force. There is no need for either dark matter or MOND.

Because the new force is sourced by neutrinos, we can comment on a few physical phenomena. First, we see that the predictions of GR near black holes remain valid, since there is no neutrino emission from the black holes. Second, there is no conflict with the Bullet Cluster, because the sources of neutrino emission are centered in the stellar medium instead of the lagging gaseous medium. Finally, it is interesting to compare the uncertainty in G_N with the variation of the square root of solar neutrino flux received at the Earth's surface between noon and midnight because the total force on the earth is due to the sun's gravity as well as the $x_{\mu ab}$ component being interpreted as a gravitational effect.

References

[1] Koltko, K.: *Attempts to find additional dynamical degrees of freedom in space-time using topological and geometric methods*. Ph.D. thesis, University of South Carolina, 2000.

[2] Koltko, K.: A gauge theory of CPT transformations to first order. Foundations of Physics Letters **15** (2002), 299–304.

[3] Koltko, K.: Gauge CPT as a possible alternative to the dark matter hypothesis. arXiv 1308.6341 [physics.gen-ph] and cross listed as [astro-ph.GA] (2013).

[4] Koltko, K.: A free-field Lagrangian for a gauge theory of the CPT symmetry, arXiv 1703.10904v3 [physics.gen-ph] and cross listed as [astro-ph.GA], [hep-th] (2018).

[5] McGaugh, S. S., Schombert, J. M., Bothun, G. D., de Blok, W. J. G.: The baryonic Tully-Fisher relation, arXiv astro-ph/0003001v1 (2000).

Conference *Cosmology on Small Scales 2020*
Michal Křížek and Yurii Dumin (Eds.)
Institute of Mathematics CAS, Prague

ON THE PROBLEM OF FLATNESS IN VARIOUS COSMOLOGICAL MODELS

Yurii V. Dumin

Sternberg Astronomical Institute (GAISh) of Lomonosov Moscow State University,
Universitetskii prosp. 13, Moscow, 119234 Russia

Space Research Institute (IKI) of Russian Academy of Sciences,
Profsoyuznaya str. 84/32, Moscow, 117997 Russia

dumin@yahoo.com, dumin@sai.msu.ru

Abstract: The problem of flatness of the Universe (i.e., an almost zero curvature of its three-dimensional space) is one of the major methodological issues, determining the viability of various cosmological models. In fact, just the inability to resolve this problem was one of the reasons to reject the old, "pre-inflationary" cosmological model in the early 1980's and to replace it by the inflationary scenario. Here, we outline the corresponding mathematical formalism and pose a question if flatness of the Universe can be satisfactorily explained in the "uncertainty-mediated" inflationary model, which was suggested in our recent works [Y. V. Dumin. In: *Cosmology on Small Scales 2018*, p. 136; Grav. Cosmol. **25** (2019), 169]? As follows from the respective calculations, the curvature term in the Friedmann equation becomes insignificant in the course of time and, therefore, the Universe tends to be flat. From this point of view, the uncertainty-mediated cosmological model can serve as a reasonable alternative to the standard (exponential) inflationary scenario.

Keywords: flatness of the Universe, inflationary model, uncertainty relation

PACS: 98.80.Bp, 98.80.Cq, 98.80.Es, 95.36.+x

1. Introduction

Since the observed three-dimensional space is almost perfectly flat, it is one of key problems of theoretical cosmology to explain how this flatness developed in the course of evolution of the Universe. In other words, does a particular cosmological model predict the flat spatial asymptotics for a sufficiently generic class of initial conditions?

A change in the cosmological paradigm in the early 1980's from the old model with power-like expansion, governed by the ordinary matter and radiation, to the inflationary scenario, governed by the vacuum energy or Λ-term [1, 2], was caused

just by the inability of the first-mentioned model to resolve a few conceptual puzzles of the observed Universe. They were the causal connectivity between the remote subregions of space–time, a presence of the initial singularity and, in particular, a surprising flatness of the three-dimensional space. In the next sections, we shall discuss how the mathematical formalism can or cannot predict such flatness for the different cosmological models; and special attention will be paid to the uncertainty-mediated scenario, which was put forward in our recent publications [3, 4].

2. Dynamics of the scale factor in various cosmological models

The commonly-accepted paradigm of the modern cosmology both for the early and late Universe is based on the Robertson–Walker space–time metric:

$$\mathrm{d}s^2 = c^2\mathrm{d}t^2 - R^2(t)\biggl[\frac{\mathrm{d}r^2}{1-kr^2} + r^2(\mathrm{d}\theta^2 + \sin^2\theta\,\mathrm{d}\varphi^2)\biggr]\,, \tag{1}$$

whose temporal dynamics is described by the Friedmann equation [5]:

$$H^2 \equiv \left(\frac{\dot{R}}{R}\right)^2 = \frac{8\pi G}{3c^2}\,\rho_0\left(\frac{R}{R_0}\right)^{-3(1+w)} + \frac{c^2}{3}\,\Lambda - kc^2\frac{1}{R^2}\,. \tag{2}$$

Here, r, θ, and φ are the dimensionless spherical coordinates, the coefficient k equals 1, 0, and -1 for the closed, flat, and open 3D space, respectively; R is the scale factor of the Universe, H is the Hubble parameter, G is the gravitational constant, c is the speed of light in vacuum, and dot denotes a differentiation with respect to the time t.

The first term in the right-hand side of formula (2) describes a contribution of the ordinary matter, whose density is ρ_0 at the instant $t = 0$, when the scale factor equals R_0. The equation-of-state parameter w is equal to 0 for the dust-like (i.e., non-relativistic) substance and 1/3 for the radiation.

The second term represents a contribution of the vacuum energy or Λ-term, which is usually assumed to be independent of time. The Λ-term can be either introduced "by hand" as a new fundamental constant or derived from the underlying theory of elementary particles; the last-mentioned case being more typical for the models of the early Universe.

Finally, the third term in equation (2) describes contribution of the spatial curvature into the temporal dynamics of the scale factor.

According to observations, the curvature should be close to zero. So, one possible option is to set $k = 0$ *a priori*. However, this looks not so good from the methodological point of view. A much more attractive option would be to construct such cosmological model where the curvature term becomes insignificant (as compared to other terms) in the course of time, starting from a generic set of the initial conditions; so that the approximately flat three-dimensional space is formed "dynamically" in a self-consistent way. In the subsequent sections, we shall study if such behavior is possible in various models of the early Universe.

2.1. The old, "pre-inflationary" model

Although the Λ-term was introduced into the equations of General Relativity already during its development in the late 1910's, it was commonly believed till the early 1980's that it is absent in the real world. Then, the general Friedmann equation (2) is reduced to

$$\left(\frac{\dot{R}}{R}\right)^2 = \frac{8\pi G}{3c^2}\,\rho_0\left(\frac{R}{R_0}\right)^{-3(1+w)} - kc^2\frac{1}{R^2}\,. \tag{3}$$

If we assume initially that $k = 0$, then the resulting equation can be easily integrated and gives

$$\tilde{R}(t) = R_0\left(\frac{t+T}{T}\right)^{\frac{2}{3(w+1)}}, \tag{4}$$

where T is the age of the Universe, which is expressed through the previously-used cosmological parameters as

$$T = \frac{2}{3(w+1)}\left(\frac{3\,c^2}{8\pi G\rho_0}\right)^{1/2}. \tag{5}$$

From here on, solutions obtained under the assumption of zero curvature, $k = 0$, will be marked by a tilde.

In fact, it is clear even without the exact temporal dependence of the scale factor that the curvature term in equation (3) will decrease slower than the first term in the course of expansion of the Universe. Really, the curvature term decays as $1/R^2$, while the first term as $1/R^{3(1+w)}$, i.e., $1/R^3$ in the case of non-relativistic matter and $1/R^4$ in the case of radiation. Therefore, the curvature term will inevitably dominate after some time, and the flat three-dimensional space cannot be formed dynamically.

2.2. The standard (exponential) inflationary scenario

The main assumption of the inflationary scenario is that the density of ordinary matter in the early Universe can be ignored, but the Λ-term is of primary importance. In other words, the general Friedmann equation (2) is reduced to

$$\left(\frac{\dot{R}}{R}\right)^2 = \frac{c^2}{3}\,\Lambda - kc^2\frac{1}{R^2}\,. \tag{6}$$

If the curvature term is initially ignored ($k = 0$), the integration of (6) is trivial and results in

$$\tilde{R}(t) = R_0\exp\left(\frac{c\sqrt{\Lambda}}{\sqrt{3}}\,t\right), \tag{7}$$

where $\Lambda = \text{const}$, and only the increasing solution was taken into account.

Again, it is clear even without the exact temporal dependence of the solution of the total equation (6) that role of the curvature term will become negligible in

the course of time as compared to the first term. Really, the curvature term decays as $1/R^2$, while the first term remains constant. So, as distinct from Sec. 2.1, solution $R(t)$ should tend to $\tilde{R}(t)$, corresponding to the flat three-dimensional space, at the sufficiently large time. Just this fact is one of the main advantages of the inflationary models.

2.3. The uncertainty-mediated inflationary model

Since the physical origin of the Λ-term remains unclear and there should be two absolutely different Λ-terms in the early Universe and nowadays, it may be reasonable to consider the cosmological model with a decaying Λ-term. A particular version of such theory was presented in our recent works [3, 4]. It is based on the qualitative idea by A. Coe [6] that the vacuum energy might be estimated from the quantum-mechanical uncertainty relation between the time and energy. Really, as was shown by L. I. Mandelstam and I. E. Tamm [7], the energy–time uncertainty relation can be used not only in the context of measurements but also for estimating the long-term evolution of quantum systems; for more details, see review [8]. Then, Λ-term appearing in equation (6) should be replaced by the function:

$$\Lambda(t) = \frac{4\pi C_{\mathrm{UR}}}{c\, l_{\mathrm{P}}} \frac{1}{t}\,, \tag{8}$$

where $l_{\mathrm{P}}{=}\sqrt{G\hbar/c^3}$ is the Planck length, and $C_{\mathrm{UR}} \geq 1$ (abbreviation "UR" means the uncertainty relation). So, a substitution of (8) into (6) gives the modified Friedmann equation:

$$\left(\frac{\dot{R}}{R}\right)^2 = \frac{4\pi C_{\mathrm{UR}}}{3\tau} \frac{1}{t} - kc^2 \frac{1}{R^2}\,, \tag{9}$$

where $\tau = l_{\mathrm{P}}/c = \sqrt{G\hbar/c^5}$ is the Planck time.

Solution of this equation at zero spatial curvature ($k = 0$) is the "quasi-exponential" function:

$$\tilde{R}(t) = R_0 \exp\left(\sqrt{\frac{16\pi C_{\mathrm{UR}}}{3}} \sqrt{\frac{t}{\tau}}\right) \tag{10}$$

if we consider only the increasing branch, *i.e.*, the expanding Universe. Discussion of its physical properties important for cosmology can be found in our papers [3, 4, 9, 10].

Next, let us return to the general ($k \neq 0$) Friedmann equation (9). To estimate the relative contributions of the energetic (first) and curvature (second) terms in the right-hand side, we can substitute there the simplified solution (10). Since

$$\lim_{t\to\infty} \frac{1/t}{1/\tilde{R}^2(t)} = \lim_{t\to\infty} \frac{\tilde{R}^2(t)}{t} = \infty \tag{11}$$

(as can be easily proved applying the L'Hôpital's rule two times), one should conclude that the role of the curvature term will be negligible at large time.[1] In other words, the situation is the same as in the standard (exponential) inflationary scenario.

3. Conclusion

Employing the simple estimates, we have shown that the problem of flatness was a serious conceptual drawback of the old cosmological model, governed by the ordinary matter and radiation. On the other hand, the flat three-dimensional space can be formed dynamically in the standard (exponential) inflationary scenario and—which is the novel result—in the inflationary model based on the quantum-mechanical uncertainty relation.

Since it was already shown before that this model resolves also the problem of causality in the early Universe [9, 10] and avoids the cosmological singularity, it can serve as a reasonable alternative to other inflationary scenarios considered currently in the literature, e.g., reviews [11, 12].

References

[1] Guth, A. H.: The inflationary Universe: A possible solution to the horizon and flatness problems. Phys. Rev. D **23** (1981), 347.

[2] Linde, A. D.: The inflationary Universe. Rep. Prog. Phys. **47** (1984), 925.

[3] Dumin, Y. V.: Cosmological inflation from the quantum-mechanical uncertainty relation. In: M. Křížek, Y. Dumin (Eds.), *Cosmology on Small Scales 2018*, *Dark matter problem and selected controversies in cosmology*. Inst. of Math., Prague, 2018, p. 136.

[4] Dumin, Y. V.: A unified model of Dark Energy based on the Mandelstam–Tamm uncertainty relation. Grav. Cosmol. **25** (2019), 169.

[5] Olive K. A., Peacock, J. A.: Big-Bang cosmology. In: Patrignani, C., et al. (Particle Data Group), *Review of Particle Physics*. Chin. Phys. C **40** (2016), 100001, p. 355.

[6] Coe, A.: *Observable Universe topology and Heisenberg uncertainty principle.* Preprint viXra:1710.0143, 2017.

[7] Mandelstam, L. I., Tamm, I. E.: The energy–time uncertainty relation in non-relativistic quantum mechanics. Izv. Akad. Nauk SSSR (Ser. Fiz.) **9** (1945), 122, in Russian.

[1] Strictly speaking, this is not a rigorous mathematical proof but rather the "plausible reasoning", because we used here solution of the simplified equation, $\tilde{R}(t)$. A more rigorous proof will be published elsewhere.

[8] Deffner, S., Campbell, S.: Quantum speed limits: from Heisenberg's uncertainty principle to optimal quantum control. J. Phys. A: Math. Theor. **50** (2017), 453001.

[9] Dumin, Y. V.: The problem of causality in the uncertainty-mediated inflationary model. In: M. Křížek, Y. Dumin (Eds.), *Cosmology on Small Scales 2020, Excessive extrapolations and selected controversies in cosmology*. Inst. of Math., Prague, 2020, this book.

[10] Dumin, Y. V.: Cosmological inflation based on the uncertainty-mediated Dark Energy. Grav. Cosmol. **26** (2020), 259.

[11] Martin, J., Ringeval, C., Vennin, V.: Encyclopædia inflationaris. Phys. Dark Universe **5–6** (2014), 75.

[12] Ellis J., Wands, D.: Inflation. In: Patrignani, C., et al. (Particle Data Group), *Review of Particle Physics*. Chin. Phys. C **40** (2016), 100001, p. 367.

Conference *Cosmology on Small Scales 2020*
Michal Křížek and Yurii Dumin (Eds.)
Institute of Mathematics CAS, Prague

ASTROPHYSICAL BOUNDS ON MIRROR DARK MATTER, DERIVED FROM BINARY PULSARS TIMING DATA

Itzhak Goldman[1,2]

[1] Department of Physics, Afeka Engineering College
Tel Aviv, Israel
goldman@afeka.ac.il
[2] Department of Astrophysics, Tel Aviv University
Tel Aviv, Israel

Abstract: Mirror Dark Matter (MDM) has been considered as an elegant framework for a particle theory of Dark Matter (DM). It is supposed that there exists a dark sector which is mirror of the ordinary matter. Some MDM models allow particle interactions mirror and ordinary matter, in addition to the gravitational interaction. The possibility of neutron to mirror neutron transition has recently been discussed both from theoretical and experimental perspectives. This paper is based on a previous work in which we obtained stringent upper limits on the possibility of converting neutrons to mirror neutrons in the interiors of neutron stars, by using timing data of binary pulsars. Such a transition would imply mass loss in neutron stars leading to a significant change of orbital period of neutron star binary systems. The observational bounds on the period changes of such binaries, therefore put strong limits on the above transition rate and hence on the neutron – mirror-neutron mixing parameter ϵ'. Our limits are much stronger than the values required to explain the neutron decay anomaly via $n - n'$ mixing.

Keywords: dark matter, neutron stars, pulsars

PACS: 95.35.+d, 97.60.Jd, 97.60.Gb

1. Introduction

The idea of mirror dark matter (MDM) has been considered by various authors [1]. In this class of models each ordinary particle p has a mirror particle p' counterpart. There is, a generic problem in that the extra mirror neutrinos (ν') and mirror photon (γ') contribute too much to the number of degrees of freedom at the Big Bang Nucleosynthesis (BBN) epoch, destroying the success of the big bang nucleosynthesis predictions. A possible way out is to assume a breaking of the Z_2 symmetry in the early universe so as to have asymmetric inflationary reheating in the two sectors (ordinary matter and MDM) resulting in a lower reheat temperature (T') of the mirror

sector compared to (T) of the visible one [4]. This breaking eventually trickles down to the low energies leading in general to a splitting the mirror and visible fermion masses [5]. The above mentioned symmetric picture could however remain almost exact if the asymmetric inflation picture is carefully chosen. Cosmologies of such scenarios have been discussed in [2] and references therein.

An interesting new phenomenon is possible in almost exact mirror models, if there are interactions mixing the neutron with the mirror neutron state (denoted by $\epsilon_{n-n'} \equiv \epsilon'$). In such a case, one can expect $n \to n'$ oscillations to take place in the laboratory [7] and indeed there are ongoing and already completed searches for such oscillations [3] at various neutron facilities.

We note that $n - n'$ oscillation is similar to neutron-anti-neutron oscillation suggested very early [9] and extensively discussed in the literature. For recent reviews, see [10]. The rate governing the $n - \bar{n}$ oscillations was limited by laboratory experiments to be

$$\epsilon_{n\bar{n}} = 1/\tau_{n\bar{n}} < 10^{-8}\,\mathrm{sec}^{-1} \text{ or } 10^{-23}\,\mathrm{eV}. \tag{1}$$

We focus on the possibility that $n \to n'$ transitions can lead to mass loss of a neutron star and if the latter is a member of a binary system, then this mass loss affects the binary period. Indeed (see [12]), the mass loss of any kind of such neutron stars implies an increase of the orbital period of the binary system P_b. In the following sections we find that observational limits on $|\dot{P}_b/P_b|$ of binary pulsars yield stringent bounds on the $n - n'$ mixing parameter ϵ'.

2. Transition of a neutron star to a mixed neutron-mirror neutron star induced by $n - n'$ mixing

We note that $n \to n'$ transitions, kinematically forbidden in nuclei, can occur in neutron stars. The neutrons in neutron stars are mainly bound by gravity and *not* by nuclear forces. Let us, suppose that an $n \to n'$ conversion occurred at some point in the star. Under the pressure a neighboring neutron then will be pushed to "hole" generated by the converted neutron, gaining in the process kinetic energy which is of order of the Fermi energy E_F. Additional energy gain is obtained, since the produced n' gravitates to the center of the star and a surface neutron replaces the neutron which went into the above mentioned "hole". Therefore the net (eventually radiated via neutrino and mirror neutrino emission) energy stemming from an early, single nn' transition is:

$$m_n c^2 \left(\mathrm{e}^{\phi(R)} - \mathrm{e}^{\phi(0)}\right) + < E_F >, \tag{2}$$

where $\mathrm{e}^{\phi(r)} = g_{oo}^{1/2}(r)$, $\mathrm{e}^{\phi(R)} = (1 - 2GM/c^2)^{1/2}$ and $< E_F >$ is the average Fermi energy of the disappeared neutron. Thus the gravitational mass of the neutron star will decrease. This has led [13] to propose that ($n \to n'$) oscillations generating completely mixed nn' stars, may explain the observed mass distribution of neutron stars.

3. The rate of $n \to n'$ transition

We express the $n \to n'$ transition rate $\Gamma(n \to n')$ by

$$\Gamma(n \to n') = \Gamma(nn) P_{nn'} \,, \tag{3}$$

where Γ_{nn} is the rate of nn collisions and $P_{nn'}$ is the probability of having n' (rather than n) at the time of the collision.

Equation (3) is based on the supposition [14] in which one assumes that:

a) The coherent buildup of the $|n' >$ component in the initial purely $|n >$ state of the two component system, proceeds unimpeded by nuclear interactions during the time of flight between two consecutive collisions.

b) The coherent build-up stops upon collision and the n' part is released as outgoing mirror neutron particles.

Denoting by t_{nn} the mean free time for neutron-neutron collisions and by ϵ' the rate for n to n' oscillation, the Hamiltonian in the two dimensional $|n >$, $|n' >$ Hilbert space leads to

$$P_{nn'} = [\epsilon' \cdot t_{nn}]^2.$$

Substituting the above $P_{nn'}$ and $\Gamma_{nn} = t_{nn}^{-1}$ in equation (3), one gets

$$\Gamma_{n \to n'} = t_{nn} \epsilon'^2. \tag{4}$$

Taking $t_{nn} \approx 10^{-23}$ sec, the flight time of a neutron a $O(Fermi)$ distance at a speed $\sim \frac{1}{3}c$ yields

$$\Gamma_{n \to n'} = 6 \times 10^{-8} [\epsilon'/10^{-11} \text{ eV}]^2 \, \text{yr}^{-1}. \tag{5}$$

In what follows we shall use astrophysical data to obtain bounds on $\Gamma_{n \to n'}$ and employ equation (5) to derive bounds on ϵ'.

4. Neutron star models and their descendant fully mixed neutron – mirror neutron stars

To obtain the resulting mass and radius decrease, we solved numerically the TOV equations with a commonly used equation of state [21]. We first solve the TOV structure equations for pure neutrons. Then for the same baryon number we solve the TOV equations for a totally mixed neutron – mirror neutron star. We employ the method used by us in [6]. In this specific case we have two fluids obeying the same nuclear equation of state where the only interaction is through the gravitational field.

We considered three different models each characterized by its total baryon number (that does not change in the transition). For each baryon mass we calculated the initial and final mass and radius. We also calculated the initial $e^{\phi(R)} - e^{\Phi(0)}$. The resulting models are:

$\underline{M_b = 1.81 M_\odot}$

$$M = 1.57 M_\odot, \quad R = 12.2\,\mathrm{km}, \quad \mathrm{e}^{\phi(R)} - \mathrm{e}^{\Phi(0)} = 0.15,$$

$$M_{nn'} = 1.43 M_\odot = 0.91 M, \quad R_{nn'} = 8.8\,\mathrm{km} = 0.72 R,$$

$\underline{M_b = 2.17 M_\odot}$

$$M = 1.82 M_\odot \quad R = 12.37\,\mathrm{km}, \quad \mathrm{e}^{\phi(R)} - \ \mathrm{e}^{\Phi(0)} = 0.17,$$

$$M_{nn'} = 1.62 M_\odot = 0.89 M, \quad R_{nn'} = 8.8\,\mathrm{km} = 0.71 R,$$

$\underline{M_b = 2.44 M_\odot}$

$$M = 1.97 M_\odot, \quad R = 12.4\,\mathrm{km}, \quad \mathrm{e}^{\phi(R)} - \ \mathrm{e}^{\Phi(0)} = 0.19,$$

$$M_{nn'} = 1.7 M_\odot = 0.86 M, \quad R_{nn'} = 8.65\,\mathrm{km} = 0.7 R.$$

5. The relation between the mixing parameter ϵ' and the mass loss rate

Returning to the main goal of the paper, namely limiting ϵ', we need to relate the rate of neutron to mirror neutron transition to the stellar $\dot{M}/M$. Since neutrons from the entire volume of the neutron star can transform to n', the resulting total mass loss of the neutron star due to this is proportional to $\Gamma_{n\to n'}$.

A great advantage is that all the different binary pulsars (with variety of masses, spin down ages and companions) should conform to a single fundamental parameter: ϵ'. Thus, we can use the youngest pulsars to set stringent limits on ϵ'. In turn, this implies that also the older pulsars are still in the process of transition. In particular, for small enough values of ϵ' even these older pulsars may be at the very initial stages of the pure to mixed star transition.

We next present two estimates of $\dot{M}/M$.

First estimate

The first estimate uses the average value $\dot{M}/M \approx \Gamma_{nn'} \Delta M/M$ during the complete transition to a mixed star where, ΔM is the total mass reduction. The $\Delta M/M = 0.09 \div 0.14$ obtained in the previous section then yields a representative value

$$\left|\frac{\dot{M}}{M}\right| \approx 0.12\,\Gamma_{nn'}. \tag{6}$$

Second Estimate

Here we use the results of the numerical solutions of the neutron stars presented in Section 4. We apply equation (2) to the very beginning of the transition process and find

$$\left|\frac{\dot{M}}{M}\right| \geq \left(\mathrm{e}^{\phi(R)} - \mathrm{e}^{\phi(0)}\right) \Gamma_{nn'} = (0.15 \div 0.19)\Gamma_{nn'}. \tag{7}$$

It reassuring that the estimates by the two methods agree up to a factor of 1.5. It also makes sense that at the very beginning the process is faster than that derived from the first method which represents a time average over the entire transition.

Thus we adopt

$$\left|\frac{\dot{M}}{M}\right| \geq 0.14\Gamma_{nn'} \tag{8}$$

as a representing value during the entire transition episode.

6. Limits on ϵ' derived from timing observations of binary pulsars

Jeans (1924) in [11] pointed out that the mass of the star that emits electromagnetic radiation decreases with time and therefore, the orbital elements of a binary system should evolve with time. Assuming that in the local frame of each star the radiation emission is spherically symmetric, he obtained

$$Ma = \text{ constant}, \tag{9}$$

where a is the semi-major axis and $M = m_1 + m_2$ is the total mass of the system. This and the expression for the binary period

$$P_b = 2\pi\sqrt{\frac{a^3}{GM}} \tag{10}$$

imply

$$\frac{\dot{P}_b}{P_b} = -2\frac{\dot{M}}{M}. \tag{11}$$

Since $\dot{M} < 0$, $\dot{P}_b > 0$ so that the orbital period keeps increasing.

Except for the nature of emission process this is the same as the situation addressed here. We consider next four binary pulsars and obtain the the limits on the present rate of the mass change for each system.

In general, only neutron stars which are still in the process of transiting to a mixed star will exhibit mass loss. A priori, for extremely "high" $\Gamma_{nn'}$ some of the older observed pulsars in binaries may be "too old".

PSR 1916+13

We use the data of [15]. The spin down age of the pulsar is $1.1 \times 10^8\,\mathrm{yr}$. It is commonly assumed that the pulsar companion is a neutron star, so that there is no mass transfer between the binary members. Also one neglects the mass accretion from the interstellar medium. After accounting for the expected gravitational radiation, Galactic acceleration, and further dynamical corrections there is still some limited room for a positive change of binary period that could have followed from the mass decrease,

$$\frac{\dot{P}_b}{P_b} < 1.36 \times 10^{-11}\,\mathrm{yr}^{-1} \tag{12}$$

implying

$$\left|\frac{\dot{M}}{M}\right| < 6.8 \times 10^{-12}\,\mathrm{yr}^{-1}$$

for the two neutron stars losing mass. Using equations (5) and (14) the bound

$$\epsilon' < 2.8 \times 10^{-13}\ \mathrm{eV}$$

follows.

PSR J1141-6545

This is a young pulsar of age about 2×10^6 yr. The companion is a massive white dwarf of mass $0.98 M_\odot$ and the neutron star has a mass $1.3 M_\odot$, see [19, 20].

This system is a superb laboratory for testing GR. Using the data from the above observational papers, one finds that the residual (subtracting from the measured value the gravitational radiation terms as well as the galactic acceleration and the kinematic effect and allowing for the uncertainties of all the above) positive possible value of the orbital period rate of change is very small

$$\frac{\dot{P}_b}{P_b} < 1.84 \times 10^{-12}\,\mathrm{yr}^{-1},$$

implying for the given masses and taking into account that only the neutron star is undergoing the mass loss

$$\left|\frac{\dot{M}}{M}\right| = \frac{M + M_c}{2M}\frac{\dot{P}_b}{P_b} < 1.6 \times 10^{-12}\,\mathrm{yr}^{-1},$$

where M_c is the mass of the white dwarf companion.

This implies a limit

$$\epsilon' < 1.4 \times 10^{-13}\ \mathrm{eV}.$$

This result is very important, as for the other three pulsars pulsars, one may have argued that the transition $n \to n'$ has already finished. This young pulsar closes the door on this argument.

PSR J0437-4715

This is a neutron star-white dwarf binary with masses of $1.76M_\odot$ and $0.25M_\odot$, respectively. The spin-down age is $1.6 \times 10^9\,\mathrm{yr}$. Using the data from the above observational papers, one finds that the residual (subtracting from the measured value the gravitational radiation terms as well as the galactic acceleration and the kinematic effect and allowing for the uncertainties of all the above) positive possible value of the orbital period rate of change is [20],

$$\frac{\dot{P}_b}{P_b} < 2.8 \times 10^{-11}\,\mathrm{yr}^{-1},$$

implying

$$\left|\frac{\dot{M}}{M}\right| < 1.6 \times 10^{-11}\,\mathrm{yr}^{-1}$$

and therefore,

$$\epsilon' < 4.4 \times 10^{-13}\,\mathrm{eV}.$$

PSR J1952+2630

This pulsar is in a binary orbit with a $(0.93 \div 1.4)M_\odot$ white dwarf companion [18]. Its spin down age is $7.7 \times 10^7\,\mathrm{yr}$, the orbital period is 0.39 days and during 800 days of follow-up the error on the period is 7×10^{-12} days. This leads to $\dot{P}_b/P_b < 8.2 \times 10^{-12}\ \mathrm{yr}^{-1}$.

Taking into account that only the pulsar losses mass, we get

$$\left|\frac{\dot{M}}{M}\right| = \frac{M + M_c}{2M}\frac{\dot{P}_b}{P_b} < 7 \times 10^{-12}\,\mathrm{yr}^{-1},$$

where M_c is the mass of the white dwarf companion.

Thus one finds

$$\epsilon' < 2.9 \times 10^{-13}\,\mathrm{eV}.$$

The expected period change due to gravitational radiation in this pulsar is 2 orders of magnitude smaller, and thus does not interfere with the derived limit.

7. Discussion

In this paper, used astrophysical data, notably, precision pulsar timing measurements to strongly constrain a putative $n \to n'$ transition in neutron stars.

We solved numerically the general relativistic structure equations for neutron stars with three different baryon mass. Using a realistic nuclear matter equation of stat, we first solved for a pure ordinary neutron star and then (for the same baryon mass) we obtained the solution for a fully mixed neutron-mirror neutron star. In this way, we found the average mass reduction rate over the the time span of the transition. From the solution of the ordinary neutron star we found the mass reduction at the very beginning of the process. We found that two methods yield

similar relations between the rate of mass change of the star and the rate of the microscopic process.

This allows us to restrict the mixing parameter between. We find that the key parameter ϵ' responsible for $n \to n'$ transition is restricted to be below 4.4×10^{-13} eV.

All four binary pulsars considered here yield quite similar limits on ϵ'. Of particular importance is the the limits are quite the same even though systems ages vary between 2×10^6 yr and 1.6×10^9 yr. The presence of the youngest binary pulsar refutes the possibility that for the older pulsars the process has been already finished.

Our limits on ϵ' also exclude the possibility that nn' oscillations can explain the neutron decay anomaly [22].

Acknowledgments

This work has been supported by the Afeka College Research Fund.

References

[1] Lee, T. D. and Yang, C. N.: Phys. Rev. **104** (1956), 254 communication; Kobzarev, Y., Okun, L., and Pomeranchuk, I. Ya: Yad. Fiz. **3** (1966), 1154; Pavsic, M.: Int. J. T. P. **9** (1974), 229; Kolb, E. W., Seckel, D., and Turner, M.: Nature, **514** (1985), 415; Foot, R., Lew, H., and Volkas, R.: Phys. Lett. B **272** (1991), 67.

[2] Foot, R.: Mirror dark matter: Cosmology, galaxy structure and direct detection. Int. J. Mod. Phys. A **29** (2014), 1430013.

[3] Broussard, L. and Kamyshkov, Y.: Talk at BLV 2017; Berezhiani, Z., Frost, M., Kamyshkov, Y., Rybolt, B., and Varriano, L.: Neutron disappearance and regeneration from mirror state. Phys. Rev. D **96** (2017), 035039.

[4] Berezhiani, Z., Dolgov, A., and Mohapatra, R. N.: Asymmetric inflationary reheating and the nature of mirror universe. Phys. Lett. B **375** (1996), 26.

[5] Mohapatra, R. N. and Nussinov, S.: Constraints on mirror models of dark matter from observable neutron-mirror neutron oscillation. Phys. Lett. B **776**, (2018), 22.

[6] Goldman, I., Mohapatra, R. N., Nussinov, S., Rosenbaum, D., and Teplitz, V.: Possible implications of asymmetric Fermionic dark matter for neutron stars. Phys. Lett. B **725** (2013), 200.

[7] Berezhiani, Z. and Bento, L.: Neutron-mirror neutron oscillations: How fast might they be? Phys. Rev. Lett. **96**, (2006), 081801; Berezhiani, Z.: More about neutron-mirror neutron oscillation. Eur. Phys. J. C **64** (2009), 421.

[8] Goldman I., Mohapatra R. N., Nussinov S.: Bounds on neutron mirror neutron mixing from pulsar timing. PhRvD **100** (2019), 123021.

[9] Kuzmin, V. A.: Cp violation and baryon asymmetry of the universe. Pisma Zh. Eksp. Teor. Fiz. **12** (1970), 335; Glashow, S. L.: The future of elementary particle physics. NATO Sci. Ser. B **61**, (1980), 687; Mohapatra, R. N. and Marshak, R. E.: Local B-L symmetry of electroweak interactions, majorana neutrinos and neutron oscillations. Phys. Rev. Lett. **44** (1980), 1316; Erratum: Phys. Rev. Lett. **44**, (1980), 1643.

[10] Mohapatra, R. N.: Neutron-anti-neutron oscillation: Theory and phenomenology. J. Phys. G **36** (2009), 104006; Phillips, D. G. et al.: Neutron-antineutron oscillations: Theoretical status and experimental Prospects. Phys. Rept. **612** (2016), 1.

[11] Jeans, J. H.: Mon. Not. Roy. Astron. Soc. **85** (1924), 2.

[12] Goldman, I. and Nussinov, S.: Limit on continuous neutrino emission from neutron stars. JHEP **1008** (2010), 091.

[13] Mannarelli, M., Berezhiani, Z., Biondi, R., and Tonnelli, F.: Talk at the Nordita ESS Workshop, December (2018).

[14] Cowsik, R. and Nussinov, S.: Some constraints on $\Delta B = 2$ n anti-n oscillations. Phys. Lett. B **101** (1981), 237.

[15] Weisberg, J. M., Nice, D. J., and Taylor, J. H.: Timing measurements of the relativistic binary pulsar PSR B1913+16. Astrophys. J. **722** (2010), 1030.

[16] Demorest, P. B., Pennucci, T., Ransom, S. M., Roberts, M. S. E., and Hessels, J. W. T.: A two-solar-mass neutron star measured using Shapiro delay. Nature **467** (2010), 1081.

[17] Ng, C., Kruckow, M. U., Tauris, T. M. et al.: A young radio pulsar with a massive compact companion. Mon. Not. Roy. Astron. Soc. **476** (2018), 4315.

[18] Lazarus, P. et al.: Timing of a young mildly recycled pulsar with a massive white dwarf companion. Mon. Not. Roy. Astron. Soc. **437** (2014), 1485.

[19] Bhat, N. D. R., Bailes, M., and Verbiest, J. P. W.: Gravitational-radiation losses from the pulsar-white-dwarf binary PSR J1141-6545. Phys. Rev. D **77** (2008), 24017.

[20] Verbiest, J. P. W. et al.: Precision timing of PSR J0437-4715: An accurate pulsar distance, a high pulsar mass, and a limit on the variation of Newton's gravitational constant. Astrophys. J. **679** (2008), 675.

[21] Steiner, A. W., Lattimer, J. M., and Brown, E. F.: The equation of state from observed masses and radii of neutron stars. Astrophys. J. **722** (2010), 33.

[22] Berezhiani, Z.: Neutron lifetime puzzle and neutron-mirror neutron oscillation. European Phys. J. C **72** (2019), 4849.

HISTORY AND PHILOSOPHY OF COSMOLOGY

Conference *Cosmology on Small Scales 2020*
Michal Křížek and Yurii Dumin (Eds.)
Institute of Mathematics CAS, Prague

COSMOLOGICAL COINCIDENCES IN THE EXPANDING UNIVERSE

Vladimír Novotný

Cosmological Section of the Czech Astronomical Society
Jašíkova 1533/4, CZ-149 00 Prague 4, Czech Republic
nasa@seznam.cz

Abstract: In the study of dimensionless combinations of fundamental physical constants and cosmological quantities, it was found that some of them reach enormous values. In addition, the order of magnitude of some of them appears to be the same or in an arithmetic relation to others. Because attempts to calculate these quantities and other (smaller ones) from first principles were unsuccessful, Paul A. M. Dirac attempted to base cosmological theory on these coincidences. The result of his relations resulted in a decreasing gravitational constant. After many more similar attempts to explain these coincidences, and after the creation of alternative theories of gravity to the general theory of relativity, it has been shown that the required degree of variability of the gravitational constant can be experimentally ruled out. With a combination of cosmological coincidences however, it is possible to establish a relationship that relates the ratio of the total mass of the observable universe to its radius. This relationship is independent of time and is given by the ratio of the square of the speed of light and the gravitational constant. The mass of the observable part of the universe thus increases in the same way as its radius. In an expanding universe, this can be explained simply by the fact that the horizon recedes and new matter enters the observable region.

Keywords: Cosmological coincidences, cosmological numbers, Dirac's Large Numbers Hypothesis, Dirac's cosmology, Eddington number, expanding universe, Einstein-de Sitter model

PACS: 01.65.+g, 04.50.Kd, 04.80.Cc, 04.90.+e, 98.80.-k, 98.80.Bp, 98.80.Jk

1. Introduction

The dimensions and evolution of cosmic objects are determined by dimensionless combinations of fundamental physical constants, see [1]. In this paper, we will deal only with the following: speed of light c in vacuum, the reduced Planck constant $\hbar = h/(2\pi)$, the gravitational constant G, the elementary charge e, as well as the mass of proton m_{p} and the mass of electron m_{e} at rest (see Table 1).

name	symbol	value	remark
speed of light in vacuum	c	$299\,792\,458$ m/s	by definition
Planck constant	h	$6.62607015 \cdot 10^{-34}$ Js	by definition
reduced Planck constant	$\hbar$	$1.05457182 \cdot 10^{-34}$ Js	$\hbar = h/(2\pi)$
gravitational constant	G	$6.674 \cdot 10^{-11}\mathrm{m^3kg^{-1}s^{-2}}$	measured value
elementary charge	e	$1.602176634 \cdot 10^{-19}$ C	by definition
mass of the proton	m_p	$1.67262192 \cdot 10^{-27}$ kg	measured value
mass of the electron	m_e	$9.10938370 \cdot 10^{-31}$ kg	measured value
Boltzmann constant	k	$1.380649 \cdot 10^{-23}$ J/K	by definition
Avogadro constant	N_A	$6.02214076 \cdot 10^{23}\,\mathrm{mol^{-1}}$	by definition
vacuum permittivity	ε_0	$8.854187812 \cdot 10^{-12}$ F/m	measured value

Table 1. Values of some fundamental constants and other quantities

In addition to the above-mentioned fundamental physical constants, quantities derived from the dimensions of the observable universe or the number of particles in it can also enter dimensionless combinations. All these dimensionless combinations form groups of order of magnitude separated by size — most combinations have a value from 10^{-3} to 10^3, but some reach extreme values of 10^{40} or even 10^{80}, see [2]. Most dimensionless quantities constructed in this way have their own names (see Table 2).

name	symbol	value	relationship
fine-structure constant	α	$1/137.036$	$\mathrm{e}^2/(4\pi\varepsilon_0\hbar c)$
grav. fine-structure constant	α_G	$5.90 \cdot 10^{-39}$	$Gm_\mathrm{p}^2/(\hbar c)$
elmag. to grav. intensity ratio	-	$1.24 \cdot 10^{36}$	$Gm_\mathrm{p}^2/(4\pi\varepsilon_0) = \alpha/\alpha_\mathrm{G}$
proton to electron mass ratio	-	1836.15	$m_\mathrm{p}/m_\mathrm{e}$
Compton wavelength of electron	λ_e	$3.86 \cdot 10^{-13}$m	$\hbar/(m_\mathrm{e}c)$
classical electron radius	r_e	$2.82 \cdot 10^{-15}$m	$\mathrm{e}^2/(4\pi\varepsilon_0 m_\mathrm{e}c^2) = \lambda_\mathrm{e}\alpha$
1st Bohr radius	r_B	$5.29 \cdot 10^{-11}$m	$4\pi\varepsilon_0\hbar^2/(m_\mathrm{e}\mathrm{e}^2) = \lambda_\mathrm{e}/\alpha$

Table 2. Values of some dimensionless and length quantities

Dimensionless quantities of the order of 10^{10} are referred to as *cosmological numbers* (sometimes also *cosmic numbers*). This group also includes the binding constant of gravity α_G and the ratio of the intensity of electromagnetic and gravitational interaction α/α_G. However, there are exceptions, because only they contain mere microphysical constants (if we consider the gravitational constant G as a microphys-

ical constant). The relationships between cosmological numbers are then referred to as *cosmological coincidences*.

One of the basic physical questions from the beginning of the 20th century was whether the whole universe affected local physics or not, and whether the very small value of the gravity coupling constant α_{G} is not conditioned by the size of the observable universe or the number of particles in it. Cosmological coincidences may have indicated whether such a possibility was realistic.

Cosmological coincidences are usually assessed only in the order of magnitude, and coefficients close to one tend to be neglected in the relationships between cosmological numbers. In our work, however, we will respect such coefficients and take them into account.

In the older literature, where the CGS system is used, the expression e^2 corresponds to our expression $\mathrm{e}^2/(4\pi\varepsilon_0)$ appearing in Coulomb's law, where ε_0 is the permittivity of vacuum. Thus the CGS system has a different unit of charge than the SI system, it is not rationalized and the permittivity of the vacuum in it is by definition equal to one (in terms of one).

Note that for the dimensionless coupling constant of the electromagnetic interaction α, called the *fine-structure constant* or *Sommerfeld's constant*, the relation $\alpha = \mathrm{e}^2/(4\pi\varepsilon_0\hbar c)$ applies in the SI system, but in the CGS system $\alpha = \mathrm{e}^2/(\hbar c)$. Since it is a dimensionless quantity, its value is independent of the selected system of units. It pays a role in the relationships for the splitting of spectral lines, which is caused by relativistic phenomena and spin-orbital interactions.

We can construct a similar dimensionless quantity, α_{G}, for the gravitational interaction. Its notation is identical in the SI system and in the CGS system. Unlike the constant of the fine structure α, in the definition of which the elementary charge unambiguously appears, we have to decide which elementary particle and its mass we choose here to be fundamental. Usually the proton is chosen here, because it is a much more massive particle than the electron and it gravitationally dominates in the universe among stable particles. Then $\alpha_{\mathrm{G}} = Gm_{\mathrm{p}}^2/(\hbar c)$.

2. Weyl and Eddington

Let N_1 denote the ratio of the intensity of the electromagnetic and gravitational interaction between the proton and electron, which does not change with distance. We will write this relationships in the SI system as follows

$$N_1 = \frac{\alpha}{\alpha_{\mathrm{G}}}\frac{m_{\mathrm{p}}}{m_{\mathrm{e}}} = \frac{\dfrac{\mathrm{e}^2}{4\pi\varepsilon_0\hbar c}}{\dfrac{Gm_{\mathrm{p}}m_{\mathrm{e}}}{\hbar c}} = \frac{\dfrac{\mathrm{e}^2}{4\pi\varepsilon_0}}{Gm_{\mathrm{p}}m_{\mathrm{e}}} = 2.27\cdot 10^{39}. \tag{1}$$

Futher, let N_2 denote the ratio of the *radius R of the observable universe* and the *classical electron radius* r_{e} (the classical electron radius $r_{\mathrm{e}} = \mathrm{e}^2/(4\pi\varepsilon_0 m_{\mathrm{e}}c^2)$ is a formal quantity denoting the radius of a sphere with uniformly spatially distributed charge, whose total electrostatic energy is equal to the rest energy of the electron).

We replace the radius R of the observable universe by the product cT, where T is the present age of the universe, which is quite famous quantity today ($13.8 \cdot 10^9$ years, i.e. $4.35 \cdot 10^{17}$ s), see [3]. We get a value of $1.31 \cdot 10^{26}$ m, i.e. cca 4200 Mpc. More precisely, there should be kcT, where the size of the constant k depends on a specific model of the universe. For instance, $k = 3$ in the Einstein-de Sitter model of the universe, which is spatially uncurved, has zero cosmological constant, and contains only material dust. We have

$$N_2 = \frac{R}{r_\mathrm{e}} = \frac{R}{\dfrac{\mathrm{e}^2}{4\pi\varepsilon_0 m_\mathrm{e} c^2}} = \frac{4\pi\varepsilon_0 m_\mathrm{e} c^2 R}{\mathrm{e}^2} = \frac{4\pi\varepsilon_0 m_\mathrm{e} c^3 T}{\mathrm{e}^2} = 4.63 \cdot 10^{40}. \tag{2}$$

The coincidence order of the dimensionless quantities N_1 and N_2, both of which have a value of about 10^{40}, was discovered in 1919 by H. Weyl in [4] and discussed in more detail in [5]. F. Zwicky called it Weyl's hypothesis [6], but later this name was not adopted.

Another cosmological number N_3 was introduced by A. S. Eddington, see [7, 8]. In the literature, it is often referred to as the *Eddington number*. It represents the number of nucleons in the observable universe and can be expressed as the ratio of the mass M of the observable part of the universe to the mass of one proton. Its size is of the order of 10^{80}. We will also use this value,

$$N_3 = \frac{M}{m_\mathrm{p}}. \tag{3}$$

Then

$$M = m_\mathrm{p} 10^{80} = 1.67 \cdot 10^{-27} \cdot 10^{80} \text{ kg} = 1.67 \cdot 10^{53} \text{ kg}.$$

The order of magnitude of N_3 is thus roughly equal to the square of the numbers N_1 or N_2. Throughout his life, Eddington tried to create a theory that would allow the theoretical calculation of the number N_3 and other dimensionless quantities, such as the fine-structure constant α or the ratio of the masses of the proton and electron $m_\mathrm{p}/m_\mathrm{e}$, see [9]. The resulting Eddington theory was not published until after his death, by E. T. Whittaker in 1946 in the book Fundamental Theory (cf. [10]), but did not receive a favorable recognition, and the general opinion is that it is wrong [11]. Eddington's successive attempts to calculate the number N_3 gave results of the order 10^{79} to 10^{80}. His formula was based on the multiplication of the factors 136 and 2^{256}, where 136 is the approximate value of the reciprocal fine-structure constant $\alpha \approx 1/137$. All there numbers N_1, N_2, and N_3 are constants in Eddingon's theory. Attempts to calculate theoretically the exact values of α and $m_\mathrm{p}/m_\mathrm{e}$ continues up to now, but without any noticeable success.

3. Dirac and Gamow

In 1937 and 1938, Paul A. M. Dirac published two works [12] and [13], in which he introduces a completely new approach to the problem of cosmological numbers. He

formulates the *Large Numbers Hypothesis* (LNH, latter called *Dirac's LNH*) in which he assumes that all very large numbers in physics are connected together by simple arithmetic relations in which coefficients of magnitude of units occur. The hypothesis was based, among other things, on the fact that obtaining theoretically very large numbers is quite difficult. LNH-based cosmology is called *Dirac's cosmology.*

Thus, according to Dirac's LNH, it should hold $N_1 = N_2$ and $N_3 = N_2^2$. Because the number N_2 increases with time, the number N_1 should grow with time, too, and the number N_3 should grow with time quadratically, namely, we have

$$N_1(t)N_2(t) = N_3(t). \tag{4}$$

Since the number N_1 contains only microphysical constants, in order to satisfy the LNH, it is necessary that some of them are variable in time. Dirac chose the gravitational constant G as a variable. First, this constant is measured with very low relative accuracy, but an important argument was that many physicists at that time believed that the marked weakness of gravity was related to the large number of particles in the observable universe. Later, in 1974 (see [14]) and is 1979 (see [15]), Dirac added to his cosmology the assumption of the formation of particles in the observable universe so that the LNH would also be satisfied for the number N_3. He considered two possibilities – matter could increase in the universe either uniformly or preferentially in areas where it already exists.

The first objection to the change of the gravitational constant over time was as early as in 1948 published by E. Teller [16]. He stated that the luminosity of the Sun depends on the 7th power of the gravitational constant, and if Dirac's LNH were valid, the Sun in the Precambrian Era would have to shine much more strongly than it does today. Water could not exist on Earth in a liquid state, and the origin of life at that time would be impossible.

Second, Dirac's hypothesis had a large number of responses in the literature. On one hand, it was a partial inspiration for constructing alternative theories of gravity, such as Jordan's theory [17], Brans-Dicke's theory [18], and Hsieh-Canuto's theory [19]. Furthermore, various modifications of its occurrence have appeared, and still appear in the literature, and several other coincidences have been studied.

Third, Dirac's hypothesis led to an experimental effort to directly measure the limits for a possible change in the gravitational constant, which led to the definitive refutation of its original version in the 1980s. It was based on the measurements of the Viking spacecraft, located on Mars, which made it possible to measure very accurately the distance of Mars from Earth. It has been shown that the orbits of the planets in the Solar system do not increase to the extent that Dirac's hypothesis assumes, see [20].

In the late 1960s, G. Gamow published an alternative hypothesis that gravity does not weaken, but the strength of the electromagnetic interaction increases as the magnitude of the elementary charge increases over time [21, 22]. However, this version was very soon refuted, see [23, 24, 25, 26].

4. Dicke and Crater

Another opinion was expressed in 1961 by R. H. Dicke [27], who calculated that the average lifetime of stars roughly corresponds to the present age of the universe. This explains the order of magnitude of the number N_2, which must reach the value of N_1 in order for the interstellar matter to be enriched with heavier elements. It is mainly the carbon needed for the development of life and then for the formation of the observer. This view was an important impulse for the formulation of the anthropic principle by B. Carter in 1974, see [28, 29]. The anthropic principle formulated in various versions is very often discussed today in both cosmological and philosophical works. In its consequences, it also led to considerations about the possible existence of a multiverse, see [30].

In Dicke's view, therefore, N_1 is constant, N_2 increases with time as in Dirac's theory, and N_3, which is their product, also increases, but only proportionally to N_2.

$$N_1 N_2(t) = N_3(t). \tag{5}$$

5. Machian condition

Below we show how (5) arises. Substituting into equation (5) from relations (1), (2), and (3), we get

$$\frac{\dfrac{\mathrm{e}^2}{4\pi\varepsilon_0\hbar c}}{\dfrac{Gm_\mathrm{p}m_\mathrm{e}}{\hbar c}} \cdot \frac{R}{\dfrac{\mathrm{e}^2}{4\pi\varepsilon_0 m_\mathrm{e}c^2}} = \frac{M}{m_\mathrm{p}} \tag{6}$$

which means

$$\frac{\mathrm{e}^2 4\pi\varepsilon_0 m_\mathrm{e}c^2 m_\mathrm{p}}{4\pi\varepsilon_0 G m_\mathrm{p} m_\mathrm{e}\mathrm{e}^2} = \frac{M}{R},$$

and finally,

$$\frac{c^2}{G} = \frac{M}{R}. \tag{7}$$

We see that the M/R ratio should remain constant for the duration of the universe and should be equal to the constant $c^2/G = 1.27 \cdot 10^{27}$ kg/m. Calculated quantities $M = 1.67 \cdot 10^{53}$ kg and $R = 1.31 \cdot 10^{26}$ m satisfy this relationship very well. Since we are only looking for an order of magnitude match, the result is fully in line with expectations.

Dividing equation (5) by the right-hand side, we get (compare also with [31])

$$\frac{N_1 N_2}{N_3} = \frac{c^2 R}{GM} = 1,$$

that is

$$\frac{GM}{Rc^2} = 1. \tag{8}$$

This equality should be considered only approximately, of course. Thus, we obtain a result corresponding to the so-called *Machian initial condition*, the fulfillment of which is assumed for any realistic model of the universe, see [32]. Since Mach's principle is not included in Einstein's General Theory of Relativity, some authors consider relation (8) to be the selection principle for a proper choice of a realistic model of the universe, see [33].

6. Solution in an expanding universe

The question remains how it is possible for the number of particles in the observable universe to grow linearly with time. The answer is very simple. The observable universe seems to be flat, as found in 2000 in the BOOMERANG experiment [34]. Because the influence of the cosmological constant was negligible in the first billions of the universe's existence, the universe behaved more or less according to the Einstein-de Sitter model. This model describes a spatially flat infinite universe with a critical mass density and zero cosmological constant [35]. The radius of the observable region R increases roughly as the product of cT. Because this model is Euclidean, the volume of the observable universe will be proportional to t^3. However, in this model, the mass density decreases at the same time proportionally to t^2, see [36]. Therefore, the number of particles in the observable part of the universe will increase proportionally with time as

$$N_3 \sim V\rho \sim t^3 t^{-2} = t,$$

where ρ is the mean density.

7. Conclusions

We have to state that from today's point of view, it is clear that since the properties of the Einstein-de Sitter model of the universe were already known in 1961 (which also applies in 1937), it was possible to withdraw from the model with decreasing gravitational constant and not try to supplement or to modify the original LNH, or to create other theories of gravity competing with the General Theory of Relativity, which sought to describe gravity as an interaction whose intensity decreases with time (although the author of this article is aware that the main reason for constructing such theories was the incorporation of Mach's principle into the theory of gravity, not only the fulfillment of LNH). It is noteworthy that the development of Dirac's LNH in terms of development of the expanding universe appears in the literature only in note 26 to Chapter 4 of the book by J. D. Barrow *The Book of the Universes*, see [37]. The main goal of this article was to draw an attention to Barrow's evaluation.

Remark. Due to the redefining of the basic units of the SI system in 2019 (especially kilograms and amperes), the quantities c, $\hbar$, e (as well as the Boltzmann constant k and the Avogadro's constant N_{A}) are already defined as real constants [38, 39], cf. also Table 1. A possible variability of the coupling constants α and

α_G, which is still being sought, would be reflected in the variability of the vacuum permittivity ε_0 and the gravitational constant G.

Acknowledgment. The author thanks Michal Křížek for his impulse to write this article and for his advice in its preparation. He is also indebted to Filip Křížek and Lawrence Somer for valuable suggestions.

References

[1] Carr, B. J., Rees, M. J.: The anthropic principle and the structure of the physical world. Nature **278** (1979), 605–612.

[2] Harrison, E. R.: The cosmic numbers. Physics Today **25** (12) (1972), 30–34.

[3] Planck Collaboration: Planck 2018 results. VI. Cosmological parameters, arXiv: 1807.06209v2 [astro-ph.CO], p. 14.

[4] Weyl, H.: Eine neue Erweiterung der Relativitätstheorie, Ann. Phys. **59** (1919), p. 129.

[5] Weyl, H.: Universum und Atom, Naturwissenschaften **22** (1934), 145–149.

[6] Zwicky, F.: On the theory and observation of highly collapsed stars, Phys. Rev. **55** (1939), 726–743.

[7] Eddington, A. S.: Preliminary note on the masses of the electron, the proton, and the universe, Math. Proc. Cambridge Phil. Soc. **27** (1931), 15–19.

[8] Eddington, A. S.: On the value of the cosmical constant, Proc. Roy. Soc. London A **133** (1931), 605–615.

[9] Eddington, A. S.: Relativity Theory of Protons and Electrons, Cambridge University Press, 1936.

[10] Eddington, A. S.: Fundamental Theory, Cambridge University Press, 1946.

[11] Barrow, J. D., Tipler F. J.: The Anthropic Cosmological Principle, Oxford University Press, 1986, p. 226.

[12] Dirac, P. A. M.: The cosmological constants, Nature **139** (1937), 323.

[13] Dirac, P. A. M.: A new basis for cosmology, Proc. Roy. Soc. London A **165** (1938), 199–208.

[14] Dirac, P. A. M.: Cosmological models and the Large Numbers Hypothesis, Proc. Roy. Soc. Lond. A **338** (1974), 439–446.

[15] Dirac, P. A. M.: The Large Numbers Hypothesis and the Einstein theory of gravitation, Proc. Roy. Soc. London A **365** (1979), 19–30.

[16] Teller, E.: On the change of physical constants, Phys. Rev. **73** (1948), 801–802.

[17] Jordan, P.: Schwerkraft und Weltall, Braunschweig, F. Vieweg & Sohn, 1952.

[18] Brans, C., Dicke, R. H.: Mach's Principle and a relativistic theory of gravitation, Phys. Rev. **124** (1961), 925–935.

[19] Canuto, V., Adams, P. J., Hsieh, S.-H., Tsiang, E.: Scale-covariant theory of gravitation and astrophysical applications, Phys. Rev. D **16** (1977), 1643–1663.

[20] Hellings, R. W., Adams, P. J., Anderson J. D. et al.: Experimental test of the variability of G using Viking Lander Ranging Data, Phys. Rev. Lett. **51** (1983), 1609–1612.

[21] Gamow, G.: Electricity, gravity, and cosmology, Phys. Rev. Lett. **19** (1967), 759–761.

[22] Gamow, G.: Variability of elementary charge and quasistellar objects, Phys. Rev. Lett. **19** (1967), 913–914.

[23] Dyson, F. J.: Time variation of the charge of the proton, Phys. Rev. Lett. **19** (1967), 1291–1293.

[24] Peres, A.: Constancy of the fundamental electric charge, Phys. Rev. Lett. **19** (1967), 1393–1294.

[25] Bahcal, J. N., Schmidt M.: Does the fine-structure constant vary with cosmic time?, Phys. Rev. Lett. **19** (1967), 1294–1295.

[26] Chitre, S. M., Pal, Y.: Limit on variation of e^2 with time, Phys. Rev. Lett. **20** (1967), 278–279.

[27] Dicke, R. H.: Dirac's Cosmology and Mach's Principle, Nature **192** (1961), 440.

[28] Carter, B.: Large Number Coincidences and the Anthropic Principle in Cosmology, in: Longair M. (ed.): Confrontation of Cosmological Theories with Observational Data, 1974, 291–298.

[29] Carter, B.: The Significance of Numerical Coincidences in Nature, Part 1 – The Role of Fundamental Microphysical Parameters in Cosmogony, arXiv:0710.3543v1 [hep-th], 1–73.

[30] Carr, B. (ed.): Universe or Multiverse?, Cambridge University Press, 2007.

[31] Alpher, R. A.: Large numbers, cosmology, and Gamow, Am. Sci. **61** (1973), 52–58.

[32] Dicke, R. H.: The many faces of Mach, in: Gravitation and Relativity, Chiu H.-Y., Hoffmann W. F. (eds.), W. A. Benjamin, Inc. 1964, 121–141.

[33] Wheeler J. A.: Mach's Principle as boundary condition for Einstein's equations, in: Gravitation and Relativity, Chiu H.-Y., Hoffmann W. F. (eds.), W. A. Benjamin, Inc., 1964, 303–349.

[34] de Bernardis, P. et al.: A flat universe from high-resolution maps of the cosmic microwave background radiation, Nature **404** (2000), 955–959.

[35] Einstein, A., de Sitter, W.: On the relation between the expansion and the mean density of the universe, Proc. Nat. Acad. Sci. **18** (1932), 213–214.

[36] Rindler, W.: Relativity – Special, General, and Cosmological, Oxford University Press, 2nd Ed., 2006, p. 401.

[37] Barrow, J. D.: The Book of the Universes, The Boldey Head, London, 2011, p. 312.

[38] Stock, M.: The revision of the SI – the result of three decades of progress in metrology, Metrologia **56** (2019), 022001.

[39] Martin-Delgado, M. A.: The new SI and the fundamental constants of Nature, arXiv: 2005.01428v1 [physics.pop-ph], 1–18.

Conference *Cosmology on Small Scales 2020*
Michal Křížek and Yurii Dumin (Eds.)
Institute of Mathematics CAS, Prague

VEDIC COSMOLOGY ON THE CHARACTERISTICS AND ROLE OF DARK MATTER: IMPLICATIONS FOR THE SEARCH OF DARK MATTER PARTICLE

Yash Aggarwal

Emeritus Research Associate
Lamont-Doherty Earth Observatory of Columbia University
Palisades, NY 10964, U.S.A.
haggarwal@hotmail.com

Abstract: Despite decades of efforts and an active intensive experimental program, the nature of dark matter (DM) remains an unsolved mystery. The problem is that we do not know what we are looking for. We submit that Vedic Cosmology (VC) expounded in Vishnu Purana (VP), an ancient Indian Text, may shed light on what DM might be and inform its search, and show why VC deserves serious scientific scrutiny. A critical examination of VP shows that it describes three constituents of the universe that are astonishingly similar to those of Standard Cosmology (SC): Vyakta or visible/ordinary matter; Pradhana, an invisible primary matter; and Purusha, an invisible nondescript energy. Vyakta or visible matter is common to both cosmologies. Pradhana is described as 'subtle, uniform, durable, self-sustained, illimitable, undecaying, and stable; devoid of sound or touch, and possessing neither colour nor form'. Thus, Pradhana has the essential widely-accepted characteristics of DM in that it does not emit or absorb light or other electromagnetic radiation, is illimitable or much more abundant than visible matter, and stable as DM is thought to be. Moreover, VP describes the morphology and constituents of a structure resembling a proto-galaxy in which a halo of this invisible primary matter surrounds ordinary matter with a central cavity/hole; which leaves little doubt that Pradhana of VP is most probably the DM of SC. Purusha, the third constituent of the universe in VC, is equated here with dark energy (DE) of SC. Pradhana is undecaying; which may explain why no decay product of DM has thus far been detected. Furthermore, consistent with the principle of conservation of mass, VP states that Pradhana/DM was not created, nor can it be destroyed, and that ordinary matter is a product of DM and converted back to DM over trillions of years. If so, the DM particle cannot be a sub-atomic elementary particle, nor a hypothetical light particle such as an axion, and has to be more massive than the sum of the masses of all elementary particles. And it implies that under certain unspecified conditions ordinary

matter could be synthesized into DM. Additionally, VC indicates that density of DM/Pradhana is constant, as is apparently the density of DE in SC and of the invisible nondescript energy Purusha in VC; which resolves the Cosmological Coincidence problem and is shown to yield a Hubble constant comparable in value to that measured locally.

Keywords: Dark matter, Dark energy, Dark matter's relationship with ordinary matter, search for Dark matter particle, ultimate fate of Universe and Earth

PACS: 98.80.-k

1. Introduction

The existence of dark matter (DE) was first suggested almost a hundred years ago by the Dutch astronomer Jacobus Cornelius Kapteyn using stellar velocities, see [8]. Since then a number of astronomical observations have affirmed its existence. Zwicky in [24] and [25] tracked the velocities of galaxies within galaxy clusters and observed that the gravity of visible matter alone was not sufficient to keep the cluster from flying apart and that additional matter that was not visible was needed to keep the cluster together. Rubin et al. in [15] observed the velocities of stars on the outskirts of individual galaxies, and a stream of observations including gravitational lensing by galaxy clusters followed in the 1980s. Rubin et al. in [16] concluded that most galaxies must contain $\sim$ six times as much dark as visible mass. And by the 1980s it came to be widely accepted that astronomically observed gravitational effects could not be accounted for by existing theories of gravity unless matter that is invisible or dark is present in the universe, see Randall [13]. Alternatively, modifications to existing theories of gravity have been proposed to explain the need for the presence of DM. These modifications are, however, unsatisfactory on theoretical grounds and apparently still require the presence of DM to correctly describe the formation of large-scale structure of the universe, see [3].

At the present, DM is inferred to be 5 to 6 times more abundant than visible/ordinary matter, constituting $\sim 85\,\%$ of the matter in the universe and $\sim 25\,\%$ of its energy density, see Planck collaboration [11]. It is thought to be non-baryonic, mostly "cold" or that it moves much more slowly than the speed of light, stable on cosmological time scales, does not interact with ordinary matter through the strong nuclear force, but through gravity and possibly through the weak nuclear force, see [3]. Candidates include primordial black holes, and new-undiscovered particles such as axions, sterile neutrinos, and WIMPs or weakly interacting massive particles, see [3]. The current search for DM particles involves: indirect detection or observation of signals from deep in the universe emanating from the annihilation or decay of DM particles; creation of DM particles through high-energy collision of protons in the Large Hadron Collider; and direct detection based on the hope that DM particles may occasionally interact with ordinary matter such as liquid xenon through the weak force, see Toomey [20]. Unfortunately, despite decades of efforts

and an ongoing intensive experimental program, the search for DM particle(s) remains elusive. The problem is that none of the observations or computer simulations involving DM give a clear indication as to what DM is made up of. In short we do not know what we are looking for.

We submit that Vedic Cosmology (VC) may shed light on the characteristics of DM, its relationship with ordinary matter, and its role in the evolution of the universe; and consequently may inform the search for the elusive DM particle. Vishnu Purana (VP), a post-Vedic ancient Text in Sanskrit translated into English by Wilson, see [23], offers the principal tenets of VC. It describes in considerable detail the origins of the universe, its cyclic nature, the ultimate fate of planet Earth and the universe, cosmic cycles spanning billions to trillions of years, and three constituents of the universe, one of which appears to be the DM of the modern-day Standard Cosmology (SC). It is noteworthy that the late astrophysicist Carl Sagan in [17] aptly observed that the cosmic cycles described in VP "correspond, **no doubt by accident**, to those of modern scientific cosmology. Its cycles run from our ordinary day and night to a day and night of Brahma, 8.64 billion years long, longer than the age of the Earth or the Sun and about half the time since the Big Bang. And there are much longer time scales still". After a careful scrutiny of VP, Aggarwal in [1] showed that the time span of 8.64 billion years (Gy) noted by Sagan **was not an accident**, but apparently corresponds to Sun's useful life comparable to the current rough estimate of 10 Gy for Sun's life on the main sequence. In addition, the age of the universe and the timing of the formation of the first solar system in the Milky Way inferred from VP, and the sequence of events leading to the incineration of planet Earth by an expanding Sun in the next 4–5 Gy described in VP, agree remarkably well with current scientific data and/or models, see [1]. Here, after additional research, we go a step further and explore the nature of DM, dark energy (DE), space, and time and their roles in the formation and evolution of the universe as expounded or inferred from VP, and discuss their implications. We begin, however, with a brief review of the conclusions in [1]), clarifying and supplementing them as warranted that provides a foundational background of this paper and offers compelling reasons why VC merits serious scientific scrutiny despite the fact that its origins remain obscure. Thereafter, we describe and discuss the findings relating to DM.

2. Background

The VP is part of an ensemble of 18 post-Vedic Texts collectively denominated as Puranas, or literally "of ancient times" in Sanskrit. The Puranas are a vast literature of stories and allegory pertaining to cosmology, history, geography, and genealogies of kings, see Krishnananda [9], and not religion per se that requires adherence or blind faith. Not all Puranas were, however, created equal or written at the same time. The VP is one of the two finest Puranas, see [9] and considered to be among the oldest dating back to the first century B.C. for its written form and many centuries older

in its oral form, see Wilson [23]. A word of caution. In addition to describing the beginnings of the universe in material terms, VP invokes non-material elements and metaphysics subject to uncertain interpretations. Also, the Puranas often ascribe a result, outcome, or action to a mythological deity/actor and use different names for the same deity. We overcame such hurdles by separating the core tenets of VC that are beyond reproach from the more tenuous or speculative interpretations, and by focusing on the action or the result and ignoring the actor. Aggarwal in [1] provides a fuller description of VP, other sources supporting the conclusions therein, and methodology used in judging the cosmological content of VP. Note also that when quoting from VP, the word(s) in parentheses are not ours except those in italics.

The VP and the Bhagavata Purana (BP) translated by Prabhupada in [12] describe two major cycles of VC: Vishnu's cycle that lasts $\sim$ 311 trillion years and corresponds to the lifespan of the universe; and the 8.64 Gy long Brahma's cycle noted by Carl Sagan that apparently corresponds to Sun's life span and comparable to the widely used estimate of 10 Gy for Sun's life on the main sequence, see [1]. This rough estimate of 10 Gy, however, suffers from large uncertainties. It is based on Sun's current luminosity, a first order approximation of the amount of Sun's mass available for conversion into solar energy, and assuming a steady state system. Models of Sun's evolution, however, indicate that Sun's luminosity increases with the age of the Sun; and if a rough correction is made assuming a linear increase in Sun's luminosity from its inception to the Red-Giant phase using the model in Schröder and Smith [19], the Sun's life span on the main sequence decreases to $\sim$ 8.9 Gy or closer to the 8.64 Gy time span of Brahma's cycle. And a relatively small change of say 10 % in the fraction of Sun's mass available for fusion would result in a change of almost 1 Gy in Sun's life span.

The VP and BP do not explicitly state the age of the universe, but it can be rather accurately inferred from the past history of Brahma's cycle described in them. The cycle is divided into two equal parts, each 4.32 Gy long called a Kalpa and 2 Kalpas constitute a Brahma's cycle. During the first half of the cycle life evolves and flourishes on an earth-like planet, and during the second half life slowly perishes ending with the incineration of Earth. The VP and BP in fact describe the past history of this cycle, naming each half of the past cycles, and making it clear that one, and only one, Brahmas' cycle or two halves preceded the current cycle (BP, Canto III, Chap. 11, Prabhupada [12]; Aggarwal [1]). And since the current cycle began with the formation of our Solar system $\sim$ 4.57 Gy ago (see [2]), one can deduce from this history that our universe is at least $4.57 + 8.64 = 13.21$ Gy but not more than $13.21 + 4.32 = 17.53$ Gy old, in agreement with current estimate of $\sim$ 13.8 Gy (see [11]) for the age of the universe.

The history of Brahma's cycle indicates that a now-defunct solar system $\sim$ 13.2 Gy old should exist in the Milky Way, and implies that planets formed within less than a billion years of the currently accepted age of the universe. In 2003 the Hubble Space Telescope discovered the existence of a planet in the Milky Way galaxy that formed around a sun-like star $\sim$ 13 Gy ago, whose identity was confirmed by NASA,

see [10]. We quote: "NASA's Hubble Space Telescope precisely measured the mass of the oldest known planet in our Milky Way galaxy. At an estimated age of 13 billion years, the planet is more than twice as old as Earth's 4.5 billion years. It's about as old as a planet can be. It formed around a young, sun-like star barely 1 billion years after our universe's birth in the Big Bang", see [10]. No claim is made here that the primeval solar system discovered by NASA is the solar system predicted by VP. Suffice to note that VP's indication that a solar system formed in the Milky Way galaxy some 13.2 Gy ago is supported by NASA's discovery. This prediction also implies that the Milky Way should be at least ~ 13.2 Gy old. And since heavy elements are generally thought to have been released in supernovae, it follows that the solar system envisioned in VP was presumably preceded by several generations of stars that produced the heavy elements necessary to form the planets. Therefore, we may conclude that VP predicts that the Milky Way should be significantly older than 13.2 Gy and possibly almost as old as the universe itself. In fact, as discussed later, VP describes the morphology and constituents of a large-scale structure resembling a galaxy that apparently formed soon after the beginning of the universe. In 2018 a 13.5 Gy old low-mass metal-poor star was discovered in the Milky Way, indicating that the Milky Way is at least 13.5 Gy old and ~ 3 Gy older than previously thought, see Schlaufman [18].

We are roughly half-way through Brahma's cycle since the inception of our Solar system, just as the Sun is about half-way through its main sequence. The VP predicts that at the end of the current cycle or in ~ 4–5 Gy Earth will be incinerated by the Sun. Succinctly, the sequence begins with a 100-year drought causing havoc because of the failure of crops, followed by extensive evaporation of water, boiling over of rivers and oceans, and a moist runaway green-house effect that leaves the Earth a molten rock before it is consumed by the Sun. And we quote: "The seas, rivers, mountain torrents, and springs are all exhaled; and so are the regions of Patala, the regions below the earth. Thus fed, through his intervention, with abundant moisture, the seven solar rays dilate to seven suns, whose radiance glows above, below, and on every side; and sets the three worlds and Patala on fire. The three worlds, consumed by these suns, become rugged and deformed throughout the whole extent of their mountains, rivers, and seas; and the earth, bare of verdure, and destitute of moisture alone remains, resembling in appearance the back of a tortoise. The great fire, when it has burnt all the divisions of Patala, proceeds to the earth, and consumes it also", see VP, Book VI, Chap. III, Wilson [23]. Compare this description to that in [19] that describes the effects of Sun's evolution on Earth. We quote: In about a billion years "the water vapour content of the atmosphere will increase substantially and the oceans will start to evaporate by Kasting, 1988 in [19]. An initially moist greenhouse effect by Laughlin, 2007 in [19] will cause runaway evaporation until the oceans have boiled dry. The subsequent dry greenhouse phase will raise the surface temperature significantly faster than would be expected from our very simple black-body assumption, and the ultimate fate of the Earth, if it survived at all as a separate body, would be to become a molten remnant". The

Schröder and Smith model (see [19]), however, predicts that eventually the Earth along with Mercury and Venus will be engulfed by the Sun. The major difference, however, between VP and the SS (see [19]) model is that the incineration of Earth in VP takes place in the next $\sim$ 4–5 Gy, whereas in the SS model it takes $\sim$ 7.5 Gy. This difference in large part can be accounted for by the fact that in the SS model Sun's life on the main sequence is fixed at 10 Gy, and as discussed earlier it could be much shorter, possibly by as much as 2 Gy.

3. Constituents of the Universe

Vedic cosmology does not per se invoke a creator as an entity separate from the creation, but posits that underlying the phenomena of creation, evolution, and destruction is an unfathomable reality personified as Vishnu and Brahma that manifests itself in the forms of "Pradhana (primary or crude matter), Purusha (spirit), Vyakta (visible substance), and Kala (time)". See VP, Book I, Chapt. II, Wilson [23]. And, irrespective of whether one accepts or not the existence of such an underlying reality, it is amply clear from VP that the universe is the result of time (Kala) and composed, "in their due proportions" of Vyakta or visible matter, Pradhana or primary matter that is invisible, and Purusha, a nondescript energy that fills all space but is not detectable by the senses. The VP, however, does not specify the quantitative proportions of the three constituents; but implies that the three constituents are in unequal/differing proportions, and we can gauge their relative importance from their descriptions.

Compare these three constituents of VC to those of the SC in which the universe is also composed of three components in unequal proportions: visible/ordinary matter, DM, and DE. Note that visible/ordinary matter is common to both cosmologies. VP describes the characteristics of primary matter (Pradhana). It is characterized as "subtle, uniform, durable, self-sustained, illimitable, undecaying, and stable; devoid of sound or touch, and possessing neither colour nor form". See VP, Book I, Chapt. II, Wilson [23]. Hence, primary matter is invisible or does not emit or absorb light or other electromagnetic radiation, just as DM; is limitless and hence much more abundant than visible matter as DM is deduced to be; and durable and stable as DM is thought to be. Hence, it appears that the primary matter of VC and DM of SC are apparently one and the same thing. And the following description in VP of the morphology and constituents of a large-scale structure resembling a galaxy provides additional evidence that the primary matter of VP is in all likelihood the DM of SC.

Succinctly, VP indicates that ordinary matter is composed of ether, air, light, water, and earth; that these components or elements did not all form simultaneously or at once, but in stages; that ether "endowed with the property of sound" was the first, which in turn produced air, followed by light, then water, and lastly earth; and that "being unconnected, they could not without combination, create living beings, not having blended into each other". See VP, Book I, Chapt. II, Wilson [23]. Here,

we digress somewhat and ponder as to the nature of these five components or elements. Rather than thinking of these five components as building blocks of ordinary matter as is generally thought, we suggest that apart from radiation/light they may represent distinct phases of ordinary matter. In that case air, water, and earth would obviously represent respectively the phases of gas, liquid, and solid; and the question would be whether the remaining component ether (akasha in Sanskrit) is also another phase of matter. We first note that it is not the aether, quintessence, or the fifth element of the Greeks because aether was thought to be non-material (see Fludd [6]), whereas akasha or ether of VP is matter. We suggest that it could be plasma or the missing fourth phase of matter. If so, VP's characterization of ether/akasha as the first stage of matter "endowed with the property of sound" from which ensued air (gas) followed by light (photons) would be remarkably consistent with the following sequence in the evolution of matter and radiation in the early universe. The early universe is thought to have been a hot soup of dense plasma of electrons and baryons (protons and neutrons) in which counteracting forces of gravity and pressure created oscillations analogous to sound waves, see Eisenstein [5]. As the universe expanded, the plasma cooled such that electrons and protons combined forming neutral hydrogen (gas) atoms, allowing photons (light) to decouple from matter and free stream through the universe, see Dodelson [4]. Furthermore, VP's assertion that water and earth were the last to form is consistent with the current understanding that heavier elements such as oxygen formed in stars only after electrons and protons had combined to form hydrogen atoms and photons had decoupled from matter.

Notwithstanding the above digression, VP clearly states that these components then combined with each other and "assumed, through their mutual association, the character of one mass of entire unity" forming an "egg, which gradually expanded like a bubble of water". In that egg "were the (*future*) continents and seas and mountains, the planets, and divisions of the universe, the gods, the demons, and mankind. And this egg was externally invested by seven natural envelopes, or by water, air, fire, ether, and Ahankara the origin of the elements, each tenfold the extent of that which it invested; next came the principle of intelligence, and finally the whole was surrounded by the Indiscrete Principle (*primary invisible / dark matter*); resembling thus the cocoa-nut filled interiorly with pulp, and exteriorly covered by husk and rind." "Its womb, vast as mountain Meru, was composed of the mountains; and the mighty oceans were the waters (*liquid*) that filled its cavity" See VP, Book I, Chapt. II, Wilson [23]. Note that the invisible primary matter Pradhana is also called the Chief principle, Indiscrete principle, or the Equilibrium of the qualities and its characteristics described earlier were shown to be akin to those of DM. Despite some ambiguity concerning the components of ordinary matter, the preceding large-scale structure apparently resembles a galaxy both in its morphology and its constituents. Its shape is analogized with that of a coconut and hence it could be round or ellipsoidal, just as the vast majority of galaxies are observed to be. It has a large central cavity, albeit filled with water (liquid), consistent with the current knowledge that a massive black hole lies at the center of virtually all large galaxies.

Its pulp is made up primarily of ordinary/visible matter in all its phases; which in turn is surrounded by a halo of primary/dark matter. The clear description that the visible part of the structure/galaxy consisting of ordinary matter is surrounded by primary matter that is invisible leaves little doubt that the primary matter of VP is in all likelihood the DM of SC. Dark matter halos play a key role in current models of galaxy formation and evolution. The DM halo envelops the galactic disc and extends well beyond the edge of the visible galaxy, and although invisible, its existence is inferred by astronomical observations of its effects on the motions of stars and galaxies, see Wechsler and Tinker [21]. It appears, however, that the structure described in VP, although large with a cavity vast as mountain Meru, is still in its infancy, gradually expanding or growing like a bubble of water and not fully developed just like an egg waiting to hatch.

Unfortunately, VP does not describe in similar detail what the third component is, except that it is some sort of undetectable energy that apparently uniformly fills the entirety of space, and hence much more abundant than visible matter. On the other hand, we do not know much about DE either, except that it too remains undetected, is much more abundant than visible matter, and thought to be a repulsive energy of space that causes it to expand. Given the deficits in our knowledge on the nature of the invisible energy/spirit of VC and DE of SC and the numerous concordances between VC and SC or current science established above, we could reasonably assume that they are one and the same, especially since in both cosmologies the universe comprises three components of which the other two are apparently common to both.

4. Role of Dark Matter and implications

Table I summarizes the foregoing correspondences between VC and current science or SC. These concurrences cannot simply be fortuitous, but provide compelling evidence why VC merits serious scientific scrutiny. Unfortunately, the narrator in VP does not know the source of the knowledge and how VC came to be expounded, but informs us that this knowledge was passed on by Brahmin scholars learned in the Vedas. Nevertheless, having established that the primary matter of VC is in all probability the DM of SC, we can now enunciate the core tenets of VC that elucidate DM's relationship to ordinary matter and its role in the evolution of the universe. The following are the core tenets of VC, and we quote from VP supporting the inference or conclusion drawn.

First, VC posits that time is without a beginning and its end is not known and that the universe is cyclic. We quote: "The deity as Time is without beginning, and his end is not known; from him the revolutions of creation, continuance, and dissolution intermittently succeed". 2) Pradhana or DM and Purusha/Puman or DE pre-existed the current cycle. We quote: "There was neither day or night, nor sky nor earth, nor darkness nor light, nor any other thing, save only One, inapprehensible by intellect, or That which is Brahma and Puman (*DE*) and Pradhana (*DM*)". 3) That Pradhana/DM is without a beginning and that visible/ordinary matter is its product

Vedic Cosmology (VC)	**Feature/Characteristic**	Standard Cosmology (SC) Current science
> 13.2 Gy and < 17.5 Gy	**Age of the universe**	13.8 billion years (Gy)
> 13.2 Gy	**Age of Milky Way**	> 13.5 Gy
~ 13.2 Gy	**Oldest planet in the Milky Way**	~ 13 Gy
8.64 Gy	**Useful lifespan of Sun**	$\sim$ 8–10 Gy (see text)
In 4–5 Gy	**Incineration of Earth by the Sun**	In $\sim$ 5.5–7.5 Gy (see text)
Long drought, followed by extensive evaporation, boiling over of the oceans and rivers, a wet runaway greenhouse effect, resulting in a molten rock resembling the back of a tortoise.	**Events preceding the incineration of Earth by the Sun**	Increase in temperatures, extensive evaporation, boiling over of oceans, runaway greenhouse effect, resulting in a molten rock.
Visible matter, primary/invisible matter, and a nondescript spiritual energy in "their due proportions"	**Constituents of the universe**	Ordinary matter, dark/invisible matter, and dark energy in unequal proportions
Shaped like a coconut (rounded or ellipsoidal), with a massive central cavity surrounded by visible matter and a halo of primary/dark matter	**Morphology and constituents of Milky Way or protogalaxy described in VC**	Spiral (round), with a massive black hole in the center surrounded by ordinary matter and an extensive halo of dark matter
Subtle, uniform, durable, stable self-sustained, illimitable, undecaying, and devoid of sound or touch, and possessing neither colour nor form.	**Primary/Dark matter**	Does not absorb or emit electromagnetic radiation, much more abundant than ordinary matter, and apparently durable and stable.

Table 1: Similarities between vedic cosmology and current science or standard cosmology

and converted back into DM by the end of a cycle. We quote: "The chief principle (Pradhana) is the mother of the world; without beginning; and that into which all that is produced is resolved. By that principle all things were invested in the period subsequent to the last dissolution of the universe, and prior to creation" See VP, Book I, Chapt. II. Wilson [23].

The foregoing principal tenets of VC lead to the following inferences and/or conclusions. Since DM is without a beginning and is limitless, and according to general relativity matter cannot exist without space, it follows that space too is without a beginning and is unbounded; and so is time. Neither DM nor DE were created; are apparently constants from one cycle to another and fill the entirety of space. The implication is that the densities of DM and DE are constant and not functions of time. In contrast, DM in SC has a beginning, was presumably created in the Big Bang, and its density decreases along with that of ordinary matter as the universe expands.

The proposition that ordinary matter is a product of DM and converted back to DM by the end of a cycle, and that DM and ordinary matter both exist during the cycle, implies that a relatively small mass of DM is converted to ordinary matter at the beginning of a cycle; which incidentally also explains why DM is much more abundant in the universe than ordinary matter. The constituents of ordinary matter (protons, neutrons, and electrons) are by products of DM; which implies that the DM particle is not a subatomic elementary particle, nor a hypothetical light particle such as an axion. In fact, the principle of conservation of mass requires that it be more massive than the sum of the masses of all elementary particles; and suggests that it cannot be created by high-energy collisions of protons alone in accelerators such as the Large Hadron Collider (LHC), but could possibly be synthesized from ordinary matter under certain unspecified conditions. Furthermore, since Pradhana/DM is non-decaying, it may explain why no decay or annihilation product of DM has thus far been observed. Note also that the proposition that the density of DM is constant, as is apparently the density of DE, resolves the so-called Cosmic Coincidence problem as to why the current densities of DM and DE happen to be of the same magnitude. Also, the proposition that DM existed before the commencement of the current cycle and that it was not created in the Big Bang makes it possible for the density inhomogeneities observed in the Cosmic Microwave Background (CMB) to have grown much faster than envisioned in SC (see [3]); thus providing a head start to the formation of galaxies. This difference between VC and SC may also explain why galaxies such as the Milky Way formed soon after the beginning of the current universe $\sim 13.8\,\mathrm{Gy}$ ago.

Lastly, the proposition that DM density is largely constant in VC may account for the incongruity between the value of Hubble constant H_0 inferred from CMB using SC or the ΛCDM model and H_0 measured locally. Riess et al. in [14] determined a value for $H_0 = 74.03 \pm 2.82\,\mathrm{km\,s^{-1}\,Mpc^{-1}}$ (2σ) measured locally using Cepheids, that is significantly higher than the value of $H_0 = 67.4 \pm \mathrm{km\,s^{-1}\,Mpc^{-1}}$ (2σ) inferred from Planck CMB data and ΛCDM, see [11]. These values taken at face value indicate that Ho measured locally is higher by $\sim 10 \pm 5\,\%$ (2σ). The following simple calculation provides a rough estimate of the difference between the values of H_0 predicted by VC and the ΛCDM model from the CMB data. The Hubble parameter is a function of redshift z (see Wei and Wu [22]) and in a flat universe with constant lambda, H_0 can be expressed as:

$$H_0 = H(z)\sqrt{\Omega_{\rm BZ}(1+z)^{-3} + \Omega_{\rm CZ}(1+z)^{-3} + \Omega_{\Lambda\rm Z}}, \tag{1}$$

where the $\Omega_{\rm BZ}$, $\Omega_{\rm CZ}$, and $\Omega_{\Lambda\rm Z}$ are, respectively, the density parameters (densities expressed as fractions of critical density) for baryons, DM, and DE at redshift z at the epoch of CMB. The density of DM in VC is, however, constant. Hence, the ratio $H_0^{(\rm vc)}/H_0^{(\rm sc)}$ of the value of H_0 inferred by VC to that by SC is given by:

$$\frac{H_0^{(\rm vc)}}{H_0^{(\rm sc)}} = \frac{\sqrt{\Omega_{\rm BZ}(1+z)^{-3} + \Omega_{\rm CZ} + \Omega_{\Lambda\rm Z}}}{\sqrt{\Omega_{\rm BZ}(1+z)^{-3} + \Omega_{\rm CZ}(1+z)^{-3} + \Omega_{\Lambda\rm Z}}}. \tag{2}$$

For $z \sim 1100$ corresponding to the epoch of CMB, the components $\Omega_{\rm BZ}(1+z)^{-3}$ and $\Omega_{\rm CZ}(1+z)^{-3}$ are small or negligibly small and the ratio $H_0^{(\rm vc)}/H_0^{(\rm sc)}$ reduces to:

$$\frac{H_0^{(\rm vc)}}{H_0^{(\rm sc)}} < \sqrt{1 + \frac{\Omega_{\rm CZ}}{\Omega_{\Lambda\rm Z}}}. \tag{3}$$

The ratio is greater than 1. Thus, VC predicts a H_0 value greater than that inferred by the ΛCDM model. And since the densities of DM and DE are both constants in VC, their ratio is also a constant and does not change with time. Hence, if this ratio Ω_c/Ω_Λ at say $z = 0$ could be determined independent of the ΛCDM model, we could quantify the difference. Hollanda et al. in [7] determined the current density parameters independent of ΛCDM using supernovae and galaxy clusters, but dependent on the value of H_0. Their study gives values for the $\Omega_{\rm CO}/\Omega_{\Lambda\rm O}$ ratio comparable to that obtained by [11]. Adopting its value of ~ 0.34 from [7] we get $H_0^{(\rm vc)}/H_0^{(\rm sc)} < 1.157 \pm 0.021$. Thus, VC predicts $H_0 \sim 15 \pm 2\,\%$ higher than that inferred using ΛCDM, and comparable (within 2σ) to that measured locally. Note that the contribution of radiation to the total density was neglected in the above calculation. Its inclusion does not change the results.

5. Conclusions

We showed that VC concurs with SC or current science on numerous key aspects of our universe. In fact, it is mind boggling to ponder that a few thousand years ago Vedic scholars could stipulate that the Milky Way is older than 13.2 Gy when until recently the Milky Way was thought to be younger by ~ 3 Gy. It is equally beguiling that the ancient Vedic scholars visualized that Earth will be incinerated in the next 4–5 Gy preceded by a wet runaway greenhouse effect, consistent with current models of Sun's evolution. And perhaps above all they were aware that one of the constituents of the universe is matter that is invisible or dark, the modern-day existence of which was postulated only about a hundred years ago, see Kapteyn [8].

The differences between VC and SC as to the origins of DM and its role in the formation and evolution of the universe are equally profound, and the two cosmologies envision dramatically different scenarios as to how the universe came into being

and what might be its ultimate fate. In VC the universe is cyclic, whereas in SC its ultimate fate remains in limbo. In VC, time is without a beginning and its end is not known; that space, DM, and DE are constants from one cycle to another; and that DM and DE existed before the beginnings of the current universe. In SC, space, time, DM came into being in or at the time of the Big Bang. In VC, ordinary matter is created from DM at the beginning of a cycle and synthesized back into DM by the end of the cycle in trillions of years. In SC, the relationship between ordinary and DM remains unknown (except that DM acts gravitationally on ordinary matter). In SC, DM having been created in the Big Bang, its density decreases as space expands while that of DE remains constant; which creates the Cosmological Coincidence problem as to why the current densities of DM and DE happen to be of similar magnitude. In VC, the density of DM is constant, just as the density of DE; which resolves the long-standing Cosmological coincidence conundrum. Additionally, we showed that the proposition that DM density is constant apparently resolves the current unexplained incongruity between the value of Hubble constant inferred from CMB and SC or the ΛCDM model and its value measured locally.

If dark matter is undecaying as described in VP, it would explain why attempts to detect products of annihilation or decay of DM have thus far not been successful. Furthermore, the proposition that ordinary matter is a product of DM implies that the elusive DM particle should be massive and not light such as neutrino or axion. In fact, conservation of mass requires that it be more massive than the sum of the masses of all elementary particles. It also suggests that under certain unspecified conditions ordinary matter could be synthesized into DM, but that attempts to create DM particle(s) by high-energy collisions of protons alone in the Large Hadron Collider may not be fruitful.

Acknowledgements

I thank Dr. Klaus Jacob for reviewing an initial version of the paper and encouragement to pursue the research. This research was not funded by any external entity. I thank the anonymous reviewer.

References

[1] Aggarwal, Y. P.: Cosmic cycles of Hindu cosmology: scientific underpinnings and implications. J. Cosmol. **13** (2011), # 32.

[2] Amelin, Y., Krot, A. N., Hutcheon, I. D., Ulyanov, A. A.: Lead isotopic ages of chondrules and calcium-aluminum-rich inclusions. Science **297** (2007), 1678–1683.

[3] Dark matter- Particle Data Group: Updated by Dress and Gerbier, pdg.lbl.gov > reviews > rpp2017-rev-dark-matter, 2017.

[4] Dodelson, S.: Modern Cosmology, Academic Press. ISBN 978-0122191411, (2003).

[5] Eisenstein, D. J. et al.: Detection of the baryon acoustic peak in the large-scale correlation function of SDSS luminous red galaxies. Astrophys. J. **633** (2) (2005).

[6] Fludd, R.: Mosaical Philosophy, London, Humphrey Mosely, 1659, page 221.

[7] Holanda, R. F. L., Gonçalves, R. S., Gonzalez, J. E., Alcaniz, J. S.: An estimate of the dark matter density from galaxy clusters and supernovae data, 2019, arXiv: 1905.09689.

[8] Kapteyn, J. C.,: First attempt at a theory of the arrangement and motion of the sidereal system. Astrophys. J. **55** (1922), 302–327.

[9] Krishnananda, S.: A Short History of Religious and Philosophic Thought in India. The Divine Life Society, Sivananda Ashram, Rishikesh, India, 1994.

[10] NASA, News Release, 2017,
`www.nasa.gov/mutimedia/imagegallery/image_feature_76.html`

[11] Planck collaboration: Planck 2018 results. VI. Cosmological parameters, 2019, arXiv: 1807.06209.

[12] Prabhupada, S. L Srimad Bhagavatam Translation. The Bhaktivedanta Book Trust Int. Inc., USA, 1962.

[13] Randall, L.: Dark Matter and the Dinosaurs: The Astounding Interconnectedness of the Universe, New York: Ecco/HarperCollins Publishers, 2015.

[14] Riess, G., Casertano, S., Yuan, W. L, Macri, M., Scolnic, D.: Large Magellanic Cloud Cepheid Standards Provide a 1% Foundation for the Determination of the Hubble Constant and Stronger Evidence for Physics Beyond ΛCDM. Astrophys. J. **876** (1) (2019), 876–885.

[15] Rubin, V., Ford, W. K. Jr., Thonnard, N.: Rotation of the Andromeda Nebula from a Spectroscopic Survey of Emission Regions. Astrophys. J. **159** (1970), 379–403.

[16] Rubin, V., Thonnard, N., Ford, W. K. Jr.: Rotational Properties of 21 Sc Galaxies with a Large Range of Luminosities and Radii from NGC 4605 (R=4 kpc) to UGC 2885 ($R = 122$ kpc). Astrophys. J. **238** (1980), 471.

[17] Sagan, C.: COSMOS, Random House, 1980.

[18] Schlaufman, K. C., Thompson, I. B. Casy, A. R.: An Ultra Metal-poor Star near the Hydrogen burning Limit, 2018, arXiv: 1811.00549.

[19] Schroeder, K. P., Smith, R. C.: Distant future of the Sun and Earth revisited. Mon. Not. R. Astron. Soc. **386** (1) (2008), 155–163.

[20] Toomey, E.: New Generation of Dark Matter Experiments Gear Up to Search for Elusive Particle, Smithsonian.com, Feb. 3, 2020.

[21] Wechsler, R. Tinker, J.: The Connection between Galaxies and their Dark Matter Halos. Annual Review of Astronomy & Astrophysics **56** (2018), 435–487, arXiv:1804.03097.

[22] Wei, J. J., Wu, X. F.: An Improved Method to measure Cosmic Curvature. ApJ **838** (2), 2017, article id 160.

[23] Wilson, H. H.: The Vishnu Purana, (Translation), Published by John Murray, London, 1840.

[24] Zwicky, F.: Die Rotverschiebung von extragalaktischen Nebeln, Helvetica Physica Acta **6** (1933), 110–127.

[25] Zwicky, F.: On the Masses of Nebulae and of Clusters of Nebulae. Astrophys. J. **86** (1937), 217.

ALTERNATIVE COSMOLOGICAL THEORIES

Conference *Cosmology on Small Scales 2020*
Michal Křížek and Yurii Dumin (Eds.)
Institute of Mathematics CAS, Prague

GEOMETRIC DISCRETE UNIFIED THEORY FRAMEWORK

Yan Breek

Nvidia, Santa Clara, CA 95051, U.S.A.
ybreek@gmail.com

Dedicated to my physics and math teachers Vadim Knizhnik, Boris Dubrovin, Sergei P. Novikov, and Sergei Nesterov

Abstract: This article proposes a unified theory framework encompassing a discrete topological interpretation of physical forces, wave functions, and the nature of space and time. It provides novel explanations for the collapse of wave functions, quantum entanglement, and offers insights into the origins of quantum probabilities. This article also explains the nature of mass, Higgs field, and suggests a path for unifying quantum mechanics and gravity. Elementary particles are represented as defects in discrete elastic topological spaces. Quantum numbers are explained as geometric and topological invariants of the discrete graph. Entangled particles are directly connected to each other through a puncture in discrete space, separated by a distance of one Planck length. Wave functions are explained as mechanical stress waves within elastic discrete space. Wave-particle duality is explained as discrete topological defects causing extended distributed stress within elastic space lattice. The results of the double-slit experiment are interpreted as wave functions maximizing the probability of rupture in high-stress areas of discrete space with obvious analogies to solid state mechanics. Black holes and Big Bang are explained as phase transitions in the discrete space graph structure. Connection to string theory is discussed. Experimental verification of the theory is proposed.

Keywords: black hole, Big Bang, Planck length, quantum gravity, lattice theory, topological unified theory, unified discrete field theory

PACS: 95.30.Sf, 98.80.-k

1. Introduction

A large portion of the work in theoretical physics currently focuses more on the mathematical formulas rather than the underlying conceptual framework. It has long been accepted that the conceptual foundation of quantum mechanics is not as consistent and appealing as the elegant framework of general relativity. For instance,

as was pointed out by Landau and Lifshitz, see [1], although quantum mechanics describes quantum phenomena, the concept of a "measurement," which is fundamental to quantum mechanics, is a classical idea, which is a foundational inconsistency. It has also proved very difficult to unify gravity with quantum mechanics. The lack of coherence and consistency in quantum mechanics is partially due to the fact that, while general relativity was developed solely by Einstein based on a powerful physical insight, quantum mechanics was developed piece-wise by multiple physicists based more on mathematical formulae than on underlying physical principles and insights.

Although mathematics is a crucial tool for expressing and developing ideas in theoretical physics, it is not the only approach. For example, the original scientific articles written by Michael Faraday contained little to no math but, nevertheless, introduced novel and useful physical concepts of magnetic fields and the behavior of magnetic field lines that later were developed into part of a powerful mathematical framework by James Maxwell. Einstein's "happiest thought" was the physical equivalence principle. Even Feynman diagrams were and are popular due to their simple and intuitive geometric interpretation. While physics has progressed tremendously since Faraday and Einstein, their physical insight-based approach, which expresses ideas in geometric or topological terms, remains valid and provides a fruitful foundation on which to develop the mathematical framework.

In this paper, I propose several concepts and insights that may lay out a foundation of a unified theory of all fundamental physical forces, which unifies gravity with quantum mechanics. While the ideas described here are not presented in a rigorous mathematical framework, I hope they can provide a foundation for one.

2. Conceptual foundation of the theory: basic postulates and assumptions

Since the theory presented here is essentially geometric in nature and Euclidian geometry is based on axioms, I have similarly formulated the basic assumptions of the theory as a set of postulates.[1]

Postulate 1 *(Discreteness): Space is discrete and composed of the underlying elementary units. The resulting discrete structure can be geometrically represented as a graph, network, or lattice (see Figure* 1*). The graph does not exist in space; rather, the graph itself is space.*

Physical Justification: The existence of fundamental constants 'Planck distance' and 'Planck time', combined with the fact that most of the physical quantities in a bound system on a quantum scale, such as energy, momentum, etc., come in discrete units (quants) suggest that space and time may likewise be discrete. This concept is supported by multiple researchers in the field of quantum gravity, such as

[1]Why Postulates? Hilbert's 6th problem calls for creating an axiomatic system of theoretical physics. If one believes that our universe can be described as a discrete graph with rule-based operations defined on it, as proposed in this article, then perhaps the 6th Hilbert's problem starts to look as potentially solvable.

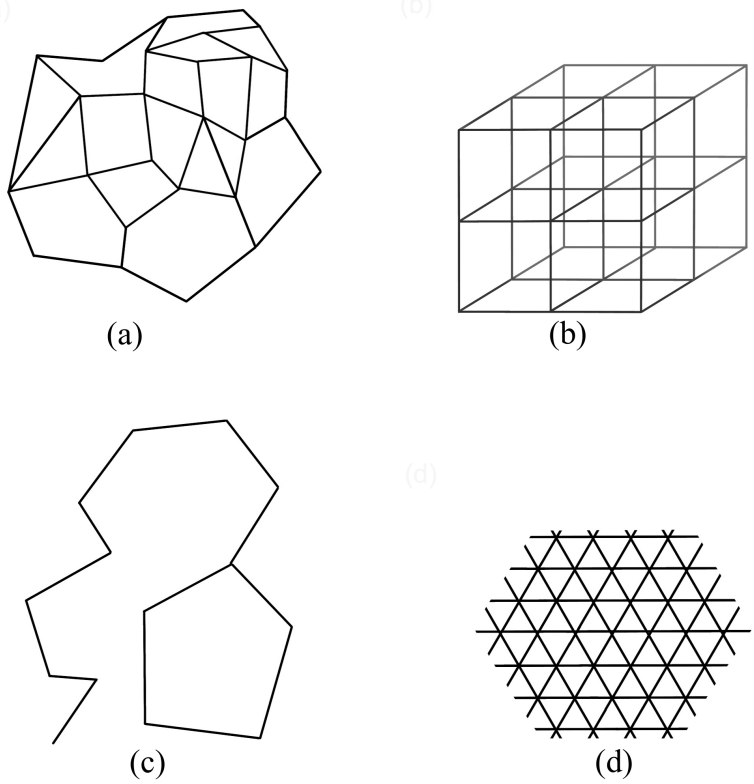

Figure 1: Examples of graphs and lattices, some of which may be used to model space structure in different Universes. (a): A well-connected graph, no regular structure, distance can be defined, can be mapped to "wrinkled 2D" space. Unlikely to correspond to any real Universe because of irregularity. (b): A well-connected lattice with 3 dimensions, regular symmetry structure for discrete translations and rotations, distance easily defined. Resembles our current Universe in many but likely not all aspects. (c): Weakly connected graph, no regular structure, distance may be defined. This graph is highly unlikely to represent any real Universe because it is way too simple and small. (d): Well-connected graph, 2 dimensions, regular triangular symmetry structure for discrete translations and rotations, distance easily defined. Does not match our Universe because the number of dimensions is too small.

Lee Smolin and Roger Penrose, see [2, 3, 4]. I assume that all of the graph's edges are on the order of one Plank length in size.[2]

Postulate 2 *(Emergence of space): Space, as we know it, is an emergent phenomenon that resulted from the underlying elementary units connecting together in a graph with certain geometric and topological structure and properties. The local*

[2]While referring to elements of the space graph, I will use the words "arc" and "edge" interchangeably; I will also use the words "node" and "vertex" interchangeably. I will also use the words "graph" and "lattice" interchangeably."

structure and properties of the space graph may vary between different universes or even between different parts of the same universe. They may also change within the same Universe over time. Space graph structure is the cause of concepts of locality, distance, dimensionality, smoothness, regularity, and symmetry; they are all emergent properties of the graph.

Physical Justification: The Big Bang was a violent dynamic process, during the course of which space appeared to be created, and time appeared to come into existence. Therefore, any truly fundamental theory must explain the nature and dynamic of space-time creation, particularly on the quantum scale (Planck length scale). A fundamental theory also has to explain what space is and what time is. As argued by Lee Smolin and Roger Penrose, it is not sufficient to merely assume spacetime as a background, like most physics theories do, see [2, 4].

It appears likely that the spatial structure and properties inside a black hole are different from the spatial structure and properties outside of it. Nothing can escape from inside a black hole, and no object can move away from the center of a black hole while inside the event horizon, but outside of a black hole a physical object can move in any direction. This suggests different symmetry properties and dynamics of space inside and outside of a black hole, representing a phase transition of the space' microscopic structure on the Planck scale. Likely, the same principle applies to the Big Bang, especially if one assumes, as has been proposed by multiple authors, that the Big Bang was what emerged on the other side of a black hole, or that Big Bang is a "black hole played backward", see [5, 6, 7, 8, 9, 10, 11, 12]. For these reasons, the properties and structure of space must be a changing, evolving phenomenon. This approach is inspired by multiple quantum gravity theories given by Lee Smolin, Roger Penrose, and others, see [2, 4].

The emergence of space is similar to how Lego blocks may be used to build a toy house or an airplane. If the elementary units had been connected differently, we could have ended up with a different number of dimensions in our universe, or perhaps with no dimensions, no symmetry, no regularity, or no locality at all (see Figure 2).

General relativity says that the curvature of space is controlled by mass and is changing over time and space. I propose to take it further and say that not only does space curvature change, but the discrete structure, symmetry, and dimensionality of space also change, and they do so on both a quantum (Planck length) and macro scale. At the moment, I make no assumptions about the specific structure and group symmetry of the space graph on a Planck scale in our universe but will discuss that important issue in more detail below.[3]

[3]It is possible that Figure 2 (a) corresponds to the state of the universe just before the Big Bang, representing a higher degree of symmetry and a compact fully connected and tightly packed space, and perhaps snapping of one edge caused the Big Bang to unravel, similar to the proposal by Cumrun Vafa and Robert Brandenberger for an ensemble of tightly wound strings some of which have later annihilated and caused the Big Bang to unravel, see [13].

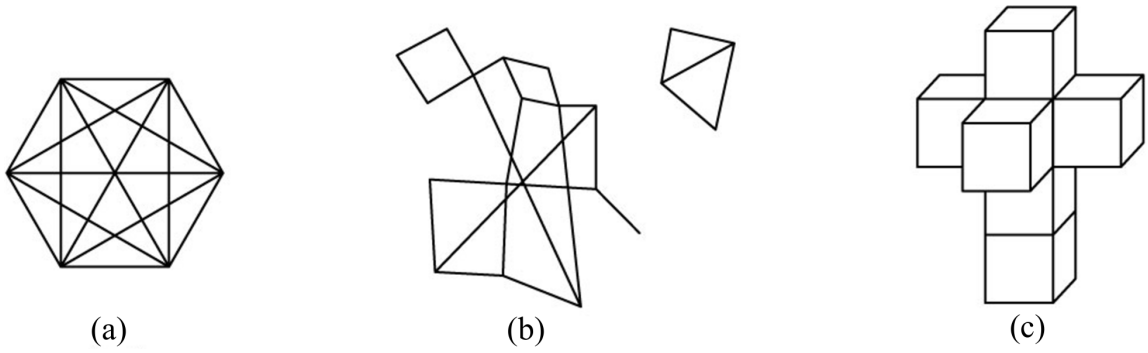

Figure 2: More examples of graphs, some of which may be used to model different Universes. (a): Everything is connected with everything. This type of graph may represent our Universe just before Big Bang, because it is highly symmetrical, possibly causing unification of fundamental forces due to high symmetry. (b): Highly irregular disconnected graph. That graph likely does not represent any physical universe due to its extreme irregularity, small size, and the presence of completely disconnected areas. (c): This is a 3D unfolding of a 4D cube. This graph probably does not map to any physical Universe, but it illustrates a concept of how a surface (3D) in high-dimensional space (4D) may be projected into a lower-dimensional space (3D).

Postulate 3 *(Elementary particles, space defects, and quantum numbers): All elementary particles in our universe are topological defects in the underlying space lattice. Each distinct type of topological defect corresponds to a specific type of elementary particle (i.e., a defect of a certain topological structure represents an electron; a different type of defect represents a graviton, etc.) (see Figure* 3*).*

Corollary: I further assert that all of the quantum numbers currently utilized in quantum physics are, in fact, geometric and topological characteristics of defects in the space graph that correspond to the particle or system being considered. This goes to the heart of the origin of quanta and discreteness in quantum mechanics, electric charge and spin, flavor quantum numbers, and other fundamental constants and quantum variables.

Clarification: Since it only makes sense to speak about "defects" if the underlying graph itself has certain regularity, I therefore have to assume that the space graph is indeed regular in a certain sense at least over short distances. While I do not claim to know the exact structure of that regularity, I will discuss several possibilities below which will be a focus of further research.

Physical Justification: The discrete lattice approach has been used very productively in solid state physics to describe material structure and various geometric defects and perturbations in a crystalline lattice, such as edge and screw dislocations in metals, point defects, holes, phonons, etc. It is appealing to describe various quantum numbers associated with elementary particles simply as topological invariants

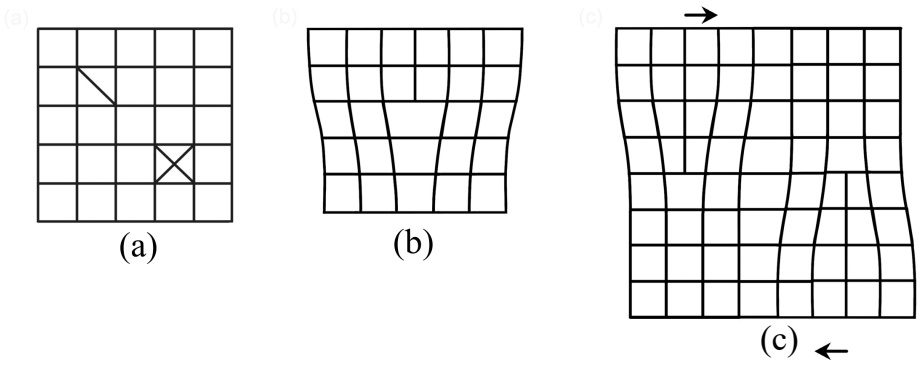

Figure 3: Topological defects representing elementary particles, and their interactions. (a): Examples of two topological defects on a regular lattice. The defects represent two different possible types of elementary particles. (b): 2D examples of "edge dislocations" representing possible elementary particles. The drawing also illustrates elastic stress within the graph introduced by defects (see Postulate 5 below for details). Edge dislocations also frequently occur in solid state crystals in 3D in our world. (c): 2D example of two "edge dislocations" of opposite signs representing a particle and an antiparticle. The drawing also illustrates elastic/mechanical stress in the graph caused by those defects (see Postulate 5). In this configuration the stress would cause the dislocations to attract to each other and annihilate. Such interactions indeed occur in solid state crystals in our world in 3D, especially in metals.

and/or graph invariants of specific types of defects in the underlying lattice. It is even more appealing that this proposal reduces the complexity and the number of assumptions in the theory. In the existing theories, space and particles are postulated and considered separately. In the proposed framework, particles are just an emergent property of the space itself.

By the way of analogy, consider what happens when two opposite but aligned edge dislocations meet in metal (see Figure 3 (c)). Dislocations can move around, as indicated by the arrows in Figure 3 (c). When the top dislocation meets the fully aligned bottom dislocation, they annihilate, elastic stress in the underlying lattice is released, and phonons (vibrations of the lattice) are produced.[4]

I propose that this is exactly what happens when elementary particles annihilate in our universe. I also propose that this exactly represents the difference between particles and antiparticles. They are geometrically and topologically opposites of each other (in relation to the undisturbed space graph state) and can therefore geometrically and topologically annihilate each other within the space graph structure. In fact, this also explains the CP symmetry.

This also raises an interesting possibility that perhaps strings are one-dimensional

[4]That process is known in metallurgy and solid state physics as annealing.

dislocations in the underlying structure of the space graph, or more generalized versions of dislocations (possibly including branes, etc.). Perhaps, a screw-like dislocation of the space graph represents one type of string, an edge-like dislocation represents another type, and so on. If true, then perhaps the much sought-after M-theory of strings is actually a generalized theory of various types of extended topological defects within the space graph (for another interpretation of M-theory, please see the Interpretation of Strings section below).

Quantum numbers discussion: If elementary particles are indeed topological defects in a discrete graph structure of space, interpreting particles' internal quantum numbers (electric charge, absolute spin, etc.) as topological invariants of such defects appears to be a natural consequence. As to exactly how to map a specific quantum number to the geometric properties of the space graph defect, while I do not have a complete answer, I can provide a few illustrations. Consider, for instance, a regular space graph, where each node has exactly K arcs connected to it. In that scenario, one of possible quantum numbers for a space graph defect may be the difference between the actual number of the arcs connected to the "defective" node and K. Alternatively, a quantum number may be the difference between the actual number of arcs within an elementary space graph cell representing the graph defect and the number of arcs within a "normal" space graph cell that contains no defects. Yet another quantum number may indicate the differences between the actual and the baseline number of nodes within an elementary cell. That example may refer to scalar quantum number such as electric charge, for example. The illustration in Figure 7 indicates that static electric field and electric charge may correspond to a topological defect of having either an interstitial node or a vacancy, representing the electric charges of opposite signs. See more detailed description of that below. Yet more complex quantum numbers would emerge when one considers the geometric aspects of the relationship between the defect and the local geometry of the graph. I would then perhaps expect vector-like quantities to emerge, such as spin, etc.

Postulate 4 *(Non-locality or quasi-locality). Any elementary unit A may potentially be directly connected by an arc to any other elementary unit B (subject to certain conservation rules), no matter how many steps along the arcs of the regular space graph lattice separate the units A and B. See Figure* 4.

Physical Justification: These connections beautifully explain quantum entanglement, as well as other quantum phenomena that appear to violate the concept of locality. I assert that the nature of quantum entanglement is exactly represented in Figure 4 (c). The paradox of entangled particles is explained here simply by assuming that entangled particles are directly connected with each other and that the distance between them is one Planck length no matter how far they appear from each other. Therefore, the "spooky action at a distance" that bothered Einstein so much can be explained as a local action! See detailed discussion below regarding that important insight.

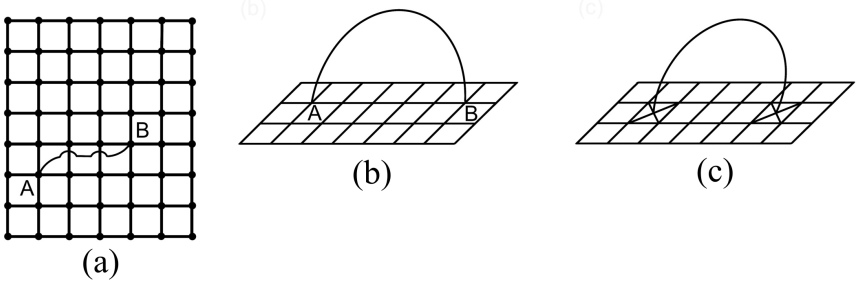

Figure 4: Direct spatial links of one Planck length between seemingly distant nodes on a regular lattice/graph. These images illustrate the nature of quantum entanglement. (a), (b): Direct links between seemingly distant nodes are depicted. This is a Riemann space puncture on discrete lattice/graph. (c): This image illustrates and explains the true nature of entangled particles. Two topological defects representing elementary particles are directly connected by a direct spatial link of one Planck length. This explains "spooky action at a distance", Bell theorem, and other non-local paradoxes of quantum mechanics. Seemingly non-local action becomes local due to a presence of direct spatial link, equivalent of Riemann surface puncture on a lattice.

Postulate 5 *(Lattice distortion, elastic stress, and the wave function): Any topological defect (elementary particle) in the space lattice results in long-range distortions and mechanical stress in the lattice. This distributed stress is mathematically represented by the wave function as described by the Schrödinger equation.*

Physical Justification: This is similar to the way dislocations, point defects, and other defects in crystals result in long-range distortions and a mechanical (elastic) stress field that both diminish gradually with distance. The physical nature of the wave function is the degree of mechanical stress in the space lattice/graph. See Figure 5 and Figure 6 for illustrations of mechanical stress fields of linear defects, and Figure 7 for illustrations of stress fields of point defects. Since the graph itself is space (as opposed to "existing in space"), when I speak about "stress," I mean stress in the force and energy sense. Formally, stress is a number that is assigned to each arc (and/or possibly to each node) of the graph. I assume that stress values are determined by the lattice configuration, just like they are in solid state physics. Our working hypothesis is that the quantitative nature of that stress is elastic, causing harmonic oscillators to appear in many equations of modern theoretical physics on the quantum level. If strings are indeed contours on the graph, this would also explain the elastic nature of strings.

Stress fields, illustrated in Figure 7, resemble corresponding electric fields of positive and negative electric charges. It is plausible that they indeed represent the nature and origin of positive and negative electric charges (an extra node causing compression, a missing node causing tension). If so, that would also explain why

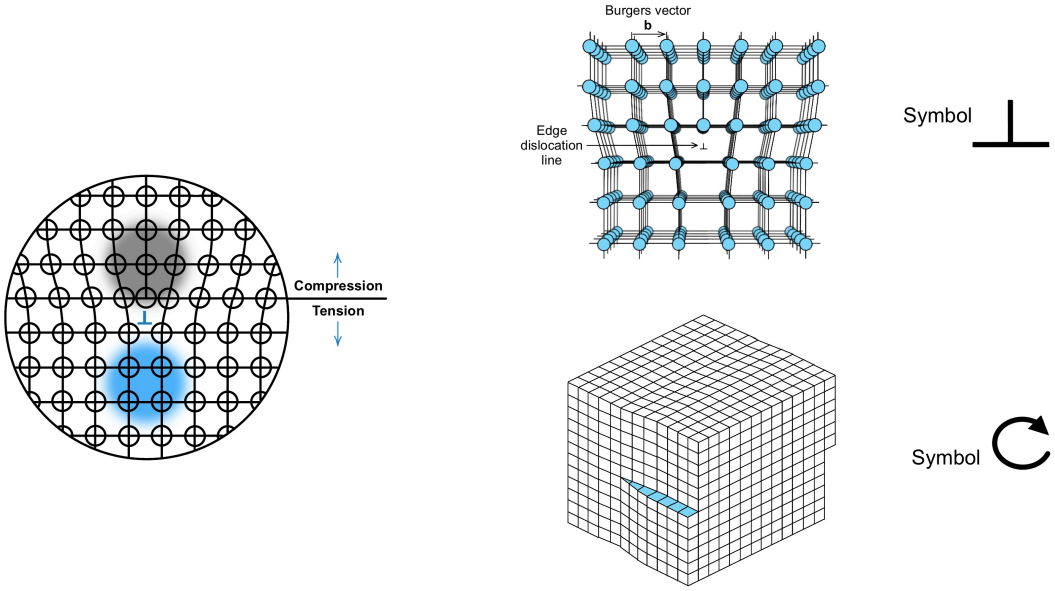

Figure 5: Edge dislocation (top right) and screw dislocation (bottom right) that occur in crystals, especially metals. Image on the left illustrates elastic stress field of an edge dislocation, explaining how topological defects in elastic structures may cause elastic stress force field to come into existence. I propose that similar mechanism is responsible for the existence of elementary particles and fundamental forces in our Universe: particles are topological defects in the elastic space lattice. These defects cause elastic stress fields of various configurations. Those stress fields manifest themselves as four fundamental forces in our world. Images on the right illustrate two different types of linear dislocations (defects) in solid crystals. Perhaps those linear defects explain the nature of strings in string theories. Image credit: `http://academic.uprm.edu/pcaceres/Courses/MechMet/MET-4A.pdf`

electric charges of the opposite sign would attract each other and why charges of the same sign would repel.

This postulate provides a compelling explanation of the nature of the wave function, and, in particular, wave function collapse and wave-particle duality. Wave-particle duality is resolved by associating the particle part of the duality with the corresponding discrete topological defect, and the wave part with the resulting spatially distributed wave-like elastic stress. It also follows Einstein's tradition of literally interpreting any fundamental mathematical quantity in physics equations, including the wave function, as physically existing. This approach is also similar to pilot-wave theory of de Broglie and Bohm. The geometric interpretation proposed here is self-consistent: if an elementary particle is a topological defect in the regular elastic structure of space, such a defect must cause elastic stress in the lattice! In this

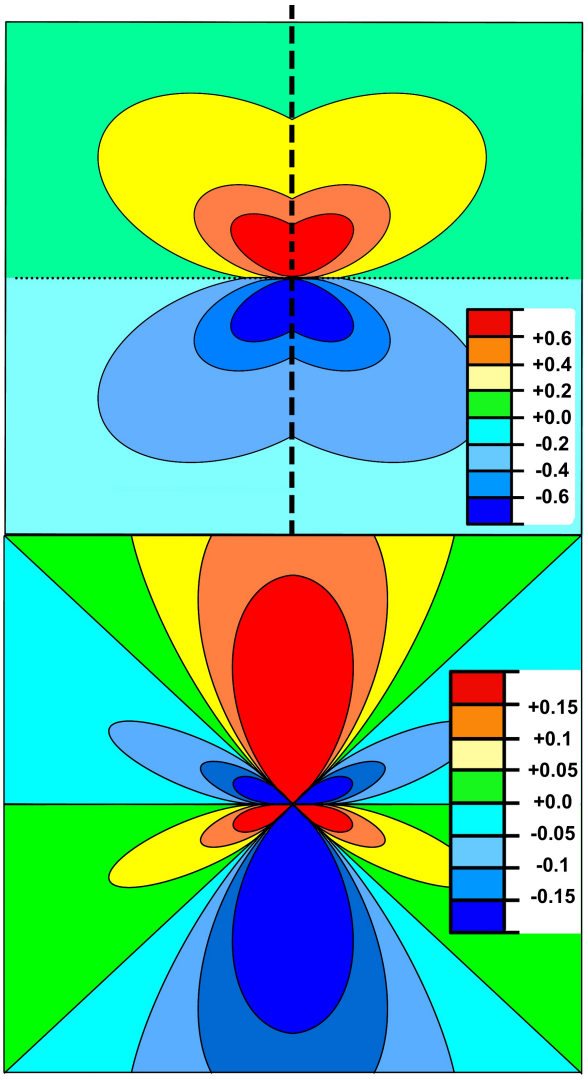

Figure 6: Mechanical stress field components (xx and yy) of an edge dislocation in a crystal. The bottom image has an uncanny resemblance to certain electron orbitals of a hydrogen atom. That resemblance may be suggesting that the proposed theory is on the right track: I propose that wave function is a degree of elastic stress caused by geometric defects in discrete space lattice. Since the stress field of a simple linear dislocation depicted here resembles electron's wave function near a simple atom, that gives us a confirmation that the proposed framework can indeed produce solutions that resemble our Universe. Image credit: `https://www.slideshare.net/vamsikrishna393950/stress-fields-around-dislocation`.

representation, the particle and the wave characteristics of an elementary particle are intrinsically and unavoidably coupled with each other, as confirmed by numerous experiments.

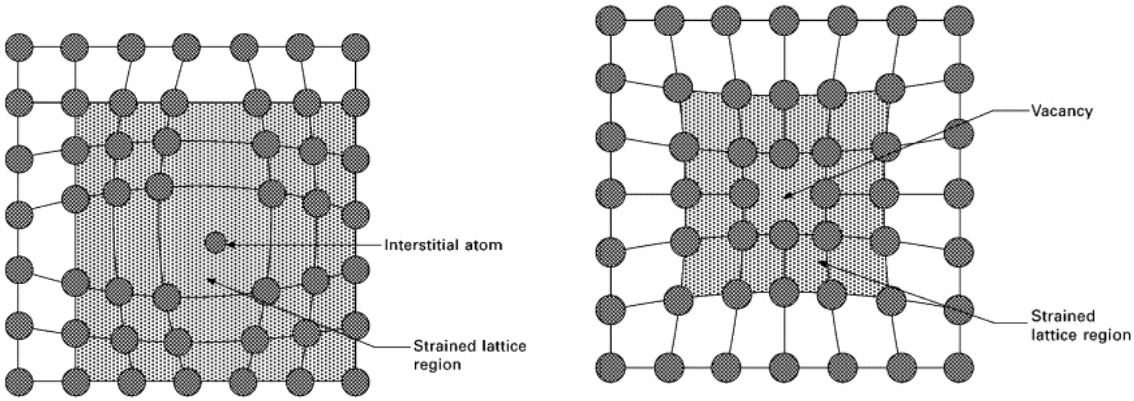

Figure 7: Elastic stress fields of point defects in crystals. They resemble the fields of positive and negative electric charges, and they interact with each other similarly: stress fields would cause an interstitial atom to be attracted to a vacancy, just like a positive charge would attract to an electric charge. An interstitial atom and a vacancy may also annihilate. These images therefore may illustrate a true nature of electrically charged particles and their oppositely charged antiparticles within the space lattice. Left: Stress field of an interstitial atom in a crystal. Right: Stress field of a vacancy in a crystal. Image credit/copyright: `https://www.sciencedirect.com/topics/chemistry/crystal-displacement`

Furthermore, sometimes high mechanical stress (or a high gradient of stress) may force a particular arc (edge) to snap and form a connection with a different node, resulting in a change in the local configuration of the graph, local energy decrease and stress relaxation, and an increase in entropy. This would explain the paradox of the dual slit experiment. See below for a detailed discussion of that insight.

2.1. Additional postulates (dynamic)

Postulate 6 *(Nature of time). An elementary unit of local time (Planck time) corresponds to one elementary unit of change in the underlying graph.*

Clarification: One of the simplest units of change is a switch of an end of a graph's arc from node A to node B (see Figure 8 (a)). Time is always a local phenomenon, just as in special and general relativity.

Other possible elementary switches may include the breaking of an arc (Figure 8 (b)) or the appearance of a new arc (Figure 8 (c)), subject to appropriate conservation laws (see more on conservation laws below). In fact, an elementary switch operation (Figure 8 (a)) can be represented as a superposition of the elementary operations (Figure 8 (b)) and (Figure 8 (c)), as illustrated in Figure 8. This is equivalent to the annihilation operator $(a-)$ (result depicted in Figure 8 (b)) and the creation operator $(a+)$ (Figure 8 (c)), which are commonly utilized in quantum mechanics. Another possible elementary unit of change is an appearance of a new node or the disappearance of an existing one, or, perhaps more likely, a pairwise

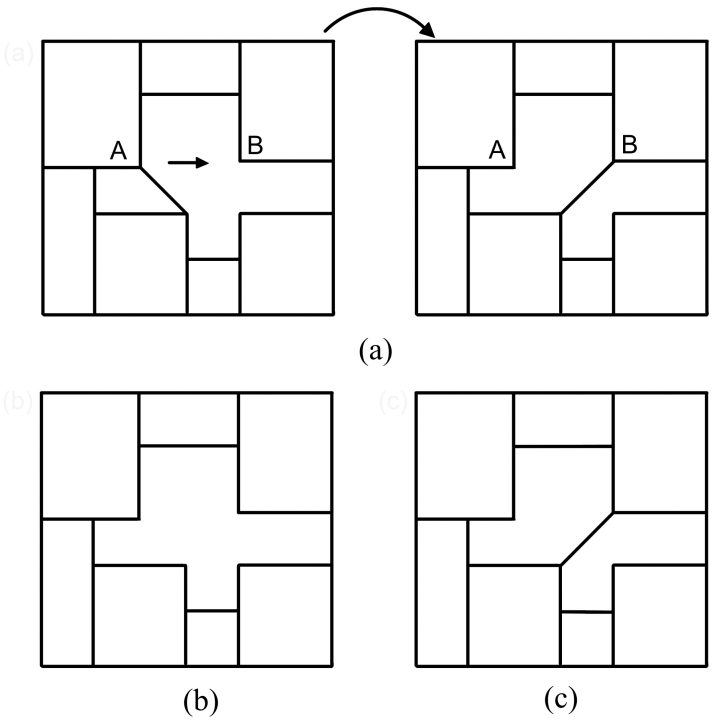

Figure 8: Elementary switch operations on space graph, representing local passage of time. Local time is defined as the number of elementary switch operations ("clock ticks") on the space lattice. (a): One-step elementary switch operation within the space lattice (also one local clock tick). (b), (c): Results of an 'arc annihilation' operation (b) and 'arc creation' operation (c), that in combination result in one elementary switch operation (a) (one local clock tick).

combination of both, if an appropriate nodes number conservation law applies (see more on that below).[5]

Physical Justification: This is a natural interpretation of time given the first five postulates. Time is generally thought of as a measure of change, and, if space is discrete at Planck's scale, then the smallest possible unit of time must correspond to the smallest possible unit of change in that graph (lattice).

Since on macro scale in the classical limit the time advances smoothly and uniformly, and since according to Postulate 6 local time is a count of local elementary switches, we have to assume that the underlying space graph is constantly undergoing a sequence of elementary switches in every location throughout its structure. Since we also assert that elementary particles are geometric defects in the space graph, it follows that therefore virtual particles will be constantly created and annihilated

[5]The pairwise option (arc plus arc hole, or extra node plus node hole) may also describe the pairs of virtual particles and antiparticles that are known to spontaneously flicker in and out of existence in a vacuum.

by those elementary switch operations, producing vacuum fluctuations of vacuum energy, and creating quantum foam that was first proposed by John Wheeler et al., see [14]. Therefore, the passage of time, quantum foam, and creation and annihilation of virtual particles are all caused by and/or refer to the same underlying physical phenomena: ongoing elementary switch operations occurring throughout the space graph. One can think of them as discrete oscillators or clocks operating in every point of the discrete space graph.[6]

Postulate 7 *(Quantum probabilities). The probabilities inherent in quantum mechanics result from the elastic stress and the underlying discrete structural symmetry of the space lattice.*

Physical Justification: The arcs (units) of the space graph with a high amount of stress concentrated in them are more likely to snap or change structure, producing a corresponding increase of entropy due to achieving a more uniform state. By the way of analogy, this is similar to bending an irregularly shaped stick by holding it at both ends and applying force. The stick may break in any location, but it is most likely to break in the area with the highest stress. This explains why the probability of finding a particle in a specific location is proportional to the square of wave function amplitude. This is also somewhat similar to how a metal structure with large number of defects (for instance, created during the process of rapid transition from liquid to solid phase) gradually relaxes the internal mechanical stress by recombining and annihilating the defects, particularly when heated, a process that is called "annealing" in metallurgy and solid state physics.

Also, when a unit of change travels along a certain path and encounters a split in the graph (say, left or right), the probability of the unit taking the next step is a function of the symmetry of the split, as well as of local elastic stress in the lattice/graph. If the graph is perfectly symmetrical and the stress of each possible path is equal, a particle will be equally likely to propagate along any of the arcs. If the graph is not symmetrical and the energy/stress is different along each arc, the particle is less likely to propagate along the arc with highest stress/energy, possibly following the Boltzmann equation or similar (see Figure 9).

One of the most appealing aspect of this approach is that it provides an explanation of the double-slit experiment (see discussion of that important subject below).

There is another consideration with regards to the elastic stress and expanding Universe. If the Big Bang was indeed what emerged on the other side of a black hole and if the space graph is elastic, it is easy to imagine that the space graph was squished through the bottleneck of a black hole singularity under tremendous stress, similar to a spring compressed to an absolute maximum. After traveling through the black hole bottleneck and emerging on the other end as the Big Bang, the highly

[6]It is also likely that the elementary switch operations described here are topological generalizations of the cellular automata operations, as described by Stephen Wolfram and others in various publications, see e.g. [15].

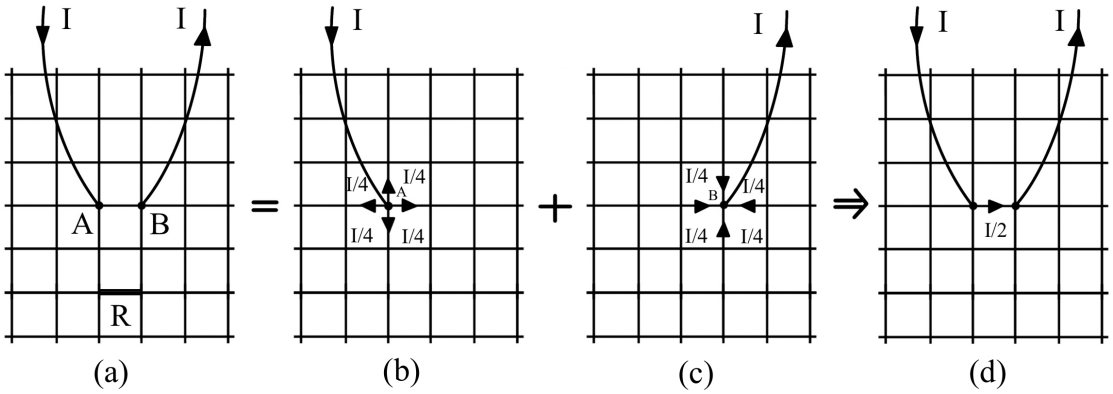

Figure 9: Illustration of solving currents flow equations on infinite conducting lattice based on symmetry considerations. Similar approach may be applicable for calculating elementary particles paths' and measurement probabilities on the space graph (lattice) based on symmetry structure and elastic stress within each arc. In this analogy electric resistance within the conducting network is analogous to elastic stress in the space graph; symmetry considerations would apply equally to the conducting network and to the space lattice. (a): Problem setting: calculate the entire lattice' electric resistance for the depicted configuration. (b): Lattice symmetry results in inflow current I splitting equally into I/4 currents in each of the four adjacent arcs. (c): Outflow currents are also symmetrical, each of them equal to I/4. (d): Due to Kirchhoff's laws, configuration in (a) is equal to a superposition of (b) and (c). Therefore the current from point A to point B must be equal to I/4 + I/4 = I/2. Hence, total resistance is R/2.

compressed space graph would very rapidly unwind and expand (likely changing its symmetry in the process), resulting in something very similar to inflation, see [18].

Postulate 8 *(Nature of mass): The mass of an elementary particle is a measure of the energy added to the lattice (due to the increased elastic stress of the lattice) that results from introducing the corresponding topological defect.*

Physical Justification: Given Einstein's equation,

$$E = mc^2, \tag{1}$$

and the assertion that elementary particles are topological defects in an elastic space graph, this appears to be a natural definition of mass.

Corollary: I further propose that the reason for the existence of inertial mass is the elastic resistance of the space lattice against the movement of mass (represented as topological defects in the lattice). This resistance is otherwise known as the Higgs field.

Physical Justification: Let us consider the implications for inertial mass. In the case of a linear non-rotational movement in an arbitrary direction, once you consider the sequence and the set of all elementary graph operations that must occur in order for a body to move in that direction, it becomes clear that in order to execute that movement the space graph has to bend elastically. The same is true for a rotational movement at an arbitrary angle. Since the graph is discrete, for an approximately round flat disc of radius R the minimal angle it can rotate at is:

$$\Phi = L_p/R, \tag{2}$$

where L_p is the Planck length and $L_p << R$. However, if one tries rotating the entire disk at that angle, points that are closer to the disc's center (at a smaller distance r from the center) cannot rotate at that angle, since the Planck length is fixed and finite; the smallest angle they can rotate at would be:

$$\Theta = L_p/r. \tag{3}$$

Since $\Phi \neq \Theta$, either the space graph, the disk, or both have to bend elastically in order to execute such rotation, with the elastic stress and resistance producing the inertial mass effect. The same is true for an arbitrary angle rotation, following the same logic.

Therefore, the concept of mass arises naturally from the elastic properties, symmetry, and structure of the space lattice (graph). This interpretation of inertial mass is similar if not identical to the definition of the Higgs field and Higgs boson. Within the framework of the Standard Model, elementary (not composite) particles that have mass (except neutrinos) acquire that mass in the process of interacting with a Higgs boson, a process that some physicists have likened to a person trying to move through a crowded room full of people, see [19].

In the framework proposed in this article, essentially the Higgs field is the elastic lattice of space, and the Higgs boson is the elastic distortion of that lattice. Particles acquire mass due to the elastic distortion of the space lattice: the lattice has to bend for a topological defect to come into existence, and the lattice has to bend again for a particle (topological defect) to move around. This is the origin of mass.

Interestingly, since the space graph is elastic and discrete, there has to be a minimum amount of force that results in movement, because, for anything to move, it has to overcome the adjacent elastic energy barrier. A weaker force than that will not have enough strength to cause an elementary space graph switch, and, therefore, the particle would not move.

For gravitational mass the reasoning is also straightforward: topological defect in elastic space lattice forces the lattice to curve, resulting in gravitational force.

A traditional interpretation of general relativity is that "mass tells space how to curve, and space tells mass how to move", see [20]. In the proposed framework, our interpretation is: mass is nothing but discrete curved (distorted) space! A curved

(distorted) space lattice IS mass! This is a deep and simple concept, which satisfies the rule of Occam's razor – entities should not be multiplied unnecessarily.

Furthermore, in our framework, all known physical forces (e.g., weak, strong, electromagnetic, gravitational) have exactly the same source: the elasticity of the underlying space graph. This is how I propose to achieve unification.[7]

Zero mass particles consideration: What about the particles that have zero rest mass such as photons and gluons? Our working hypothesis is that they represent defects that cannot topologically be static, since this would result in a graph configuration that is topologically prohibited. It is perhaps similar to a falling stack of dominoes with each falling domino knocking over the next one, creating an ever-spreading dynamic wave.

2.2. Additional postulate needed: conservation laws

It appears that appropriate discrete conservation postulates have to be defined on the graph.[8] Since I do not know the exact functional form of these conservation postulates, I will refrain from formulating them as a definite list. However, I would like to propose several possible candidates (for an isolated system):[9]

- The total number of arcs of the graph may be conserved.
- The total number of nodes of the graph may be conserved.
- A discrete generalized version of the energy stress momentum tensor may be conserved.
- The total information content of an isolated system is conserved.

3. Discussion

3.1. Guiding considerations of the proposed theory

The following guiding principles and considerations have been a driving force for me in the development of this theory. In my view, any variable that occurs in valid equations of theoretical physics must have a very specific and tangible physical meaning and should be taken literally whenever possible. For example, Planck has

[7]The observable difference between the four fundamental forces results from specific local geometries of the space graph and specific local defects (particles) involved. But, as the symmetry of the space graph increases (perhaps inside a black hole or at the beginning of the Big Bang), at the highest symmetry state, all four forces will merge into one.

[8]A plausible alternative to conservation postulates would be to explicitly list all allowable operations on the graph in the style of generalized cellular automata. If an appropriate set of allowed operations is chosen, the conservation laws would be a result of the collective properties of this set of allowable operations. This is a logical duality.

[9]In a continuous space, Noether's theorem, see [21] relates symmetries to conservation laws. There already exists a number of published papers on expanding Noether's theorem to discrete lattices, including but not limited to an article by Wendlandt and Marsden [22]. Those approaches may help derive exact conservation laws and space lattice symmetries for discrete models of the Universe such as our proposed framework.

originally considered his quants a mere calculational trick rather than physically existing objects. Einstein instead took them literally as physical objects and, in doing so, laid down the foundation of quantum mechanics, as well as explained the photoelectric effect.

Conventional interpretation of Schrödinger's equation and the wave function is that the square of the amplitude of the wave function is a probability density. In my view, probability is not a tangible physical quantity; even less so is the square root of a probability density. Therefore, conventional interpretation of quantum mechanics misrepresents the true nature of the wave function. Assuming that Schrödinger's equation is correct, at least to a high degree of approximation in continuous space limit, I therefore must treat the wave function as a representation of a physical object. In the proposed theory described in this article, the wave function has a very specific physical interpretation. It is a measure of mechanical/elastic stress caused by distortion in the underlying space graph. Unlike the square root of probability, stress and distortion have straightforward physical meanings.

Furthermore, Schrödinger's equation and the wave function incorporate complex numbers in the formulas, without necessarily explaining what complex numbers physically mean. But what is the physical meaning of a complex number? In mathematics, complex numbers are interpreted through introducing an additional dimension (i), together with appropriate commutation, addition, and multiplication rules. Therefore, if Schrödinger's equation is to be taken seriously as it should, the presence of complex numbers in these equations indicates that our Universe has an additional dimension described by the imaginary part of the wave function. This dimension must physically exist with slightly different commutation, addition, and multiplication rules (as compared to real numbers) that follow the algebra of complex numbers.

Another hint that this interpretation is on the right track is the Kaluza-Klein theory, see [23]. Although the theory was eventually discarded, the fact that Kaluza was able to derive both Maxwell's equations and the equations of general relativity from a single unified framework by assuming the existence of a fourth dimension that is bound in a tight circle is deeply profound, as well as puzzling and mysterious. I do not believe that this was a mere coincidence. Even if Kaluza's formulas did not correctly account for all of observable physics, he must have been at least partially on the right track, and it may be quite worthwhile to try to reproduce the Kaluza-Klein theory on the discrete space graph framework proposed in this article. It appears plausible that our Universe may indeed have 4 discrete spatial dimensions, with the fourth dimension corresponding to the imaginary part of the wave function and bound in a circle as proposed by Kaluza-Klein.

Another argument along the same lines is the explanation of the quantum tunneling effect. If one assumes extra spatial dimensions (as described in the paragraph above) or non-local links as described in Postulate 4, the tunneling effect explanation becomes clear. Instead of going through the energy barrier, a tunneling particle goes around the barrier (see details below).

The presence of Planck distance and Planck time in the equations of theoretical physics suggests that the Universe may be discrete at its most basic level. If so, a discrete graph appears to be a natural framework for modeling the Universe. General relativity must be correct on the macroscopic level because of its profound elegance and consistent experimental confirmation. If so, a discrete version of general relativity would be a space graph with dimensions that fit our observations, and an elementary unit of space curvature would be an elementary local discrete topological distortion of that space graph.

3.2. Qualitative explanation of important physical phenomena

In this section, I propose and discuss a qualitative explanation of important physical phenomena, concepts, and equations utilizing the framework of the space graph described in this article.

3.2.1. Wave function nature and wave-particle dualism

The dual wave-particle nature of elementary particles is explained as follows. The physical meaning of a wave function corresponds to a degree of elastic stress in the underlying space lattice. The elastic stress field created in the space lattice by a topological defect that IS an elementary particle (see Postulates 4 and 5 above) is responsible for the wave-like properties of a particle, while the topological defect at the core of the particle is responsible for its particle-like properties. Stress and distortion waves, caused by topological defects (elementary particles), propagate through the lattice in a distributed manner analogous to mechanical stress waves, which can produce wave interference effects, while the topological defect (the center and 'heart' of an elementary particle) has a specific location within the graph/lattice and behaves like a particle. Because a topological defect causes an associated distributed elastic stress field (wave) to exist, wave-like and particle-like properties of elementary particles are always coupled with each other.

3.2.2. Quantum entanglement

Entangled particles are simply connected through a direct graph link as illustrated in the Figure 4 (c). This completely resolves the apparent non-locality and Bell Theorem contradictions.

The so-called "spooky action at a distance" that troubled Einstein so much is simply explained by the fact that entangled particles are directly connected by a graph's arc (a discrete quantum version of the Riemann fold puncture). Even though the entangled particles appear to be far away from each other, the presence of a direct spatial link between them on the order of one Planck length (see path 1 in Figure 10) enables their respective states to affect each other instantaneously or almost instantaneously. Therefore, quantum entanglement is not an 'action at a distance'; it is, in fact, a local action due to the presence of an arc (one Planck length in size) that directly connects the entangled particles. This also explains the non-local paradoxes of Bell's theorem.

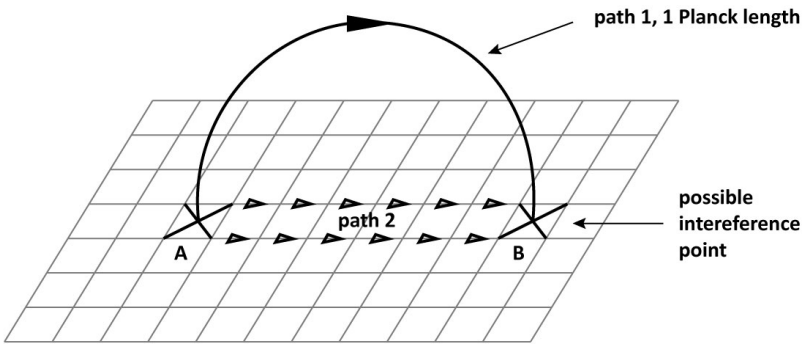

Figure 10: Propagation of signal between entangled particles can follow "fast & direct" 1-Planck-length path. It should take 1 Planck time interval for the signal to propagate between entangled particles following the short path. Interference between the waves traveling through the short path and long path is also possible, although unlikely for most configurations due to the vast differences in distance ratios between a short path and long path. The changes might also propagate instantaneously between A and B due to topological conservation laws on the lattice.

3.2.3. Wave function collapse

The collapse of the wave function is the process of topological transformation or breaking of the topological defect/knot representing an elementary particle. The local stress produced by the topological defect disappears because the knot/defect snaps, releasing the elastic stress through rearrangement of the connections (arcs/ edges) between the graph's nodes. Therefore, the wave-like long-range stress in the space lattice also relaxes to zero either through the propagation of stress waves (which are presumably spreading at the speed of light in our universe) or through discrete Riemann puncture of the graph. During this process, the information represented by the knot leaks into the environment, following conservation laws. In this context, information is an irreducible quantitative description of the space graph geometry/topology and dynamics, essentially a digital encoding of the graph configuration in the sense of information theory and Shannon's formula, see [24].

A snap in the space graph would most likely occur in the location of the highest stress (with the highest probability), but it might also occur in less stressed areas of the graph (albeit with a lower probability). The probability of a snap in a particular location is proportional to the square of the amplitude of the elastic stress in that location, which is why the probability density of finding a particle in a specific location classically is proportional to the square of the amplitude of the wave function.

3.2.4. Degrees of freedom in a multi-particle system

One of the strange aspects of quantum mechanics is why the number of degrees of freedom in a multi-particle quantum system grows exponentially faster than the number of particles, rather than always being proportional to the number of particles (as it would in a classical system). In the proposed framework, the answer for this

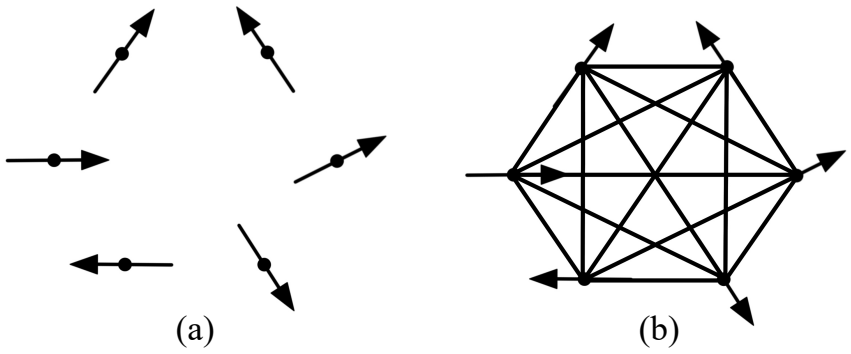

Figure 11: Degrees of freedom in classical and quantum systems. (a): The number of degrees of freedom in a classical system is proportional to the number of particles. (b): The number of degrees of freedom in a quantum system is a tensor product of the degrees of freedom of individual particles due to the possibility of entanglement between particles. Entanglement is explained as direct spatial links of one Planck length between the particles on the space graph.

is straightforward. The extra degrees of freedom describe the presence (or absence) of direct spatial links between the particles (see Postulate 2 and 3 and Figure 11).

Furthermore, for a system of N quantum particles, the reason why the number of degrees of freedom grows geometrically rather than as N^2 is that the degrees of freedom describe the configuration space (a tensor product), where the degrees of freedom multiply rather than add. The reason for why the configuration space is a tensor product is inherently in the possibility of direct spatial links between the particles, meaning entanglement features. This point is well illustrated in the article by T-D Bradley, which says: "The tensor product captures all ways that basic things can interact with each other." See [25].

3.2.5. Pathway to the unification of four fundamental forces

The approach presented here asserts that all four known fundamental physical forces are interpreted as four different types of elastic stress patterns caused by different types of topological defects within a discrete space graph, as described above. The exact details of geometry and topology of those four distortion types have yet to be discovered, as well as the local symmetry structure of the proposed space graph, and the structure of specific topological defects representing elementary particles in our Universe. This will be a challenging area of further research for us.

3.2.6. The Big Bang

In the framework of the proposed space graph theory, the Big Bang is interpreted as a phase transition of the space graph.

Current theories suggest that the four fundamental forces exist as a result of a series of stepwise breaks in symmetry. Using a similar approach, I assume that

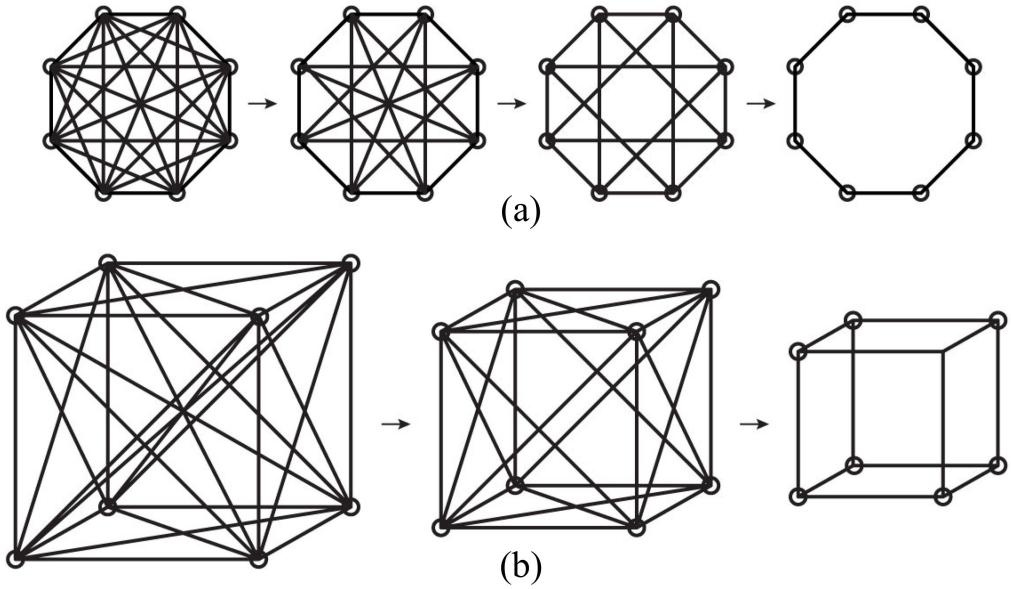

Figure 12: Step-wise symmetry breaking on two small graphs. (b) may indeed resemble the discrete symmetry breaking process that our Universe went through right after the Big Bang, although it appears more likely that our Universe microscopic symmetry incorporates tetrahedral rather than cubic symmetry (see discussion below).

initially the proposed space graph at the moment of the Big Bang stage was highly symmetric, resulting in the unification of all four fundamental forces. Presumably, the graph then went through three sequential phase transitions with each transition resulting in less symmetry and producing a new split between the previously unified fundamental forces. After three subsequent breaks in symmetry, the Universe ended up with the four fundamental forces as we know them today.

Figure 12 illustrates two possible scenarios of symmetry breaking on small graphs with each transition resulting in a lower symmetry state. The end state in Figure 12 (b) may be mapped to the three-dimensional structure of a cube which resembles the three-dimensional space of our universe. I do not mean to assert that the actual symmetry groups of our universe are exactly represented by these images; I merely wanted to illustrate the concept of symmetry breaking of the space graph. In fact, our best guess of the true symmetry of our Universe is that it contains a triangular symmetry as a subsystem, as proposed below in this paper.

3.2.7. Black holes

Similar to the Big Bang (see above), within the proposed framework of the space graph, black holes represent a specific topological phase state of the space graph that is different and distinct from "normal" space.

It has been suggested by multiple researchers that the Big Bang is what emerged on the other side of a black hole. If we also assume that complete time reversal symmetry plays out in that scenario, since the Big Bang underwent three subsequent breaks in symmetry, I propose that inside a black hole three subsequent symmetry unifications take place step-wise as one gets closer to the center.

3.2.8. Interactions between elementary particles

Topological defects of the space graph (elementary particles) may recombine, sometimes resulting in new particles or in annihilation (see Postulate 4 and Figure 3), subject to conservation laws (Postulate 7), while preserving certain geometric and topological invariants of the space graph (e.g., the sum of the quantum numbers of particles for each distinct type of quantum number).

In addition to the local transformations that occur when particles meet and transform through a rearrangement of arcs and/or nodes in the space graph (transmutation), particles may also affect each other at a distance (but not instantaneously, unless directly connected by an arc, as all interactions should move no faster than the speed of light), resulting in scattering or attraction. The mechanics of this interaction is through the elastic stress field of the space graph. This is very similar to how defects in crystalline matter (for example, dislocations in metals) attract or repel each other through the mechanical stress field that they induce within the space lattice.

3.2.9. Quantum tunneling

In the quantum tunneling effect, a particle is assumed to go through the energy barrier. In our framework, I propose that the particle actually goes around the barrier. The process of 'going around' may either happen step-wise alongside (around) the energy barrier or in one long jump of one Planck length around the barrier (see Figure 13 for a graphical illustration).

3.2.10. Interpretation of strings theories

The Big Bang was a highly dynamic process, producing our Universe as a consequence. Furthermore, it had been known for a while that our Universe is expanding, and it has been recently proven that the expansion is accelerating, see [26, 27]. These findings suggest that there exists a physical process responsible for the creation of space. Therefore, any truly fundamental physical theory must explain how space is created and cannot merely assume that space is just a background. For this reason, string theories in any form are unlikely to be the final answer because they take space for granted as a background. This point has been previously emphasized by many quantum gravity researchers, including Lee Smolin and others, see [28].

There exist two distinct possibilities as to how to interpret strings within the framework of the proposed space graph. At the moment, I am not taking a definite position on which one of these two possibilities is actualized in our Universe; this will be an area of further research. The possibilities are:

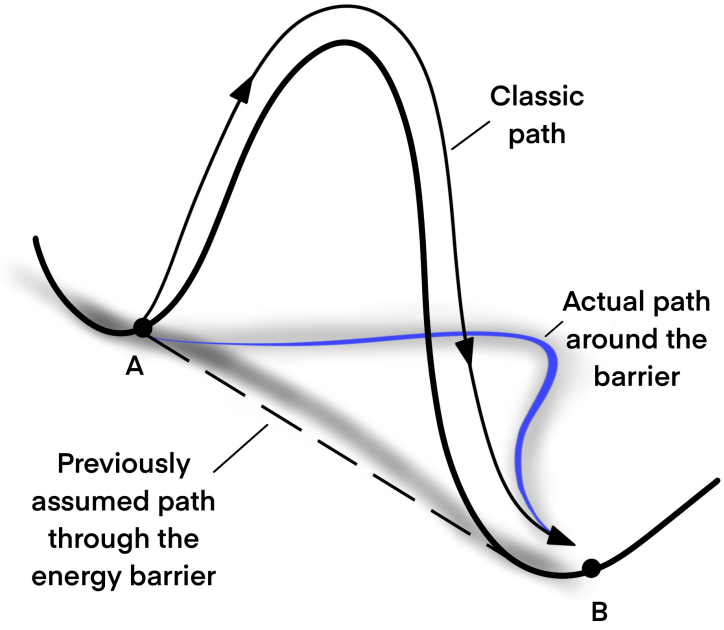

Figure 13: Explanation of quantum tunneling effect: particle goes around the energy barrier into the fourth dimension.

Option 1: Strings can be interpreted as discrete imaginary contours (either open or closed) or branes on the underlying discrete space graph. They do not correspond to any physically existing objects, aside from the fact that those imaginary contours can be arbitrarily chosen within the space graph and follow the edges of the space graph. As such, strings are a made-up construct similar to the discrete elements approach utilized in civil engineering models of stress analysis. (Figure 14) offers a visual illustration.

Even if strings are imaginary objects, they may still offer calculational benefits. First, they encode the topology and geometry of the space graph as they have to follow the graph's surface. Second, because they are extended objects, they may help avoid singularities in our calculations, just like in the calculus of complex numbers, where one can calculate an integral over a singularity by following a closed contour path integral around the singularity. Third, as strings are usually thought of as elastic objects, they might also be utilized to represent the elastic properties of the underlying space graph for computational purposes.

There is yet another interesting take on the M-theory of strings along these same lines. One can consider all contours on the space graph to be strings, which have elastic properties as described above (and as described by equations from popular string theories). Any connected contour or line one draws on the space graph along the edges can be considered a string. Therefore, the entire space graph can be viewed as being interwoven from a set of strings. Perhaps this is the ultimate description and explanation of the M-theory of strings.

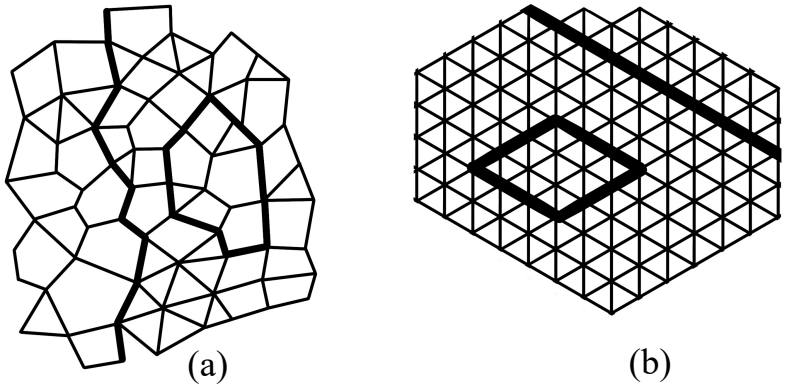

Figure 14: Plausible interpretation of strings: imaginary contours on the discrete space lattice. One open string and one closed string are shown here on an irregular space lattice A and a regular space lattice B.

Option 2: Alternatively, another possibility is that strings could also be interpreted as physically existing extended topological defects within the underlying discrete space graph, similar to linear dislocations in crystals (see Figure 5). In this case, the energy of a dislocation would be (at least to a first order of approximation) proportional to its length, which is similar to some of the energy equations derived from string theory.

3.2.11. Quarks

For a one-dimensional dislocation in solid state physics, its energy is generally proportional to its length. It appears plausible to suggest that quarks are topological defects that must be connected for geometrical and topological reasons by a one-dimensional space graph dislocation. This would explain why it is so hard to separate quarks and why the energy of such a system would grow linearly with distance.

3.2.12. Magnetic monopoles

Perhaps the reason that no one has ever observed magnetic monopoles is that the corresponding topological defect structure would require adding an infinite amount of mechanical stress energy to the space lattice if one tries to calculate an integral over the entire lattice.

3.2.13. Screw dislocations

The geometric structure of a screw dislocation has a certain resemblance to an electromagnetic wave (see Figure 15). Further research will explore whether that resemblance is merely superficial or whether there is indeed a deeper physical connection, perhaps an identity, between screw dislocations in the space graph and electromagnetic waves.

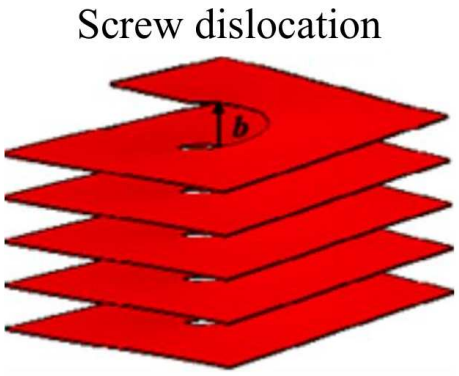

Figure 15: Screw dislocation in a regular 3D lattice has an uncanny resemblance to an electromagnetic wave. Image credit:
`http://www.crpp-bordeaux.cnrs.fr/spip.php?article1324&lang=en`

3.2.14. Singularities

Since I am proposing a discrete spatial structure with a certain minimum unit of length (Plank length), I expect that no singularities would be predicted by our theory, not even in the center of a black hole. This is analogous to how singularities disappear in string theory as a result of a non-zero string length. Singularities seem to arise when one allows the size of a physical object to become zero or makes other unrealistic "absolute" assumptions, such as absolutely hard objects, etc. Einstein postulated that nothing moves faster than light in a vacuum. Similarly, I assert that nothing can get smaller than the Planck length, which I believe will eliminate singularities.

3.2.15. Calculation of a Black Hole's entropy

Since I assert that the Planck length is the minimum size allowed in the Universe (being the size of an elementary arc of the space graph) and that the space lattice has a regular structure, the number of elementary objects one can fit on the surface of the event horizon of a black hole is proportional to the surface area of the event horizon divided by the square of Planck length. Objects inside a black hole cannot contribute to its entropy because they are not in thermodynamic relationship with the space outside the event horizon and cannot interact with it. Therefore, only the objects on the surface of the event horizon can contribute to its entropy (see Figure 16), and therefore black hole entropy must be proportional to its surface area. This reasoning is practically identical to the one published by Carlo Rovelli in 1996, see [29].[10]

The entropy of a black hole can also be calculated using other approaches, as demonstrated by Stephen Hawking, Jacob Beckenstein, and others, see [30]. However, within the framework proposed in this paper, the number of elementary space graph nodes on the event horizon of a black hole should depend on the local symme-

[10]Special thanks to Ian Smith for suggesting the entropy of a black hole as a calculation target.

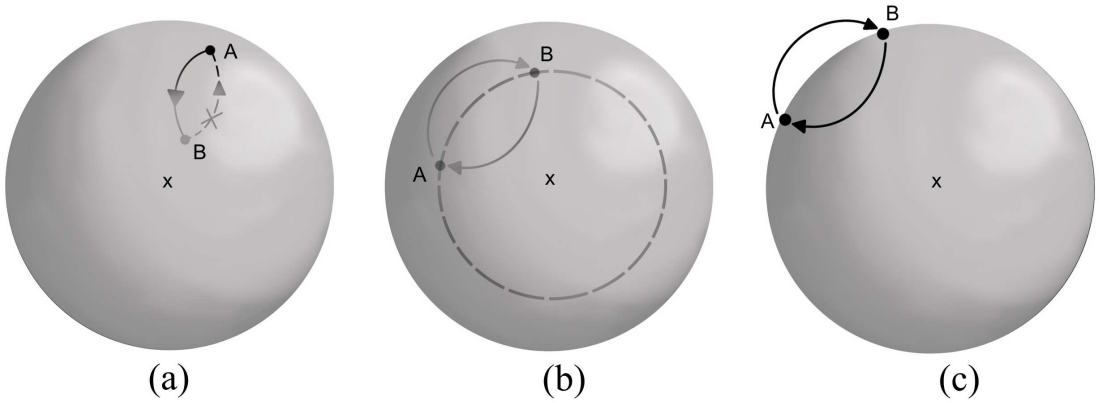

Figure 16: Qualitative calculation of a black hole entropy. (a): That transposition operation is physically prohibited since nothing can escape a black hole, and therefore it should not count towards black hole entropy. (b): Objects inside black hole are not in thermodynamic equilibrium with the objects outside of black hole, and therefore this transposition should not count towards black hole entropy. (c): Only transpositions between the objects located right on the event horizon should count towards black hole entropy. Since Planck length and Plank area are finite, and the smallest physically existing object should have a cross-section on the order of one square Planck length, therefore total black hole entropy must be proportional to its surface and be a function of how many elementary Planck areas can fit on the surface of the event horizon.

try group and the geometry of the graph, because different local symmetries would result in different packing densities. Hawking has shown that the proportionality coefficient in the black hole entropy formula is 1/4, see [31]. Further work will focus on calculating the precise local symmetry of the space graph from that proportionality coefficient proposed by Hawking, Beckenstein, and others, which I hope will help to determine the true symmetry structure of the space graph on the event horizon of a black hole and may also provide ideas as to how to extrapolate the structure and symmetry of the space graph away from the surface of the event horizon and into our "normal" space outside of a black hole.

3.2.16. Interpretation of the double-slit experiment

Feynman once wrote that all the mystery and strangeness of quantum mechanics boils down to the double-slit experiment, see [32]. Within the space graph framework, the double-slit experiment is explained as follows.

A particle's center (topological defect of the space graph) goes through either one slit or another. However, the expanded space graph elastic stress field caused by the defect is distributed and wave-like in nature. This stress field, being essentially a wave, goes through both slits and creates the interference pattern. However, when

it is time for the particle to hit the screen, that collision impact forces the wave-particle configuration to "decide" what specific arc in the space graph should break in order to release the elastic stress in the space lattice. Analogous to static mechanics, where a material is most likely to break in the area of greatest stress, the arc of the space graph that is most likely to break and reconfigure will be the one that is under the most stress (see Postulate 5 above). The stress is the largest in the areas, where the space graph elastic stress field wave interfered with itself in a way that increased the stress (areas where the constructive interference of the wave is the largest). Therefore, the particle dots will cover the screen most densely in the areas that exactly match the experimentally observed interference pattern.

Once an arc is broken in a specific location, the particle will materialize in that location, but, since quantum numbers and topological and geometric invariants of the graph must be conserved, as suggested above in section "Conservation Postulate Needed," this would cause the topological defect at the heart of the elementary particle to "untie" and cease to exist in all other possible locations. My guess is that the specific mechanism for doing so would most likely be a discrete Riemann fold puncture forming a direct connection between the area, where the arc broke and the 'previous' heart of the original topological defect (particle). Another possibility is that this 'defect untie' process would spread through regular space at the speed of light.

If, in the double-slit experiment, one could measure which specific slit the particle traveled through, it would destroy the phase coherence within the wave, and the interference pattern would not emerge on the screen, as seen in numerous experiments.

I also suggest that the difference between experimental "weak measurements" and "strong measurements" of quantum systems is the following: strong measurements involve breaking (rearranging) the space graph; weak measurements do not cause any space graph rearrangements but they do cause elastic stress fields to interact and affect each other and to convey a certain amount of information in the process of doing so.

3.3. Open questions and future research areas

3.3.1. Space graph geometry

What is the structure and symmetry of the space graph and exactly what type of defect corresponds to each known elementary particle? This is an open question. I would like to mention several possibilities, which are all areas of further research.

One plausible option is that the local space graph symmetry group is triangular-based, or that it includes triangular symmetry as a sub-system,[11] since this is the simplest discrete symmetry group that can produce an area (triangular) and volume (tetrahedron). It is also one that is the easiest to form statistically in a super-dynamic and chaotic process, such as the Big Bang or the collapse of a black hole.

[11]Special thanks to Vladimir Mikhalev for collaborating on that insight, as well as on the discussion of rotational symmetry.

If the probability of an arc or a node in a space graph to be available for forming a bond or a cell in a certain local symmetry configuration is less than 1, then the probability of finding three such objects to form a triangular cell must be greater than for a quadratic, hexagonal or other cell type (assuming that the underlying probabilities are at least partially independent). Once a triangular cell is formed, other cells are likely to condense on it in the same triangular geometry, similar to the crystallization process in solid state physics. Therefore, a triangular symmetry group appears to be a natural guess.

It is well known that the regular tetrahedron cannot tile 3D Euclidean space fully. However, in the framework of this theory, the space graph does not exist in space, but rather it creates and defines space. Therefore full tiling considerations may not necessarily apply here.

In case if we consider the ability to fully tile 3D space a desirable property then we can also consider various tetrahedral and hexagonal crystal symmetries as possible candidates.

It is also quite plausible that the actual structure of discrete space graph may resemble a quasicrystal rather that a crystal (more on that below).

There is experimental evidence suggesting that the space lattice symmetry group may indeed contain triangular symmetry at least as a sub-system. The electric charge of an electron is a multiple of 3 electric charges of the d quark. In the framework of the proposed theory, an electric charge is a local geometrical/topological characteristic of the space lattice and its defects. If those characteristics differ by exactly a factor of 3, this is a good indication that indeed the symmetry of the space lattice and its defects contains triangular symmetry! [12][13]

Additional arguments in favor of the symmetry group that incorporates both triangular symmetry and mirror symmetry is the structure of the Standard Model: it contains three families of matter particles, as well as a mapping between electron-muon-tau and corresponding neutrinos, and a similar dual mapping within quarks family. Therefore both triangular symmetry and mirror symmetry are likely to be subsystems of the total discrete space graph symmetry group.

It is also very important to try to guess correctly the number of dimensions in the spatial graph representing our Universe. That would also establish a base for considering the geometry and topology of defects representing elementary particles. I do not know the true answer in regards to the number of dimensions, but my

[12]In this example, the color and flavors of quarks would naturally be interpreted as certain geometrical and topological characteristics of the space lattice defects that correspond to quarks. The same is true for gluons.

[13]It is important to note that some quantum numbers of elementary particles, specifically spin, differ from each other by a factor of two for certain particles (quarks and leptons have spin 1/2, photon, gluon, $W^{\pm}$ and Z^0 bosons have spin 1). This must also be a consequence of the space lattice symmetry and particle geometry within the graph. That may indicate a mirror symmetry, and, in combination with the multiple of 3 for electric charge, as discussed above, a full tetrahedral, a hexagonal or chiral-tetrahedral symmetry for the space lattice and space lattice defects.

best guess is that it is 4-dimensional (not considering time, I mean only spatial dimensions here), with the 4th dimension representing imaginary numbers axis and rolled in a circle. There are two reasons for my guess: (1) imaginary component of wave function in Schrödinger's equation; and (2) Kaluza-Klein theory equations.

Another intriguing, although probably less likely possibility is some higher dimensional generalized form of Penrose tiling or variant tiling.

It also appears plausible, as suggested above, that fermions should be represented by the types of geometric defects that allow only one particle of its kind to occupy a particular location (more than one particle in any one location would presumably result in configurations that are logically impossible or prohibited within the space graph). Bosons, on the other hand, can be represented by the types of defects that allow a limitless number of particles in any one location, without violating any conservation laws or resulting in any geometric configurations that are logically prohibited by the nature of the space graph.

These questions can be further explored either by analytical approaches or by brute force computation methods on sufficiently powerful computers.

3.3.2. The paradox of rotational symmetry

This issue has caused me a lot of concern in relation to the proposed space graph theory. If the space structure is discrete, how can that be reconciled with the fact that, at least on the classical level in our Universe, we observe seemingly continuous rotational symmetry consistent with SO(3) group?[14]

Some possible explanations may include but are not limited to the following:
(1) Perhaps, on the smallest scale, rotation is discrete, but, on macro scales, rotations get 'averaged' to a practically continuous SO(3) rotation as a result of quasi-random irregularities in the lattice structure, space grain boundaries between the adjacent small areas of fixed orientation, and/or the elasticity of the space lattice. This is very similar to the small-crystal grain structure in metals, where each grain has a fixed orientation of the crystal lattice but is oriented randomly (or quasi-randomly) in relation to its neighboring grains. As a result, the entire metal slab exhibits continuous rotationally symmetry on a classical scale due to the random orientation of the grains with respect to each other averaging out uniformly in all directions on a macroscopic scale. Since the Planck length is so incredibly small, on a macroscopic

[14]So far, I have primarily discussed the simplest form of a space graph, where all nodes are identical, aside from a variable number of arcs that may be connected to them. However, following the solid-state physics analogy, one can also imagine a graph with more than one distinct type of node, such as a salt crystal, where some nodes represent Na+ and some nodes represent Cl-, as opposed to a diamond crystal where all nodes are the same. Also, in the simplest case, we may assume that not only are all nodes identical but also that the number of arcs connected to each node must be exactly the same. Of course, another possibility is that the number of arcs can vary between 0 and some fixed integer number. Finally, we must also consider the possibility of a directed graph with some arcs having a preferred direction, perhaps explaining one-way movement towards the center of a black hole. I would nevertheless hope that a simple solution would accurately correspond to our Universe, as often is the case in nature.

level, the rotations and translations of the space graph may be made to look smooth, giving the illusion of continuous rather than discrete movement, both translational and rotational.
(2) Alternatively, the space graph structure may be similar to the structure of amorphous metals or water, which have short-range but no long-range order.
(3) Elastic bending of the space graph structure may also play a role, as discussed above after the Postulate 7, with regards to the nature of inertial mass.[15]

Some of these assumptions might make good physical sense if one considers how the space graph could have evolved or came into existence. In solid state physics, large crystals are rare in nature because arranging elementary nodes (atoms in the case of solid-state physics) in a perfectly regular solid structure with an infinite long-range order usually takes a long time and requires ensuring reasonably stable conditions, such as a fairly fixed temperature, pressure, and chemical composition of the surrounding media. In nature, crystals typically form either when the temperature drops and a liquid freezes into a solid or through a slow process of chemical deposition from a concentrated solution. Furthermore, the growth of a crystal typically starts in a location that has some kind of fluctuation or defect. In most cases in nature, the solvent in the liquid phase typically contains many small fluctuations and the walls of the container holding the liquid contain many irregularities. Also, the temperature usually changes quickly enough in most physical processes that involve crystals. As a result, a large number of small crystals typically start to form almost simultaneously in multiple locations and in random or quasi-random orientations. Once the material completely solidifies, it becomes an ensemble of many small crystals with random orientations.

In a similar manner, if one assumes that space was created during the Big Bang and/or perhaps that the Big Bang was what emerged on the other side of a black hole, all indications are that this would have been a violent and dynamic process. There are also indications that the Universe rapidly cooled down after the Big Bang. Under these fast-moving and chaotic circumstances, there would not have been enough time for one infinitely uniform regular space graph crystal to evolve through the entire space graph. Instead, the Universe should have plausibly ended up with an extremely large number of small space graph crystals (grains) with different orientations connected at their boundaries, similar to what happens when liquid iron cools rapidly and solidifies.

One should be even more confident of this expectation if we consider the random quantum fluctuations that are an inherent nature of the quantum systems. Quantum fluctuations must have been present in the early universe, as confirmed by studies of cosmic microwave background radiation (CMBR). Fluctuations are needed to seed the origins of multiple crystal grains simultaneously, as seen in solid state physics.

[15]Einstein arrived at the idea of curved space by considering the geometry of a rapidly rotating disk, see [33]. Perhaps, we also could derive valuable insights by considering the geometry of a rotating body within a discrete space.

Therefore, quantum fluctuations would have likely resulted in multiple crystalline areas of the space graph growing almost simultaneously in random orientations with respect to each other. Perhaps a more detailed analysis of CMBR may even contain clues to the symmetry structure of the space graph. Perhaps the largest visible universe-size patterns of CMBR is an imprint of the very first elementary graph cell that has formed during the Big Bang? It would also be worthwhile to examine the range of all scales in CMBR.

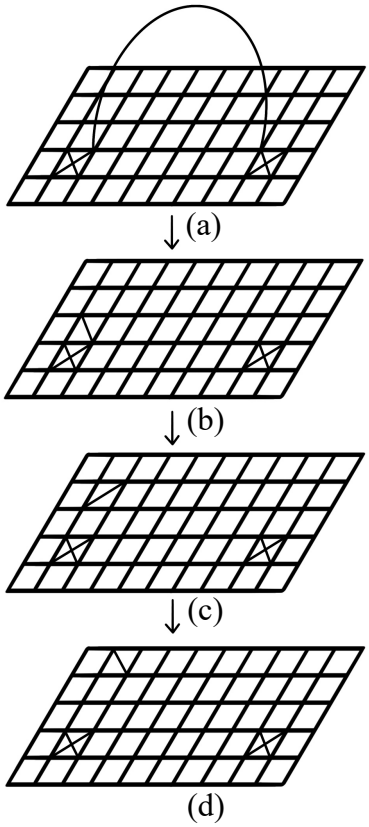

Figure 17: This image illustrates that when entangled particles stop being entangled, a new particle must be emitted. (a): represents entangled state: two entangled particles (topological defects of the lattice) are directly connected by a spatial link of one Planck length. (b): The entanglement breaks, but assuming that the total number of arc must be conserved due to a conservation law, another arc should appear, likely in an adjacent location. That new arc is also a topological defect, and therefore must represent a newly born emitted particle. (c),(d): The emitted particle moves further away from the original location. Therefore, the proposed discrete geometric theory may be verified experimentally by analyzing whether entanglement breaking results in a new particle emission. If detected, the geometric nature of the emitted particle would also become clear as it must correspond to one extra arc in the space graph.

Finally, if one assumes that the Big Bang was what emerged on the other side of a black hole, matter would have likely fallen into the black hole in a chaotic, violent random process, possibly seeding the fluctuations on the other side of the black hole, which became our Universe.

For all these reasons, the small grain-structure of the space graph may indeed be plausible. If we assume a sufficiently small size of the grains within the space graph and a random orientation with respect to each other, we would end up with a Universe that has a discrete rotational and/or translational symmetry on the Planck length scale and a continuous SO(3) symmetry on the classical scale, such as we observe in our Universe.

3.3.3. Experimental verification and predictions of the proposed model

For a physical theory to be credible, it should be verifiable through experimental means. Within the proposed framework, there is a specific prediction that might be verified utilizing current experimental methods.

I have suggested that entangled particles are connected through a direct spatial link of one Planck length (Figure 4 (c)). Consider entangled particles which stop being entangled. At first, the link between the entangled particles breaks. Since an arc has just disappeared, assuming that conservation laws preserve the total number of arcs in a closed system (see the section "Conservation Postulates Needed" above), an extra arc would appear in a topologically adjacent area and perhaps then propagate through the space graph (Figure 17). This extra arc would also represent a topological defect, which, by definition, would be an elementary particle. What kind of elementary particle would be represented by an extra arc in the space graph? Since it appears that an extra arc would introduce a relatively light deformation of the space lattice compared to other possible types of topological defects, the particle emitted when entanglement breaks should therefore have a small mass. The most likely candidate would be neutrino (which has a very low but non-zero rest mass). A less likely possibility would be a photon. More speculative candidates include dark mass particles, dark energy, or perhaps a graviton. The antiparticles of these particles are also a possibility.

In summary, a break in entanglement would result in the emission of an elementary particle. With some ingenuity, the emitted particle may be experimentally detected.[16,17]

Another possible experimental verification is the following. Although the Planck length is much much smaller than anything modern experimental technologies can

[16]This idea has been suggested by Alexey Solovey in a private discussion.

[17]The suggestion that termination of entanglement connection results in a new particle being emitted would only work if the number of arcs is indeed conserved. But since I am unsure on the exact form of the conservation laws, it is also possible that only the number of nodes is conserved, but not the number of arcs, similar to well-known situations in atomic matter when the number of atoms is conserved but not necessarily the number of chemical bonds. If the number of arcs is not conserved then termination of entanglement would not have to result in particle emission.

probe directly, we could try to observe the aggregated effects of discrete space composition on particles that travel over large distances. This has been originally suggested in a research paper by Rodolpho Gambini and Jorge Pullin, see [37]. We can analyze light (or any radiation) arriving to Earth from far-away galaxies billions of light-years away. Over such vast distances, there must be a measurable imprint on that radiation by the structure of space. This signature imprint would be different, depending on whether space is discrete or continuous. We might even be able to derive the exact space geometry and local symmetry on the Planck scale from its imprint on particles of light/radiation traveling over vast distances. We might even be able to detect whether the structure of the space graph is constant throughout the observable Universe.

4. Summary and conclusions

(1) This article proposes a unified framework based on a discrete graph model to explain the nature of space and time, the nature of elementary particles, the origin of quantum numbers, wave functions, wave-particle duality, wave function collapse, quantum entanglement, quantum probabilities, degrees of freedom in multi-particle systems and provides an interpretation of quantum tunneling. This framework also explains the origin of mass, fundamental forces, Higgs field and Higgs boson.
(2) An illustrative calculation of the entropy of a black hole is interpreted within the proposed framework.
(3) A new prospective on strings theories and M-theory is proposed in the spirit of generalized quantum gravity models.
(4) Cosmological implications of the proposed theory, including the Big Bang and black holes, are explored.
(5) Interpretations of fermions, bosons, and zero rest mass particles are proposed.
(6) Various possibilities for modeling the discrete structure of space are proposed and discussed.
(7) Ideas for experimental verification of the proposed theory are suggested.
(8) Further areas of research include the dynamics and structure of the space graph, identifying the structure of specific geometric and topological defects corresponding to known elementary particles, and elementary operations and conservation laws on the space graph.

Acknowledgments. Special thanks to Roger Penrose, Brian Greene, and Lee Smolin, whose books inspired me to seek new approaches, and to Vladimir Novikov who taught me foundations of solid state physics. I also would like to express my gratitude to Vladimir Mikhalev, Ian Smith, and Alexey Solovey for their useful discussions, and to Nathan Hageman for helping to edit this paper.

Publication note. This paper has been approximately 20 years in the making. I was originally trained in solid state physics and topology in Russia, and was taught by Sergei P. Novikov, the Fields Medal Winner, and Dmitri Knizhnik, the author of the Knizhnik-Zamolodchikov equation. I developed most of the ideas presented here

during the time period 2000–2006. Since 2006 I have privately shared my theory with a number of physicists as I was looking to add more mathematical rigor to it, and some of those scientists have since published papers containing similar ideas. This paper contains much less math than I would have preferred because I have not worked in the academia since 1991. I have finally decided to publish my theory as is in the hope to attract colleagues who can help develop this further. Any physicists or mathematicians interested in collaborating please contact me at ybreek@gmail.com. Thank you!

References

[1] Landau, L., Lifshitz, E.: *Quantum mechanics*. New York: Pergamon Press, 1977.

[2] Smolin, L.: *Three roads to quantum gravity*. New York: Basic Books, 2001.

[3] Smolin, L.: Atoms of space and time. Scientific American **290** (1) (2014), 66–75.

[4] Penrose, R.: On the nature of quantum geometry. Magic without Magic (1972), 333–354.

[5] Bojowald, M.: The semiclassical limit of loop quantum cosmology. Classical and Quantum Gravity **18** (18) (2001), L109.

[6] Bojowald, M.: Dynamical initial conditions in quantum cosmology. Physical Review Letters **87** (12) (2001), 121301.

[7] Bojowald, M.: Inflation from quantum geometry. Physical Review Letters **89** (26) (2002), 261301.

[8] Bojowald, M.: Isotropic loop quantum cosmology. Classical and Quantum Gravity **19** (10) (2002), 2717.

[9] Frolov, V. P., Markov, M., Mukhanov, V. F.: Through a black hole into a new universe? Physics Letters B **216** (3–4) (1989), 272–276.

[10] Tsujikawa, S., Singh, P., Maartens, R.: Loop quantum gravity effects on inflation and the cmb. Classical and Quantum Gravity **21** (24) (2004), 5767.

[11] Lawrence, A., Martinec, E.: String field theory in curved spacetime and the resolution of spacelike singularities. Classical and Quantum Gravity **13** (1) (1996), 63.

[12] Rees, M., Ruffini, R., Wheeler, J. A.: Black holes, gravitational waves and cosmology: an introduction to current research. New York, Gordon and Breach, Science Publishers, Inc.(Topics in Astrophysics and Space Physics. Volume 10), 1974, p. 182.

[13] Brandenberger, R., Vafa, C.: Superstrings in the early universe. Nuclear Physics B **316** (2) (1989), 391–410.

[14] Wheeler, J. A., Ford, K.: Geons **97** (January 1995), 511.

[15] Wolfram, S.: *A new kind of science*. Champaign, IL: Wolfram media, 2002.

[16] O'Sullivan, D.: Graph-cellular automata: a generalised discrete urban and regional model. Environment and Planning B: Planning and Design **28** (5) (2001), 687–705.

[17] Gell-Mann, M.: *The quark and the jaguar: adventures in the simple and the complex.* Macmillan, 1995.

[18] Guth, A. H.: Inflationary universe: a possible solution to the horizon and flatness problems. Physical Review D **23** (2) (1981), 347.

[19] Miller, D.: Politics, solid state and the Higgs. Physics World **6** (9) (1993).

[20] Wheeler J. A., Ford, K.: *Geons, black holes and quantum foam: a life in physics*. W. W. Norton & Company, New York, London, 2000.

[21] Noether, E.: Invariante variationsprobleme. nachr. d. könig. gesellsch. d. wiss. zu göttingen, math-phys. Klasse (1918), 235–257.

[22] Wendlandt, J. M., Marsden, J. E.: Mechanical integrators derived from a discrete variational principle. Physica D, Nonlinear Phenomena **106** (1–3) (1997), 223–246.

[23] Kaluza, T.: Zum unitätsproblem der physik. Sitzungsber. Preuss. Akad. Wiss. Berlin (Math. Phys.), vol. 1921, no. arXiv: 1803.08616, pp. 966–972, 1921.

[24] Shannon, C. E.: A mathematical theory of communication. Bell System Technical Journal **27** (3) (1948), 379–423.

[25] Bradley, T.-D.: The tensor product, demystified, 2018, `https://www.math3ma.com/blog/the-tensor-product-demystified`

[26] Riess, A. G., Filippenko, A. V., Challis, P., Clocchiatti, A., Diercks, A., Garnavich, P. M., Gilliland, R. L., Hogan, C. J., Jha, S., Kirshner, R. P., et al.: Observational evidence from supernovae for an accelerating universe and a cosmological constant. The Astronomical Journal **116** (3), 1009.

[27] Perlmutter, S., Aldering, G., Goldhaber, G., Knop, R., Nugent, P., Castro, P., Deustua, S., Fabbro, S., Goobar, A., Groom, D., et al.: Measurements of ω and λ from 42 high-redshift supernovae. The Astrophysical Journal **517** (2), (1999), 565.

[28] Rickles, D., French, S., Saatsi, J. T.: *The structural foundations of quantum gravity*. Oxford University Press, 2006.

[29] Rovelli, C.: Black hole entropy from loop quantum gravity. Physical Review Letters **77** (16) (1996), 3288.

[30] Bekenstein, J. D.: Black holes and entropy. Physical Review D **7**, (8) (1973), 2333.

[31] Hawking, S.: Particle creation by black holes. Communications in Mathematical Physics **46** (2) (1976), 206–206.

[32] Feynman, R. P., Sands, M., Leighton, R. B.: *The Feynman lectures on physics: quantum mechanics. III*. Addison-Wesley, 1965.

[33] Einstein, A., Davis, F. A.: *The principle of relativity*. Courier Corporation, 2013.

[34] Penrose, R.: The role of aesthetics in pure and applied mathematical research. Bull. Inst. Math. Appl. **10** (1974), 266–271.

[35] Gummelt, P.: Penrose tilings as coverings of congruent decagons. Geometriae Dedicata **62** (1) (1996), 1–17.

[36] Levine D., Steinhardt, P. J.: Quasicrystals: a new class of ordered structures. Physical Review Letters **53** (26) (1984), 2477.

[37] Gambini, R., Pullin, J.: Nonstandard optics from quantum space-time. Physical Review D **59** (12) (1999), 124021.

Conference *Cosmology on Small Scales 2020*
Michal Křížek and Yurii Dumin (Eds.)
Institute of Mathematics CAS, Prague

GRAVITATIONAL MODEL OF THE THREE ELEMENTS THEORY: ILLUSTRATIVE EXPERIMENTS

Frederic Lassiaille

FL Research
Saint-Mandrier-sur-Mer, France
frederic.lassiaille@yahoo.com

Abstract: Some following comments are made about the Gravitational Model of the Three Elements Theory: Formalizing (GMTETF) [1]. Some illustrative experiments related to GMTETF are depicted. Apart from the cutting tests of the model which are designed in order to validate the model, more ambitious tests are proposed, which are only naturally suggested by the model. The astrophysics scale experiments concern only the surrounding model [2], which is a simplified version of the model. At laboratory scale, some of the model's predictions might be revealed by the precision of the future interferometers.

Keywords: relativity, gravitation, surrounding, critical density

PACS: 95.30.Sf, 98.80.-k

1. Introduction

In the present document some comments will be tried about GMTETF, which will be named "the model".

An important focus will be applied to the second assumption of the model. The macroscopic relation between the privileged frame of the model and energy distribution can be searched for. This will reveal an algebraic structure for the set of boosts.

Another detailed description concerns the fitting process which has been used at the construction of surrounding. It will tune in return the relative values of the contributions of the galaxy and Universe for the calculation of the privileged frame.

An experimentation designed in order to measure the "counteracting effect", a dizzling effect predicted by the model, will be imagined. The three cutting tests of surrounding will be reminded, since this large scale model is derived directly from the model. Then some more ambitious experiments will be imagined, suggesting clues for the search of a new physics.

2. Reminder of the assumptions of the model

Let us remind briefly the four assumptions of the model.

1. Matter is made up of indivisible particles always moving at the speed of light along geodesics. Let us name "IP" such a particle.

2. The space-time structure is determined by a set of successive deformations, each of them is described by a boost. Let us name "boost-like deformation" such a deformation.

3. Each IP is propagating a boost-like deformation through space-time. This propagation evolves at the speed of light. An energy is propagated along this propagation. Let us name "IP gravitational wave" such a wave.

4. The space-time structure is determined only at the intersections of the "future light cones of the IPs". The rule yielding the final space-time deformation resulting from numerous IP gravitational waves, occurring in the same space-time event, is dictated by the principle of energy conservation.

3. Algebraic structure of the set of boosts

The purpose of this paragraph is to study the set of boosts in the context of the model. In this context, the question of the algebraic structure of the set of boosts gets a physical signification through the question of the determination of the privileged frame. Concretely, the question is the evolution of this privileged frame in case of multiple macroscopic particles in motion. The significance of "macroscopic particle" here is "a particle which contains multiple IPs".

The first GR issue which will be reviewed is the issue of the absence of algebraic structure for the set of boosts with the composition operator. Now this question is reformulated the following way. What is the algebraic structure of the set of boosts which describe the evolution of the privileged frame? How is this structure connected to energy distribution of multiple macroscopic particles? This gets here a direct answer in the context of the model. Indeed, after the determination of a privileged R_0 frame, the algebraic structure of the set of (a, B) couples appears, where a is the energy at rest of an object, and B is the boost associated with its motion in R_0. Let us call S this set of couples. The algebraic structure of S is inherited from the f isomorphism from S to the set of energy-momentum four-vectors, such as $f((\mathrm{d}E, B^{\mu}_{\nu})) = \mathrm{d}D^{\mu}$, using the notations of the equations of [1]. It should be noticed that the image of f is the set of energy-momentum four-vectors describing an energy having a speed always strictly below the speed of light. The definition of the induced $*$ operator acting on S is $(a_1, B_1) * (a_2, B_2) = f^{-1}(f((a_1, B_1)) + f((a_2, B_2)))$, with obvious notations. The resulting structure of $(S, *)$ is isomorphic to $(\mathbb{R}^{+*} \times \mathbb{R}^3, \mathrm{op})$, where $\mathbb{R}$ is the set of real numbers, $\mathbb{R}^{+*}$ is the set of strictly positive real numbers, and op is the barycentric operator. Physically it is more relevant to say that this is

isomorphic to the set of (a_t, v) couples, where a_t is the total energy of the object, and v, being strictly weaker than c is the speed of the inertial center of the object in a given frame, using the barycentric operator.

Now in this context the GR issue of the order of the boosts in their three dimensional composition can be addressed. Because now this question is reformulated the following way. Is it possible to use the composition of the boosts in three dimensions, for describing the evolution of the privileged frame, and, if so, what is the correct order which must be used? For trying to answer those questions, let us suppose the Universe filled with a constant and uniform distribution of matter, and let us study two A and B objects in this context. If A and B are far enough from each other, the space-time deformation due to A is not noticeable around B and vice versa. In this case an inertial privileged frame R_B attached to B will appear in an inertial privileged frame R_A attached to A following roughly the rule of the composition of the boosts and it will appear a Wigner rotation [3, 4, 5]. But in the context of the model, the space-time structure will be determined without ambiguity. The answer to the question of the order will be conspicuous: R_A to R and then R to R_B. (Here the meaning of "an inertial privileged frame attached to a given particle" is a frame such as its origin is always located in the particle, sharing the same speed as the particle. It is always theoretically possible to obtain such a frame almost approximately, by either decreasing Universe matter density or by increasing the particle matter density.) Now if the Universe becomes empty except A and B then no boost composition will be required and no Wigner rotation will appear. Also if E_A and E_B are the respective energies at rest of A and B, if $E_A \gg E_B$ and if A and B are closed enough to each other so that the space-time deformation of the Universe is not noticeable around A, (that is, the deformations of A and B are the only one noticeable around B), then R_B will appear in R with a Wigner rotation and the choice of the order will be obvious too: R to R_A and then R_A to R_B. The final result is that the answer to the questions of which composition of boosts and which chosen composition order between the macroscopic privileged frames depends of the relative energies associated to those frames.

4. Fitting the surrounding coefficient

The full detail of the fitting process which has been giving the surrounding coefficient will be required further on in the present document. The following surrounding coefficient has been created from a macroscopic simplification of the C_{GMTET} coefficient introduced in [1],

$$C_{\mathrm{surrounding}} = \frac{a\rho_0 + b\rho_{u0}}{c\rho + d\rho_{\mathrm{Universe}}}, \tag{1}$$

where ρ is matter density around the observer below $10\,h^{-1}\,\mathrm{kpc}$ (roughly $15\,\mathrm{kpc}$), ρ_0 is this matter density in the Solar system, ρ_{Universe} is matter density in the Universe, and ρ_{u0} is matter density in the Universe at today's time. The symbols a, b, c, and d denote the fitting parameters.

The value of the gravitational constant G in Solar system would imply $a = c$ and $b = d$. The degree of liberty of the ratio allows to fix $b = d = 1$. It remains only a which is constraint mainly by two different requirements.

- The equivalent G in the IGM.
- The critical matter density of the Universe.

But those two requirements yield different values of a. They can be approximately met but this would not allow a correct simulation of the galaxy speed profiles. The equality $b = d$ is required, because $C_{\text{surrounding}} = 1$ in Solar system. But for the same reason there is $a = c$ in the galaxy. That is why it has been supposed the existence of a shielding effect in a galaxy. Then, in place of supposing $a \neq c$, it has been supposed the existence of an α coefficient taking the role of such a shielding effect. It has two different values, α_{in} for an observer located in the Milky Way, and α_{out} for an observer located outside of any galaxy. The new formulation of the ratio is the following

$$C_{\text{surrounding}} = \frac{\alpha_{\text{in}}\rho_0 + \rho_{u0}}{\alpha\rho + \rho_{\text{Universe}}}. \tag{2}$$

However, this simple formulation remains constraint by the four following requirements:

1. The equivalent G in the IGM.
2. The critical matter density of the Universe.
3. The equivalent G in a void.
4. The simulations of the speed profiles of the galaxies.

And this is quite an achievement: it is possible to find values for those two variables, α_{in} and α_{out}, while matching those four requirements.

- α_{out} gets the value 1. By itself this is also noticeable.
- α_{in} gets the value $1.6 \cdot 10^{-5}$. The order of magnitude of this particular value can be directly observed when simulating galaxies. One starts from the following equation.

$$C_{\text{surrounding}} = \frac{A}{B + C\rho}. \tag{3}$$

Then it is seen immediatly $B \neq 0$. Because of $B = 0$, the simulated speed profile of a galaxy becomes irrelevant. On the contrary, $B \gg C\rho_0$ simply yields no modification of Newton's law. When trying different configurations for the values of B and C (A is only the degree of liberty of the ratio), it appears quickly that B and $C\rho$ must not differ by more than one order of magnitude. And interestingly

this is in accordance with the four previous requirements altogether. The second requirement above implies $(\alpha_{\text{in}}\rho_0 + \rho_{u0})/(2\rho_{u0}) = 1/\Omega$, where the used value for the relative critical density is $\Omega = 0.05$. Then we have the following result:

$$\alpha_{\text{in}}\rho_0 = 39\rho_{u0}. \tag{4}$$

It is in contradiction with the results of the calculations of [1], which supposes that Newton's law is valid at any scale. Hence, it tends to show that gravitation would be weaker than Newton's law for interacting distances beyond 15 kpc which is approximately the ray of the galaxy we are living in. This has also consequences in the determination of the privileged frame, which will be used further on in the present document.

5. Experimentations

It will be studied two different kind of experimentations relative to the model.

The first kind of experimentation will be named "cutting test", that is an experimentation which is intended to validate or invalidate the model. It means that if such an experientation succeed, then either the model is validated, that is, confirmed, either it is invalidated.

The second kind of experimentation will be called "clue for the search of a new physics". Such an experimentation is testing only a suggestion of the model. This more or less direct suggestion is not a prediction, or it might be called a "very soft" prediction.

5.1. Cutting tests

Let us try to list the set of tests which are able to validate or invalidate the model (the "cutting tests"). The following features of the model will be concerned.

1. The "counteracting effect" of the second assumption.
2. The surrounding effect at large scale (for interaction distances greater than 15 kpc).

5.1.1. Testing the counteracting effect

The "boost" which is refered to in the second assumption describes the space-time deformation of the model. It does so by determining successively the evolution of a particular frame, called the "privileged frame". At each step of the dicrete GMTETF model, locally the speed of this frame with respect to the previous one, is exactly opposite to the speed, with respect to the previous frame, of the interleaved added matter. This particular behavior will be called "counteracting effect".

This dizzling characteristic suggests a cutting test of the model. It consists in testing this counteracting effect.

Therefore, it consists in testing the space-time deformation generated by matter in motion as predicted by the model. What happens is that the privileged frame

is modified by the motion of matter, at the location of this matter. It means that if some important amount of matter is at rest in the laboratory at time $t = t_0$, and then put into motion at a high speed V at $t = t_1 > t_0$, it will generates the following consequence (now in the present document this matter in motion will be simply named "matter in motion").

- The privileged frame of the laboratory at $t = t_0$ goes into motion at $t = t_1$ with a v speed opposite to V, with respect to its previous location at $t = t_0$.

Of course, the privileged frame on Earth, far from the matter in motion, is still the same. It means that at a location far from the matter in motion no change is noticed between t_0 and t_1. But the privileged frame located close to the matter in motion is not the same. If the effect is strong enough it will produce matter distorsion and stress in the laboratory. The speed v is given by the following equation:

$$v \simeq -V \frac{\sum_{n=0}^{N} \mathbb{1}(x, y_n, u_n) \sqrt{\frac{E_t(y_n)}{\|x - y_n\|_3}}}{\sum_{n=0}^{M} \mathbb{1}(x, y_n, u_n) \sqrt{\frac{E_t(y_n)}{\|x - y_n\|_3}}}. \tag{5}$$

This equation is in fact an approximation, but it's a good aproximation on earth. The notations has been defined in [1], let us remind them:

- n is the IP number of the IP located at the y_n event.
- x is the location of the laboratory.
- $\|x - y_n\|_3$ is the distance between x and y_n (space distance, calculated in a covariant manner).
- $\mathbb{1}(x, y_n, u_n) = \delta(\|x - y_n\|_3 - x^0 + y_n^0)\delta_E(u_n \cdot u - \sqrt{2}/2)$ is used for selecting the IPs which are taken into account in the sums.
- $\delta(\|x - y_n\|_3 - x^0 + y_n^0)$ tells that the IPs must be located on the past light cone centered in x.
- $\delta_E(u_n \cdot u - \sqrt{2}/2)$ tells that the IPs on this cone propagate a gravitational wave in x only if their initial orientation allows it. But in the macroscopic version of (5), in which only the means values are considered, for IPs pertaining to matter, not pertaining to light, matter being approximately at rest with respect to the earth, this $\delta_E(u_n \cdot u - \sqrt{2}/2)$ term is always equal to 1. It means also that the energy of light in the Universe is considered relatively negligible.

The IPs which are numbered with a n number between 0 and N are those which are parts of the matter in motion.

The IPs which are numbered with a n number between 0 and M are simply the IPs of the observable Universe.

In order to only illustrate this particular behavior, let us imagine an experimentation. In the present document any comments about experimental physics will be done only on this purpose of illustration. So as a matter of example, one related experiment might consist in using a 300 m high and 2 m diameter pipeline connected to an upward lake. Far from the location of the measurement the pipeline is vertical or almost vertical, then it is slowly curved in order to be horizontal at the location of the measurement. At this location a mirror is placed into the tube, or very closed to it. Its horizontal location is measured by an interferometer. This one measures the distance between this first mirror, and a second mirror located far from the pipeline in order to avoid the predicted effect. The experiment is trying to detect a modification of this measured distance, therefore, to detect a motion of the first mirror with respect to the second one. A first measurement is done at $t = t_0$ when the pipeline is empty. A second one is done at $t = t_1$ when the pipeline is full of water in motion at 10 m/s.

The prediction of the model is the following. Between t_0 and t_1 the first mirror should be put into motion at the v speed given by equation (5).

Let us rewrite some of the equations and inequalities of [1]:

$$\frac{S_w(\text{laboratory})}{S_w(\text{galaxy})} = \frac{\rho_{\text{laboratory}}}{\rho_{\text{galaxy}}}\left(\frac{R_{\text{laboratory}}}{R_{\text{galaxy}}}\right)^{5/2} \simeq 3\ 10^{-29} \tag{6}$$

$$\frac{\rho_{\text{galaxy}}}{\rho_{\text{Universe}}}\left(\frac{R_{\text{galaxy}}}{R_U}\right)^{5/2} Ex \simeq 10^{-7} < \frac{S_w(\text{galaxy})}{S_{\text{Universe}}} < 1 \tag{7}$$

where $S_w(\text{laboratory})$ is the value of the sum which is the numerator of the ratio of the rhs of (5) in the particular case in which the matter in motion is a sphere of ray equal to $R_{\text{laboratory}}$, and in which x is the center of this sphere. Furthermore, $S_w(\text{galaxy})$ is the same calculation modelizing in a very rough manner the galaxy by such a sphere with a ray equal to R_{galaxy}, and S_{Universe} is the value of the sum which is the denominator of the ratio of (5). $Ex \simeq 0.22$ is the coefficient due to expansion. The symbols $\rho_{\text{laboratory}}$, ρ_{galaxy}, and ρ_{Universe} are the associated matter densities with obvious notations. Also $R_{\text{laboratory}}$ and R_{galaxy} are the respective rays, and R_U is the particle horizon. It has been used $\rho_{\text{laboratory}} = 10^3\,\text{kg/m}^3$, $R_{\text{laboratory}} = 1\,\text{m}$, for taking into account the 2 m diameter pipeline. It has been used $\rho_{\text{galaxy}} = 0.003\ M_0/\text{ly}^3$, where M_0 is the mass of the Sun, $R_{\text{galaxy}} = 15\,\text{kpc}$, and $\rho_{\text{Universe}} = 9.24 \cdot 10^{-27}\,\text{kg/m}^3$.

But it has been shown above that the behaviour of surrounding allows to expect a much greater value for the weaker bound of (7). Indeed, the $S_w(\text{galaxy})/S_{\text{Universe}}$ ratio is driving the numerator of the surrounding modifying coefficient, which is reminded in equation (2). And the latter one is strongly constraint as it has been shown. The related terms of equation (2) are $\alpha_{\text{in}}\rho_0 = S_w(\text{galaxy})$, $\alpha_{\text{in}}\rho_0 + \rho_{u0} = S_{\text{Universe}}$. Then

with equation (4) it goes $S_w(\text{galaxy}) = (39/40)S_{\text{Universe}} \simeq S_{\text{Universe}}$. The result is that the inequalities of (7) are replaced by the following approximation.

$$\frac{S_w(\text{galaxy})}{S_{\text{Universe}}} \simeq 1. \tag{8}$$

Now it results the following R ratio and the resulting speed of (5):

$$R = \frac{S_w(\text{laboratory})}{S_{\text{Universe}}} \simeq 3 \cdot 10^{-29}, \tag{9}$$

$$v = VR \simeq 3 \cdot 10^{-28}\,\text{m/s}. \tag{10}$$

A mirror moving freely horizontally, close to the matter in motion, would travel approximately the following $d = vT_{\text{meas}}$ distance after $T_{\text{meas}} = 1\,\text{hour}$,

$$d \simeq 10^{-24}\,\text{m}. \tag{11}$$

This very low value might generate no stress in matter, even for a mirror solidely attached to the laboratory. Nevertheless, it might be compared to the possible strain sensitivity of the future KAGRA interferometer [6]. For example, a $L = 1\,\text{km}$ long KAGRA interferometer (distance between the two mirrors) having a strain sensitivity of $s = 10^{-29}\,\text{Hz}^{-1/2}$ operating at $\nu = 100\,\text{Hz}$ would admit a N absolute noise given by the following equation

$$N = Ls\sqrt{\nu} = 10^{-25}\,\text{m}. \tag{12}$$

Therefore, it sounds possible to compare the prediction of equation (11) with the measurement. But, among others, the presence of the matter in motion close to the first mirror will produce vibrations which might forbid this detection even with the values given by equations (11) and (12).

5.1.2. Testing surrounding

There are also theoretical differences between GR and the model at astrophysical scale, concerning the determination of the privileged frame. They have been discussed in [1], and they seem to be difficult to test at this scale.

Compared to the counteracting effect, which is an inner part of the second assumption, the surrounding effect is a behavior which is induced by the assumptions. Nevertheless, this effect is inherent to the main equation of the model. Therefore, testing this effect is testing the model with a cutting test. In [2] it was noticed that there are three tests of surrounding. They are reminded below and in Table 1.

Intragalactic
This test consists in continuing the simulation of a galaxy under the surrounding model. A specific focus on flat profiles of giant galaxies might be done.

Extragalactic
This test consists in detecting a particular correlation between matter density and the equivalent G, outside of any galaxy. The following equation is predicted.

$$\frac{G'}{G} = 2\frac{\rho_c}{\rho + \rho_u}, \tag{13}$$

G is the gravitational constant,
G' is the equivalent value of G as predicted by the model,
ρ is the matter density calculated in a 15 kpc ray sphere centered in M,
ρ_u is the matter density of the Universe at the time of the M event, and
ρ_c is Universe critical matter density.

Large scale structure

Surrounding predicts a particular stable equilibrium and a particular matter distribution in this equilibrium state. This distribution of matter is given by the following equations

$$\rho = (\rho_{\text{wall}} + \rho_u)\,\frac{x_{\text{wall}}}{x} - \rho_u, \tag{14}$$

where x is the distance from the nearest wall, x_{wall} is half the width of this wall, ρ_{wall} is the matter density of the wall, and ρ_u is Universe matter density.

Equation (14) shows a void falling into complete emptiness at this x_e distance from the nearest wall,

$$x_e \simeq \frac{\rho_{\text{wall}}}{\rho_u} x_{\text{wall}}. \tag{15}$$

Therefore, the test consists in measuring the observed matter density distribution which is used in those equations, and then checking if those equations are retrieved.

5.2. Clues for the search of a new physics

The model gives some clues for the search of a new physics. Indeed it suggests quite naturally a particle physics in which the four forces would be driven by its equation. This would result in surrounding effects occuring in particle physics. It means that as well as gravitation, each of the three remaining forces would be weakened or increased by surrounding matter density, depending on wether this matter density is increased or decreased, respectively.

This remark might lead to clues for the search of a new physics. But for this a simple modelization of the electron and the photon in the context of the model has to be introduced.

5.2.1. The model and particle physics

The GMTETF model was untitled a "Gravitational Model" (GM). But one might notice that this model by itself naturally suggests a unifying theory. The first step would be to describe the composition of each particle of the standard model under the context of the first assumption. The trajectory of IPs inside each particle would be detailed. And the second step would be trying to retrieve particle physics from this "extended GMTETF". Of course, this would be a huge work.

In order to retrieve the Planck-Einstein relation, the trajectory of an IP pertaining to a photon would be an helix. And in oder to retrieve electromagnetism,

an electron would be quickly modelized by an IP trajectory having the shape of an helix engraved on the surface of a torus. Indeed this seems to be the way to retrieve electromagnetism in this context. Those descriptions are of course only suggested, not proven by any means. Let us remind that the aim is to find clues for the search of a new physics. In the present document such a modelization will be called TET ("Three Elements Theory").

Another remark about particle physics is that the surrounding effects predicted by the model suggests [7] a solution to the mass gap and confinement problems [8, 9].

5.2.2. Surrounding effects in particle physics

Interestingly some apparently good ideas there might lead nowhere. For example, a measurement of the hydrogen spectral rays under different surrounding contexts would probably shows no variation at all. Indeed, the energy levels are function of the fine structure constant. But recent developments [10] tend to show that this constant having no unit is related to the geometry of a particular modelization of the electron. And this modelization is similar to the GMTETF modelization introduced above. Therefore, measuring the atom spectral rays might not show anything new.

This absence of surrounding effects might concern other measurements in the field of particle physics. Hence, a good practice would be to restrict ourselves only to explicit or implicit measurements of space-time trajectories.

One of these measurements are the cross sections of particles, since they measure the trajectories of the interacting particles. But on earth the required precision might not be enough as compared to the R ratio of equation (9). The same "double" experiment on earth and also far from earth (in orbit for example) would allow to test the prediction of a much stronger ratio:

$$\frac{S_w(\text{Earth})}{S_{\text{Universe}}} \simeq \frac{S_w(\text{Earth})}{S_{\text{galaxy}}} \simeq 10^{-11}$$

with the notations and values of [1].

Once again a good precision might be obtained by an interferometer, measuring either a distance or a light frequency. In the context of the model the Planck-Einstein $E = h\nu$ relation suggests that the energy of the IP pertaining to the photon modifies its own helicoidal trajectory, and therefore its own frequency. Indeed, the space-time deformation would be increased with the IP energy, decreasing the helix's ray. In such a case it would appear also surrounding effects. Decreasing or increasing respectively the surrounding matter density would result respectively in increasing or decreasing the space-time "elasticity", hence decreasing or increasing the ray of this helix, and then increasing or decreasing the photon's frequency. The conclusion here is that the surrounding effect of the model might modify the Planck constant.

Let us try to illustrate this by the description of a possible experimentation. An already existing gravitational wave interferometer [11] is modified, covering only one arm of the two arms ot the interferometer with a 1 m ray pipeline, without modifying the arm itself. The result is that this arm is located in the axis of this pipeline. Then

the first measurement detects the location of the interference fringes with an empty pipeline. The second measurement is exactly the same one but using a pipeline full of water. The prediction is a relative difference of the measured frequencies given by the R ratio of equation (9). Using a reference frequency of 100 Hz, it would result in a frequency shift of 10^{-27} Hz. Of course, the recent interferometers do not allow such a precision, but this value might be obtained by future versions [6]. Also the suggested experimentation might be improved for example replacing the pipeline by a channel.

5.2.3. Miscellaneous experiments

Another idea would be of searching for possible violations of the linearity of the gravitational force. Indeed it has been shown in [1] that a slight modification of the model can lead to such a violation. For example, the eclipse anomaly [12] might find here the beginning of an explanation, since the lenticular effect occuring during an eclipse increases light beam densities and also the intensity of the microscopic waves predicted by GMTET. Unfortunatly, the observed anomaly is a decreasing gravity, whereas the prediction would be an increase. But this is an example of what might be searched for. Another example might be the Pioneer anomaly [13]. Indeed, if any non-linearity would be predicted by the model, then of course this location would be one of the locations, in the Solar system, in which this non linearity would be very strong. Those best locations would be the ones wich are aligned with the sun and Saturn, or with the Sun and Jupiter, and of course having the coresponding planet and the Sun on the same side.

It might be possible also to search for this non-linearity at laboratory scale. The experiment would be for example aligning numerous spheres of lead and measuring the value of the gravitational constant on this straight line while successively modifying the number of aligned spheres.

Another clue for this quest of a new physics is given by TET. Then the experiment would try to detect the existence of any magnetic or electrostatic field in the vicinity of a light beam propagating in an optic fiber following a particular shape. The simplest shape would be the shape of an helix having its axis following a circle. A complicated shape would be the shape of an helix having its axis following a bigger helix, with the axis of this bigger helix following a circle.

Table 1 shows the cutting tests of the model. Table 2 shows the "clue" experiments for the search of a new physics, which are suggested by the model.

6. Discussion

The determination of the privileged frame of the model reveals macroscopically an algebraic structure of the set of boosts, which is related to energy distribution.

The fitting process of surrounding tends to show that gravitation would be weaker than Newton's law for interacting distances beyond 15 kpc. This has also consequences in the determination of the privileged frame.

Scale	Tested behavior	Cutting test experiment
Astrophysical	Galaxy speed profiles	Simulating and comparing with experimental data
Astrophysical	Surrounding effect in IGM[a]	Measuring the equivalent G and matter densities
Astrophysical	Large scale structures	Measuring matter distribution at large scale
Laboratory	Counteracting effect	Detecting an induced motion[b]

Table 1: Cutting tests of the model: [a]Intergalactic medium, [b]The particular counteracting effect of the second assumption is tested.

Scale	Tested behavior	Experiment
Laboratory	Surrounding effects	Measuring a light frequency[a]
Laboratory	Linearity[b]	Measurement of G using aligned spheres
Solar system	Linearity[b]	Measurement of the gravitational force[c]
Laboratory	Generation of an EM[d] field	Measurement of an EM field[e]

Table 2: Suggested experiments based on the model, imagined in order to give clues for the search of a new physics: [a]A possible variation of the Planck constant with surrounding matter density is suggested by the model, [b]A possible violation of the linearity of the gravitational force is suggested by the model, [c]Measurement of the evolution of the gravitational force along the "Saturn-Sun" line, and "behind" Saturn from the Sun, [d]"EM" is an acronym for electromagnetic, [e]Measurement of electrostatic and magnetic fields close to a dedicated fiber optic apparatus.

The most promising experimentation suggested by the model has been depicted. It consists of testing the conteracting effect predicted by the model. It seems to be difficult to realize, because of the added noise generated by the motion of matter during the experiment. It requires a sensitivity which is not afforded by the existing interferometers. But this could be afforded by the future interferometers.

The other cutting tests concern only surrounding. Those are astrophysical measurements.

In the laboratory scale, there exist also tests which are not cutting tests but only tests which are suggested by the model. One of them is testing the evolution of the Planck constant with surrounding matter density.

Can we expect to reveal a new physics?

Acknowledgements

I thank the organizers of CSS 2020 for their invitation to give this lecture.

References

[1] Lassiaille, F.: Gravitational model of the three elements theory: formalizing. In: the Proceedings of *8th International Conference on New Frontiers in Physics (ICNFP 2019)*.

[2] Lassiaille, F.: Surrounding matter theory. In: M. Křížek, Y. Dumin (Eds.), *Cosmology on Small Scales 2018*, *Dark matter problem and selected controversies in cosmology*. Inst. of Math., Prague, 2018, pp. 204–228.

[3] Rhodes, J., Semon, M.: Relativistic velocity space, Wigner rotation and Thomas precession. Amer. J. Phys. **72** (2005).

[4] O'Donnell, K., Visser, M.: Elementary analysis of the special relativistic combination of velocities, Wigner rotation and Thomas precession. Eur. J. Phys. **32** (2011), 1033–1047.

[5] Rebilas, K.: Comment on 'Elementary analysis of the special relativistic combination of velocities, Wigner rotation and Thomas precession'. Eur. J. Phys. **34**(3) (2013), L55–L61.

[6] Abbott, B. P., Abbott, R., Abbott, T. D. et al.: Prospects for observing and localizing gravitational-wave transients with Advanced LIGO, Advanced Virgo and KAGRA. Living Rev Relativ **21**(3) (2018), `https://doi.org/10.1007/s41114-018-0012-9`.

[7] Lassiaille, F.: Surrounding principle applied to Yang-Mills theory: introduction, Boson Journal of Modern Physics 4(2) (2018), 426–434.

[8] Jaffe, A., Witten, E.: Millennium Prize Problems, Amer. Math. Soc., Providence, RI, 2006, 125–152.

[9] Faddeev, L. D.: Mass in Quantum Yang-Mills Theory (Comment on a Clay Millennium Problem) In: Benedicks M., Jones P. W., Smirnov S., Winckler B. (Eds.), *Perspectives in Analysis. Mathematical Physics Studies*, **vol. 27** Springer, Berlin, Heidelberg (2005), arXiv: 0911.1013 [math-ph].

[10] Poelz, G.: An Electron Model with Synchrotron Radiation, (2020), arXiv: 1206.0620v34 [physics.class-ph]

[11] Abbott, B. P. et al.: GW150914: The Advanced LIGO Detectors in the Era of First Discoveries. Phys. Rev. Lett. **116** (2016), 131103.

[12] Wang, Q. et al.: Precise Measurement of Gravity Variations During A Total Solar Eclipse, (2010), arXiv: 1003.4947v1 [astro-ph.EP].

[13] Turyshev, S. G., Toth, V. T.: The pioneer anomaly. Living Rev. Relativity **13** (2010), 4.

LIST OF PARTICIPANTS

Yash P. Aggarwal
Lamont-Doherty Earth Observatory of Columbia University, 822 Winton Drive, Petaluma, CA 94954, U.S.A.
haggarwal(at)hotmail.com

Pavel N. Antonyuk
Faculty of Mechanics and Mathematics, Lomonosov Moscow State University, Leninskie Gory 1, Moscow, R-119 991 Russia; Moscow Institute of Physics and Technology, 9 Institutskiy per., Dolgoprudny, R-141 701 Russia
pavera(at)bk.ru

Hana Bílková
Institute of Mathematics, Czech Academy of Sciences, Žitná 25, CZ-115 67 Prague 1, Czech Republic
hbilkova(at)math.cas.cz

Yan Breek
Nvidia, Santa Clara, California, U.S.A.
ybreek(at)nvidia.com

Joerg Dabringhausen
Astronomical Institute, Faculty of Mathematics and Physics, Charles University, V Holešovičkách 2, CZ-180 00 Praha, Czech Republic
joerg(at)sirrah.troja.mff.cuni.cz

Yurii V. Dumin
P.K . Sternberg Astronomical Institute of M. V. Lomonosov Moscow State University, Universitetskii pr. 13, R-119 234 Moscow, Russia; Space Research Institute, Russian Academy of Sciences, Profsoyznaya str. 84/32, R-117 997 Moscow, Russia
dumin(at)sai.msu.ru, dumin(at)yahoo.com

Antonín Dvořák
Kovoprojekta Brno a.s., Poznaňská 22, CZ-616 00 Brno, Czech Republic
antonin.dvorak(at)centrum.cz, advorak(at)kovoprojekta.cz

Ismael Ferrero
Institute of Theoretical Astrophysics, University of Oslo, Duehaugveien 6b, Oslo, Norway
s.i.ferrero(at)astro.uio.no

Itzhak Goldman
Afeka Engineering College and Tel Aviv University, Mivtza Kadesh 38, Tel Aviv, Israel
goldman(at)afeka.ac.il

Vesselin G. Gueorguiev
Institute for Advanced Physical Studies, Montevideo Street, Sofia 1618, Bulgaria; Ronin Institute for Independent Scholarship, 127 Haddon Pl., Montclair, NJ 07043, U.S.A.
Vesselin(at)MailAPS.org

Moritz Haslbauer
Helmholtz-Institut fuer Strahlen- und Kernphysik, University of Bonn, Nussallee 14–16, D-53121 Bonn, Germany
mhaslbauer(at)astro.uni-bonn.de

Ahmad Hujeirat
University of Heilelberg, Berlinerstr. 41, D-69120 Heidelberg, Germany
AHujeirat(at)urz.uni-hd.de

Albin Joseph
Indian Institute of Science Education and Research, AB 1, Room No. 402, Bhouri, Bhopal, MP, 462066, India
albinje(at)iiserb.ac.in

David Kaftan
Nad Soutokem 1418/9, CZ-143 00 Prague 4, Czech Republic
david.kaftan(at)post.cz

Igor Dmitrievich Karachentsev
Special Astrophysical Observatory, Russian Academy of Sciences, Nizhnij Arkhyz, Zelenchukski region, Karachai-Cherkessian Republic, R-369 167 Russia
ikar(at)sao.ru

Jaroslav Klokočník
Astronomical Institute, Czech Academy of Sciences, CZ-251 65 Ondřejov, Czech Republic
jklokocn(at)asu.cas.cz

Roman Knobloch
Department of Mathematics, Technical University of Liberec, Studentská 2, Liberec, Czech Republic
Roman.Knobloch(at)tul.cz

Vladimír Kocour
Faculty of Transportation Sciences, Czech Technical University, Konviktská 20, CZ-110 00 Prague 1, Czech Republic
kocouvl(at)fd.cvut.cz

Kurt Koltko
P. O. Box 100595, Denver, CO 80250, U.S.A.
localcpt(at)yahoo.com

Sergei Kopeikin
Department of Physics and Astronomy, University of Missouri in Columbia, U.S.A.
kopeikinS(at)missouri.edu

Michal Křížek
Institute of Mathematics, Czech Academy of Sciences, Žitná 25, CZ-115 67 Prague 1, Czech Republic
krizek(at)cesnet.cz, krizek(at)math.cas.cz

Pavel Kroupa
Astronomical Institute, Faculty of Mathematics and Physics, Charles University, V Holešovičkách 2, CZ-180 00 Praha, Czech Republic; University of Bonn, Helmholtz-Institut für Strahlen- und Kemphysik, Nussallee 14–16, D-53115 Bonn, Germany
pavel(at)astro.uni-bonn.de, pkroupa(at)uni-bonn.de,

Frederic Lassiaille
Saint-Mandrier-sur-Mer, France
lumimi2003(at)hotmail.com, frederic.lassiaille(at)yahoo.com

Eric J. Lerner
LPPFusion, Inc., 128 Lincoln Blvd., Middlesex, NJ, 08846-1022 U.S.A.
eric(at)lppfusion.com

Andrej Liška
Astronomical Institute of Charles University, V Holešovičkách 2, CZ-180 00 Prague 8, Czech Republic
liska.andrej123(at)gmail.com

František Lomoz
Sedlčany Astronomical Observatory, CZ-115 67 Sedlčany, Czech Republic
F.Lomoz(at)seznam.cz

André Maeder
Geneva Observatory, 19, chemin des Marais, CH-1234 Vessy, Switzerland
Andre.Maeder(at)unige.ch

Jan Maršák
Pedagogical Institute, Prague, Czech Republic
jmarsak(at)seznam.cz

Attila Mészáros
Astronomical Institute of Charles University, V Holešovičkách 2, CZ-180 00 Prague 8, Czech Republic
meszaros(at)cesnet.cz

Jaroslav Mlýnek
Department of Mathematics, Technical University of Liberec, Studentská 2, Liberec, Czech Republic
Jaroslav.Mlynek(at)tul.cz

Klaus Morawetz
Münster University of Applied Sciences, Stegerwaldstrasse 39, D-48565 Steinfurt, Germany; International Institute of Physics – UFRN, Campus Universitário Lagoa nova, 59078-970 Natal, Brazil
morawetz(at)fh-muenster.de, morawetz(at)physik.tu-chemnitz.de

Vladimír Novotný
Cosmological Section of the Czech Astronomical Society, Jašíkova 1533/4, CZ-149 00 Prague 4, Czech Republic
nasa(at)seznam.cz

Marek Nowakovski
Departamento de Fisica, Universidad de los Andes, Cra 1E, 18A-10, Bogota, Colombia
mnowakos(at)uniandes.edu.co

Wolfgang Oehm
An Quirinusbrunnen 14, D-53129 Bonn, Germany
physik(at)wolfgang-oehm.com

Tomáš Ondro
Mendel University in Brno, Zemědělská 1665/1, CZ-613 00 Czech Republic
tomas.ondro(at)mendelu.cz

Jan Papež
Institute of Mathematics, Czech Academy of Sciences, Žitná 25, CZ-115 67 Prague 1, Czech Republic
papez(at)math.cas.cz

Soňa Peková
Tilia Laboratories, s.r.o., Laboratory for Molecular Diagnostics, 5. května 44, CZ-273 08 Pchery, Czech Republic
sona.pekova(at)tilialaboratories.cz

Thomas Prevenslik
QED Radiations, Kelheimer Strasse 8, Berlin, D-10777 Germany
thomas.prevenslik(at)gmail.com

Petr Sadílek
Cosmological Section of the Czech Astronomical Society, Prague, Czech Republic
petr.sadilek(at)post.cz

Karel Segeth
Institute of Mathematics, Czech Academy of Sciences, Žitná 25, CZ-115 67 Prague 1, Czech Republic
segeth(at)math.cas.cz

Lawrence Somer
Department of Mathematics, Catholic University of America, Washington, D.C., 20064, U.S.A.
somer(at)cua.cz

Daniele Sorini
Institute for Astronomy, University of Edinburgh, Royal Observatory, Blackford Hill, EH9 3HJ, Edinburgh, United Kingdom
sorini(at)roe.ac.uk

Alessandro D. A. M. Spallicci
Université d'Orléans, Observatoire des Sciences de l'Univers, Campus CNRS, 3A Av. de la Recherche Scientifique, F-45071 Orléans, France
spallicci(at)cnrs-orleans.fr

Alexei A. Starobinsky
L. D. Landau Institute for Theoretical Physics, Russian Academy of Sciences, 2, Kosygina, R-119 334 Moscow, Russian Federation
alstar(at)landau.ac.ru

Charles Sven
41242 North Westlake Avenue, Antioch, Illinois 60002, U.S.A.
cjsven(at)allnewuniverse.com

Ingo Thies
University of Bonn, Helmholtz-Institut für Strahlen- und Kemphysik, Nussallee 14–16, D-53115 Bonn, Germany
ithies(at)astro.uni-bonn.de

Václav Vavryčuk
Institute of Geophysics, Czech Academy of Sciences, Boční II, CZ-141 00 Prague 4, Czech Republic
vv(at)ig.cas.cz

Tomáš Vejchodský
Institute of Mathematics, Czech Academy of Sciences, Žitná 25, CZ-115 67 Prague 1, Czech Republic
vejchod(at)math.cas.cz

Vladimír Wagner
Nuclear Physics Institute, Czech Academy of Sciences, Hlavní 130, CZ-250 68 Řež, Czech Republic
wagner(at)ujf.cas.cz

Jana Žďárská
Institute of Physics, Czech Academy of Sciences, Na Slovance 2, CZ-182 21 Prague 8, Czech Republic
zdarskaj(at)fzu.cz

PROGRAM OF THE CONFERENCE

Wednesday, September 23

12:00–14:00 Registration

14:00–14:10 Opening

Chair: Yurii V. Dumin

14:10–14:50 **Pavel Kroupa**, The star-formation histories of nearby galaxies raises questions on cosmology

14:50–15:30 **Moritz Haslbauer**, Structure formation in LCDM and MOND

15:30–16:00 Coffee Break

Chair: Michal Křížek

16:00–16:30 **Wolfgang Oehm**, A possible constraint on the validity of general relativity for very strong gravitational fields

16:30–17:00 **Yurii V. Dumin**, The problem of causality in the uncertainty-mediated inflationary model

17:00–17:20 **Yurii V. Dumin**, The problem of flatness in various cosmological models

Thursday, September 24

Chair: Itzhak Goldman

9:00–9:45 **Václav Vavryčuk**, Cosmic microwave background as thermal radiation of intergalactic dust?

9:45–10:15 **Jan Papež**, Linear algebraic solvers in Cosmic Microwave Background data analysis

10:15–10:45 Coffee Break

Chair: Pavel Kroupa

10:45–11:05 **Joerg Dabringhausen**, Elliptical galaxies without dark matter

11:05–11:30 **Pavel N. Antonyuk**, Mathematics of the Hubble law

11:30–12:00 **Yash P. Aggarwal**, Vedic cosmology on the characteristics of dark matter: Implications for the search for dark matter particle

12:00–14:00 Lunch Break

Chair: Klaus Morawetz

14:00–14:50 **Itzhak Goldman**, Astrophysical bounds on mirror dark matter

14:50–15:20 **Ismael Ferrero**, A unified scenario for the origin of disk and elliptical galaxy structural scaling laws

15:20–15:30 **Conference photo**

15:30–16:00 Coffee Break

Chair: Wolfgang Oehm

16:00–16:50 **Michal Křížek**, Excessive extrapolations of Einstein's equations

16:50–17:10 **Daniele Sorini**, Radiation-Lambda equality and reionisation: coincidence or anthropic prediction?

17:10–17:40 **Charles Sven**, Physics of dark energy

Friday, September 25

Chair: Václav Vavryčuk

9:00–9:30 **Klaus Morawetz**, Exact solution of Einstein-Cartan equations with torsion

9:30–10:00 **Frederic Lassiaille**, Gravitational model of the three elements theory: Formalizing comments

10:00–10:30 **Ahmad Hujeirat**, The cosmological fate of neutron stars and their connection to dark matter and dark energy

10:30–11:00 Coffee Break

Chair: Moritz Haslbauer

11:00–11:20 **Thomas Prevenslik**, Cosmology and redshift in cosmic dust

11:20–11:50 **Václav Vavryčuk**, Considering light-matter interactions in Friedmann equations

11:50–12:10 **Kurt Koltko**, Gauge CPT and the baryonic Tully-Fisher law

12:10–14:00 Lunch Break

Chair: Yurii V. Dumin

14:00–14:30 **Michal Křížek**, A critical review of paradoxes in the special theory of relativity

14:30–15:00 **Yan Breek**, Imprint of quantum gravity model on observable cosmology

15:00–15:20 **Yash P. Aggarwal**, A working hypothesis of a cyclic universe that neither undergoes cosmic inflation or a Big Crunch based on Vedic cosmology

15:20–15:25 **Vladimír Novotný**, Cosmological coincidences in the expanding universe (Poster presentation)

15:25–15:30 **Albin Joseph**, Exact solutions of some dynamical variables in FRW universe with scalar field dynamics (Poster presentation)

15:30–16:00 Video presentations

Saturday, September 26

9:00–12:00 Excursion to the astronomical and cosmological sights of Prague guided by **Michal Křížek**. We will meet at 9:00 in front of the main gate of the Institute of Mathematics at Žitná 25.

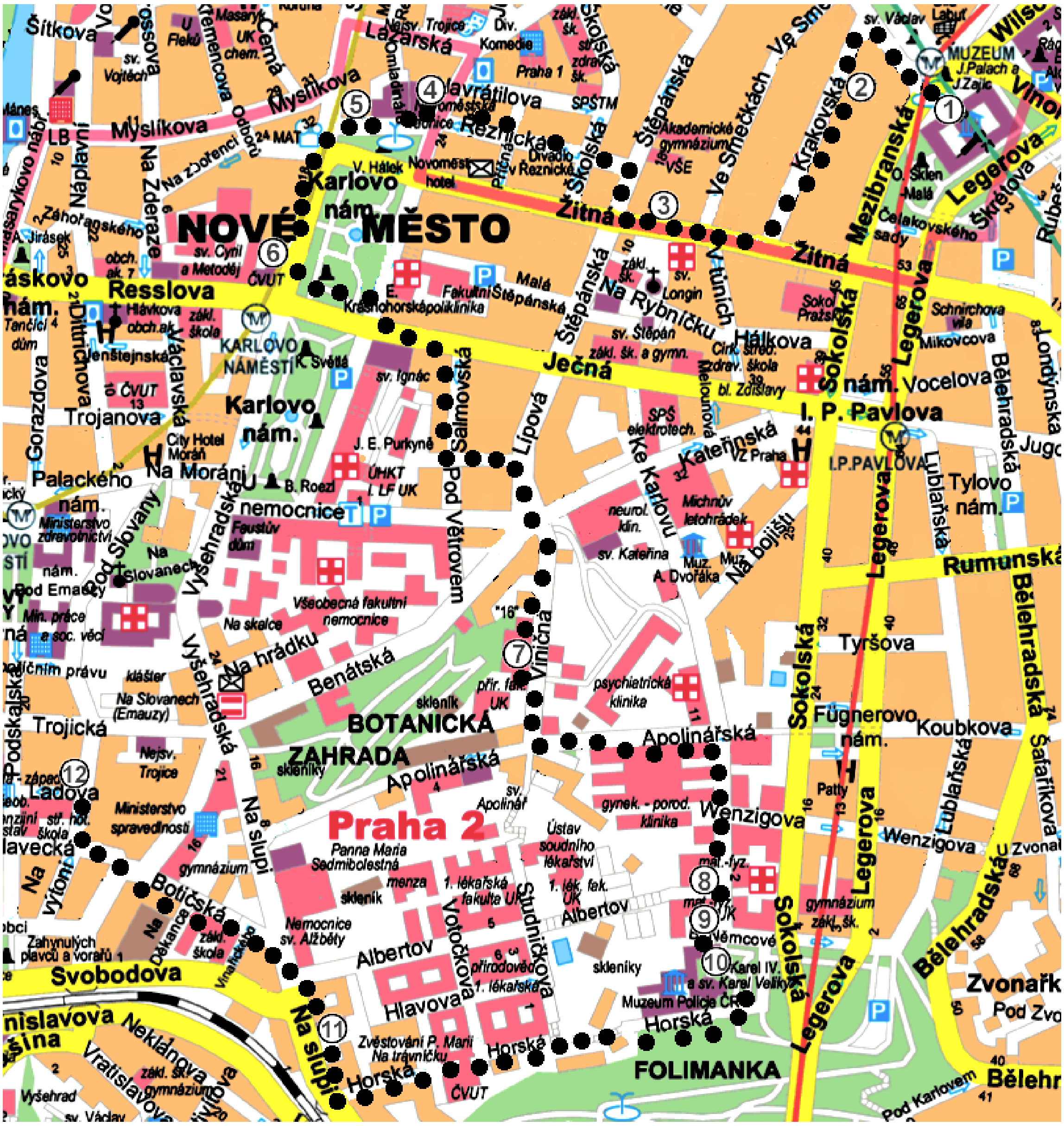

Map of the proposed walk through the astronomical and cosmological sightseeings of Nové Město (New Town) according to [3].

Stop 1. Our walk will start at the main building of the National Museum which was completed in 1891. It originally housed the Czech Academy of Science and the Arts (ČAVU). In 1902, 72 plaques of red Meissen granite were placed on the outside walls of the building. We can find among them many famous mathematicians, physicists, and astronomers, for example, Křišťan from Prachatice (the author of a book on the astrolabe), Tycho Brahe (incorrectly spelled as Tycho de Brahe [2]), Tadeáš Hájek from Hájek, Martin Bacháček from Nauměřice, Johannes Kepler (see Figure 1) Jan Marek Marci, Prokop Diviš, Josef Stepling, Stanislav Vydra, František Josef Gerstner, Bernard Bolzano, and Christian Doppler.

Figure 1

Stop 2. In Krakovská Street No. 14/1362, Pavel Josef Šafařík has a memorial plaque. He is the father of the astronomer Vojtěch Šafařík who produced glass and metal mirrors. V. Šfařík had a private observatory in Vinohrady and was a professor of chemistry and descriptive astronomy at the University of Prague.

Stop 3. The Union of Czech Mathematicians and Physicists and the Institute of Mathematics of the Czech Academy of Sciences are located in Žitná No. 25/609. There is also the largest mathematical library in the Czech Republic which counts over 80 000 library units. Many of them are digitized, see `www.dml.cz`.

St. Longin's Rotunda stands nearby the Institute of Mathematics. It is one of the few preserved Romanesque rotundas in Prague. It originated from the 12th century as a parish church for the village Rybníček which was there before the founding of the Prague New Town in the middle of the 14th century. The astronomer Martin Bacháček from Nauměřice (professor at the University of Prague and a friend of Johannes Kepler) worked in a parish school of the nearby Church of St. Štěpán in Štěpánská Street.

Stop 4. On the eastern wall of the New Town City Hall, the standard of the Prague elbow (= 591.4 mm) is presented (see Figure 2). It was established in 1268 by the Czech king Přemysl Otakar II and remained unchanged[1] until 1765, i.e. for five centuries. For comparison, the definition of 1 meter changed during the last 60 years several times. Let us note further that the New Town Hall Tower contained an astronomical clock (horologe) like the Old Town City Hall Tower, see [3, p. 139].

Figure 2

[1] In 1765, the Austrian archduchess Maria Theresa ordered the use of the Austrian units of measurement in Prague.

Stop 5. A memorial plaque on Charles Square No. 20 marks the place, where Christian Doppler (1803–1853), professor of mathematics at the Czech Technical University in Prague and the founder of the Institute of Physics in Vienna, lived before 1840 (see Figure 3). The date of his death on the plaque is incorrect and an unusual first name in the form of Kristian is presented. In 1842, he gave his famous lecture *On the colored light of binary stars* in the Patriotic Hall of Karolinum (formerly in Latin: Collegium Carolinum; at present the seat of Charles University). For the first time he introduced there relations that describe the Doppler phenomenon, see [1].

Figure 3

Stop 6. Foucault's pendulum 21 m long is situated in the entrance hall of the Czech Technical University on Charles Square No. 13/293. The French physicist Jean B. L. Foucault used a similar 67 m long pendulum in 1851 to demonstrate the Earth's rotation.

On the way to Stop 7, we can see a memorial plaque in honor of the Nobel Prize Winner Carl Ferdinand Cori (1896–1984) which is placed on his birthplace house in Salmovská Street No. 6/1693. He studied medicine in Prague in the next street U Nemocnice No. 5, where is another plaque and a memorial hall (see Figures 4 and 5). Then he left for the U.S.A. with his wife Gerty Cori. Here they received the Nobel Prize in Physiology or Medicine in 1947.

Figure 4

Figure 5

Figure 6

Stop 7. A memorial plaque (see Figure 6) in the lobby of the Faculty of Science of Charles University in Viničná Street No. 7/1594 recalls that Albert Einstein worked in this building in 1911–1912. He also had his office here, where he found the peace he needed to formulate basic ideas of the General Theory of Relativity. He received the Nobel Prize for Physics in 1921.

Stop 8. The Czech Institute of Physics of the Charles University of Prague is located in Ke Karlovu Street No. 5/2026. The construction of this building was realized mainly due to Professor of experimental physics Čeněk Strouhal (1850–1922). Teaching in this building was established from January 1908.

Stop 9. Dean's office of the Faculty of Mathematics and Physics of Charles University is situated in Ke Karlovu Street No. 3/2027.

Stop 10. James W. Herschel, the grandson of the famous William Herschel (the discoverer of the planet Uranus), is one of the founders of dactyloscopy. He is remembered in a dactyloscopic collection in the Museum of the Police of the Czech Republic in the former Augustinian Monastery Panny Marie a sv. Karla Velikého.

Stop 11. We shall proceed downstairs around the fortifications of Prague from the epoch of Charles IV. to the octagonal tower of a Gothic church Panny Marie Bolestné to Na Slupi Street No. 4a. The number 8 in the Middle Ages symbolized eternity. The known planets at that time together with the Sun and the Moon were supposed to move in seven spheres and according to the Aristotelian tradition, the eighth sphere of fixed stars was motionless.

Figure 7

Stop 12. The Czech Nobel Prize Winner in Chemistry Jaroslav Heyrovský lived in the period 1926–1951 in Ladova Street No. 8. At present there is a commemorative plaque (see Figure 7).

References

[1] Doppler, Ch.: Ueber das farbige Licht der Doppelsterne und einiger anderer Gestirne des Himmels. Abh. böhm. Ges. Wiss. **2** (1842), 466–482.

[2] Šolcová, A.: From Tycho Brahe to incorrect "Tycho de Brahe". A searching for the first occurrence when the mistaken name of famous astronomer appeared. Acta Univ. Carolin. Math. Phys. **S46** (2005), 29–36.

[3] Šolcová, A., Křížek, M.: Procházky Prahou matematickou, fyzikální a astronomickou (2. část). Pokroky Mat. Fyz. Astronom. **52** (2007), 127–141, available at `www.dml.cz`

SUBJECT INDEX